Characterisation of molecular variations in human C-reactive protein

By Robert D Williams

Thesis submitted for the degree of Doctor of Philosophy

June 2017

Keele University

SUBMISSION OF THESIS FOR A RESEARCH DEGREE

Degree for which thesis being submitted: Doctor of Philosophy

Title of thesis: Characterisation of molecular variations in human C-reactive protein

Date of submission:

Original registration date: 24.09.2012

Name of candidate: Robert D Williams

Research Institute:

Name of Lead Supervisor: Dr A. K. Shrive

I certify that:

(a) The thesis being submitted for examination is my own account of my own research
(b) My research has been conducted ethically. Where relevant a letter from the approving body confirming that ethical approval has been given has been bound in the thesis as an Annex
(c) The data and results presented are the genuine data and results actually obtained by me during the conduct of the research
(d) Where I have drawn on the work, ideas and results of others this has been appropriately acknowledged in the thesis
(e) Where any collaboration has taken place with one or more other researchers, I have included within an 'Acknowledgments' section in the thesis a clear statement of their contributions, in line with the relevant statement in the Code of Practice (see Note overleaf).
(f) The greater portion of the work described in the thesis has been undertaken subsequent to my registration for the higher degree for which I am submitting for examination
(g) Where part of the work described in the thesis has previously been incorporated in another thesis submitted by me for a higher degree (if any), this has been identified and acknowledged in the thesis
(h) The thesis submitted is within the required word limit as specified in the Regulations

Total words in submitted thesis (including text and footnotes, but excluding references and appendices): **61,731**

Signature of candidate …… Date ……

Abstract

The research described here focuses on the molecular variations, clinical significance and structural interactions of the innate immune protein, C-reactive protein (CRP).

Monomeric CRP (mCRP) was produced through urea-induced dissociation, at an optimum concentration of 3M urea over a 10-week period. Dissociated samples were purified via size exclusion chromatography and confirmation was provided via Western Blot analysis. In contrast with previous published works, this mCRP retained the ability to reversibly bind to phosphocholine. Furthermore, the binding of mCRP with cell wall polysaccharide does not result in the generic precipitation trend as that seen with pentameric CRP (pCRP).

Human serum samples with raised CRP levels (>100mg/L) were analysed (*n =40)* to determine whether circulating mCRP could be detected *in vivo*. All 40 samples tested positive for pCRP via Western Blot and ELISA analysis, with further quantification via the UV Spectrophotometer supporting the calculated pCRP levels. Monomeric CRP was identified in all the 40 patient samples tested, with an average value recorded of 0.88mg/L (SE = ±0.142). Informed by the results from *in vitro* mCRP studies, the mCRP displayed a molecular weight of approximately 25kDa based on size exclusion chromatography and Western Blot analysis and demonstrated an ability to reversibly bind phosphocholine. To our knowledge, we are the first to successfully purify and identify a monomeric form of CRP from human serum through these procedures.

Crystallisation trials of *in vitro* produced mCRP and the complex of pCRP with C1qGHR and CWPS did not result in the growth of any protein crystals of sufficient diffraction quality. One crystal from the complex crystallisation trials diffracted to 9Å with follow up conditions currently being pursued. Furthermore, additional crystallisation trials

from both experiments have generated potential conditions which may be refined in future research to produce high-quality diffraction grade crystals.

List of Figures

Chapter 1.0

Chapter 2.0

Chapter 3.0

Chapter 4.0

List of Tables

Chapter 1.0

Chapter 2.0

Chapter 3.0

Chapter 4.0

Table of Amino Acids

Amino Acid	Single Letter Code	Three Letter Code
Alanine	A	Ala
Cysteine	C	Cys
Aspartic acid	D	Asp
Glutamic acid	E	Glu
Phenylalanine	F	Phe
Glycine	G	Gly
Histidine	H	His
Isoleucine	I	Ile
Lysine	K	Lys
Leucine	L	Leu
Methionine	M	Met
Asparagine	N	Asn
Proline	P	Pro
Glutamine	Q	Gln
Arginine	R	Arg
Serine	S	Ser
Threonine	T	Thr
Valine	V	Val
Tryptophan	W	Trp
Tyrosine	Y	Tyr

Abbreviations Used

AMI:	Acute Myocardial Infarction
AP:	Alkaline Phosphatase
APC:	Antigen Presenting Cell
APS:	Ammonium Persulfate
BSA:	Bovine Serum Albumin
CaC_2:	Calcium Chloride
CI:	Chief Investigator
CLR:	Collagen-like Region
CRP:	C-reactive Protein
CWPS:	Cell Wall Polysaccharide
DLS:	Diamond Light Source
DNA:	Deoxyribose Nucleic Acid
ECL:	Enzyme Chemiluminescence
EDTA:	Ethylenediaminetetraacetic acid
ELISA:	Enzyme-linked Immunosorbent Assay
FPLC:	Fast Protein Liquid Chromatography
GHR:	Globular Head Region
HCl:	Hydrochloric Acid
HEPES:	4-(2-Hydroxyethyl) Piperazine-1-Ethanesulfonic Acid
HRP:	Horseradish Peroxidase
ICAM-1:	Intercellular Adhesion Molecule 1
IgG:	Immunoglobulin G
IL:	Interleukin
IRAS:	Integrated Research Application System
LDL/HDL:	Low/High Density Lipoprotein
mAb:	Monoclonal Antibody
MCP-1:	Monocyte Chemoattractant Protein-1
mCRP:	Monomeric C-reactive Protein

MES:	2-(*N*-Morpholino)Ethanesulfonic Acid
MP:	Micro-particles
MPD:	Methyl Pentanediol
MWCO:	Molecular Weight Cut Off
NaCl:	Sodium Chloride
NHS:	National Health Service
PAGE:	Polyacrylamide Gel Electrophoresis
PAMP:	Pathogen Associated Molecular Pathogens
PBS:	Phosphate Buffered Saline
PC:	Phosphocholine
PCF:	Participant Consent Form
pCRP:	Pentameric C-reactive Protein
PEG:	Polyethylene Glycol
PIS:	Participant Information Sheet
PRR:	Patter Recognition Receptors
PVDF:	Polyvinylidene Fluoride
RNA:	Ribonucleic Acid
SAP:	Serum Amyloid P Component
SDS PAGE:	Sodium Dodecyl Sulfate Polyacrylamide Gel Electrophoresis
SMC:	Smooth Muscle Cells
TBS:	Tris Buffered Saline
TEMED:	Tetramethylethylenediamine
TMB:	Tetramethylbenzidine
UHNM:	University Hospital of North Midlands
VCAM-1:	Vascular Cell Adhesion Molecule 1

Acknowledgements

When I first started my PhD, I was advised that it would be the hardest, yet most rewarding thing I would ever undertake in my life. Four years on and to say this advice was true is such an understatement. That said, if given the opportunity to go back and do it all again, I wouldn't think twice about saying yes. My PhD has helped me develop both personally and professionally into the person I am today.

Firstly, I would like to give a massive thank you to both of my supervisors, Dr. Annette Shrive, and Professor Trevor Greenhough for the support, guidance and encouragement they have given me throughout the past four years. Their indispensable knowledge and advice on both my experimental work and what is required to complete a PhD has helped me achieve so much. For that I am truly grateful. Secondly, thanks go out to our collaborators, Professor Tony Fryer, members of R&D and the pathology department at UHNM. Without their help, assistance, and extensive clinical knowledge, a large part of this research would have not been possible.

I would also like to give a special thank you to Ian Burns. His laboratory assistance and willingness to help whenever I needed it has been greatly appreciated throughout my PhD. Thanks, go out to Jamie for helping to create the structural images in my thesis. Also, to all the other members of the Structural Biology team at Keele; Jenny, Ruben, Will and others, thank you for all the support, advice and laughs over the years. I would also like to thank my amazing demonstrating team. Four years of second year labs has given me some amazing memories to look back on!

I would like to give a massive, heart-felt thank you to all my friends, family, and most importantly parents for all the help, support, love and encouragement they have given me, not just over the past four years, but throughout my entire life. Without any of this I

would not be where I am today and I will be forever grateful. Finally, I would like to thank Jordan. Thank you for your support, love, advice and believing in me.

Chapter 1.0 – Introduction

1.1 Overview

C-reactive protein belongs to a family of proteins known as the pentraxins and has been highly conserved throughout evolution. The pentraxin family is named for its appearance in electron micrograph from the Greek words *penta* (five) and *ragos* (berries) (Pepys *et al.* 1978b; Pepys & Hirschfield, 2003).

When the human body becomes infected with an invading pathogen, liver cells will begin synthesising C-reactive protein rapidly as part of the innate immune response. Due to this acute rise of the plasma protein's levels within serum, it is routinely used worldwide as a biological marker for infection, inflammation and tissue damage.

C-reactive protein has been identified within a whole range of species including the mammalian class, fish and even within the primitive Atlantic horseshoe crab, *Limulus polyphemus* (Pepys *et al*., 1978b). Additionally, there is no record of any human being identified as having a deficiency of C-reactive protein Coupled with a persistence to resist evolutionary change, this underlies the importance of C-reactive protein to the host's innate immune function (Pepys & Baltz, 1983).

1.2 The Human Immune System

The study of the human immune system is a relatively new science, thought to originate from Edward Jenner, who observed in the late 18th century that the relatively mild disease of cowpox seemed to confer protection against the often-fatal disease of smallpox. In 1796, Jenner demonstrated that inoculation with cowpox protected from smallpox, and named this procedure a 'vaccination'. It was not until the 19th century that Robert Koch proved that infectious diseases are caused by microorganisms, each responsible for their own disease. In modern-day medicine, we now recognise four broad categories of disease-causing microorganisms, more commonly known as pathogens: viruses, bacteria, fungi and unicellular & multicellular eukaryotic organisms (collectively known as parasites) (Berg *et al*., 2011; Murphy *et al.,* 2008).

The human immune system can be split into two different sub-categories. These two categories are; the innate immune system, a short lasting, non-specific primary line of defence, and the adaptive immune system, which provides a 'tailored' response specific to the pathogen it targets. Both systems contain proteins, cells and organs that are concerned with defence of the individual, primarily against the threat of disease caused by these infectious organisms. The animal or human that an infectious organism (or pathogen) invades is known as the host. Not all infectious organisms are harmful to the host they invade, with some being beneficial. Bacteria living within our gut aid in the digestion of food and are known as commensal organisms. However, there are many pathogens to which we as a species are constantly in danger of infection, and the diseases caused by them. Without the protection from our immune system, we would be vulnerable to these pathogens that we are exposed to daily (Wood, 2006).

The function of the human immune system is primarily to protect the host against the threat of disease. This defence can be further split into four main tasks. The first is known as immunological recognition; the presence of an infection must be detectable by the immune system. This immediate response is carried out by white blood cells of the innate immune system, and lymphocytes of the adaptive immune system. The second task is to contain the infection, eventually removing the pathogen from the host completely. This is known as immune effector functions. The human body has a whole range of defence mechanisms within its arsenal; activation of one of the three complement cascades through a system of blood proteins, production of antibodies, recruitment of lymphocytes and other white blood cells (Murphy *et al.,* 2008). The third task is immune regulation; the ability of the immune system to regulate itself to prevent causing harm to the host. Dysfunction of this system can result in exacerbation of the immune response, thus exploiting conditions such as allergies and auto-immune disease (Muphy *et al.,* 2008). Finally, the fourth point is immunological memory, a unique feature of the adaptive immune system. Memory from the immune system is paramount if preventing recurrence of disease from the same pathogen. Having already been exposed to that same pathogen previously in a person's life, allows the human body to generate an immediate and stronger response against subsequent exposure (Berg *et al*., 2011).

The human body has two main different forms of protection barriers which prevent invasion of pathogens which may cause disease. Physical barriers include skin and mucosa, cilia lining the respiratory tracts and mucus secreted in the epithelial cells of the gut. Chemical and biochemical barriers include the acidic conditions, fatty acids, lysozymes present in sweat and tears and collectins which can bind to sugars of microbial surfaces and promote elimination. Despite these primary defences, pathogens are constantly developing,

and adapting to these barriers, meaning more complex defence features are required from the human immune system (Berg *et al*., 2011; Muphy, *et al* 2008; Wood, 2006).

1.2.1 Inflammation and the Immune System

When the host's initial defences are breached, the invading pathogen will encounter cells that will recognise the organism as 'foreign'. This results in the initiation of the immediate innate immune response. One of the main functions of the innate immune system is to propagate an inflammatory response at the site of infection (Berg *et al*., 2011). Physiological changes within the body, including vasodilation, endothelial cell activation, increased vascular permeability and the secretion of chemotactic factors, are all contributing factors. Immune cells, such as macrophages engulf these pathogens and present fragmented pieces of the pathogen on their surface. This phagocytosis of the invading organism also results in the release of proteins known as chemokines and cytokines, alongside other immune-stimulating biologically active molecules (Alberts *et al.*, 2014; Wood, 2006).

Chemokines are chemotactic agents which are responsible for the migration of certain immune cells. Furthermore, they can also indirectly increase the expression of cell adhesion molecules, such as selectins and integrins. Alteration in these cell adhesion molecules allows immune cells (neutrophils, macrophages) to bind to the epithelium at a site around the body and enter the tissues. The process by which these cells leave the bloodstream is known as extravasation (Wood, 2006). This is usually carried out in four main stages, the first being 'rolling'. Vasodilation of blood vessels reduces blood flow and allows immune cells to 'roll and bump' along the endothelial cell wall, interacting with 'E' and 'P' selectin. Attachment then occurs through adhesion molecules such as the intercellular adhesion molecule 1 (ICAM-1), which allows cells to migrate across the epithelium towards the site

of inflammation, where concentrations of certain chemokines will be higher, usually interleukin (IL) 8 (Wood, 2006).

Whereas chemokines function as chemo-attraction proteins, cytokines function as signalling molecules between cells. They are secreted through a broad range of cells from the immune system through interactions with receptors on the cell surface. Chemokines are responsible for regulation of the immune response, and can also evoke biological activities through binding to certain receptors. Although inflammation is a natural response of the human immune system to toxins or foreign substances, more commonly known as antigens, aggressive immune responses can occasionally inflict undue harm to the host. Diseases such as rheumatoid arthritis, cardiovascular disease and diabetes mellitus are all thought to contain an element of immune dysregulation. This occurs when immune cells fail to recognise the host's cells and start destroying them. In addition, the uncontrolled release of inflammatory cytokines can further result in damaging levels of inflammation at localised sites throughout the body (Alberts *et al.,* 2014; Berg *et al*., 2011; Murphy *et al.,* 2008; Wood, 2006).

1.2.2 The Innate Immune System

The innate immune system is a part of a host's defence, which has been passed down through the generations. Unlike the adaptive immune system which is 'learnt', organisms are born with innate immunity, with vertebrates, invertebrates, plants, and even the most primitive of organisms being recorded to display this line of defence (Alberts *et al.*, 2014; Janeway & Medzhitov, 2002). These pre-existing defence mechanisms are designed to prevent infection and mount an immediate, primary defence against invading infectious agents. The innate immune response is not specific to a pathogen in the way the adaptive immune system is, and can generate a response within a matter of hours. The system depends

on a group of proteins and phagocytic cells that recognise conserved features of pathogens and become activated quickly to help destroy and remove pathogens (Alberts *et al.,* 2014; Wood, 2008).

The innate immune system can be sub-divided into the humoral arm and the cellular arm of defence. The humoral arm of the innate immune system is extremely diverse and is so named as it involves substances which are found in the humorous or bodily fluids. Macromolecules such as antibodies (adaptive immunity), blood proteins and antimicrobial peptides are secreted into the extracellular space upon recognition of a foreign stimulus. Once infectious agents have breached anatomical barriers, or penetrated tissues, acute inflammation is stimulated, typically manifesting symptoms such as redness, swelling, heat and possible pain. Blood proteins responsible for these pathological changes include collectins (surfactant protein A and D, C1q, mannose-binding lectin), ficolins and pentraxins (C-reactive protein, PTX3, serum amyloid protein) (Garlanda *et al.,* 2005). Activation of the complement system also occurs, enhancing the immune response through recruitment of immune cells and antibodies, whilst also promoting intensified states of inflammation. These immune components play a crucial role in the discrimination between host and foreign cells through recognition of highly conserved motifs called pathogen-associated molecular patterns (PAMPS) (Berg *et al*., 2011). PAMPS often occur in repeating patterns of microbial molecules, including nucleic acids, proteins, lipids and polysaccharides. Special receptor proteins, shown through the above listed examples, can recognise PAMPS, and are known as pattern recognition receptors (PRRs). PRRs can be expressed on the surface of immune cells (including macrophages and dendritic cells), in addition to intracellularly. There are four main classes of PRR families which have been identified. These include transmembrane proteins, such as toll-like receptors (TLRs), C-type lectin receptors as well as cytoplasmic proteins such as retinoic acid-inducible gene receptors and nucleotide oligomerisation

domain (NOD)-like receptors. Upon detection of PAMPs by PRRs, an inflammatory immune response is triggered, which leads to the destruction and removal of invading pathogens from the host (Alberts *et al.,* 2014; Murphy *et al.,* 2008; Takeuchi & Akira, 2010; Wood, 2006).

The cellular arm of the innate immune system involves the recruitment of immune cells to a site of infection and production of intensified states of inflammation, through the secretion of inflammatory mediators such as cytokines (interleukin-6) and chemokines (interleukin-8). These are produced by immune cells such as macrophages and mast cells (Janeway & Medzhitov, 2002). Among these recruited cells are phagocytes. Phagocytes are a group of cells, including dendritic cells and mast cells. The most commonly recruited phagocyte during an inflammatory response are neutrophils, which are capable of ingesting foreign particles such as bacteria, parasites, dead host cells and foreign debris and digesting their contents. This process is known as phagocytosis (Berg *et al*., 2011). Harmful pathogens (or peptides) which have been opsonised, agglutinated, neutralised or rendered harmless through interactions with antibodies or alternative immune proteins are engulfed by phagocytes. These are then digested through lysosome killing mechanisms (usually digestive enzymes). Alternative lysosome-independent killing mechanisms also exist, which involve the generation of oxygen radicals and the production of nitric oxide (Janeway & Medzhitov, 2002, Wood, 2006). Although the innate immune system differs in specificity, response time, memory to the adaptive immune response, there is a large amount of overlap, with both arms of the immune system working together to protect the host.

1.2.3 The Adaptive Immune System

Occasionally, a microorganism will infect a host, which requires a stronger immune response than that provided through innate immunity. Complex creatures, such as vertebrates can elicit a more sophisticated and specialised response, known as the adaptive immune response. This system contains an extensive range of diverse cells, which can mount an augmented defence against one pathogen (Berg *et al*., 2011). Although the response time takes longer than that seen for the innate system, the adaptive immune system also provides long-lasting protection, or 'memory' against specific pathogens. A person who has recovered from a measles infection, for example, will be protected for life against that virus which invaded the body, although not against other common viruses. For the adaptive system's memory to work, the host must have meet the organism previously and initiated an adaptive immune response (Alberts *et al.*, 2014; Berg *et al*., 2011).

Part of the innate immune system's role is the initiation of the adaptive immune response. Cytokines and chemokines released through the first line of defence results in the migration of immune cells to the site of infection. Lymphocytes play a crucial role within this adaptive response. There are two different types of lymphocytes; B and T cells (Murphy *et al.,* 2008). The main role of B lymphocytes within the human body is the production of immunoglobulin proteins called antibodies. Antibodies circulate within the human blood stream, permeating other bodily fluids where they will bind to specific antigens (or epitope) which stimulated their production. B cells contain membrane-bound immunoglobulins (B-cell receptors) which serve as the cell's receptors for antigens. Cells known as antigen presenting cells (APC) will engulf pathogens upon contact, and present peptide fragments of the pathogen on the surface of their cell membrane through major histocompatibility complexes (MHC) (type 1 and 2). The presentation of these antigens allows interaction with T lymphocytes to further elicit an adaptive immune response. APC include dendritic cells,

macrophages and B cells (Murphy *et al.,* 2008; Wood, 2006). Activation of these B cells occurs through this antigen presentation to T-helper cells. The T-helper cells bind to the presented antigen via T cell receptors which results in the release of cytokines, inducing the proliferation of B cells into memory cells and antibody-secreting plasma cells. Antibodies have two main roles within the body; the first is binding to a specific antigen, rendering the pathogen harmless via neutralisation, agglutination or precipitation. Secondly, antibodies propagate the immune response, to recruit other cells and molecules which can destroy the pathogen once the antibody has bound to it (Berg *et al*., 2011s; Murphy *et al.,* 2008).

T lymphocytes provide the cell mediated response of the adaptive immune system. The main role of T cells within the immune system involves the killing and removal of foreign pathogens from the human body (Alberts *et al.,* 2014). There are several types of T cells which make up this cell mediated response. T helper cells, as described previously, are responsible for the activation of several other immune cells through MHC proteins expressed on the surface of APC. Activation of B cells results in the production of antibodies, whilst macrophages are stimulated to further release inflammatory cytokines (Berg *et al*., 2011; Murphy *et al.,* 2008). Cytotoxic T cells aid in the destruction of virus-infected cells or cancerous cells. Cells which are infected with a foreign pathogen will present fragments of foreign antigens on their surface which allows T cells to distinguish between healthy and infected cells. In addition, there are also T memory cells, which are antigen- specific cells which provide long-lasting immunity post infection, and regulatory T cells which provide crucial maintenance of the adaptive immune system (Alberts, *et al.,* 2014; Wood, 2006).

1.3 Components of the Immune System

1.3.1 Monocytes & Macrophages

Monocytes are a type of leukocyte (more commonly known as white blood cell) which, when matured, differentiate into macrophages or dendritic cells. Monocytes are an integral part of the innate immune system and participate within the first line of response against invading pathogens (Kinne *et al.,* 2007). Located within the circulating blood stream of the human body, they can be recruited to localised sites of inflammation, through monocyte chemotactic protein 1 (MCP-1). Increased transcription of cell adhesion molecules at inflamed sites, through the release of cytokines and chemokines promotes transmigration of monocytes from the lumen of blood vessels into the arterial intima. Once infiltrated, monocytes can differentiate into macrophages in the presence of macrophage colony-stimulating factor (M-CSF) produced through endothelial cells and smooth muscle cells (Lundberg & Hansson, 2010).

Macrophages are matured monocytes, which engulf and digest cellular debris, foreign substances and microbes through phagocytosis. Foreign material is broken down and rendered harmless via digestive enzymes contained within the cells lysosomal sacks. In addition to phagocytosis, macrophages are also involved in the recruitment of additional immune cells, such as lymphocytes, to localised sites of infection and inflammation, and regulation of the immune response, by the release of anti-inflammatory cytokines when necessary.

1.3.2 Neutrophils

Neutrophils are the most abundant type of granular leukocyte within the human immune system. They are known as granulocytes due to the presence of granules in their cytoplasm. Formed in the stem cells of bone marrow, neutrophils are an integral part of the innate immune system, participating in the first line of defence upon infection and inflammation. Their primary function within the immune system is to phagocytose and eliminate foreign microorganisms that are recognised as harmful to the host. In addition, they participate in the breakdown and elimination of dead or damaged tissues (Springer, 1995). Neutrophils also contribute towards the inflammatory response through the production of immune-stimulating components including lipids, cytokines, proteases, microbial products and reactive oxygen intermediaries (Murphy *et al.*, 2008; Sampson, 2000; Wood, 2006).

1.3.3 Lymphocytes

Lymphocytes are a type of white blood cell, found in the immune system of vertebrates and are derived from pluripotential stem cells within the bone marrow. Types of lymphocytes include natural killer (NK) cells, T cells and B cells. Natural killer cells are a form of cytotoxic lymphocyte which is critical to the functioning of the innate immune system. They provide rapid responses to viral-infected cells, alongside combatting tumour formation from cancerous cells. NK are unique in the sense that they do not need to recognise antigens presented on the surface of a cell's MHC protein to elicit an immune response. Their role within the immune system also extends to regulation, through the release of cytokines and chemokines during an immune response which helps recruit further immune cells to localised sites. Their main role however, is their ability to lyse target cells, usually infected with foreign pathogens. Upon proximity to the target cell, NK cells releases

enzymes such as perforin and proteases which form a pore in the target cells membrane, creating an aqueous channel into the cell. This therefore allows further enzymes to enter target cells and induce apoptosis or osmotic lysis (Alberts, *et al.*, 2014; Berg *et al*., 2011; Murphy *et al.*, 2008).

T lymphocytes are also derived from the bone marrow, but mature within the thymus of the body (hence the name 'T'). They are distinguishable from NK cells and B lymphocytes as they display T cell receptors on their surface. T cells can multiply into various sub-categories including: T helper cells, cytotoxic T cells or memory cells. The role of T cells within the immune system is widespread, ranging from the facilitation of the immune response, destroying virus-infected cells and providing the immune system with a 'memory' of previous antigens which have infected the host. Additionally, T cells are involved in the activation of B lymphocytes upon presentation of antigens on their T cell receptors. The resulting consequence is the production and release of antigen specific antibodies from mast cells which are crucial in the neutralisation of harmful invading pathogens. B cells, unlike T cells derive and mature within the bone marrow. They are part of the humoral arm of the immune system and are mainly responsible to produce antibodies. B cell receptors are expressed on their cell surface, which can ingest, process and present antigen sequences, which results in the initiation of an immune response. B cells can also be divided into sub-categories, with each B cell derivative responsible for a different role within the adaptive immune system. The most common types of B cells are plasma cells and memory cells. Plasma cells, usually T cell-dependent upon activation, are responsible for the formation of antibodies. Memory cells, like those seen for T cells, provide host defence against pathogens, or antigenic sequences, which have previously invaded the host (Alberts, *et al.*, 2014; Berg *et al*., 2011; Wood, 2006).

1.3.4 Eosinophils & Basophils

Eosinophils and basophils are forms of white blood cells found within the human immune system. Eosinophils are responsible for combating invading parasites and various infections within the body, alongside the regulation of mechanisms involved in allergies. Eosinophils develop in the bone marrow, and circulate the body for sites of infection or inflammation once they have fully matured (Murphy *et al.,* 2008). Upon activation, these cells are involved in the production of inflammatory cytokines, release of granular proteins through degranulation and the production of RNases to help fight viral infections. Basophils are the most uncommon of all white blood cells; however, they display the largest morphology. Alongside eosinophils, they are also involved in allergic reactions. Basophils contain relatively large amounts of the vasodilator histamine, which is released from the cell when activated (Alberts, *et al.,* 2014; Berg *et al*., 2011; Wood, 2006).

1.3.5 Platelets

Platelets, also known as thrombocytes, are highly abundant haematopoietic cells; stem cells which give rise to blood cells including white and red blood cells. They are produced from large bone marrow cells, known as megakaryocytes, constituting a minority fraction of the total blood volume. Within the bone marrow, megakaryocytes undergo a fragmentation process which results in the release of thousands of platelets per cell, controlled by the hormone thrombopoietin. Platelets contain no nucleus, and are commonly not classed as true cells, but merely fragments of cells within circulation. Their main role within the human body is focused around wound repair to prevent continuous bleeding when tissue is damaged.

Damaged endothelium results in the exposure of fibrous proteins such as collagen, allowing platelets to bind through glycoprotein surface receptors. Adhesion to the

endothelium wall is further strengthened through the release of Von Willebrand factor, from both platelets and the endothelium. Platelets are activated by the release of integrins into the circulating plasma, which results in alterations to their shape, structure and membrane-bound glycoproteins. Activation of intracellular enzymes and the recruitment of additional platelets are also processes which occur (Murphy *et al.*, 2008). In addition, the coagulation cascade is initiated, promoting the conversion of fibrinogen to fibrin; crucial for blood clotting. Together with platelets, a clot or thrombus will eventually form (providing the damage is not too severe), and prevent the host from bleeding to death (Alberts, *et al.*, 2014; Berg *et al*., 2011; Wood, 2006).

1.3.6 Antibodies

Antibodies, also known as immunoglobulins, are glycoproteins of the immune system which are involved in the identification and elimination of foreign pathogens from the human body. Bacteria, fungi and other harmful invading organisms are eliminated through processes such as agglutination, neutralisation or precipitation. These integral members of the adaptive immune system can be located either bound to the surface of B cells, ready to bind and interact with invading pathogens, or circulating within the blood (Murphy *et al.*, 2008).

Antibody molecules are roughly 'Y-shaped', composed of four polypeptide chains. Each 'Y'; contains two identical 'light' chains, and two identical 'heavy' chains. Held together by disulfide bonds, they both differ in their sequence and length, with a hinge region within the middle of the 'Y' promoting flexibility upon binding. The light chains can be classified as either κ or λ based on differences in their primary protein sequence. It is the composition of the heavy chain however, which determines the overall class of the antibody. Antibodies can be categorised into five main isotypes based on the number of 'Y' units and

the type of heavy chain: IgG, IgM, IgA, IgD and IgE. Each isotype differs in their biological properties and their functional ability when dealing with foreign antigens (Murphy *et al.*, 2008).

The 'Y' shape of antibodies can be divided into three sections: two Fab regions and one Fc region. The F(ab) regions contain variable domains and are located at the apex of the 'Y' shape. It is this region which recognises and binds specific antigen sequences which simulated their initial production. The Fc region provides a binding site for endogenous Fc receptors on the surface of lymphocytes. The region is also the site for the binding of secondary (usually non-specific) antibodies. Dyes and enzymes can be covalently bound to the Fc region of antibodies for visualisation of specific proteins/antigens, a technique commonly used in clinical assays (Alberts, *et al.*, 2014; Berg *et al*., 2011; Wood, 2006).

1.4 Human C-reactive Protein

1.4.1 Overview of C-reactive Protein

CRP was discovered by Tillett & Francis in the 1930's in the sera of patients with various infectious and inflammatory diseases. They discovered that mixing acute human sera from patients with pneumonia containing a fraction of the *pneumococcus* bacteria (fraction 'C'), would result in the precipitation of the C-polysaccharide (CPS) that is expressed on the cell wall surface of the *Streptococcus pneumoniae* (McCarthy, 1982; Pepys & Hirschfield, 2003; Tillett & Francis, 1930; Volanakis & Kaplan, 1971). Subsequently Abernethy & Avery characterised this protein and identified the protein's need for calcium ions to interact with CPS (Abernethy & Avery, 1940). They and others went on to establish that the appearance of CRP within serum is the result of a non-specific reaction in response to infection, inflammation and tissue damage (Abernathy & Avery, 1940; Ash, 1933; Baltz *et al.*, 1982; Tillett & Francis, 1930). CRP was the first acute-phase protein to be described and

subsequently the term; ‘acute phase protein’, was applied to many other plasma proteins, whereby their concentrations would rise in acute phase sera (Baltz *et al.,* 1982; Pepys & Hirschfield, 2003). Because of these findings, CRP is now routinely used as an extremely sensitive systemic marker of infection, inflammation or tissue damage (Gewurz *et al.,* 1982; Pepys & Hirschfield, 2003).

The acute-phase response comprises both nonspecific physiological and biochemical reactions in endothermic animals in response to most forms of tissue damage, infection and inflammation (Pepys & Hirschfield, 2003). Acute-phase proteins, such as CRP, are rapidly upregulated under these conditions, most commonly within hepatocytes, under the control of cytokines produced at the site of pathology. One acute phase protein which displays similar characteristics to CRP is Serum Amyloid-P component (SAP). SAP is a pentraxin serum protein, involved in the handling of chromatin and resistance to bacterial infection. It is also a universal constituent of amyloid deposits commonly observed in Alzheimer’s disease. The pentameric protein displays an ability to form decamers in the absence of calcium with two cyclic disk-like pentamers interacting face to face (Emsley *et al*., 1994; Hutchinson *et al.*, 2000).

CRP, alongside SAP, is an oligomeric, calcium binding protein which demonstrates high sequence homology with a family of proteins known as the pentraxins (Osmand *et al.*, 1977; Pepys & Hirschfield, 2003). Based on the primary structure of their subunit, the pentraxins can be divided into two groups: the short pentraxins and the long pentraxins. CRP and SAP are classed as short pentraxins which are produced in the liver, whereas PTX3 is an example of a long pentraxin. PTX3 is produced from both vascular and immune cells in response to pro-inflammatory stimuli, binding to ligands including growth factors, pathogens and complement proteins (Luchetti *et al*., 2000).

CRP and SAP show substantial homology of amino acid sequence and subunit composition and both proteins are characterised by their cyclic pentameric assembly of generally non-covalently associated subunits. CRP displays only one pentameric ring, whereas SAP exists in a pentameric form, but can also aggregate to form a decamer of two pentameric rings, which interact through their double-calcium ligand binding sites (Hohenester *et al.,* 1997). SAP is known to be present within amyloid deposits due to its calcium dependent binding to amyloid fibrils and like CRP, SAP serum levels rise during an acute phase response (Pepys *et al.*, 1978b).

1.4.2 Structure of Human C-reactive Protein

Human CRP displays a five-membered ring structure, all non-covalently bound around a central pore, with each subunit containing 206 amino acids folded into two antiparallel β-sheets with a flattened jellyroll topology (Shrive *et al.*, 1996). Each protomer contains two calcium ions, which help coordinate the binding of ligands, such as phosphocholine (PC), expressed on the surface of pathogens and dead or damaged cells, as shown in Figure 1.1 (Shrive *et al.*, 1996; Thompson *et al.*, 1999). CRP interprotomer contacts consists of three salt bridges; Glu101 – Lys201, Lys123 – Glu197 and Asp155 – Arg118 involving the 115 – 123 loop of one protomer and 40 – 42 and 197 – 202 on the adjoining loop. An effector face of CRP is located on the opposite side of the ligand binding face which contains a cleft-like region, situated around the middle of each protomer and extending to the central pore of the pentamer (Shrive *et al.*, 1996; Thompson *et al.*, 1999).

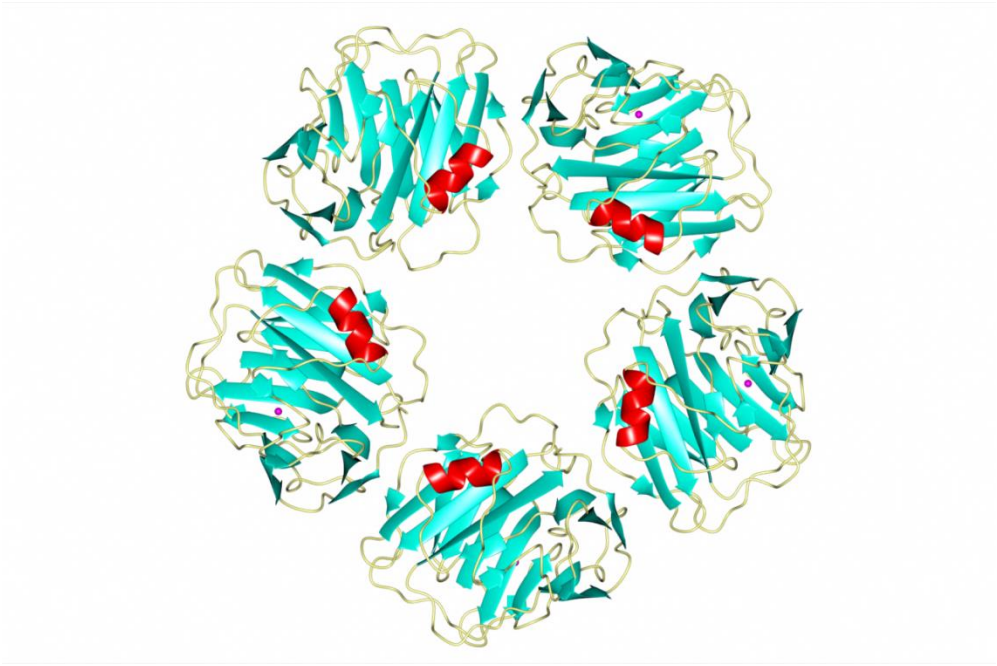

Figure 1.1 The three-dimensional structure of pentameric C-reactive protein. The α-helix is displayed in red, with the β-sheets displayed in turquoise. Calcium ions bound to each protomer are displayed as purple spheres. CRP contains five protomers, all non-covalently bound, arranged around a central pore. Levels of this acute phase protein rise rapidly in response to infection, inflammation or injury. Image of 1GNH (Shrive *et al*., 1997) created with CCP4mg (McNicholas *et al*., 2011).

1.4.3 Ligands of C-reactive Protein

The pentraxin family of proteins are mainly characterised by their five identical subunits and their calcium dependent interaction with phosphate-containing ligands, such as phosphocholine and phosphoethanolamine (PE) (Schwalbe *et al*., 1992). CRP has been documented to interact with a wide range of autologous and extrinsic ligands in a calcium dependent manner. Modified plasma lipoproteins, small ribonucleoprotein particles and apoptotic cells within the human body have all been shown to interact with CRP. Foreign pathogens to the human body, including parasites, fungi, bacteria and microorganisms present ligands such as PE and various glycans to which CRP will bind to elicit an immune response (Clos, 1989; Gershov *et al.,* 2000; Pepys & Hirschfield, Volanakis & Narkates; 1981). The main principal ligand for CRP is PC which can be found in teichoic acids,

capsular carbohydrates and lipopolysaccharides of bacteria, galactan polysaccharides, the polar head group of phospholipids and microorganisms such as *Streptococcus pneumoniae* (Narkates & Volanakis, 1982; Gotschlich, 1982).

PC is a major constituent of cell membranes from both prokaryotic and eukaryotic cells. In normal, healthy eukaryotic cells within the human body, PC is inaccessible, as the PC unit is usually part of a larger structure such as phosphatidylcholine. Any damage to these cell membranes results in the cleavage of phospholipids by the enzyme phospholipase A2, which exposes PC and enables CRP to distinguish between damaged and healthy cells (Hack *et al.*, 1997; Narkates & Volanakis, 1982). The PC unit to which CRP binds contains a choline group alongside a phosphate atom, which is double bonded to one oxygen atom and two hydroxyl groups, as shown in Figure 1.2.

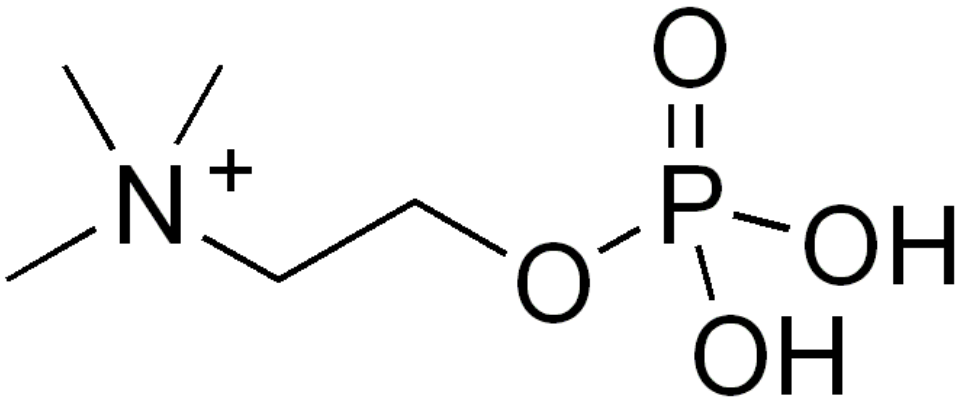

Figure 1.2. The chemical structure of phosphocholine. PC is CRP's main ligand and a major constituent in most cell membranes. PC is expressed on the surface of dead or dying cells, which allows CRP to distinguish them between healthy cells.

PC units to which CRP will bind on the surface of bacteria are usually bound to larger structures, such as the C-polysaccharide present on *Streptococcus pneumoniae*. Since the first description of 'fraction C' of the *pneumococcus* by Tillett & Francis (1930), structural studies have shown C-polysaccharide to be a teichoic acid, comprising repeating units of ribitol phosphate, *N*-acetylgalactosamine, *N*-acetyldiaminotrideoxyhexose, choline phosphate and glucose residues. Teichoic acids are gram-positive (contain a thick layer of

peptidoglycan within their cell wall) bacterial co-polymers of either glycerol phosphate or ribitol phosphate and carbohydrates, linked via phosphodiester bonds. The results showed that these repeating units can display molecular weights from 65,000Da to over 200,000Da. Furthermore, it was noted that all fractions analysed contained the same hexosamine and amino acid components but in markedly different proportions (Gotshclich & Liu, 1966; Poxton *et al*., 1978). Chemical composition analysis had previously established C-polysaccharide to originate from the bacterial cell wall, with the molecule containing four main amino acids (lysine, serine, glutamic acid and alanine) and four main sugars (D-glucosamine, D-galactosamine 6-phosphate, muramic acid and muramic acid phosphate) (Liu & Gotschlich, 1963).

1.4.4 The Calcium Binding Site

There are two calcium ions located within each of the five subunits of CRP (Shrive *et al.,* 1996). Both calcium ions are crucial in both the stability of the protein and the interaction between CRP and its ligands. The absence of calcium induces conformational changes within the protein. Residues 140-150 form a large loop away from the body of the molecule, exposing hidden sites which are susceptible to proteolysis (Ramadan *et al*., 2002). The first calcium ion is coordinated by Asp60, which presents an acidic oxygen, along with residues Asn61, Glu138, Asp140 and the main chain carbonyl of Gln139 (Shrive *et al.,* 1996; Thompson *et al.,* 1999). The second calcium ion is bound to residues Gln138, Asp140, Gln150 and Glu147. Glutamic acid-147 extends sufficiently so it can close the pocket when the addition calcium is bound (Shrive *et al.,* 1996).

1.4.5 The Phosphocholine Binding Site

The binding of PC is mediated by a phosphate-calcium interaction at the calcium binding site. The two calcium ions, displayed as red spheres in Figure 1.3, interact with two

oxygen atoms of PC, positioning the third oxygen towards the solvent, allowing PC to form an ester linkage with other, larger molecules within the vicinity.

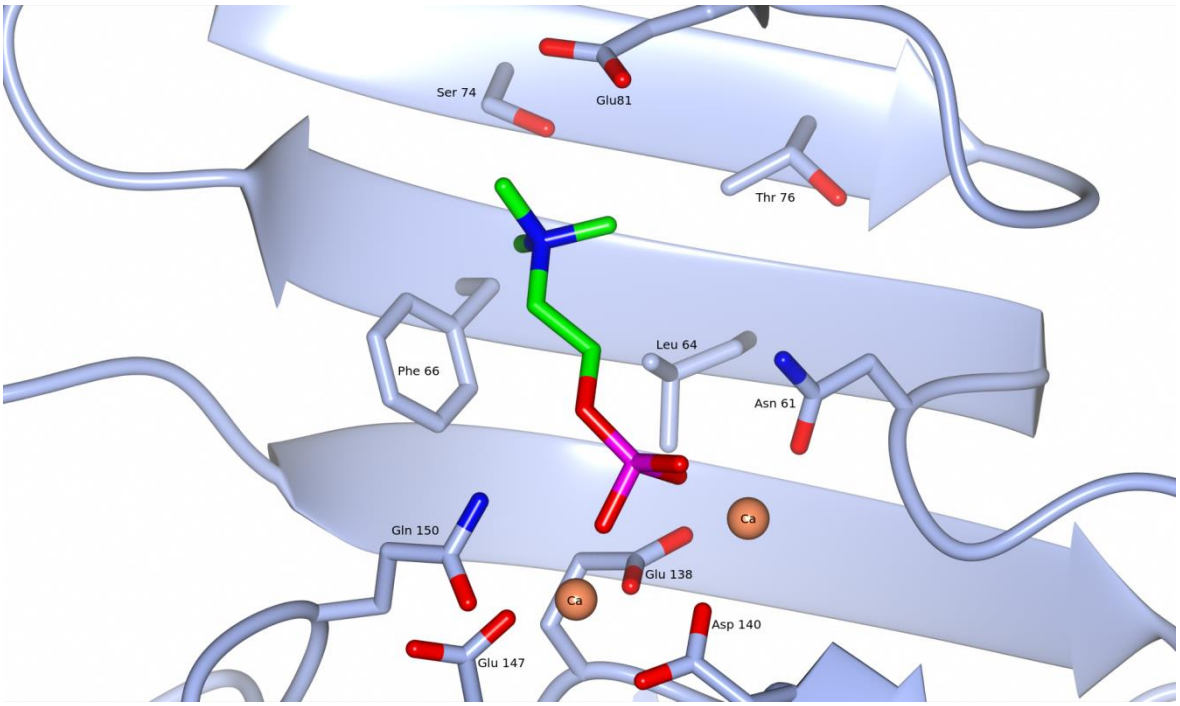

Figure 1.3 A stick model of PC interacting with CRP which is coordinated by two calcium ions. The nitrogen in the choline moiety is displayed in blue with carbon atoms displayed as green. The phosphate is displayed in pink, with oxygen atoms coloured red. The two calcium ions are displayed as maroon spheres. Image of 1B09 (Thompson *et al*., 1999) created with CCP4mg (McNicholas *et al*., 2011).

The choline moiety is then extended away from the calcium binding site and runs along the surface of the CRP molecule where the side chains from Phe66, Thr76 and Leu64 in CRP (see figure 1.3) form a large hydrophobic pocket (Shrive *et al.,* 1996; Thompson *et al.,* 1999). Hydrophobic interactions occur between three choline methyl groups and the exposed face of Phe66 and Glu81, as shown in in figure 1.3. The aromatic face of Phe66 is shifted away from the calcium site and exposed in an ideal position for the hydrophobic interaction with the tertiary methyl groups of the choline moiety (Agrawal, 2004; Thompson *et al.,* 1999).

1.4.6 The Effector Face

The effector face of CRP is located on the opposite site of the ligand binding face. A cleft-like region is situated around the middle of each protomer and extends to the central pore of the pentamer (Shrive *et al.*, 1996). A long α-helix, from residues 168 – 176 lies folded against one of the two β-sheets. The carboxyl terminal end of the helix, including the loop from residues 177 – 182, form one of the two sides of the cleft that extend from about the centre of the protomer, to its edge and the central pore of the pentamer (Shrive *et al.*, 1996; Thompson *et al.*, 1999). The opposite side of the cleft is formed by the amino and carboxyl termini of the protomer, giving a deep and narrow origin, but becoming shallower towards the pore of the pentamer, with residues His38, His95 and Trp205 protrude from the cleft floor (Thompson *et al*., 1999). The outer part of the cleft is positively charged with inner parts of the cleft halfway through, such as Asp112, providing a ring of negative charges lining the pore (Volanakis *et al.*, 2001).

It is suggested that this region is where CRP interacts with the complement protein C1q to activate, in a PC dependent manner, the classical complement pathway (Agrawal *et al.*, 2001; Kaplan & Volanakis, 1974; Shrive *et al*., 1996; Thompson *et al.*, 1999; Volanakis, 1982).

1.4.7 Levels of C-reactive Protein

In normal, healthy individuals, baseline levels of CRP range from 1-3mg/L (Pepys & Hirschfield, 2003). There are some associations which have been suggested between the production of CRP and genetic polymorphisms in IL-1 and Il-6, whereby an individual's CRP baseline level is raised (>3mg/L). Furthermore, a polymorphic GT repeat in the intron on the CRP gene is reportedly associated with the differences in the baseline of CRP concentrations in normal individuals (Berger *et al*., 2002; Pepys & Hirschfield, 2003; Vickers *et al*., 2002). Clearance of human CRP from the blood depends on its half-life;

calculated to be at 19 hours, and is constant, regardless of synthesis rate and severity of disease (Pepys & Hirschfield, 2003). Raised baseline levels of CRP have also been linked as an indicator for the development of disease and will be discussed in further sections.

1.4.8 C-reactive Protein as a Clinical Biomarker

During infection and inflammation within the human body, CRP levels will rise acutely to elicit a sufficient immune response. Interleukin 6, 1 and transforming growth factor-β are responsible for the rise in plasma levels of the acute phase protein, due to the accelerated transcription of their genes within the liver (Mackiewicz *et al.,* 1990). The general baseline level of CRP in a healthy patient's serum is around 1-2mg/L. This can increase up to 100-fold within 24-72 hours of infection or inflammation. It is due to this rapid increase in serum levels that CRP is routinely used as a clinical biomarker for injury, infection and inflammation (Pepys & Baltz, 1983; Shine *et al.,* 1981). The plasma half-life of CRP is about 19 hours and is constant under all conditions of health and disease, meaning the sole determinant of circulating pCRP is the synthesis rate, which directly reflects that intensity of pathological processes stimulating the pCRP production (Pepys & Hirschfield, 2003).

In a clinical setting, the most common technique to obtain a fast analysis of CRP levels is through automated laboratory analysis. Machines which incorporate the Enzyme-linked Immunosorbent Assay (ELISA) concept of antigen to antibody complexes can determine CRP concentrations within a sample. This is due to their ease of use, sensitivity to the assay, biochemical stability and result in international standards and inter-assay prevision. Unfortunately, these are limited to detecting elevated concentrations of CRP (Algarra *et al.,* 2013). There are several analytical methods which have been developed for the measurement of CRP levels within the blood. These tests vary in their use, with some

measuring more sensitive changes in lower CRP levels, compared to those which detect in larger rises; indicating an infection of the body. These clinical tests utilise methods such as; immunoturbidimetry, immunosorbent assays, surface plasmon resonance, chemiluminescence, impedimetry, beads, reflectometric interference spectroscopy, electrochemistry and microfluids (Choi *et al.,* 2012; Bryan *et al.,* 2013; Deegan *et al.,* 2003; Islam & Kang, 2011; Kim *et al.,* 2008; Kjelgaard-Hansen *et al.,* 2007; Lee *et al.,* 2011; Punyadeera *et al.,* 2011; Vashist *et al.,* 2014; Vashist *et al.,* 2015; Vermeeren *et al.,* 2011). These highly sensitive methods for measuring CRP levels are nephelometric assays (light scattering assays). Light scattered from antigen-antibody complexes is measured based on the principle that higher concentrations of antigen result in an increase in the scattered light. This highly sensitive method is used for measuring lower levels of CRP (<3mg/L) and to assess the risk of developing diseases such as cardiovascular disease in an apparently healthy population, which is further discussed in section 1.8.3 (Koivunen & Krogsrud, 2006; Rifai *et al.,* 2006).

1.5 Genetics of C-reactive Protein

1.5.1 Production of C-reactive Protein

The degree to which an amino acid mutates within a protein sequence depends largely on its structural and functional importance. Amino acids involved in maintaining the structural integrity of the protein, or crucial to the proteins overall function, are unlikely to change over time (Mayrose *et al*., 2004). The evolutionary rate of an amino acid is therefore indicative of how conserved that site is, allowing evaluation of that amino acid, or sequence within the protein (Mayrose *et al*., 2004). Analogues of the same protein can be traced through various species, with the conservation of specific amino acids and/or sequences highlighting areas important in functionality. Furthermore, it can highlight residues which

may endure change throughout evolution, whilst resisting a change in the proteins overall structure and function (Mayrose *et al*., 2004). Proteins which show a high percentage of homogeneity through a wide range of species, even down to the most primitive of animals, suggests a crucial importance in not only specific regions in their amino acid sequence, but their contribution to the organism's survival.

The gene sequence for human CRP is located on chromosome 1 (Whitehead *et al*., 1983). Regulators of the gene are located 1 kilo base (KB) upstream, with two inducible elements located closer to the site of transcription (Li *et al*., 1990). There are also two enhancer-line elements located distal to the protomer, with a negative regulatory region located between the two (Li *et al*., 1990). The primary translation product is larger than native serum CRP by an 18-amino acid terminal extension, which forms the signal peptide (Tucci *et al*., 1983). Sequence analysis indicates that after the signal peptides lies two amino acids of the mature, serum protein, followed by an intron of 278 base pairs, with the remaining 204 amino acids following that (Lei *et al*., 1985). The CRP gene displays a typical protomer which contains the sequences TATAAAT (TATA) and CATT box 29 and 81 nucleotides upstream. The mRNA cap site is located 104 nucleotides from the start of the signal peptide with a 3' polyadenylated noncoding region (AATAAA), 1.2 kilo base pairs in length and the 5' non-coding region at 0.1kilo base pairs (Lei *et al*., 1985)

Once transcription has occurred, the individual 206 amino acid protomers are assembled into their pentameric, quaternary structure within the endoplasmic reticulum of hepatocytes (Yue *et al*., 1996). Here the CRP protein can be stored until needed through an interaction with two carboxylesterases (gp60a and gp60b), which themselves are restricted to the endoplasmic reticulum (ER). During an acute phase response within the body, the synthesis of CRP within hepatocytes is dramatically increased, coupled with a decrease in the retention of the protein within the ER (Yue *et al*., 1996). To help fight off infection, the

acute phase response must be extremely fast and efficient. Ciliberto *et al* (1987) demonstrated that levels of CRP RNA are detectable, within hepatocytes, 2 hours after stimulation, with mature protein being detected after only just 6 hours. Furthermore, larger, intense and prolonged periods of an acute phase stimulus, results in the production of higher levels of CRP, among other proteins, to aid the body's defences (Ciliberto *et al*., 1987).

1.5.2 Induction of the C-reactive Protein Gene

The acute phase response is a normal, physiological reaction to tissue injury or infection and is therefore a fundamental aspect of many disease processes. During this response, in addition to protein synthesis upregulation, pre-formed proteins are released to limit damage and promote cellular repair or apoptosis (Pepys & Baltz, 1983). All hepatic cells within the liver are thought to be capable of synthesising acute phase proteins simultaneously, in response to infection or inflammation. However, the location of hepatic cells producing the acute phase proteins depends on the timescale of the acute response. At early periods of the inflammatory reaction, cells synthesising acute phase proteins were detected in the periportal zone, but later (24 hours), synthesising cells were detected principally in the hepatic lobule (Courtoy *et al*., 1981).

The primary inducer of the CRP gene was initially hypothesised to be IL-1, although since then, several other hormones, known to be involved within the acute phase response have also been linked. These include IL-6, interferon-γ, tumour necrosis factor α (TNFα) and transforming growth factor β (Pied *et al*., 1989; Steel & Whitehead, 1994). Despite IL-1 having a large role in the induction of the inflammatory response, experimental research by Ganapathi *et al.,* (1991) has shown that on its own, the hormone is unable induce the production of certain acute phase proteins, including CRP. Furthermore, they demonstrated that the induction of CRP required more than one inducer to be present; larger levels of IL-

1 with even lower levels of IL-6 were required (Ganapathi *et al*., 1991). Since this study, additional experimental research has established that IL-6 is the major inducer of the CRP gene, with IL-1 and other compounds acting as synergists (Li *et* al., 1996; Mackiewicz *et al*., 1990; Szalai *et al*., 2000).

1.6 Human C-reactive Protein within Additional Species

1.6.1 Mammalian C-reactive Protein

CRP is a physiologically highly conserved protein, which can be found within a variety of species across the animal kingdom. Mammalian species in which CRP has been confirmed include; monkey, rat, dog, cat, horse, goat, cow, rabbit and sheep (Mitra & Bhattacharya, 1992). Throughout these species, there are several consistencies in CRP's structure, amino acid composition and role within the host. The most common between all CRP analogues, is a primary role within the host's innate immune system, through binding to phosphocholine-containing ligands, in a calcium dependent manner (Baltz *et al*., 1982). CRP levels will rise rapidly during the acute phase response in all CRP-containing species (Schwalbe *et al*., 1992). CRP serum levels in mammals are known to differ slightly, with concentrations in healthy rats ranging from 300-600ug/ml – much greater than in other species (de Beer *et al*., 1982a). Levels in rat sera will increase about 2-3-fold during their acute phase response, therefore rat CRP being described as a minor acute phase protein (Schwalbe *et al*., 1992). Most mammalian CRP molecules display five identical subunits, all non-covalently formed around a central pore (de Beer *et al*., 1982a).

The high percentage of sequence homology observed for CRP throughout various species is a testament to the protein's resilience to evolutionary change. This similarity between protein sequences is displayed in Figure 1.4, whereby four other CRP sequences are compared against that of the human sequence. Residue Phe66 aids in the formation of

the hydrophobic pocket to which phosphocholine binds. Furthermore, Glu81 is crucial in interaction with the choline group upon binding. These ligand binding regions are highlighted within Figure 1.4 to display their homology between the various species. Similarity is also observed in the amino acids which are known to bind calcium; Glu138, Asp140 and Gln150 (Shrive *et al*., 1996).

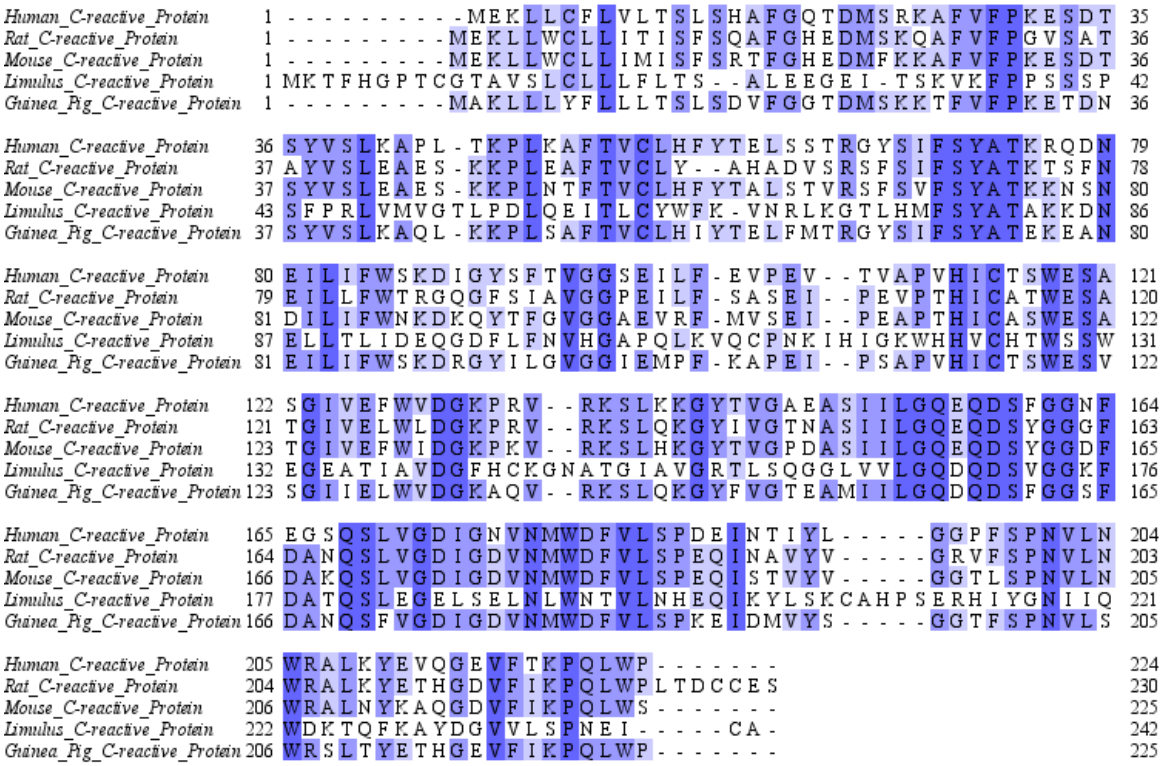

Figure 1.4 A comparison of CRP sequences from several different species to highlight the high percentage of sequence homology. Areas which are shaded dark blue display identical amino acids for all five species. The lighter shades of blue indicate identical amino acids for four out of the five species. The sequence comparison was obtained from http://www.uniprot.org/.

Rabbit CRP, like humans also retains the ability to bind PC in a calcium dependent manner (Syin *et al*., 1986). Its half-life is much shorter than human CRP, at approximately five hours, and is can be located within areas of localised inflammation and necrosis (Kushner & Kaplan, 1961). CRP subunit composition does differ slightly throughout species, mice CRP subunits are roughly 25-27kDa in size, compared to human CRP at

roughly 22-23kDa. Interestingly, dissimilar to most mammals, the major acute phase protein in mice is SAP and not CRP, despite the fact it contains both (Schwalbe *et al*., 1992).

1.6.2 C-reactive Protein within Fish

Homologues of CRP have been detected in fish species including Plaice (*Pleuronectes platessa* L.), the Common Carp (*Cyprinus carpio)*, Snapper Fish (*Pagrus auratus*, S.) and Rainbow Trout (*Oncorhynchus mykiss)*. The CRP analogues within plaice, alongside other fish species, share substantial homology in amino acid sequence, similar subunit composition, and a similar molecular appearance when observed through an electron microscope when compared to human CRP (Pepys *et al*., 1978a; Pepys *et al*., 1982). Although, plaice CRP differs from human CRP in that it contains subunits of two different molecular weights, as one is glycosylated (Baltz *et al*., 1982). Fish pentraxins, like those identified within other species can bind to phosphocholine, displayed on the surface of bacterial cell walls, in a calcium dependent manner (Cartwright *et al*., 2004). Currently, there is rather limited information regarding the *in vivo* function of pentraxin-like molecules within fish, although studies have established their ability in both complement activation and opsonisation of particles (Cook *et al*., 2005; Nakanishi *et al*., 1999)

1.6.3 *Limulus* C-reactive Protein

The Atlantic horseshoe crab, *Limulus polyphemus*, is one of the oldest surviving multicellular organisms on the planet, being over 500 million years old in existence (Enghild *et al*., 1990). In *Limulus*, CRP and SAP have been identified and described as an important component of the innate immune response and host defence (Armstrong, 1996; Pepys *et al*., 1978a; Robey & Liu, 1981). The molecular mass of *Limulus* CRP was first estimated to be approximately 300kDa, with each subunit around 22.5kDa. The subunits are arranged in cyclic pentameric symmetry and amino acid sequence homology with a range of species

(Nguyen *et* al., 1986; Tennent *et* al., 1993) Experimental evidence has reported several different forms of *Limulus* CRP with numerous genes (Nguyen *et al*., 1986). These genes give rise to three different subunit types, which are identical in N- and C- termini.

Unlike human CRP, *Limulus* CRP has been documented to be a glycosylated protein, with an N-linked oligosaccharide on each subunit. The structure of this oligosaccharide is unknown, but several different structures have been suggested (Amatayakul-Chantler *et al*., 1993). At the glycosylation site of Asn123, the cysteine residues involved in the formation of disulfide bridges appear to be the same in all *Limulus* CRP genes. Furthermore, these disulfide bridges are still present within human CRP, SAP and rabbit CRP (Nguyen *et al*., 1986). All forms of *Limulus* CRP display the ability to bind to PC in a calcium dependent manner. PC-binding sites display homology with that of the human CRP binding site, with ten out of sixteen residues identical. Furthermore, nine out of fifteen residues are also conserved in the calcium binding site. Sequence comparison of both *Limulus* and human CRP revealed a 25% identity, although *Limulus* does not contain the intron between the signal peptide and mature protein like human CRP (Nguyen *et al*., 1986).

1.7 Interaction of C-reactive Protein with Components of the Immune System

1.7.1 Macrophages and Monocytes

Alongside the activation of the inflammatory response, through the binding of dead or damaged cells, CRP plays a role in the recruitment and modulation of several other immune components within the human body. During the inflammatory response, levels of monocytes rise rapidly, which mature into macrophages at the site of infection or inflammation. It has been hypothesised that CRP can play a role in the recruitment, maturation and regulation of macrophages; although there is a debate among researchers as

to which cellular receptors are involved in these interactions (Tron *et al*., 2008). The maturation of monocytes has been shown to be susceptible to CRP-dependent inhibition, through binding to Fc receptors on their cellular surface. Although this can be inhibited via IgG, which further supports the theory of CRP binding via Fc receptors. Furthermore, CRP is known to be a negative regulator of macrophage activation, via binding to lymphocyte-derived apoptotic DNA (Mortensen *et al*., 1982; Zhang *et al*., 2011).

Flow cytometry studies involving monocytes has established the presence of CRP-binding receptors on their surface. The study by Ballou & Cleveland, demonstrated that there is specific low-affinity binding of CRP to phagocytic cells, which occurs in a calcium dependent manner (Ballou & Cleveland, 1990). As early as 1977, it was reported that CRP interacts with Fcγ receptors. This was however, later disputed, due to inconsistencies within experimental research involving inhibition of binding CRP to Fc receptors by use of antibodies, and the inability of CRP receptor modulation to inhibit IgG binding to monocytes (Gewurz *et al*., 1982; Mortensen & Duszkiewicz, 1977). Although it is not certain which receptors are involved within these interactions. The primary contenders which have been proposed are various subclasses of Fcγ-receptors known as FcγRI and FcγRIIa, which are expressed on the surface of various haematopoietic cells. FcγR contain tyrosine-based motifs, which are activated through clustering on the cellular surface, caused by ligand binding (Marnell *et al.*, 2005; Tron *et al*., 2008). These receptors function through the recognition of the Fc portion of IgG and provide a link between the humoral and cellular responses. The binding of CRP to these FcγR is proposed to have a similar effect to that seen with IgG.

CRP is thought to share several functional activities with IgG in relation to interactions with macrophage cells. These include; complement activation, opsonisation, cytokine secretion for the recruitment of additional immune cells, facilitation of

phagocytosis of CPS-coated cells, and the induction of the release of tissue factor, a potent pro-coagulant within the body (Cermak *et* al., 1993; Mortensen & Duszkiewicz, 1977; Stein *et al*., 2000; Torzewski *et al*., 2000; Zhang *et al*., 2011). The cytokine response to CRP is like that observed for IgG and includes the production of IL-1β, IL-6 and TNF-α (Gewurz *et al*., 1982). These immunological responses highlight not only a role of complement activation and promotion of the inflammatory response, but a more regulatory role with other immune components. The role of monocytes and macrophages in the immune response is typically known for their recruitment of further immune cells and phagocytosis of harmful pathogens within the body. The functional relationship between these two immune cells and CRP highlighted here demonstrates one of regulation and synergistic actions, when initiating the acute phase response.

1.7.2 Lymphocytes

The interaction between CRP and lymphocytes was first suggested by Abernathy & Francis in 1937 (Abernathy & Francis, 1937). Early investigations of CRP interactions with cells showed that the binding of CRP to immune cells, such as lymphocytes, could be readily inhibited by IgG, thus suggesting a CRP-type receptor, like that seen with Fc receptors. Eventually, these findings were disregarded, with interactions now thought to occur through certain Fc receptors, like that observed with monocytes and macrophages (Gewurz *et al*., 1982). CRP has been found to bind human T lymphocytes, and inhibit their functions, preventing T cell proliferation. Mortensen & Gewurz found that this CRP-induced inhibition was prevented by the addition of CPS (Mortensen & Gewurz, 1976). This thus suggests CRP may exert a regulatory effect of cellular immune responsiveness during inflammatory reactions (Mortensen & Gewurz, 1976). CRP has also been shown to selectively bind to T lymphocytes, inhibiting their ability to form spontaneous rosettes with sheep erythrocytes and their response to allogenic cells in mixed lymphocyte reactions. In contrast with these

results, CRP was not shown to bind B lymphocytes, and does not alter B cell functions such as binding and activation of complement components (Mortensen *et al*., 1975).

More recent experimental research has revealed that CRP can bind specifically to Jurkat T cells and to mouse naïve cells, modulating their activity during an immune response (Zhang *et al*., 2015). Furthermore, CRP inhibited differentiation of the T helper 1 cells, whilst augmenting the differentiation of the T helper 2 cells, derived from native CD4+ T cells. These results additionally portray CRP acting as a tonic regulator of the immune system (Zhang *et al*., 2015). CRP, alongside complexes of CRP with CPS increases lymphocyte toxicity in addition to enhancing the mixed lymphocyte culture reaction (Vetter *et al*., 1983). Furthermore, low levels of CRP have been shown to increase lymphocyte blastogenesis, thus increasing their numbers within serum (Hornung, 1972), as well as stimulating lymphocytes to destroy myeloma cells. Patients also suffering with diseases such as rheumatic fever are thought to promote the interactions between CRP and lymphocytes, to elicit a greater immune response (Hornung, 1972; Williams *et al*., 1978).

1.7.3 Platelets

During an immune response, inflammation at sites throughout the body will cause a rise in the level of circulating platelets (Crosby, 1971; Skoglund *et al*., 2008). Their primary role is clotting of the blood and wound repair, through activation of the coagulation cascade (Sato *et al*., 2014). Dysregulation of lipids can exacerbate the physiological events that are commonly observed in numerous inflammatory diseases. Platelet activating factor (PAF) is involved in the activation of platelets, thrombotic cascades and triggering inflammation (Sato *et al*., 2014). PAF is specifically enhanced, upon binding with CRP, which results in platelet activation & degranulation, dysregulation of and the inflammatory response and the recruitment and mediation of various leukocytes (Sato *et al*., 2014). Further to this,

experimental evidence demonstrates CRP enhancing the aggregation between monocytes and platelets during an immune response. Mediated through cell adhesion molecule P-selectin (among others), these findings suggest a more pro-inflammatory role for CRP (Danenberg *et al*., 2007). In contrast to these results, Skoglund *et al.,* conclude that CRP, in conjunction with the complement protein C1q, provide an immunoregulatory role for platelets during inflammatory conditions through the reduction of thromboxane B2, a lipid known to induce platelet aggregation. Although it is worth noting, CRP alone had no regulatory effect on the platelets, and required the presence of C1q (Skoglund *et al*., 2008).

1.7.4 Tissue Factor

Tissue factor (TF) is a transmembrane protein receptor for Factor VII/VIIa, which is commonly expressed in fibroblasts, monocytes and the sub-endothelial tissue layer (Cermak *et al*., 1993). One of TF main roles within the human body is the conversion of thrombin to prothrombin, initiating the coagulation cascade. The interaction between smooth muscle cells and endothelial cells with CRP, via FcγRIIIa receptors, has been documented to promote proliferation and TF expression, whilst decreasing the tissue factor pathway inhibitor protein (Cirillo *et al.*, 2005; Wu *et al*., 2008). CRP also induces the production and activity of TF on the surface of peripheral blood monocytes, although these results have been contested (Cermak *et al*., 1993; Paffen *et al*., 2004). Cermak *et al.,* proposed that CRP may be contributing towards the development and dissemination of intravascular coagulation and thrombosis at inflammatory sites throughout the body; although this is not conclusive (Cermak *et al*., 1993).

1.7.5 High and Low Density Lipoproteins

Lipoproteins are a soluble group of proteins that are bound to fat or lipids within the blood plasma. The main role of these proteins is to emulsify the lipid molecules to enable them to be transported around the body (Fredrickson *et al*., 1967). Common examples of lipoproteins include low density lipoproteins (LDL), very LDL (VLDL) and high density lipoproteins (HDL) (Fredrickson *et al*., 1967; Pepys & Hirschfield, 2003). CRP has been specifically shown to bind LDL and traces of VLDL when aggregated on a solid phase at a sufficient density, alongside damaged cell membranes which display these epitopes (de Beer *et al*., 1982b; Pepys *et al*., 1985). The form in which these lipoproteins must be present has been reported to be crucial though (Chang *et al*., 2002). Chang *et al.* demonstrated that CRP binds to oxidised LDL and oxidised phosphatidylcholine, but does not bind their non-oxidised native forms. With binding mediated through the available PC head group, they hypothesise that PC becomes accessible upon oxidation (Chang *et al*., 2002), thus suggesting that oxidised LDL may potentially impose a pro-inflammatory stimulus upon the body. Further to this, enzymatically degraded products of LDL can activate the complement pathway in conjunction with CRP, with the degraded product being reported to have been found within atherosclerotic lesions (Bhakdi *et al.*, 1999). Interactions between CRP and HDL display an alternative role within the immune system, with HDL being shown to neutralise the pro-inflammatory actions of CRP. HDL also demonstrated an ability to prevent CRP-induced upregulation of cell adhesion molecules and cytokine-induced expression from of endothelial cells, a common phenotype observed in atherosclerosis and other inflammatory diseases (McGrowder *et al.,* 2010; Pepys & Hirschfield, 2003; Pepys *et al*., 1985).

1.8 C-reactive Protein and Cardiovascular Disease

1.8.1 Overview of Cardiovascular Disease

Cardiovascular disease is one of the leading causes of death and illness in developed countries, causing world-wide health problems and severe pressure for the funding and capacity of national health services (Libby, 2002). Atherosclerosis is one of the main factors which contribute towards cardiovascular disease, distinguishable by the formation of lesions in larger arteries throughout the body, characterised by inflammation, lipid accumulation, cell death and fibrosis (Hansson & Libby, 2006). Research that has been provided based on animal experiments and human specimens indicates a qualitative change in the monolayer of endothelial cells which line the inner arterial surface (Libby *et al.,* 2011; Ross, 1999). Over time, these lesions, also known as atherosclerotic plaques mature and eventually result in severe clinical events including plaque rupture resulting in thrombotic material being exposed to the blood. Atherosclerosis within the heart can further lead to myocardial infraction and heart failure, whereas rupturing arteries within the brain can lead to ischemic stroke (Hansson & Libby, 2006).

1.8.2 Atherosclerosis & Thrombosis Formation

Laboratory and clinical evidence has demonstrated that atherosclerosis is not a simple disease of lipid deposition as once thought, but rather a systemic inflammation which plays a significant role in atherothrombotic inception and progression. Cells such as mononuclear cells, macrophages and T lymphocytes are prominent in atheromatous plaques and within the arterial wall (Blake & Ridker, 2002; Rifai *et al.,* 2001). The accumulation of these immune cells within the lesions typically presents an asymmetrical focal thickening of the intima, the innermost layer of the artery (Jonasson *et al.,* 1986; Ross, 1999). The cells lining the artery are normally resistant to the attachment of white blood cells onto their walls.

When the artery walls are subject to an irritative stimulus, the expression of cell adhesion molecules are upregulated on their surface (Libby *et al.,* 2011). The endothelial-leukocyte cell adhesion molecule has been proposed to be one of the first to be upregulated upon irritation. Mononuclear leukocytes migrate through the arterial endothelium through binding to vascular cell adhesion molecule 1 (VCAM-1) (Cybulsky & Gimbrone, 1991; Jialal *et al.*, 2004; Libby, 2002). LDL can also diffuse from the blood into the innermost layer of the artery. The extracellular pool of enzymes and oxygen free radicals modifies the LDL to form oxidised forms. Constituents of modified lipoprotein particles, such as oxidised phospholipids, and short chain aldehydes arising from this oxidation reaction, can induce transcriptional activation of the VCAM-1 gene. Pro-inflammatory cytokines, such as IL-1β and TNF-α, released from immune cells, can also induce the expression of VCAM-1 in endothelial cells (Cybulsky & Gimbrone, 1991; Libby, 2002; Ross, 1999; Yudkin *et al.*, 2000).

Once monocytes have migrated through the endothelial cell layer into the arterial intima, they can differentiate into macrophages. These macrophages are capable of engulfing accumulating free lipoprotein particles, eventually differentiating into foam cells (Chang *et al*., 2002; Fredrickson *et al*., 1967; Tabas, 2010). Furthermore, these macrophages within the atheroma are induced to produce and release pro-inflammatory cytokines, intensifying the localised state of inflammation and resulting in the recruitment of further immune cells (Libby *et al.*, 2011). Additionally, smooth muscle cells (SMC) are recruited from the tunica media, the middle layer of the arterial cell wall. They are induced to proliferate in response to mediators such as platelet-derived growth factor, into the tunica intima. These SMC then produce extracellular matrix molecules, such as collagen and elastin, and form a fibrous cap which covers the plaque (Hansson & Libby, 2006; Yudkin *et al.,* 2000).

One of the first responses to vascular injury involves the adhesion of platelets to the damaged vessel wall, or to the exposed tissue components. This is mediated by flow-regulated interactions, which have a key influence on subsequent thrombus growth; often cumulating in life threatening situations (Molins *et al.,* 2008). Activation of endothelial cells plays an extremely important role in the development of atherosclerosis, and is accompanied by the up-regulation and exposure to cell adhesion molecules at the site of thrombosis or infarction. P-selectin, ICAM-1 and VCAM-1 are all strongly expressed on the endothelium overlying atherosclerotic plaques. Regulation of the VCAM-1 gene is thought to be coupled with the oxidative stress of endothelial cells, through specific reduction-oxidation sensitive transcriptional and post-transcriptional regulation (Mauri *et al.,* 1993). Vascular endothelial growth factor is responsible for the induction of adhesion molecules, and the adhesiveness of leukocytes within circulation (Kim *et al.,* 2001). Upon exposure to environmental signal such as cytokines, endothelial cells can undergo profound changes which allow them to participate within the inflammatory response (Mantovani *et al.,* 1992). This activation results in the release of IL-8 and MCP-1, production of reactive oxygen specific and upregulation of adhesion molecules; all which indirectly contribute to thrombus formation.

Circulating platelets play a significant role in the pathology commonly seen in atherosclerosis. Activated platelets secrete chemotactic substances (cytokines, chemokines) which facilitate the binding and transmigration of leukocytes across the endothelium layer through the upregulation of VCAM-1 (Coppinger *et al.,* 2004; Klinger, 1997). In addition, upon activation, P-selectin, a component of the platelet alpha granule membrane, is translocated to the platelet's surface and meditates the binding of various leukocytes; forming aggregates within circulation. This response observed from platelets is a primary event that occurs in arterial thrombosis. Platelet activation is a multistep process, initiated through an interaction between platelets and the adhesive molecules collagen and Von

Willebrand factor upon the surface of the sub-endothelial extracellular matrix (Chen, *et al.*, 2001; Ruggeri, 2002). This activation of platelets results in the production of high affinity integrins, thus promoting thrombus growth, and the development of atherosclerosis within the body (Nieswandt & Watson, 2003; Chen *et al.*, 2002).

This increased presence of activated immune cells within the plaque result in enzymes, such as proteases, being released within the local vicinity. These proteases attack the collagenous cap, resulting in a significantly weaker and unstable lining. This can lead to a severe cardiovascular event, known as thrombosis; the rupturing of the plaque from forces such as arterial blood pressure. Areas which usually rupture commonly have thin, collagen-poor fibrous caps, with few SMC, but abundance in macrophages (or foam cells). These immune cells present within the plaque, produce the enzymes which degrade the collagen, alongside producing coagulant tissue factor which renders the lipid core thrombogenic. This indirectly contributes to a severe thrombotic event, causing the plaque's contents to spill out into the lumen of the blood vessel, resulting in severe clinical complications, such as heart attack and stroke (Hansson and Libby, 2011; Rifai *et al.*, 2001; Yudkin *et al.*, 2000).

1.8.3 C-reactive Protein levels and Risk of Heart Disease

Traditionally levels of CRP are clinically measured to assess the level of infection, inflammation or tissue damage within the body (Pepys & Hirschfield, 2003; Zhang *et al*., 2012). Increasing experimental evidence suggests an alternative, pro-inflammatory role for native CRP in the progression of disease. Deposition of CRP within the arterial wall is a common pathological feature in early atherosclerotic lesions. Inflammatory mediators released as a direct result of CRP include; monocyte chemoattractant protein, ICAM, VCAM-1, tissue factor and the release of cytokines (Pasceri *et al*., 2000; Pasceri *et* a*l*., 2001; Pepys & Hirschfield, 2003; Torzewski *et al*., 1998; Zhang *et al*., 1999; Zhang *et al*., 2012).

Levels of IL-10, a major anti-inflammatory cytokine, are also decreased as a direct result of CRP; all pathological features common to atherosclerosis (Singh *et al*., 2006). This CRP-dependent response has been recorded in endothelial cells, vascular smooth muscle cells and macrophages. Fcγ receptors expressed on these immune and vascular cells, is thought to mediate this binding of CRP, which can also result in opsonisation of ligands and the release of prothrombic factors at localised sites of inflammation and aortic plaques (Pepys & Hirschfield, 2003; Zhang *et al*., 2012). Local CRP synthesis through macrophages and smooth muscle cells has been reported within these atherosclerotic plaques, due to the detection of mRNA for CRP. However, this has been contested, with doubt still existing on whether CRP within atherosclerotic lesions originates from circulation or is locally synthesised (Dong & Wright, 1996; Jabs *et al*., 2003).

As previously discussed, CRP is known to selectively bind to LDL and to a lesser extent, VLDL from whole serum. Additionally, native CRP binds to oxidised and partially degraded LDL, components commonly found within atheromatous plaques. Localisation of CRP within premature atherosclerotic plaques aids in the formation of foam cells *in vivo*, with cell culture experimental work supporting this (Bhakdi *et al*., 1999; Chang *et al*., 2002; Fredrickson *et al*., 1967; Pepys & Hirschfield, 2003; Zhang *et al*., 2012; Zwaka *et al*., 2001). Alternative to human CRP, experimental research with rat CRP demonstrates an inability to bind to damaged cells and activate the complement pathway. Rats which have also been subjected to middle cerebral artery occlusion, and then treated with human CRP developed significantly larger cerebral infarcts compared to the control cohort receiving serum albumin (Gill *et al*., 2004; Griselli *et al*., 1999). In contrast with previous results, a study carried out Khera *et al.*, recorded that subjects with higher CRP levels, had a modest increase in the prevalence of subclinical atherosclerosis, with their conclusions suggesting CRP is a poor predictor of an atherosclerotic burden (Khera *et al*., 2006). Collectively, these studies are

consistent with the current theory that CRP may exert a pro-atherogenic stimulus within the human body through the expression of cell adhesion molecules, release of inflammatory mediators and activation of complement (Zhang *et al*., 2012).

Therapeutic inhibition of CRP has been suggested to be a promising new approach to cardio-protection in acute myocardial infarction, per an experimental study headed by Pepys *et al* (2006). The administration of 1,6-bis(phosphocholine)-hexane to rats which were undergoing acute myocardial infarction, abrogates the increase in infarct size and cardiac dysfunction produced by the injection of human CRP (Pepys *et al*., 2006). They state that their rationally designed drug demonstrates that CRP inhibition is a valid therapeutic strategy, which is unlikely to result in adverse effects, and thus provides informative about the physiological and pathological roles of human CRP (Pepys *et al*., 2006). Currently, statins are a form of medication which is given to patients suffering with heart disease to reduce levels of CRP (Albert *et al*., 2001; Jialal *et al*., 2001; Ridker *et al*., 1999; Ridker *et al*., 2001). The administration of statins influences the status of an atherosclerotic plaque, as inflammation and CRP levels are reduced. Statins can also be used to reduce the levels of LDL-cholesterol in patients, as well as CRP. Patients who display generally lower levels of CRP consistently show a better response to statin treatment. Medication which is commonly used to reduce levels of CRP is pravastatin and simvastatin, which inhibit CRP production at the transcriptional level within hepatocytes (Ridker *et al*., 2005; Voleti & Agrawal, 2006).

To improve global cardiovascular risk prediction, considerable interest has focused on CRP which has been shown in multiple epidemiological studies to predict an incident of myocardial infarction, stroke, peripheral arterial disease or sudden cardiac death (Koenig *et al*., 1999; Ridker, 2001; Ridker, 2003; Tracy *et al*., 1997). The hypothesis that testing CRP may have prognostic usefulness for patients with acute myocardial infarction dates to the 1940's, when levels of CRP were observed to increase as part of the acute phase response

associated with ischemia (Ridker 2001). In terms of clinical application, the measurement of CRP levels is suggested to be a stronger predictor of cardiovascular events later in a patient's lifetime, than levels of LDL cholesterol. High-sensitivity CRP tests were developed to measure the desired levels of inflammation within a 'normal' range, as standard CRP assays lacked the required sensitivity, with a lower detection limit of 3-8mg/L (Danesh *et al*., 2000; Jialal *et al*., 2004; Ridker 2001). Table 1.1 highlights the general risk category patients are grouped in depending on their reading from a high sensitive CRP (hsCRP) test.

CRP Level (mg/L)	**Risk**
<1	Low
1-3	Moderate
>3	High

Table 1.1 Levels of CRP which determine the risk category patients are placed in depending on their reading from the hsCRP test. The risks define the general likelihood of developing a severe cardiovascular condition later in life.

It is worth noting that in clinical practice, results generated from a high sensitivity CRP measurement would not be used solely to define the patient's likelihood of developing a certain condition; these results would be assessed alongside a variety of other clinical tests. Individuals with cholesterol below 130mg/L who have CRP levels >3mg/L represent high-risk groups in clinical practice (Danesh *et al*., 2000; Jialal *et al*., 2004; Ridker 2003). This relationship between a patient's baseline level of CRP and future vascular risk has been consistent in studies from the United States and Europe. Compared to novel risk factors, such as the Framingham score, hsCRP is set to be the most promising. The Framingham risk score is a gender specific algorithm commonly used to estimate the 10-year cardiovascular risk of an individual. Cohort studies have confirmed that hsCRP evaluation adds prognostic information beyond this test (Danesh *et al*., 2000; Jialal *et al*., 2004; Ridker *et al*., 2004). CRP is not the only biomarker that can be used to predict cardiovascular events. More

sophisticated measurements of cytokine activity, cellular adhesion and immunologic function have all been shown to be elevated among those at increased vascular risk. These approaches, however are unlikely to have clinical utility because the assays required for their assessment are either inappropriate for routine clinical analysis, or the protein of interest has too short a half-life for clinical evaluation (Danesh *et al*., 2000; Jialal *et al*., 2004; Ridker, 2003).

Despite the accumulating evidence suggesting a pro-inflammatory role for native CRP in the progression of disease, there is a continuous debate as to whether CRP plays a causal role in the development of disease, or whether it is simply an important clinical marker of inflammation.

1.9 Monomeric C-reactive Protein

1.9.1 Overview of Monomeric C-reactive Protein

Pentameric C-reactive protein (pCRP) is extremely stable under physiological conditions. There are increasing reports which suggest a biological role for a monomeric form of CRP named monomeric CRP (mCRP) or membrane-bound CRP (mbCRP) (Ciubotaru *et al.*, 2005; Ji *et al.*, 2009; Li *et al.*, 2012; Zhao & Shi, 2010).

The *in vitro* production of mCRP, by treatment of pCRP with high concentrations of urea (up to 8M), was first described by Potempa *et al.*, (1983). They showed that this monomeric form had decreased solubility, a difference in isoelectric point and a loss of calcium dependent binding to C-polysaccharide (Potempa *et al.*, 1983). Interestingly, once pCRP has been dissociated into mCRP, it is unable to re-associate back into its native form, raising important questions as to whether the treatment in such harsh conditions results in a

conformational change in the protein's structure, with unknown consequences for its function (Kresl *et al.*, 1998).

There is some confusion within the literature concerning the definitions of CRP isoforms. 'Monomeric CRP' can be produced *in vitro*, but references are also made to a 'membrane-bound CRP' or 'modified CRP'. It is unclear whether this isoform is monomeric or pentameric, but it is suggested to form through membrane binding of pCRP, which induces dissociation. Furthermore, it is unclear whether the 'modified' or 'membrane-bound' CRP can be located freely within human serum (Eisenhardt *et al.*, 2009; Habersberger *et al.*, 2012; Ji *et al.*, 2007; Ji *et al.*, 2009; Li *et al.*, 2012; Molins *et al.*, 2008; Slevin & Krupinski, 2009; Zhao & Shi, 2010).

1.9.2 The Formation of Monomeric C-reactive Protein

Several models have been proposed for the *in vivo* formation of mCRP, with cell membranes and liposomes being the more commonly accepted theories (Eisenhardt *et al.*, 2009; Habersberger *et al.*, 2012; Ji *et al.*, 2007; Ji *et al.*, 2009; Li *et al.*, 2012; Slevin & Krumpinski, 2009). Although, as previously stated, native CRP is known to be relatively stable under physiological conditions, evidence has been published which suggests dissociation may occur under a normal, physiological environment. Calcium dependent binding of circulating pCRP to liposomes or cell membranes can induce rapid dissociation of the pentamer with apoptotic THP-1 and Jurkat T cells, mediating this form of dissociation into a membrane bound form of CRP, thought to be monomeric (Eisenhardt *et al.*, 2009; Filep, 2009; Ji *et al.*, 2009; Sjowall and Wettero, 2007).

The dissociation of pCRP has been proposed to occur through various epitopes presented on the cell surface of endothelial cells, including lipid raft domains. Lipid rafts are specialised membrane microdomains which are enriched with cholesterol and sphingolipids

which play an important role in cellular signalling. They also contain other saturated long-chain lipids that create a dynamic 'liquid-ordered' zone in the bulk fluid membrane. These areas provide the capacity for rafts to sequester or exclude certain proteins and organise a signal transduction platform (Ji *et al.,* 2009). Sequence analysis of CRP identified a region of amino acids 35-47 which displayed a sequence resembling the putative cholesterol recognition consensus. In its pentameric form, amino acids 35-47 would largely be buried within the apolar core of the subunits and overlap with the inter-subunit contacting sequence. Moreover, upon dissociation, this sequence would then become exposed and capable of binding to regions on the membrane of high cholesterol content (Ji *et al.,* 2009). Alongside cholesterol, other key lipid components that have been identified as being able to induce dissociation of pCRP upon binding are *Pneumococcal* C-polysaccharide and polylysine. In addition to multipoint attachment of pCRP to induce dissociation, a hydrophobic microenvironment has been identified as a key determinant. This mild hydrophobic environment, such as the cell membrane, can lead to rapid dissociation of pCRP subunits, with partially retained native confirmation (Ji *et al.,* 2007).

1.9.3 Monomeric C-reactive Protein and Disease

Experimental work documented within the literature has hypothesised a link between the mCRP and the progression of certain diseases within the body. Monomeric CRP is documented to have reduced aqueous ability, with a tendency to aggregate into matrix-like lattices in various tissues, such as blood vessel walls (Slevin *et al.,* 2009). As discussed previously, activation of endothelial cells and their dysfunction is a common event leading contributing to the development of cardiovascular disease. It is believed that CRP may contribute towards this dysfunction, through the production and recruitment of pro-inflammatory cytokines, alongside the upregulation of cell adhesion molecules.

It is suggested that pCRP may undergo some form of structural rearrangement to a modified version of CRP (usually denoted mCRP), for this activation and dysfunction of endothelial cells to occur alongside asserting pro-inflammatory stimuli upon vascular cells (Khreiss *et al.,* 2004; Ji *et al.,* 2009). A study carried out by Molins *et al.,* demonstrated that mCRP, unlike pCRP was shown to induce thrombus growth on the collagen surface, and not only significantly increase the adhesion of platelets, but also the aggregate size and thrombus height (Molins *et al.,* 2008). P-selectin up regulation by mCRP demonstrates an ability to stabilise platelet-platelet and platelet-leukocyte aggregates; a potential explanation for the increase in thrombus growth as mCRP has been linked to the recruitment of platelets and thrombus growth (Molins *et al.,* 2008).

In human neutrophils, mCRP has been shown to stimulate rapid production of IL-8 (<4 hours), required *de novo* synthesis and transcription of the IL-8 gene (Khreiss *et al.,* 2005). In addition to this study, Khreiss *et al.,* showed that modified CRP, thought to be mCRP, induced the production of peroxynitrite, formed through the reaction of superoxides and nitric oxide. Peroxynitrite functions as an intracellular signalling molecule to produce IL-8 through the activation of transcription factors nuclear factor-κB and activator protein-1 (Khreiss *et al.,* 2005). The adhesion of neutrophils to endothelial cells in areas of intensified inflammation can also be increased because of mCRP. Dissimilar to pCRP, cellular adhesion molecules CD11b and CD18 are upregulated on the surface of neutrophils when they interact with mCRP (Zouki *et al.,* 2001). The properties of fibrin in human artery endothelial cells have been shown to be altered upon interactions with mCRP. Incubation with mCRP on the cell surface resulted in increased fibrin polymerisation and tissue factor expression. This increase in tissue factor alters the formation of fibrin and its clotting properties, which may contribute towards potential pro-thrombotic events that can occur at injured vessel walls (Li *et al.,* 2012). Furthermore, levels of IL-8 and monocyte

chemoattractant protein, alongside increased mRNA levels and expression of ICAM-1, E-selectin and VCAM-1 were also observed (Khreiss *et al.,* 2004). The physiological changes which have been recorded here could potentially translate into severe biological alterations within the pathology and, in turn, contribute towards the development and progression of inflammatory diseases.

Circulating platelets have also been documented to play a role in the mCRP-induced progression of inflammatory disease. Phosphatidylcholine is a major lipid contained within the membrane of eukaryotic cells, serving as a reservoir for several lipid messengers, including lysophosphatidycholine. On activation and cell death, cell membranes express derivatives of phosphatidylcholine, expressing phosphocholine residues to which CRP can bind too (Eisenhardt *et al.,* 2009). This binding site has been hypothesised to be the region where CRP binds to activated platelets, present within atherosclerotic lesions, and induce the dissociation of pCRP into mCRP. This resulting formation of mCRP leads to increased expression of adhesion molecules, like that described during endothelial cell dysfunction (Eisenhardt *et al.,* 2009). Verma *et al* proposed a method of pCRP dissociation in the peripheral circulation that would enhance the pro-inflammatory properties of CRP (Verma *et al.,* 2004). This was backed up by Eisenhardt *et al* as they could demonstrate a dissociation process showing that activated platelet membranes exposing phosphocholine, which mediates this dissociation (Eisenhardt *et al.,* 2009; Verma *et al.,* 2004).

Upon platelet activation, lipids located within their membranes are known to undergo a change in morphology and composition; one of these changes being the exposure of binding sites for immune proteins such as CRP. This rapid change in the membrane structure of lipids also results in the shedding of microparticles (MP) (Owens & Mackman, 2011). A study by Habersberger *et al.,* has hypothesised that circulating microparticles can bind and

induce dissociation of pCRP, in addition to act as a mode of transport around the body, to sites of intensified inflammation (Habersberger *et al.,* 2012). More recently, an experimental study has highlighted the failure of standard clinical CRP tests to detect mCRP that is bound to MP. This could potentially have a devastating impact on the type and quality of treatment a patient could receive (Crawford *et al*., 2016). The experimental evidence highlighted here displays a damaging pro-inflammatory role of the elusive monomeric form of CRP, which may potentially exacerbate the progression of inflammatory diseases.

1.10 Complement

1.10.1 Introduction to Complement

The complement system is part of the innate immune system and is one of the key effector mechanisms of antibody-mediated immunity in the classical pathway. It was first identified as a process in serum that 'complemented' antibodies in the killing of bacteria (Walport, 2001). There is a total of three complement pathways; the classical pathway, mannose-binding lectin pathway and the alternative pathway (Walport, 2001). The C1 complex is an initiator for the classical complement pathway by binding to immunoglobulins such as IgM, IgG or the acute phase protein CRP, bound on the surface of host cell walls (Carland *et al.,* 2010).

The C1 complex is a 790 kDa complex, which is formed by the association of the recognition protein, C1q, and a calcium dependent tetramer, comprising of two copies of the proteases C1r and C1s (Gaboriaud *et al.,* 2004). The proteases are elongated tetramers that become more compact when they bind to the collagen-like domains of the C1q molecule (Girija *et al*., 2013). Binding of the C1q protein induces a conformational change which drives the activation of the proteases in a stepwise fashion: C1r first auto-activates, then activates C1s. C1s subsequently cleaves the additional complement proteins C4 and C4b-

bound C2, forming the C3 convertase – a downstream component of the complement cascade (Girija *et al*., 2013). The role of the C1 complex within the human immune system is to activate the classical complement pathway, which results in the recruitment of inflammatory mediators and eventually the cell lysis through the formation of the membrane attack complex (MAC) (Black *et al*., 2004; Girija *et al*., 2013; Kishore *et al.*, 2004; Mold *et al*., 1999). Most major complement components are synthesised within the hepatocytes of the liver; however, the C1 complex proteins are produced, primarily within the epithelium of the gut, along with a growing list of immune cells such as macrophages and endothelial cells (Arlaud & Colomb, 2001).

1.10.2 C-reactive Protein and Complement

Activation of the complement system by CRP was first demonstrated by Kaplan and Volanakis in 1974 (Kaplan & Volanakis, 1974). They reported that the addition of pneumococcal C-polysaccharide to acute phase serum caused complement depletion, and that this process required the presence of both CRP and C1q. This activation was also shown by Sigel *et al.*, using CRP-protamine complexes (Kaplan & Volanakis, 1974; Sigel *et al*., 1974). These studies established that CRP, complexed with polyvalent or chemically cross-linked ligands, binds to C1q and activates the classical complement pathway (Mold *et al*., 1999).

The proteins C1-C9 are the major components of the classical complement cascade and are most commonly activated through the binding of various immune complexes to C1q. The initial stage of the classical complement pathway results in the cleavage of products C3 and C4, which act as opsonins (Black *et al*., 2004; Mold *et al*., 1999). The later stage of the classical complement pathway involves activation of the C5-C9, generating highly inflammatory chemotactic peptides and the formation of the membrane attack complex

causing lysis of the bacteria or cell to which they bind. The complexing of the ligand-bound CRP to C1q leads to the formation of the C3 convertase protein which assembles in a formation like that initiated by antigen-antibody complexes (Mold *et al*., 1999). The examination of individual complement components suggests that CRP mediated complement activation is limited its initial stages, involving C1-C4, with little activation of late complement proteins C5-C9 (Black *et al*., 2004; Mold *et al*., 1999). This contrasts with the complement cascade which is initiated via the antibody-antigen complex, which recruits the later phase components of the complement cascade. This difference between complement activation through CRP and that resulting from other immune complexes is presumably down to CRP's ability to interact and with factor H, leading to the inhibition of pathways that result from the formation of C5 convertases. Thus, strong inflammatory responses typically associated with C5a and the C5-9 membrane attack complexes are limited (Black *et al*., 2004; Clos & Mold, 2004; Mold *et al*., 1999; Zhu *et al*., 2005).

CRP has been shown to bind to artificial membranes, via the positively charged fatty acid derivatives, stearylamine, which results in the activation of the complement pathway (Mold *et al*., 1981; Richards *et al*., 1977). PC subunits protruding from liposomal membranes can interact and bind with CRP, and activate the complement cascade whilst simultaneously stimulating the release of glucose from the liposomes. Adequate membrane binding of CRP to PC is essential when activating the complement cascade, as lysis of the liposomal membrane was reduced when incorrect binding occurred (Richards *et al*., 1977). The complement components that were consumed during this experimental process demonstrated that activation occurred through the classical pathway. The interaction of CRP with protamines (arginine-rich, nuclear proteins) also appears to consume components of the classical complement pathway (Siegel *et al*., 1974). The consumption of classical complement components has also been described when CRP interacts with PC units present

of the surface of lecithin and sphingomyelin, both different types of phosphatides (Kaplan & Volanakis, 1974).

1.10.3 Introduction to the Human C1q Protein

The importance of C1q as a biological molecule is shown by its wide range of biological processes. Activation of the classical complement pathway by C1q usually results in the formation of the membrane attack complex (MAC) on the target cell, including cell lysis (Kishore *et al.*, 2002; Kishore *et al.*, 2004; Kishore & Reid, 2000).

The interlocking of antigens and antibodies in a complex is a natural and successful attempt to neutralise antigens. C1q plays a vital role in the solubilisation and clearance of these complexes (Kishore *et al.*, 2004; Navratil *et al.*, 1999). The complement protein, C1q, also acts as an opsonin in the removal of bacterial products by coating the bacteria and enhancing the uptake by phagocytic cells (Kishore *et al.*, 2004).

Production of pro-inflammatory cytokines such as IL-8, IL-6 and monocyte chemoattractant protein (MCP) 1 from endothelial cells is also an important role for the C1q protein. The interaction involving a collagen-like region of the C1q protein and calreticulin-CD91 receptor complex enhances p38 MAPK activation, NF-κB activity and the production of pro-inflammatory cytokines in macrophages (Berg *et al.*, 1998; Kishore *et al.*, 2004).

1.10.4 The Structure of Human C1q

The human C1q molecule is composed of three different polypeptide chains, A, B and C. There is a total of 6 subunits, each containing one A, B and C polypeptide chain with a total of 18 polypeptide chains within the C1q protein. The protein, as shown in Figure 1.5 is commonly described to take on the appearance of a ‘bouquet of flowers’.

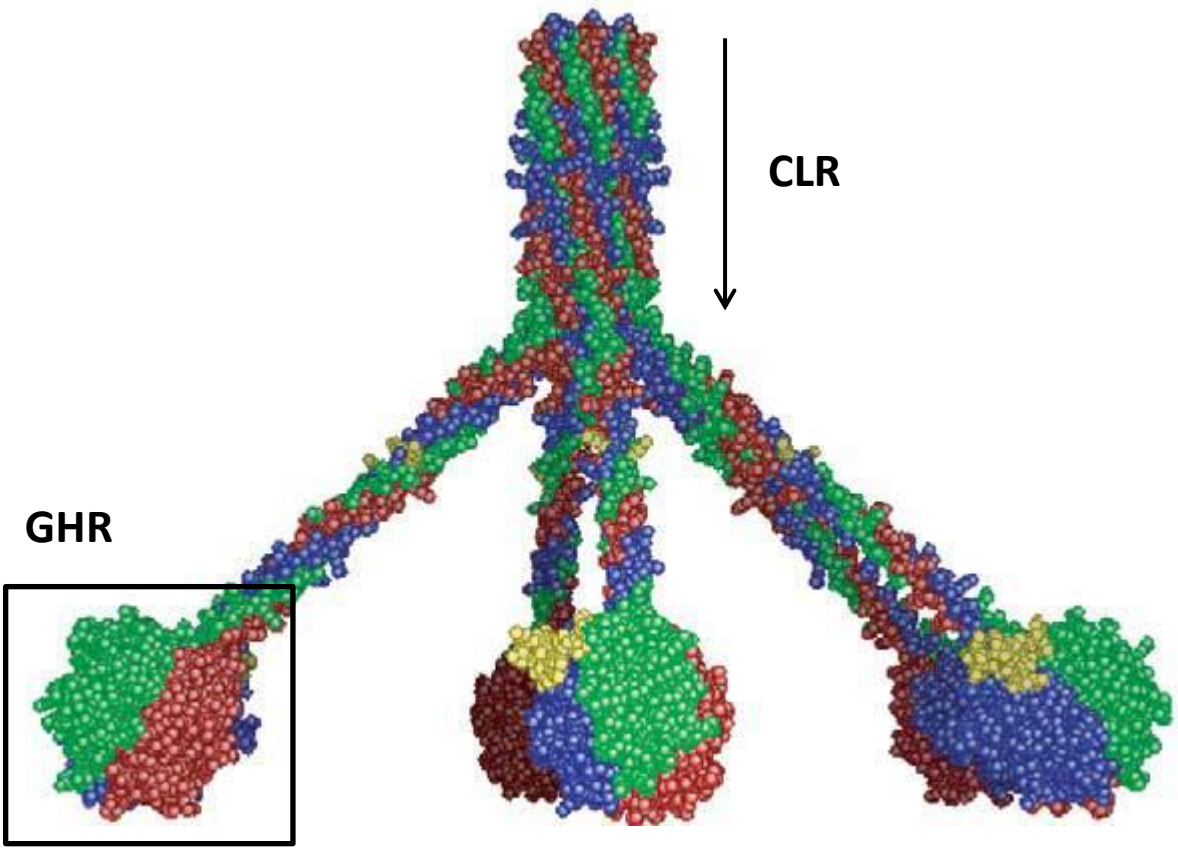

Figure 1.5 Model of the three-dimensional structure of the C1q protein. The central collagen-like region is shown at the apex of the image which diverges into six stems, eventually forming the globular head region. Each polypeptide chain is represented via a different colour; blue (A), red (B) and green (C). The glycosylated region attached to the globular head is shown in yellow. Figure has been adapted from Gaboriaud *et al*. (2004)

Each chain has a short amino-terminal region, containing a half-cysteine residue, which is involved in inter-chain disulfide bond formation. This is followed by a collagen-like region (CLR) of around 81 residues (comprising of Gly-X-Y repeats) which is linked to a C-terminal globular head region (GHR) of approximately 135 residues (Kishore & Reid, 2000; Kishore *et al.*, 2004).

The GHR fragment of C1q has been crystallised and the structure determined to a 1.9-Å resolution by Gaboriaud, *et al* (2003). The structure shows a tight, heterotrimeric assembly with non-crystallographic pseudo-3-fold symmetry (Gaboriaud *et al.*, 2003). The N- and C- termini for each of the subunits, A, B and C of the GHR emerge at the base of the trimer. Each subunit has a 10-stranded β-sandwich with jellyroll topology, homologous to

the structure that has also been described for tumour necrosis factor (TNF). There is strong conservation shown within the β-sheets of the A, B and C subunits, with significant variability occurring within the loops protruding from the apex of globular head (Gaboriaud *et al.,* 2003). There is a predominance of positive charge at the top of the C1q GHR, mainly due to lysine residues. The calcium ion at the apex of the GHR is coordinated by six oxygen ligands; the oxygen present on the side chain of AspB172, one from the main chain carbonyl of TryB173, two from the side chain carbonyls of GlnA177 & GlnB179 and two water molecules (Gaboriaud *et al.,* 2003).

Furthermore, there are exposed hydrophobic patches with several aromatic residues available to the solvent (Gaboriaud *et al.,* 2003; Kishore *et al.,* 2004). The subunits A and C both show a combination of basic and acidic residues scattered over their external face, whereas subunit B shows a predominance of positive charge, especially focused around a concentrated patch of arginine residues (Arg101, 112 and 129). This modular organisation of heterotrimer assembly, in addition with the diverse surface patterns around the three subunits of the GHR, allows C1q to interact with a diverse range of ligands (Kishore *et al.,* 2004).

1.10.5 Interactions Between C-reactive Protein and C1q

The mechanical and structural interactions that occur between C1q and CRP on an atomic level are not fully understood. Two main theories exist, based on previous experimental evidence which suggest how this interaction occurs. The first theory hypothesises that C1q interacts with the effector face of CRP through its collagen-like region, with the alternative theory suggesting an interaction between CRP and the globular head region of C1q. Moreover, there is strong experimental evidence from both mutagenesis

and binding studies which supports the latter hypothesis (Agrawal *et al.*, 2001; Gaboriaud *et al.*, 2003; Kishore *et al.*, 2004).

Previous binding studies carried out, to determine the location of the CRP binding site on the C1q molecule, demonstrated two regions of amino acids which originate from the A chain within the CLR (Jiang *et al.*, 1992). To establish whether this region was crucial for binding, two C1q A chain peptides were synthesised, identical to the amino acids in regions 76-92 and 14-26; regions which were predicted to bind to the CRP protein. The results demonstrated that the peptide fragment 76-92 partially and peptide 14-26 completely inhibited the binding of CRP to the fully intact C1q protein (Jiang *et al.*, 1992). Further, replacement of amino acids within both sequences resulted in a complete loss of inhibition, which interestingly suggests sequence specificity, and binding does not just specifically rely on charge alone when forming a theoretical basis for the inhibitory effects of the peptide sequence (Jiang *et al.*, 1992).

The immunoglobulin IgG is known to bind to the globular head region of the C1q protein. Experimental research by Jiang *et al.*, 1991, showed that heat-aggregated IgG did not block the binding of CRP-trimers to C1q, nor did CRP-trimers block the binding of IgG to C1q, suggesting that the binding sites were located at different regions on C1q (Jiang *et al.*, 1991). Monoclonal antibodies that were directed towards the CLR of C1q (anti-CLR mAb) could inhibit the binding of CRP towards C1q, whereas when using the anti-GHR mAb, it was unable to elicit the same effect. The results demonstrated here provide indirect evidence which supports the theory that binding occurs through the CLR of the C1q protein, thus initiating the classical complement pathway (Jiang *et al.*, 1991; Jiang *et al.*, 1992). However, it is now generally accepted that the interaction between CRP and C1q occurs through the globular head region of the protein.

Alternatively, experimental evidence described by McGrath *et al.*, supports the latter hypothesis (McGrath *et al.,* 2005). McGrath *et al.,* demonstrate how five monoclonal antibodies against the globular head region of C1q inhibited the binding of CRP to C1q, failing to initiate complement. Whereas four monoclonal antibodies, which were specific to the collagen-like region, failed to induce any inhibition at all. Furthermore, the five monoclonal antibodies which were specific to the globular head region inhibited the binding of C1q the solid-phase IgG, demonstrating the binding site for IgG is also located on the globular head. Finally, McGrath also showed that binding of C1q to CRP could also be inhibited by IgG, suggesting further evidence that both binding sites are located upon the globular head, as opposed to the collagen-like region (Gaboriaud *et al.,* 2003; McGrath *et al.,* 2005).

Modelling studies, researching potential structural and charge based interactions between the two proteins has also been carried out. The three-dimensional structure of CRP sports a deep cleft, which extends between each protomer on the face of the pentamer opposite to that of the phosphocholine binding site (Agrawal *et al.,* 2001; Gaboriaud *et al.,* 2003; Shrive *et al.,* 1996). Gaboriaud *et al* suggest that this cleft on the CRP molecules is where the interaction between the globular head region of C1q interacts. The apex of the globular head displays a predominantly basic charge, which could be accommodated by the negatively charged central pore of CRP; an interaction which involves the A and B subunits of C1q (Agrawal *et al.,* 2001; Gaboriaud *et al.,* 2003; Gaboriaud *et al.,* 2004). Structural elements that are suggested to be involved in the interaction between CRP and C1q are more than likely to be located on the effector face of the pentamer, as shown in Figure 1.6.

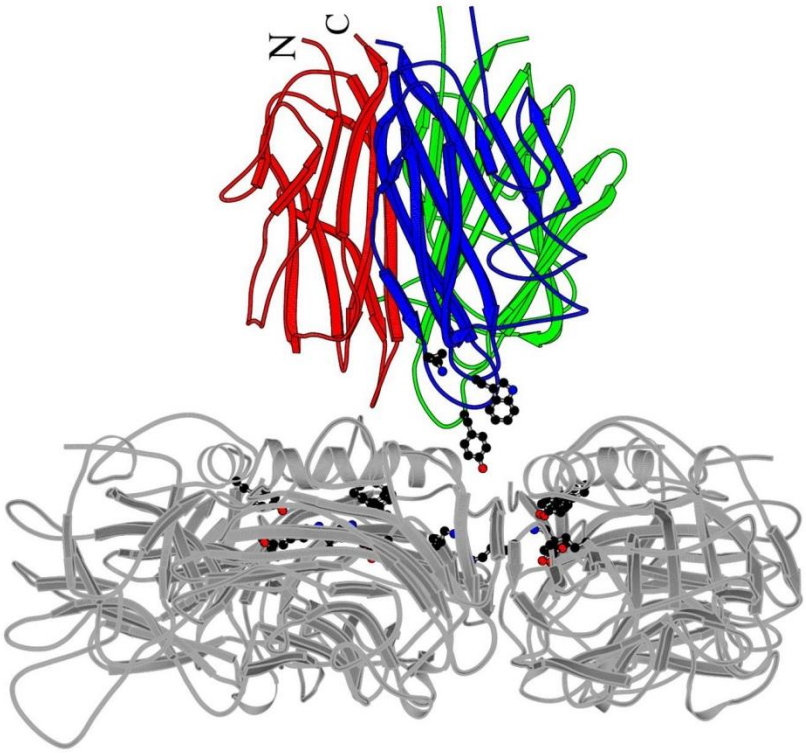

Figure 1.6 Schematic illustration of the hypothesised interaction between the GHR of C1q with the effector face of pentameric CRP. The globular head region A is shown in blue, B is shown in green and C is shown in red. The model was designed to facilitate the exploration of the potential interaction between the globular head region of C1q and CRP. Residues shown include Asp112 and Tyr175 of CRP, and Tyr175B, Lyc200A and Trp147A. The residues suggested to interact between the two proteins are highlighted as ball and stick models. Image adapted from Kishore *et al.* (2004).

The residues Asp112 and Tyr174 from CRP, show striking shape complementarity between the two proteins and have been identified as major contact residues with C1q (Agrawal *et al.*, 2001; Kishore *et al*., 2004). Asp112 from CRP is located within the open cleft, towards the centre of the pentamer; suggesting an important role for this region of the protein (Agrawal *et al.*, 2001). Further mutagenesis studies to define the topology of the C1q binding site has also demonstrated the importance of Asp112 and Tyr175, although the positively charged reside of Lys114 hinders the binding of C1q as substitution, as a negatively charged residue enhanced the binding of C1q and complement activation (Agrawal, 2004; Gaboriaud *et al.*, 2003).

The structural interactions between C1q and CRP are extremely important when researching the activation of complement, and to a wider extent, the innate immune response. Determination of individual amino acid interactions, location of binding sites and structural changes to both proteins overall will help provide a greater overall understanding of how these two proteins work and interact. Furthermore, alternative physiological forms of CRP, such as mCRP, have been linked to binding and activating the classical complement pathway (Mihlan, *et al*., 2011). This ability of mCRP to interact with mCRP is thought to result in the exacerbation of inflammation in certain diseases. Further research into understanding providing detailed structural information of how the protein binds and interacts with its constituent immune proteins may help drive areas of research and understanding.

1.11 Research Aims

The overall aims of this research were split into two areas. The first was to provide some insight into the current ambiguities around the molecular variations of CRP. This will involve the production, purification and characterisation of *in vitro* produced mCRP, alongside analysis of human serum samples for an *in vivo* form. The presence of a monomeric form of CRP within human serum may have an impact on both current clinical practice and the treatment and care a patient receives as it is not clear whether raised levels of the protein may indicate a different set of circumstances to that of its native counterpart, pCRP. Furthermore, it is unknown whether current clinical tests may be able to detect the presence of a monomeric form of CRP, or whether current clinical practice needs to be re-evaluated to accommodate for its presence.

The latter part of this research involved crystallisation studies of *in vitro* produced mCRP, alongside complex crystallisation trials involving native CRP, C1q and CWPS. Crystallisation trials involving the *in vitro* produced mCRP were initiated to identify a

potential structural map of the protein, should we identify it. Additionally, an atomic map of the monomer may highlight any structural differences between itself and the native pentameric form. Additionally, we wanted to visualise the structural interactions that occurred between CRP and its natural ligands; more specifically CPS and C1q. The crystallisation trials involving CRP, C1q and CWPS aimed at providing greater detail into the structural interactions within this complex on an atomic scale. It is not yet certain as to how CRP binds the C1q complement protein; does this occur via the globular head or the collagen-like region? Furthermore, it remains unclear why CRP can only activate complement when bound to a larger structure, and not just PC. The evidence suggests a conformational change may occur within CRP, once bound to both proteins. Solving the atomic structure of this complex will answer these questions, alongside providing a greater understanding to CRP's role and function within the immune system

Overall, this research will further the knowledge on CRP's role within the immune system, both structurally and clinically. It will also provide insight into common misconceptions of the acute phase protein, whilst contributing to the quality assurance of current clinical practice, when measuring patient CRP levels.

Chapter 2.0 – Production & Characterisation of Monomeric C-reactive Protein

2.1 Introduction

2.1.1 Overview

Native, pCRP is extremely stable under normal, human physiological conditions. However, there is increasing evidence within the literature which suggests a role for an isoform of pCRP, known as monomeric C-reactive protein (hereon referred to as mCRP). Although slightly unclear whether this protein is 'modified', or 'membrane-bound', the consensus suggests a pro-inflammatory role within the human body, compared to its native pentameric isoform (Ciubotaru *et al.,* 2005; Eisenhardt *et al.,* 2009; Ji *et al.,* 2009; Li *et al.,* 2012; Zhao & Shi, 2010).

The described mCRP displays a reduction in solubility, a change in isoelectric point and a complete loss of the calcium dependent binding to C-polysaccharide (Potempa *et al.,* 1983). The biological relevance of mCRP is yet to be fully established, with some debating whether the protein exists *in vivo* and asking if mCRP is not just a product of *in vitro* dissociated pCRP which displays these pro-inflammatory properties. There is some experimental evidence that has recently been published which demonstrates a model for the production and transportation of mCRP *in vivo*, with some researchers claiming they have successfully detected the protein *in vivo* (Wang *et al.,* 2015).

This chapter will discuss the production and characterisation of an *in vitro* produced form of mCRP, from native pCRP. The experimental work is based upon previous production of mCRP both within the literature and previous experimental work carried out within our own research lab. The aim of this research is to develop a sound methodology which allowed us to produce mCRP (*in vitro*) in the least harsh conditions possible.

2.1.2 Production of *in vitro* Monomeric C-reactive Protein

The production of a monomeric form of CRP was first described by Potempa *et al.*, in 1983. They used methods including; heat treatment, altering the pH to extremely acidic conditions and dissociation through high concentrations of urea (Potempa *et al.*, 1983). Interestingly, in addition to the characteristics previously described, once dissociated into mCRP, it was unable to re-associate back into its native form. This raises important questions as to whether treatment in such harsh conditions results in a conformational change to the structure and function of the protein. It is worth noting that many of the published works on the damaging pro-inflammatory effects exhibited by mCRP have produced their mCRP in the same way, bringing into question whether there is any physiological relevance to their work.

2.1.3 Affinity Chromatography

The technique affinity chromatography separates out protein molecules based on a reversible interaction between a protein (or a group of proteins) and a specific ligand which is coupled to a chromatography matrix. Crude samples such as human serum can be passed through this chromatography matrix to which a specific ligand is immobilised. This is called a coupled ligand, as it is coupled to the matrix, and the protein in the sample binds to this (Wilchek & Chaiken, 2000). The technique offers a highly selective method of protein purification which displays a high capacity for the protein of interest. The purification of a specific protein can be in the order of several thousand-fold, with recoveries of active material generally very high. For successful purification, affinity chromatography relies on intact protein structure and function. Thus, the process can also be used to separate out active biomolecules from denatured or functionally different forms (Wilchek & Chaiken, 2000).

The biological interactions that occur between the ligand and the target molecule can be a result of electrostatic or hydrophobic interactions, van der Waals' forces or hydrogen bonding. It is these interactions which allow target molecules to be purified from complex biological mixtures. A ligand which displays binding to very few proteins, or even just one protein, will allow greater purification than a ligand which is less specific and can bind to many proteins (Amersham Biosciences, 2003).

The matrix of the column used in this project is Sepharose made from agarose sugar beads. This material is stable and not affected by changes in pH or ionic strength in addition to being relatively inert meaning it does not interact with the proteins within the sample. The column is tightly packed with the Sepharose matrix, arranged in a matrix structure with a rigidity allowing for varying flow rates. This is known as the 'affinity medium' (Amersham Biosciences, 2003).

The ligand which is bound to the column matrix is bound via a covalent bond, whilst still retaining the crucial binding properties for interaction with protein(s). The bound ligand possesses several important qualities which are crucial for affinity chromatography. Firstly, the ligand binds reversibly to the protein in question and does not alter the protein's biological activity or properties in anyway. Secondly, the binding affinity between the ligand and the protein must be strong enough to ensure that most, if not all the target protein is bound providing a high purification yield from the crude sample. Thirdly, the interaction between the protein and ligand must not be too strong to prevent recovery once the whole sample has been passed through the column (Amersham Biosciences, 2003).

Once the entire sample has been run through the chromatography matrix, and the protein has bound to the coupled ligand, the sample must be recovered from the column. Elution of the sample can be performed specifically, by using a competitive ligand, or non-

specifically, by altering the pH, ionic strength or polarity of the solution running through the column. The most common method of purifying a sample from the column is using a competitive ligand. The competitive ligand will display a higher binding affinity for either the protein in question, or the ligand bound to the chromatography matrix (Villems & Toomik, 1993). The concentration of the competitive ligand depends on the affinity of the protein for the competitor. A lower binding affinity of the protein to the competitive ligand usually results in a higher concentration being used, whereas a higher binding affinity can generally mean a lower concentration will suffice for the removal of the protein from the column.

Crude samples such as blood and serum can be purified by affinity chromatography, as can any liquid containing a mixture of proteins. Larger volume samples do not necessarily affect the purification process, although a larger sample will increase the time taken to load onto the column. It is the amount of protein within the initial sample that is crucial for purification as overloading the column with too much protein will result in protein being wasted and incorrect feedback values when calculating the recovery yield.

The flowrate used for applying and eluting the protein sample to the column should be optimised. Too high a flowrate and the proteins within the solution may not bind adequately, therefore losing valuable protein through washing steps. However, if there is high binding affinity between the protein and ligand, slightly higher flow rates are acceptable as this will save time with a negligible loss of protein from the sample.

Prior to the addition of the sample, the column is thoroughly cleaned, usually with a recommended wash buffer appropriate for the sample being used. The wash buffer will help remove any protein that failed to elute off from the previous run. Equilibration buffer is also

run through the column before and after each step in the purification process to wash through unbound material and to ensure a constant flow through the column.

2.1.4 Gel Filtration Size Exclusion Chromatography

Gel filtration chromatography is the simplest and mildest of all chromatography techniques. It plays a key role in the purification of biological macromolecules including proteins, polysaccharides and nucleic acids. This robust technique is well suited to the handling of biomolecules that are sensitive to changes in pH, concentration of metal ions or harsh environmental conditions. Sample purification can be performed in the presence of harmful substances such as urea, guanidine, hydrochloric acid, alongside a range of temperatures. The main functions of gel filtration chromatography include; sample purification, buffer exchange and molecular weight determination. The separation and purification of these biomolecules is achieved by passing the solution through a gel filtration medium, which has been tightly packed into a column. Unlike affinity or ion exchange chromatography, the molecules within the sample do not bind to the chromatography medium, meaning buffer composition does not affect the resolution. This highlights an advantage over other chromatography techniques, as buffer conditions can be altered to suit each sample (Amersham Biosciences, 2003).

The gel filtration medium is tightly packed inside the column, forming what is known as the ‘packed bed’. This medium consists of a porous matrix of spherical particles which are used due to their chemical and physical stability, in addition to their inertness. There are several different types of gel filtration medium that can be used in size exclusion chromatography, each suited to a different type of protein purification. One common example of the medium used in size exclusion columns is Sephadex, which is ideal for rapid group separation of molecules, desalting and buffer exchange. Prior to the addition of the

sample, the column is equilibrated with buffer which fills the pores of the matrix and the space between each of the particles. The liquid within the matrix is known as the 'stationary phase', which is in equilibrium with the liquid outside of the matrix, known as the 'mobile phase' (Amersham Biosciences, 2003).

The sample is applied to the column via a syringe. To achieve the best possible resolution of the elution profile, a sample volume between 0.1-2% of the column volume is recommended. Once the sample has been applied to the column, the buffer (and sample) slowly migrates through the column tubing, towards the column. Optimum flow rates will increase the resolution of the elution profile in addition to conserving the yield of protein collected post-purification. Molecules within the sample diffuse in and out of the pores within the matrix. Smaller molecules can move further into the matrix, whereas larger molecules are restricted as to where they penetrate the pores due to their size. This ability to 'visit' more areas of the porous matrix facilitates the separation of the molecules throughout the solution based on their molecular weight. As the buffer continuously passes through the column, larger molecules which are no longer able to move further into the matrix are eluted off into fraction collection tubes. As samples are eluted off the column, their ultra-violet (UV) absorbance is measured (wavelength will depend on the type of biomolecule) to create an elution profile. The entire separation process takes place over a total of one column volume (equivalent to the volume of the packed bed) of buffer passing through the column. Calibration graphs, constructed from the elution volumes of known molecular weight standards can be used to determine the molecular weight of unknowns, based on their elution volumes (Amersham Biosciences, 2003).

Samples such as blood and serum are advised not to be run through the column due to their crude composition. This could potentially block the size exclusion column and would require constant rigorous cleaning procedures after each run. Typically, samples will have

been initially purified via a different form of chromatography (such as affinity) before being applied to the size exclusion column. Unlike affinity chromatography, the amount of protein within the sample is not a crucial factor, whereas sample volume size is. Larger volumes can affect the resolution of the sample elution profile, providing inaccurate and unreliable results.

The flowrate for applying the sample should also be optimised. The flowrate cannot exceed 1.6ml/minute for the column used in these experiments. Exceeding this could damage the column matrix. The columns are typically stored in a 20% ethanol solution to prevent any bacterial growth when not in use. Prior to running a sample through the column, deionised water is flushed through at a high flowrate (1.6ml/min) to remove all ethanol and any potential proteins that may be residing within the column from the previous run. The removal of waste is monitored through UV absorbance. When the required volume of deionised water (and equilibration buffer) has been run through, and the UV absorbance reading has baselined, the column is then ready for use (Amersham Biosciences, 2003).

2.1.5 Gel Electrophoresis

Electrophoresis is a relatively simple, rapid and highly sensitive tool which can be used to identify and characterise sample contents. Agarose gels are mainly used to separate out larger macromolecules, such as deoxyribonucleic acid (DNA) or ribonucleic acid (RNA), whereas polyacrylamide is used for the separation of proteins (Hames, 1998). Polyacrylamide gel electrophoresis can be used to analyse the size, amount, purity and isoelectric point of polypeptides or proteins. In both types of gels, a matrix is formed containing pores through which loaded samples on the gel will separate out when an electrical current is applied (Hames 1998). Components within the sample will be separated

out per their electrophoretic mobility, migrating from the negative anode, towards the positively charged cathode.

The components used to form the polyacrylamide gels are monomeric acrylamide and N, N'-methylene-bisacrylamide (bisacrylamide) (Hames, 1998). The polymerisation between acrylamide and bisacrylamide is initiated by either a chemical or photochemical free-radical generating system. Tetramethylethylenediamine (TEMED) initiates the chemical polymerisation with ammonium persulfate (APS), while photochemical polymerisation is initiated by riboflavin-5'-phosphate, or methylene blue (Hames, 1998). Dissolving APS in water causes the formation of free radicals, which in turn activates the acrylamide monomer. TEMED serves as a catalyst to accelerate the polymerisation reaction due to its ability to carry electrons. The activated acrylamide monomer can therefore react with inactivated monomeric units, producing a long polymer chain. Bisacrylamide subunits randomly cross-links with the elongating polymer chains forming a 'net' or matrix of acrylamide chains (Hames, 1998).

The ratio between the acrylamide and bisacrylamide, or the percentage used in the gel, determines the solidity/fluidity of the gel. The size of the pores within the polymerised gel is governed by the total amount of acrylamide used per unit volume and the degree of cross-linkage (Hames, 1998). The composition of acrylamide mixtures is defined by the letters T and C per Hjerten, 1962. 'T' denotes the percentage of both acrylamide and bisacrylamide in grams per 100ml, whereas 'C' denotes the percentage (by weight) of the cross-linker, relative to the total monomer (Hames, 1998; Hjerten, 1962). In practice, the suggested range for uniform acrylamide gels is between 5-20%. Samples containing larger molecular weight proteins require a lower percentage of acrylamide. High percentage acrylamide gels form smaller pores, meaning the gel would be unable to resolve these larger

molecular weight proteins (and *visa-versa* for small molecular weight proteins) (Hames, 1998).

When casting an acrylamide gel, two types of gel are cast; a stacking gel and a resolving gel. The stacking gel is where samples are loaded onto the gel and allows proteins to concentrate into a band prior to entering the resolving gel, increasing the resolution. The resolving gel is where proteins are separated out per their properties (Hames, 1998).

There are two types of systems that can be used to separate out proteins through electrophoresis; denaturing and non-denaturing systems. Non-denaturing systems are designed to separate out native proteins under conditions that preserve the proteins' function, structure and activity (usually denoted native PAGE: polyacrylamide gel electrophoresis). Separation is based not only on the protein's size, but its charge and shape. In a denaturing system, proteins are denatured to their constituent polypeptides, allowing examination of the composition, size and number of polypeptide units within the sample (usually denoted SDS PAGE: sodium dodecyl sulfate polyacrylamide gel electrophoresis) (Hames, 1998). Unlike non-denaturing systems, SDS PAGE is easier to run, stain and de-stain, without compromising on resolution (Hames, 1998).

Prior to protein samples being loaded onto the gel, they are mixed with a sample buffer. The sample buffer components depend on the type of electrophoresis system that is being run. For the denaturing system, SDS is added. SDS is an anionic detergent which binds to the proteins within the sample giving an overall negative charge (Hames, 1998). Samples are heated at 95^{o}C for 5 minutes to further denature the protein. The heating of the samples helps break the electrostatic forces that hold the three-dimensional protein structure together, except for disulfide bonds. The addition of β-mercaptoethanol reduces any disulfide bonds present in the protein. Under these conditions, all polypeptide units bind the same amount

of SDS, independent of their composition or sequence, and will migrate through the gel (when a current is applied) based only on their size (Hames, 1998). In addition to these components the sample buffer also contains bromophenol blue, a loading dye which allows visualisation of the dye front whilst the gel is running, as well as glycerol, a density reagent ensuring samples sink into the well during loading. Non-denaturing systems require no denaturing components in their sample buffer.

2.1.6 Western Blotting

A blot in molecular biology is the process of transferring proteins, DNA or RNA onto a carrier surface. There are a variety of blotting methods which can be used, depending on the sample being transferred. Southern blotting involves the transfer of DNA onto a carrier for detection, whereas northern blotting involves RNA. Western Blotting is the process of detecting specific proteins by use of antibodies which have been transferred onto a membrane, post-gel electrophoresis. The method originated in the laboratory of Harry Towbin at the Friedrich Miescher Institute and is now used across the world in both clinical and research settings (Dunbar, 1994; Towbin *et al.*, 1979).

Proteins within a sample are initially separated out, usually by SDS gel electrophoresis, as described in section 2.1.5. The proteins within the gel are then transferred onto a membrane. An electric current is applied, which 'pulls' the proteins from the gel and onto the membrane. Proteins that have been run on an SDS PAGE gel will have an overall negative charge due to the SDS; therefore, this will aid in the transfer of the proteins onto the membrane (Dunbar, 1994; Towbin *et al.*, 1979).

Typical membranes used in Western Blotting are either nitrocellulose or PVDF. Nitrocellulose is produced by treating cellulose with nitric acid and spreading the solution over a thin film. Each glucose unit in the cellulose polymer is esterified with three nitrate

groups, which are responsible for the negative charge of the membrane. Both electrostatic and hydrophobic interacts are thought to be the possible binding mechanisms between macromolecules, such as proteins, on the membrane. Nitrocellulose is widely used due to its high affinity and retention for protein, cost and ease of use (Johnstone & Thorpe, 1987; Towbin *et al*., 1979). PVDF is a highly non-reactive fluoropolymer produced by the polymerisation of vinylidene difluoride. It is also commonly used in Western Blotting procedures due to its non-specific binding capacity of amino acids (higher than nitrocellulose) and mechanical strength. PVDF is an extremely hydrophobic surface and therefore must be hydrated in methanol prior to use to improve transfer and binding (Dunbar, 1994; Johnstone & Thorpe, 1987; Towbin *et al*., 1979).

As the membranes used in Western Blotting are chosen for their ability to bind proteins, necessary steps are required to prevent interactions between the membrane and the antibody used for detection of the target protein. To prevent this non-specific binding, the membrane is blocked with non-fat dry milk powder or bovine serum albumin (BSA). Proteins within the milk powder bind to regions of the membrane where the target protein has not yet bound (Johnstone & Thorpe, 1987; Towbin *et al*., 1979).

The primary antibody is then added to 'probe' the membrane. Primary monoclonal antibodies are generated when their host species, or cell culture, is exposed to the protein (or fragment of that protein) of interest. The primary antibody will therefore be specific to the target protein. Once a sufficient amount of time has passed, the primary antibody is removed, and a secondary, species specific, enzyme-conjugated antibody is added. If the primary antibody had been raised within a mouse, an anti-mouse secondary antibody will bind to almost any mouse-sourced primary antibody (Murphy, 2008; Johnstone & Thorpe; 1987; Towbin *et al*., 1979). The secondary antibody is conjugated to an enzyme, usually horseradish peroxidase (HRP) or alkaline phosphatase (AP). Once the secondary antibody

has been allowed sufficient time to probe the membrane, a substrate for the conjugated enzyme is added. The substrate usually depends on the type of conjugated enzyme used. Horseradish peroxidase can be used to cleave chemiluminescent agents. The product formed from the reaction produces light, which therefore confirms the presence of the target protein (Johnstone & Thorpe, 1987; Towbin *et al*., 1979). The emitted light is then detected on a charged coupled device camera, which captures digital images of the blot. Cheaper detection methods are also used; 4-chloronaphthol stain with 1% hydrogen peroxide is one example. The reaction of peroxide radicals with 4-chloronapthol produces a dark purple stain that can be photographed without using specialised equipment. Although cheaper detection methods are significantly cheaper, the sensitivity of the assay is reduced dramatically (Dunbar, 1994; Murphy, 2008; Johnstone & Thorpe, 1987; Towbin *et al*., 1979).

2.1.7 The Enzyme-linked Immunosorbent Assay

An Enzyme-linked immunosorbent assay (ELISA) is a basic immunology concept of an antigen binding to a specific antibody, allowing detection of small antigens such as proteins, peptides, hormones or antibody in a fluid sample (Gan & Patel, 2013). ELISA utilises enzyme-conjugated antibodies for the detection of biological molecules. The three enzymes most commonly used are HRP, AP and β-D-galactosidase (Kemeny, 1991). The ELISA is a quantitative method that measures interactions through a colorimetric reading, serving to identify and determine the presence and concentration of specific biological molecules (Gan & Patel, 2013; Hornbeck, 2001).

The ELISA method was invented simultaneously by two research groups at the same time (Engvall & Perlmann, 1971; Van-Weemen & Schuurs, 1971). The method and technique of an ELISA was developed largely from modifying a radioimmunoassay (RIA), which dates back as far as 1941 (Coons *et al.*, 1941). RIA is a sensitive method for measuring

small amounts of substance in biological fluids, with the method first being used by Yalow & Berson in the 1960s to measure endogenous plasma insulin levels (Yalow & Berson, 1960). The use of ELISA is now routinely used method in research and diagnostic laboratories around the world (Aydin, 2015).

The antigen utilised in the ELISA is bound to a solid-phase carrier (Aydin, 2015). Carriers for ELISA can be divided into two broad categories based on their ability to bind the protein. High-capacity materials include cyanogen bromide-activated agarose, cellulose and nitrocellulose. The advantage being that they can make use of relatively impure antigen preparations and are stable for several months. Disadvantages include high background binding and difficult washing steps. Low-capacity materials such as polystyrene, polyvinyl and polypropylene are used which are easier to wash and give a lower background noise; although they can be more difficult to coat with antigen. The choice of carrier used depends on several factors, the most important of these being the purity of the coating material. Assays using immunoglobulin G (IgG) antibodies can display non-specific binding; therefore, a low-capacity material is preferable (Engvall & Perlmann, 1971; Kemeny, 1991; Van-Weemen & Schuurs, 1971).

Once the antigen has bound to the 96-well microplates, vacant binding sites are blocked with an excess of irrelevant protein, such as BSA. This blocking step prevents any unnecessary binding of the antibody to the plate, and only allowing binding to the antigen (Kemeny, 1991). A primary antibody, specific to the antigen, can bind, which is itself subsequently detected by a secondary, species specific, enzyme-conjugated, antibody. The use of secondary, enzyme-conjugated antibodies allows an amplification of the signal for when detecting the antigen, in addition to the beneficial economic costs. Conjugating an enzyme to a secondary antibody that possesses the ability to bind to multiple monoclonal specific primary antibodies is significantly more cost effective. Washing is performed after

each step, usually with phosphate-buffered saline at neutral pH, in order for the removal of any unbound antigen/antibody. Addition of the enzyme substrate yields a visible colour change or fluorescence, indicating the presence of the antigen (Gan & Patel, 2013). The reaction is usually completed within 30 minutes and can be stopped by using either sodium hydroxide or sulfuric acid (Gan & Patel, 2013). Unlike the Western Blotting technique, the sensitivity of the reaction is heightened within an ELISA, allowing for the detection of significantly smaller amounts of protein. In addition, the quantitative method of analysis also allows for antigen concentrations to be calculated. One downside compared to a Western Blot however, is that the molecular weight of the antigen (usually a protein) is unknown alongside sample purity and they are prone to false positive/negative results (Gan & Patel, 2013; Murphy *et al.,* 2008). There are several types of ELISA commonly used in scientific practice, each modified slightly for a quantitative analysis of the antigen-antibody interaction. Capture or sandwich ELISA can be used to detect secreted products such as cytokines, rather than binding the antigen directly to the plate (Murphy *et al.,* 2008) These involve antigen specific antibodies (sometimes raised against different epitopes on the antigen) being bound to the base of the plate prior to the addition of antigen, to 'capture' the antigen in question (Murphy *et al.,* 2008).

2.1.8 Experimental Aims

Our aim here within this research is to implement our developed methodology, incorporating the discussed techniques, which can result in the production, purification and where possible, characterisation of *in vitro* produced mCRP. Furthermore, it was important that we aimed at reducing any damage to the proteins structural and biological integrity through these dissociation experiments. The techniques discussed within this chapter will help develop the groundwork needed in future studies when testing human serum samples.

2.2 Materials & Methods

2.2.1 Preparation of C-reactive Protein

Native, pCRP was purchased from SCRIPPS at 2.48mg/ml in a standard storage calcium buffer (20mM Tris, 280mM NaCl, 5mM $CaCl_2$, 0.01% Sodium Azide at pH 7.4). The samples provided were stored at 4^{o}C and confirmed by the supplier to be >99% pure by SDS PAGE analysis.

Dissociation buffers were produced (20mM Tris, 280mM NaCl, and 1mM EDTA) with varying concentrations of Urea (2, 2.5, 3 and 4M Urea) from a stock of 8M Urea. Dissociation samples were mixed thoroughly in a vortex and stored in the cold room at 4^{o}C for a minimum of 10 weeks.

2.2.2 Calibration of the Size Exclusion Chromatography Column

Prior to running any samples through the column, it first needed to be calibrated for protein sizes to be accurately determined via elution volumes. The AKTA explorer 100, Fast Protein Liquid Chromatography (FPLC) system from GE Healthcare was used, with a HiLoad 16/60 Superdex 200pg Column. The system runs on the software UNICORN 5.11. To monitor the elution volumes of the proteins the UV absorbance is measured at 280nm, creating an elution profile (Amersham Biosciences, 2003).

A Gel Filtration Calibration Kit of high and low molecular weight markers was purchased from GE Healthcare. The molecular weight markers included are shown in Table 2.1. Blue Dextran was also included to determine the void volume of the column. All samples were provided in a lyophilised form and reconstituted to a 20mg/ml stock solution, as recommended via the product booklet.

Protein Standard	**Known Molecular Weight (Da)**
Ferritin	440,000
Aldolase	158,000
Conalbumin	75,000
Ovalbumin	44,000
Ribonuclease A	13,700

Table 2.1 A Table of the protein standards and their respective molecular weights, which were used to construct the calibration graph for the HiLoad 16/60 Superdex 200pg size exclusion chromatography column.

The buffers and solutions used for preparing the column are outlined in Table 2.2. The column is stored in 20% ethanol. Three column volumes (120ml/column volume) of deionised water were used to remove the ethanol solution from the system tubing and the column. The column and tubing were equilibrated with three column volumes of elution buffer (see Table 2.2). Tris and NaCl were both purchased from Fisher Scientific and sodium azide was purchased from Sigma Aldrich. All buffers and solutions used on the column were filtered through a 0.2µm cellulose acetate filter (Sartorius Stedim Biotech, Geottingem, Germany) to remove any particulate matter that may clog the system and de-gassed, to avoid introducing air into the system. All buffers and solutions were stored at 4^{o}C and allowed to equilibrate to room temperature before use.

Buffer/Solution	Components	pH
Wash Solution	Deionised H_20	7.0
Elution Buffer	50mM Tris, 150mM NaCl, 0.01% Sodium Azide	7.2
Storage Solution	20% Ethanol	7.0

Table 2.2 Buffers and solutions that were used to equilibrate the HiLoad 16/60 Superdex 200pg size exclusion chromatography column.

To achieve the most reliable results, the product booklet for the molecular weight standards contained a list of parameters that needed to be adhered to. An elution buffer with an ionic strength ≤ 0.15 (e.g. 0.15M NaCl, see Table 2.2) needed to be used. Suitable protein mixtures of the molecular weight standards also needed to be prepared; running incorrect samples together could cause either protein precipitation or the potential clashing of elution peaks on the chromatogram. This therefore resulted in two separate chromatography runs; the first containing Ferritin, Conalbumin and Ribonuclease A, and the second containing Aldolase and Ovalbumin. Blue dextran was run separately to determine the void volume of the column.

Molecular weight standards were prepared from stocks as shown in Table 2.3. The protein standards were diluted with the same elution buffer that was used to equilibrate the column (see Table 2.3). The total volume of the sample was recommended to be between 0.1 to 2% of the total column volume to achieve the best resolution on the chromatogram, therefore a final volume of 500µl was used.

Protein Standard	Required Final Concentration (mg/ml)
Ferritin	0.3
Aldolase	4
Conalbumin	3
Ovalbumin	4
Ribonuclease A	3

Table 2.3. A table listing the protein standards used to construct the calibration graph and their respective final concentrations that were required.

The prepared samples containing the molecular weight standards were loaded onto the column via a 2ml sample injection loop. A flow rate of 1ml/min was used, as recommended via the product booklet, with the absorbance measured at 280nm. Sample fractions of 5ml were collected up to a total volume of 120ml (one column volume). All size exclusion chromatography was carried out at room temperature.

2.2.3 Purification of Pentameric and Monomeric C-reactive Protein

Once the column had been calibrated, the size exclusion column was used to assess the dissociation of pCRP into mCRP and to purify both isoforms from the sample. The system, column and software used for the size exclusion chromatography are the same as described in Section 2.2.2. All chromatography runs were carried out at room temperature.

The buffer and solutions used for preparing the column are outlined in Table 2.4. The column is stored in 20% ethanol and was purged with 3 column volumes of deionised water, as described in section 2.2.2. The column and tubing were equilibrated with three column volumes of standard CRP storage buffer (Table 2.4). NaCl and $CaCl_2$ were purchased from Fisher Scientific. Tris buffer and sodium azide were purchased from Sigma Aldrich. The

CRP storage buffer pH was adjusted by the addition of hydrochloric acid (HCl). All buffers and solutions used on the column were filtered through a 0.2µm cellulose acetate filter (Sartorius Stedim Biotech, Geottingem, Germany) to remove any particulate matter that may clog the system and de-gassed, to avoid introducing air into the system. All buffers and solutions were stored at 4^{o}C and allowed to equilibrate to room temperature before use.

Buffer/Solution	**Components**	**pH**
Wash Solution	Deionised H_2O	7.0
CRP Storage Buffer	280mM NaCl, 20mM Tris, 5mM $CaCl_2$, 0.01% Sodium Azide	7.4
Storage Solution	20% Ethanol	7.0

Table 2.4. A table listing the buffers and solutions that were used to equilibrate the size-exclusion column. All buffers were filtered through a 0.2µm filter and degassed before use.

Dissociation samples containing CRP were, as described in section 2.2.1, loaded onto the column via a 2ml sample injection loop. Based on the user guide recommendations, the sample volume did not exceed 0.1-2% of the column volume (120µL – 2.4mL) to obtain the best resolution. A flow rate of 0.5ml/min was used in all samples and the absorbance measured at 280nm. All experiments were carried out at room temperature. Sample fractions of 5ml were collected up to a total volume of 120ml (one column volume).

2.2.4 Concentration of C-reactive Protein Samples

Eluted protein samples were concentrated using a Vivaspin Centrifugal Concentrator, 10kDa molecular weight cut off (MWCO), purchased through Fisher Scientific. The centrifugal concentrator was initially primed with deionised water and spun

at 1,000 x g, 4°C for 10 minutes. The protein sample was then spun at 1,000 x g, 4°C for 15 minutes or until the desired concentration had been achieved.

2.2.5 Protein Quantification

The protein content of the CRP samples was determined by using a spectrophotometer, which measures the absorbance unit for full scale deflection of the protein solution at UV280nm. A UV reading at 320nm was also taken as background absorbance, as proteins do not absorb at this wavelength. The protein concentration of the CRP samples was determined by Equations 2.1 and 2.2.

Equation 2.1: $Absorbance\ at\ UV_{280mm} = UV_{280nm} - UV_{320nm}$

Equation 2.2: *Concentration (mg/ml) = Absorbance at 280nm / Extinction Coefficient*

Extinction coefficient values are worked out using the online programme *ProtParam* from Expasy (http://web.expasy.org/protparam/) which uses the protein sequence to calculate to the total absorbance of tyrosine and tryptophan and any disulfide bonds (Gasteiger *et al.,* 2003). The extinction coefficient value of 1.7 for human CRP was used to give concentration values in mg/ml.

2.2.6 Sodium Dodecyl Sulfate Polyacrylamide Gel Electrophoresis

SDS PAGE was used to assess the purity and size of the eluted protein from the size exclusion column. SDS PAGE gels usually consist of a 12.5%T resolving gel and a 4%T stacking gel. SDS, TEMED and 30%T acrylamide/bisacrylamide were all purchased from

Sigma. The stock acrylamide/bisacrylamide was stored at -20°C and was thawed at room temperature prior to use. APS (VWR) was made to a 10% solution prior to use.

Samples were added to either reducing or non-reducing sample buffer at a 1:1 ratio and the gel was run in a standard SDS PAGE running buffer (see Table 2.5). Glycine, glycerol and Tris were all purchased from Sigma. Reduced sample buffer requires the addition of β-Mercaptoethanol (Sigma) to 5% prior to use. Bromophenol blue (VWR) was used to visualise dye front whilst the gel was running. Low range molecular weight markers (BioRad) were ran alongside the samples for the estimation of band sizes. The molecular weight markers were stored in reducing buffer and kept at -20°C prior to use. All samples and markers were heated at 95°C for 5 minutes prior to being run on the gel. The typical well volume for each sample loaded was 10µL.

Gels were run vertically in a BioRad mini-PROTEIN II cell (BioRad), connected to a PowerPac 300 (BioRad). The gels were run at a voltage of 200V for approximately 45-50 minutes, in 500mL of running buffer (see Table 2.5).

Gel Type	**Components**	**Amount**
12%T Resolving Gel	Deionised Water	2.55ml
	30%T acrylamide/bisacrylamide	3.33ml
	1.5M Tris pH 8.8	2.0ml
	10% SDS	80µl
	10% APS	60µl
	100% TEMED	6µl

4%T Stacking Gel	Deionised Water	3.0ml
	30%T acrylamide/bisacrylamide	670µl
	0.5M Tris pH 6.8	1.25ml
	10% SDS	60µl
	10% APS	60µl
	100% TEMED	6µl
Sample Buffer	Tris-HCl pH 6.8	125mM
	SDS	4%
	Glycerol	20%
	Bromophenol Blue	0.02%
Reduced Sample Buffer	β-Mercaptoethanol	5%
Running Buffer 500ml	SDS	0.5g
	Glycine	7.21g
	Tris	1.515g

Table 2.5. Components for the casting and running of an SDS PAGE gel. The amounts given are enough to cast two identical 0.75mm SDS PAGE gels. Amounts are also given for sample and running buffers.

After 45 minutes, had elapsed, or the dye front had run off the gel, the gels were removed from the tank. Coomassie Brilliant Blue (BioRad), a total protein stain was used for SDS PAGE gel lanes containing molecular weight markers, whereas lanes containing eluted CRP samples were subject to Western Blot analysis. The section of gel containing the

molecular weight markers was immersed in Coomassie Brilliant Blue for a minimum of thirty minutes for the stain to penetrate the gel's pores and stain the protein. Once a sufficient level of staining had been achieved for the protein bands, to reduce background staining, gels were gently washed in deionised water and then photographed on a Syngene GBOX image detector. Coomassie Brilliant Blue has a detection limit of around 1µg of protein; therefore, a sufficient volume of sample was added to avoid this limitation.

2.2.7 Western Blotting of C-reactive Protein Samples

Samples which were used within the Western Blot transfer had previously been subject to SDS PAGE, as described in section 2.2.6. All western blot analyses were performed in the absence of staining the SDS PAGE gel with Coomassie Brilliant Blue. A minimum of 1µg per sample was used in the SDS PAGE. Sample quantification was determined as described in section 2.2.5. Once 45 minutes had elapsed, or the dye front had run off the gel, the gel was removed from the tank and immersed into equilibration buffer (as shown in Table 2.6) for up to 30 minutes. Prior to running the SDS PAGE, nitrocellulose membrane blotting paper (0.2µm, 7x8.4cm, pre-cut) and filter pads (BioRad) were pre-soaked for up to 1 hour in equilibration buffer (Table 2.6). Resolving gels were then added to the equilibration buffer for a further 30 minutes.

The gel, nitrocellulose blotting paper and filter pads were assembled in cassette cases of the Mini Trans-Blot Electrophoretic Transfer Cell (BioRad). Prior to the transfer, an ice pack, to prevent overheating, and a magnetic stirrer, to maintain a consistent flow of running buffer (Table 2.6) throughout the tank were added. The transfer cell was connected to the PowerPac 300 (BioRad) and run at 350mA for 1 hour at 4^{o}C. Approximately 500ml of running buffer was added to the tank during protein transfer.

Buffer/Solution	Components	Amount
Running Buffer/Equilibration Buffer	SDS	0.5g
	Tris	7.21g
	Glycine	1.515g

Table 2.6. A Table of components for the running and equilibration buffers needed for protein transfer during the Western Blot analysis. Amounts of each component are also given.

Once the transfer was complete, the nitrocellulose membrane was removed from the cassette and placed in a container with blocking solution (protein side facing up) and blocked overnight. Marvel dried milk powder was used with Tris-buffered saline (TBS) for the blocking solution (see Table 2.7). Marvel dried milk was purchased from the local supermarket. The membrane was then washed 5 times with BLOTTO solution (5 minutes for each wash, see Table 2.7). Triton-X-100 was purchased from Sigma. The primary antibody was added at a dilution of 1:1,000, made up in BLOTTO, and left for a minimum of 5 hours. The primary antibody used was a monoclonal anti-C-reactive protein antibody (Clone-8), produced in a mouse. The monoclonal antibody was purchased from Sigma and was provided in ascites fluid. The antibody concentration reading was 9.1mg/ml and was stored at -20^{o}C, with the sample being thawed out prior to use. A volume sufficient to immerse the nitrocellulose membrane was used (>20ml).

The membrane was then washed 5 times with BLOTTO (5 minutes for each wash). The secondary antibody used was an anti-mouse IgG (whole molecule) HRP antibody, produced in a rabbit. The enzyme conjugated IgG antibody was purchased from Sigma and provided as a fraction of antiserum, buffered in aqueous solution. The antibody concentration reading was 10.6mg/ml and stored at -20^{o}C, with the sample being thawed out prior to use. The secondary antibody was diluted in BLOTTO at 1:40,000 and added to the

nitrocellulose membrane for a minimum of 1 hour. A volume sufficient to immerse the nitrocellulose membrane was used (>20ml).

Buffer/Solution	**Components**	**Amount**
Tris-buffered Saline (TBS) pH 7.4 with HCl	Sodium Chloride	150mM
	Tris	50mM
Blocking Solution	Marvel Dried Milk	1g
	TBS	40ml
BLOTTO	Marvel Dried Milk	0.5g
	Triton-X-100	1ml
	TBS	50ml
Primary Antibody Dilution	Monoclonal anti-CRP Antibody	6µl
	BLOTTO	23.994ml
Secondary Antibody Dilution	Anti-mouse IgG (whole molecule) peroxidase Antibody	1µl
	BLOTTO	39.999ml
ECL Reagent	Clarity peroxidase reagent	7ml

	Clarity western luminol/enhancer reagent	7ml

Table 2.7. A Table of components for the staining of the nitrocellulose membrane during the Western Blot analysis. Amounts for each component are also given.

The membrane was then washed 7 times with BLOTTO (5 minutes for each wash). Chemiluminescence was used to enable visualisation of the bands on the nitrocellulose membrane. The reagent used was the Clarity Western Enzyme Chemiluminescence (ECL) Substrate, purchased from BioRad. The ECL reagent provided high sensitivity for detecting protein on a nitrocellulose membrane when using an enzyme-conjugated horseradish peroxidase antibody (secondary antibody). Two reagents were included in the ECL Clarity package; Clarity peroxide reagent and Clarity western luminol/enhancer reagent. For mini-sized membranes (7x8.5cm), 7ml of each reagent was advised and made prior to use (see Table 2.7). All steps were carried out on the rocking machine to encourage gentle agitation of the solution with the nitrocellulose membrane.

The combined ECL reagents were added to the membrane and left for a minimum of 5 minutes. The membrane was then removed from the reagent and was wrapped in Saran Wrap (protein side up) to prevent the membrane from drying out. The membrane was then viewed on a CCD digital image detector and exposed for up to 30 minutes, depending on the intensity of the band required.

2.2.8 Binding Studies of Monomeric and Pentameric C-reactive Protein with Phosphocholine

Immobilised *p*-Aminophenyl Phosphoryl Choline (APC) was purchased from Fisher Scientific in the form of a gel, cross-linked with 6% beaded agarose. The gel had a constant storage temperature of 4^{o}C, with 5ml provided. The binding capacity of the APC was >3mg of CRP per 1ml of gel. The sample was purified from ascites fluid by centrifugation and

filtration. All affinity chromatography experiments were run using the Biologic LP Chromatography System, purchased from BioRad. The software used was LP Data View (BioRad). The absorbance was measured at 280nm. Prior to mCRP being run through the column, 20 column volumes of equilibration buffer were run through the column at 0.5ml/min (see Table 2.8). The UV absorbance baseline reading was blanked to a value of 0 absorbance units (Au). 500µl of the CRP (both monomeric and pentameric) sample was diluted in 5ml of the equilibration buffer. Larger volumes of samples were used to prevent air bubbles entering the column whilst applying a sample. The mCRP sample was run through the column at 0.5ml/min. Once the entire sample had been applied, 5 column volumes of equilibration buffer were run through the column at a flowrate of 0.5ml/min.

The chelating buffer was then added to the column. Around 3-4 column volumes of chelating buffer were run through the column, or until the UV absorbance reading had returned to its baseline value of 0Au. The column was then washed with 10 column volumes of equilibration buffer, ready for storage.

Buffer/Solution	**Components**	**Concentration**
Equilibration Buffer pH 7.4	Calcium Chloride	10mM
	Tris	50mM
	Sodium Chloride	150mM
	Sodium Azide	0.01%
Chelating Buffer pH 7.4	EDTA	10mM
	Tris	50mM

	Sodium Chloride	150mM
	Sodium Azide	0.01%

Table 2.8. A list of the components for the equilibration and chelating buffers required during a run of the phosphocholine-bound affinity chromatography column. Concentrations of each component used are also given.

Following the PC-based purification of pCRP, the sample was subject to size exclusion chromatography as described in Section 2.2.3. Eluted affinity chromatography fractions were concentrated as described in Section 2.2.4 prior to application on the size exclusion column.

2.2.9 Precipitation Studies with Cell Wall Polysaccharide

The precipitation experiment involving pCRP and mCRP was adapted from previous work carried out by Volanakis, (1982), when researching into how pCRP precipitates out with varying amounts of ligand. Native, pCRP (purchased from SCRIPPS) alongside mCRP (dissociated with 3M urea) were incubated with varying amounts of CWPS. Precipitation levels were calculated based on the remaining concentration of protein within the supernatant via an ELISA. Prior to this, calibration of both proteins was required, to calculate the precipitated levels of both proteins. All ELISA analysis was performed on 96-well microplates. Table 2.9 displays the amounts of CRP used (µg) for the calibration experiments using either pCRP (SCRIPPS) and *in vitro* produced mCRP (via 3M Urea).

		1	2	3	4	5	6	7	8	9	10
A	**pCRP (µg)**	0.75	0.375	0.187	0.093	0.046	0.023	0.011	0.005	0.002	Blank
B		0.75	0.375	0.187	0.093	0.046	0.023	0.011	0.005	0.002	Blank
C		0.75	0.375	0.187	0.093	0.046	0.023	0.011	0.005	0.002	Blank
D	**mCRP (µg)**	0.75	0.375	0.187	0.093	0.046	0.023	0.011	0.005	0.002	Blank
E		0.75	0.375	0.187	0.093	0.046	0.023	0.011	0.005	0.002	Blank
F		0.75	0.375	0.187	0.093	0.046	0.023	0.011	0.005	0.002	Blank

Table 2.9 The varying amounts of both pCRP and mCRP used for the construction of calibration graphs via ELISA analysis. All samples were triplicated with the average value used when constructing the calibration graph.

Samples for both pCRP and mCRP used in ELISAs were treated and developed as described in section 3.2.9. The primary monoclonal antibody dilution used was 40,000 as suggested by the supplier, as was the secondary antibody dilution. Samples were developed with TMB for 5-10 (2M sulphuric acid added to stop the reaction) and then read at 450nm on a BioTek EL800 plate reader using the Gen5 Software.

Pentameric CRP and *in vitro* produced mCRP (20µg per sample) were incubated with varying amounts of CWPS, as shown in Table 2.10.

		Amount of CWPS (µg)									
		1	**2**	**3**	**4**	**5**	**6**	**7**	**8**	**9**	**10**
A	**pCRP**	0.1	0.5	1	10	20	50	100	200	300	Blank
B	**(20µg**	0.1	0.5	1	10	20	50	100	200	300	Blank
C	**used)**	0.1	0.5	1	10	20	50	100	200	300	Blank
D	**mCRP**	0.1	0.5	1	10	20	50	100	200	300	Blank
E	**(20µg**	0.1	0.5	1	10	20	50	100	200	300	Blank
F	**used)**	0.1	0.5	1	10	20	50	100	200	300	Blank

Table 2.10 The varying amounts of CWPS used within the precipitation experiments. Precipitation levels for both pCRP and the *in vitro* produced mCRP were calculated by ELISA analysis of the remaining supernatant, once mixed with CWPS and centrifuged.

Samples were made up to 400µl using a standard storage calcium buffer (see section 2.2.1). All samples were then incubated at 37^{o}C for 1 hour whilst being gently agitated. The samples were then centrifuged at 6,500 x g for 15 minutes to pellet the precipitate within the sample. The supernatant from each sample was transferred to separate tubes.

The supernatant from each sample was then subject to an ELISA, as described in section 3.2.9. Primary and secondary antibody dilutions used were as per the calibration (40,000), with samples being developed in TMB (for the same period as the calibration). Samples were then read at 450nm. CRP concentrations were determined using the calibration line equations. Total level of precipitation was calculated by subtracting the total amount of CRP remaining from the initial amount (20µg).

2.3 Results

2.3.1 Calibration of the Size Exclusion Chromatography Column

Size exclusion chromatography was used to assess the level of dissociation of pCRP into *in vitro* produced mCRP and to purify out both protein forms from the sample. Prior to the use of this technique within our research, the column needed to be calibrated for us to determine/establish accurately where pentameric, monomeric and other possible CRP isoforms would be eluted. The gel filtration calibration kit purchased from GE Healthcare provided a range of proteins with known molecular weights. A calibration graph was plotted based on the elution volume of each protein standard. This calibration was used throughout our research to determine the molecular weight of protein which had been run through the size exclusion column.

For the calibration of the size exclusion column, three separate runs were carried out as suggested by the GE Healthcare Calibration User Guide. This was to avoid the clashing of peaks on the chromatogram and to avoid mixing protein standards which may cause precipitation within the sample. Figure 2.1 shows the chromatography trace for the molecular weight standards aldolase (158kDa) and ovalbumin (43kDa). The sample was injected into the column at 0ml and two peaks were observed at elution volumes of 76.37ml (55.98mAu) and 87.64ml (87.63mAu) for aldolase and ovalbumin respectively.

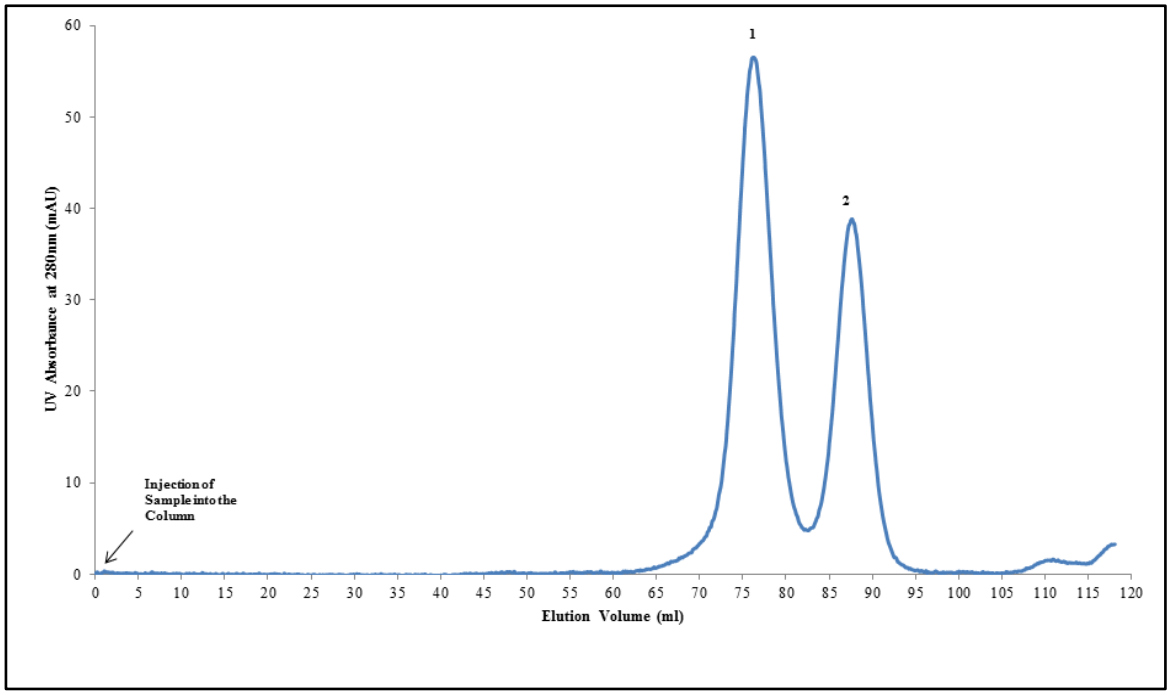

Figure 2.1 A size exclusion chromatography trace of the molecular weight standards Aldolase (158kDa) and Ovalbumin (43kDa). Aldolase, peak 1, has an elution volume of 76.37ml. Ovalbumin, peak 2, has an elution volume of 87.64.

The second chromatography run used molecular weight standards ferritin (440kDa), conalbumin (75kDa) and ribonuclease A (13.7kDa) (see Figure 2.2). Three main peaks were

observed (peaks 2-4, Figure 2.2) with elution volumes of 64.41ml (7.55mAu), 83.2ml (40.59mAu) and 100.32ml (38.49mAu), as expected. A fourth, smaller peak was observed at 46.07ml (1.01mAu). Based on the calculated molecular weight and absorbance reading of this fourth peak, it was unclear what it represented. It was therefore disregarded within our line of experiments as it did not contribute towards the calibration of the size exclusion column.

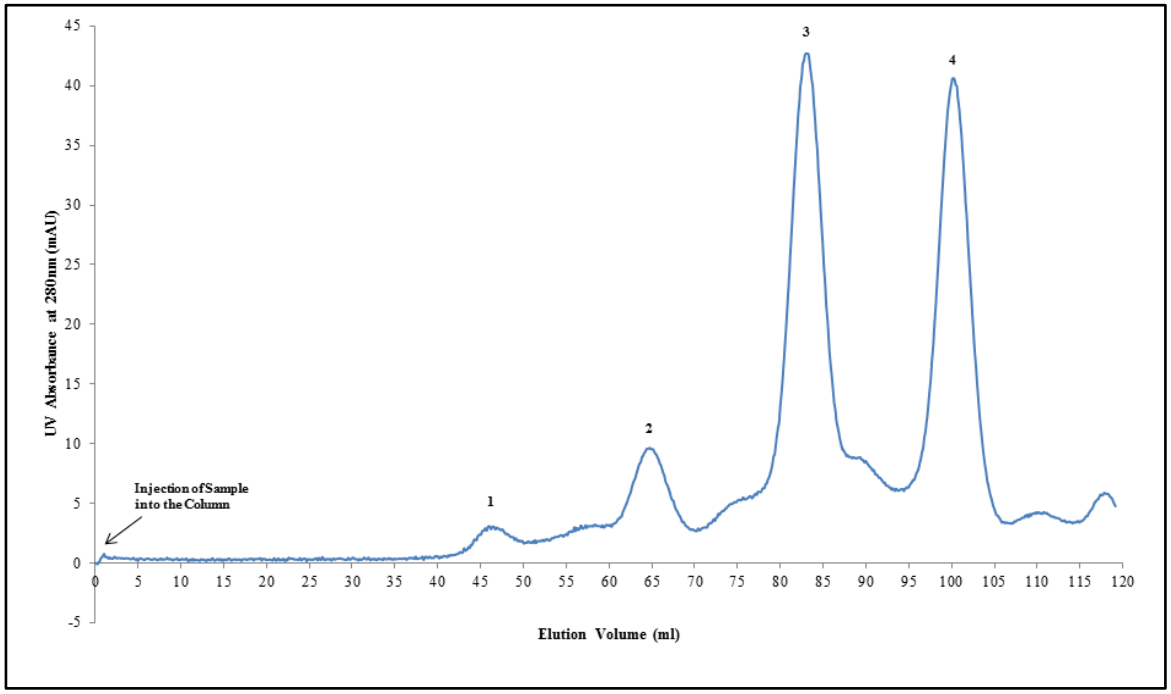

Figure 2.2 A size exclusion chromatography trace of the molecular weight standards Ferritin (440kDa), Conalbumin (75kDa) and Ribonuclease A (13.7kDa). Ferritin, peak 2, has an elution volume of 64.41ml. Conalbumin, peak 3, has an elution volume of 83.2ml. Ribonuclease A, peak 4, has an elution volume of 100.32ml. Peak 1 displayed an elution volume of 46.07, although it is unclear what this peak represents.

The third calibration only used Blue Dextran, a high molecular weight glucose polymer which can be used to determine the void volume of the column. Blue Dextran was used to determine the void volume of the column. The chromatography trace of Blue Dextran

shows one sharp single peak (see Figure 2.3). The peak displays a slight 'shoulder' on its right-hand side and extends all the way to the end of the chromatography trace as expected, with UV absorbance not returning to baseline levels

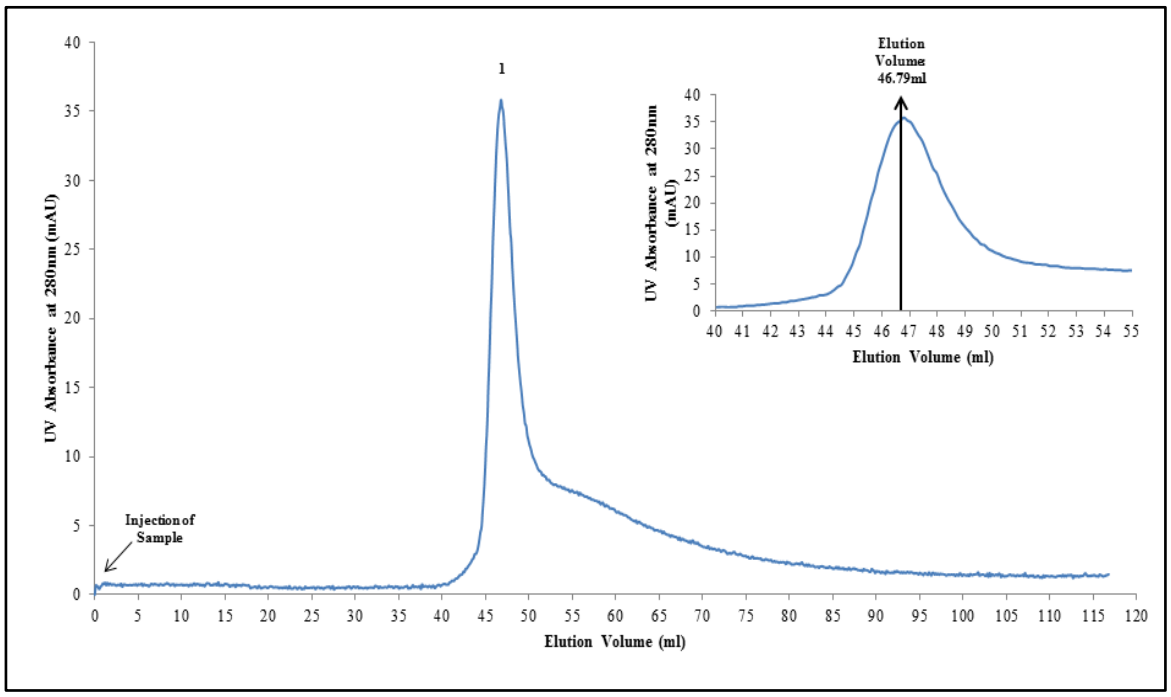

Figure 2.3 A size exclusion chromatography trace for Blue Dextran, a high molecular weight glucose polymer. Peak 1 is labelled on the graph, with an elution volume of 46.79ml. This is highlighted in the magnified graph of the elution region of 40-55ml. The absorbance was measured at 280nm.

The elution profiles of the molecular weight standards were then used to construct a calibration graph for the size exclusion chromatography column. Based on each individual elution volume for the protein standards, a Kav value was determined. This was calculated from the following equation:

Equation 2.3: *Kav = (Elution Volume – Void Volume)/(Total Column Volume – Void Volume)*

The total column volume was calculated to be 120.63ml (π x radius x length) and the void volume of the column was calculated to be 46.79ml from the chromatography run with Blue Dextran, as shown in Figure 2.3.

Protein	**Molecular Weight (Da)**	**Elution Volume (ml)**	**Kav Value**	**Log of Molecular Weight**
Ferritin	440, 000	64.41	0.239	5.64
Aldolase	158, 000	76.37	0.401	5.19
Conalbumin	75, 000	83.20	0.493	4.87
Ovalbumin	43, 000	87.64	0.553	4.63
Ribonuclease A	13, 700	100.32	0.725	4.13

Table 2.11 Elution volumes for all the molecular weight standards and their calculated Kav values. The Log of the molecular weight for all standards is also shown.

Table 2.11 shows the calculated Kav values for each of the protein molecular weight standards in addition to the Log of each of the protein standards' molecular weight. These two values for each molecular weight standard were plotted against each other to construct a calibration graph, as shown in Figure 2.4.

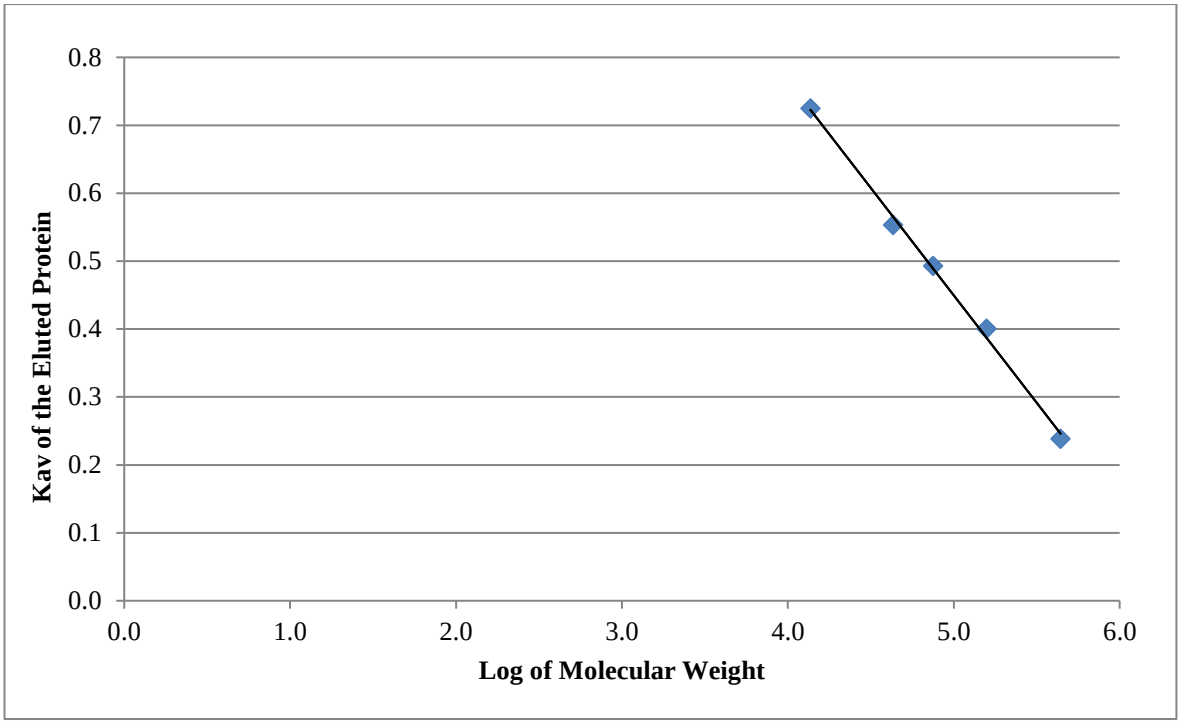

Figure 2.4 A graph of the Kav of each of the molecular weight standards plotted against the log of their molecular weight. The R^2 value is 0.9968. The line equation for the graph is as follows: $y = -0.3163x + 2.0311$.

The calibration graph displays an R^2 value of 0.9968, indicating a strong negative correlation for the data points, which indicates an inverse relationship, where the larger the elution volume, the smaller the molecular weight of the protein. The line equation of the calibration graph is as follows:

Equation 2.4: $y = -0.3163x + 2.0311$

Equation 2.4 describes the relationship between the Kav of the molecular weight protein standards and the Log of their molecular weight. By running a protein through the size exclusion chromatography column, its molecular weight can therefore be determined through this equation. The ability to calculate a protein's molecular weight based on its elution volume will enable reliable/accurate identification of CRP molecular variants based

on the number of monomers present in the molecule from *in vitro*-produced and purified serum samples – or some similar sentence.

2.3.2 Purification of Monomeric C-reactive Protein

In addition to the calibration of the size exclusion chromatography column, a control sample of the pCRP (which was not subject to dissociation) was run through the column to establish an elution volume for the native protein. The chromatography trace for pCRP is shown in Figure 2.5. One peak is observed, at an elution volume of 79ml (8.2mAU). Based on the calibration graph, this elution volume corresponds to a size of around 110kDa for the eluted protein. This corresponds to the known molecular weight of pCRP of 115kDa (Shrive *et al.*, 1996).

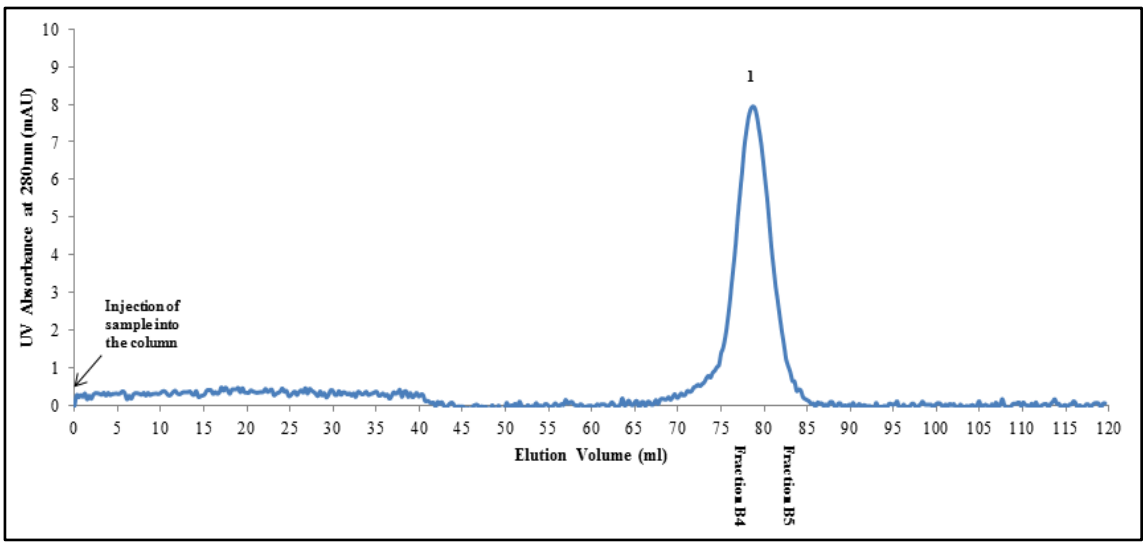

Figure 2.5 A size exclusion chromatography trace for the pCRP control run. 200µg of the protein was run through the column. The one main peak on the chromatogram, labelled 1, has an elution volume at 79ml (8.2mAU).

To dissociate native, pCRP into mCRP the protein was exposed to a dissociation buffer containing urea and the calcium chelator, EDTA. Research within the group (J Moran, unpublished results) has shown that removal of calcium is required to effectively dissociate pCRP with urea buffer. A period of 10 weeks for a dissociation trial with 2M urea and 5mM EDTA resulted in only approximately 10% of the pCRP to dissociate into mCRP (J Moran,

unpublished results). To determine whether moderate concentrations could be used to successfully dissociate all the pCRP in a 10-week period, several different dissociation trials were initiated with varying concentrations of urea. Figure 2.6 shows a size exclusion chromatography trace for a 2M urea dissociation trial after a 10-week period. Two peaks are observed on the chromatography trace, like that recorded from J. Moran's unpublished results. The larger of the two peaks, peak 1, was eluted off at a volume of 79.02ml into the fraction collection tubes B4 and B5. Based on the calibration graph, the elution volume for peak 1 indicates a protein with a molecular weight of 108kDa. The elution profile and volume of peak 1 is like that of the pCRP (see Figure 2.6). Peak 2, which was significantly smaller, eluted at 95.65ml into the fraction collection tubes B7 and B8, corresponding to a calculated molecular weight of 21.3kDa, which corresponds to an expected monomer molecular weight. Fractions which corresponded to elution peaks for all size exclusion chromatography runs were combined respectively and concentrated to the appropriate protein concentration (as described in section 2.2.4) and stored at 4ºC for further experimental analysis. All samples were injected at 0ml with the UV absorbance being read at 280nm.

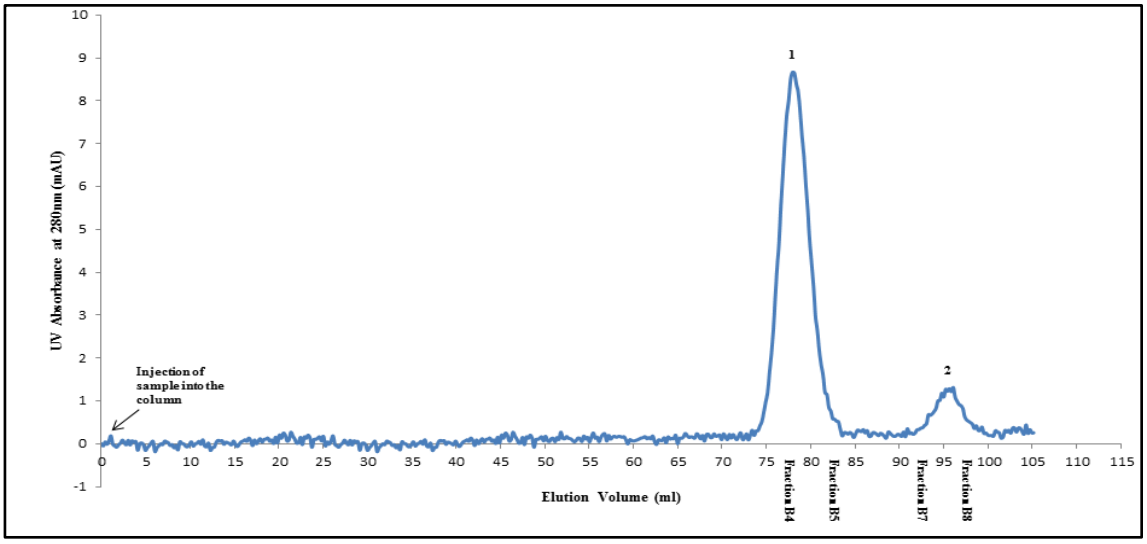

Figure 2.6 A size exclusion chromatography trace for the CRP 2M urea dissociation experiment. The sample was run through the system 10 weeks after the initiation of the

experiment. Both peaks are labelled on the graph (1 and 2). The elution volume for peak one is 79.02ml and the elution volume for peak 2 is 95.65ml. Fractions that were collected for further experimental analysis are also labelled (B4, 5, 7 and 8).

Figure 2.7 shows the size exclusion chromatography trace for a 2.5M urea dissociation trial after 10 weeks. The chromatogram shows similarities to the 2M urea dissociation in that two peaks are observed at similar elution volumes. Peak 1 was eluted off at 79.09ml, and peak 2 at 95.68ml, corresponding to 109kDa and 21.2kDa respectively. The peaks observed in Figure 2.7 show a marked difference in absorbance compared to that from the 2M urea dissociation trial. Peak 1 gave an absorbance of 2.4mAU whereas the absorbance for peak 2 was 8.9mAU. Comparison with Figure 2.6 shows a significant change in the absorbance, with peak 2 now displaying a higher level of absorbance. Eluted fractions B4 and B5 were combined and B7 and B8 combined and concentrated to the appropriate volumes for further experimental analysis. An additional, smaller peak was recorded in the chromatography trace with an elution volume of 113.2ml. Based on the calculated molecular weight of the elution volume, and the absorbance value, it was unknown what this additional peak represented. Based on these points, the peak was disregarded as irrelevant within these experimental trials and was not pursued any further.

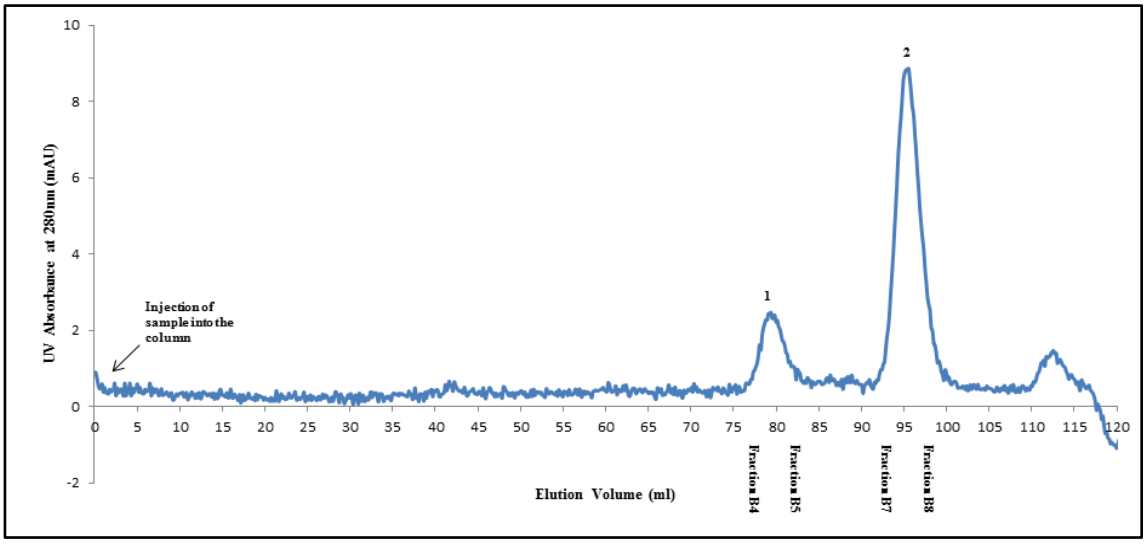

Figure 2.7 A size exclusion chromatography trace for the CRP 2.5M urea dissociation

experiment. The sample was run through the system 10 weeks after the initiation of the experiment. Both peaks are labelled on the graph (1 and 2). The elution volume for peak one is 79.09 and the elution volume for peak 2 is 95.68ml. Fractions that were collected for further experimental analysis are also labelled (B4, 5, 7 and 8).

The corresponding chromatography trace for treatment of pCRP with a 3M urea dissociation buffer for 10 weeks is shown in Figure 2.8. As previously observed, two peaks were seen at 79.60ml (103kDa), and at 94.97ml (22kDa). Although there are similarities with those shown in Figures 2.6 and 2.7, there is a marked increase in absorbance for Peak 2 which gives a reading at 32mAU. Peak 1 showed an absorbance value of 1.14mAu, slightly reduced to Peak one in Figure 2.7.

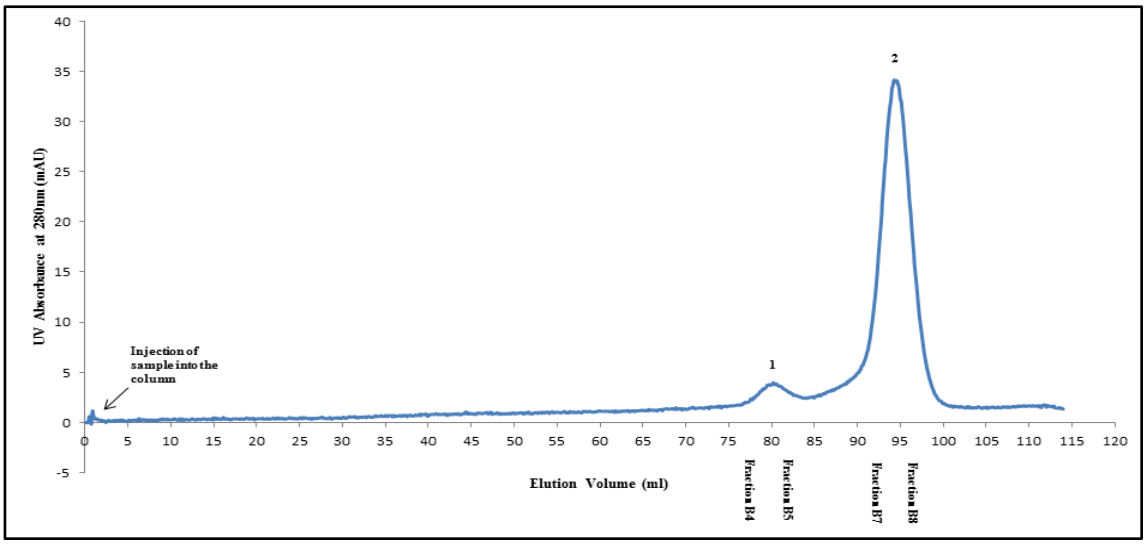

Figure 2.8 A size exclusion chromatography trace for the CRP 3M urea dissociation experiment. The sample was run through the system 10 weeks after the initiation of the experiment. Both peaks are labelled on the graph (1 and 2). The elution volume for peak 1 is 79.60ml and the elution volume for peak 2 is 94.97ml. Fractions that were collected for further experimental analysis are also labelled (B4, 5, 7 and 8).

Figure 2.9 shows the final dissociation trial of 4M urea with pCRP when run through the size exclusion chromatography column. As demonstrated in previous trials, two main peaks were observed (1 and 2) on the chromatogram. Peak 1 was eluted off at 79.27ml

(1mAU), which was calculated to be a protein with a molecular weight of around 107kDa. Peak 2 was eluted off at 94.90ml (6.01mAU), giving a protein with a molecular weight of around 22kDa. It is worth noting that although there is a similar pattern to the peaks observed in Figure 2.9 to previous dissociation trials, there is an overall decreased absorbance to that of Figures 2.8, 7 and 6 due to a smaller amount of protein being used in this dissociation trial. A third unexpected peak is also shown in Figure 2.9, eluting off at 112.25ml, with an absorbance of.5mAU. This elution volume was calculated to represent a protein with a molecular weight of 4.15kDa. Based on the calculated molecular weight of the peak, the sample in question was deemed not relevant to our study and was thus not pursued any further.

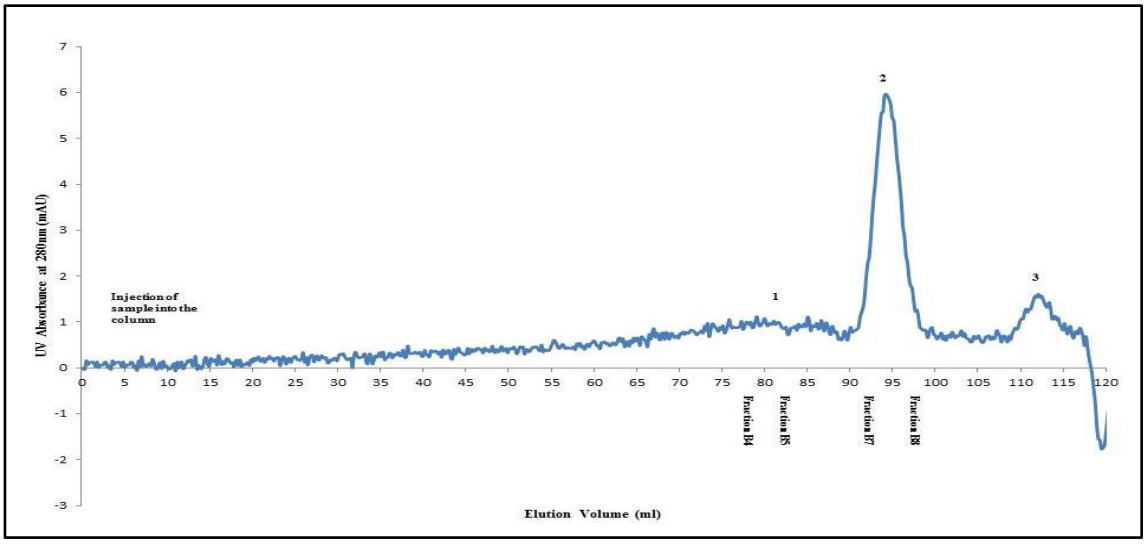

Figure 2.9 A size exclusion chromatography trace for the CRP 4M urea dissociation experiment. The sample was run through the system 10 weeks after the initiation of the experiment. All peaks are labelled on the graph (1-3). The elution volume for peak 1 is 79.27ml, the elution volume for peak 2 is 94.90ml and the elution volume for peak 3 is 112.25ml. Fractions that were collected for further experimental analysis are also labelled (B4, 5, 7 and 8).

Upon purification via size exclusion chromatography, all urea-induced dissociated CRP samples were stored in a standard calcium storage buffer (see Section 2.2.1) at 4^{o}C. It

is worth noting that during storage periods, none of the samples from any of the dissociation trials displayed any indication of re-association into higher molecular weight aggregates.

2.3.3 Western Blotting of Monomeric and Pentameric C-reactive Protein

As the size exclusion chromatography system only separates out proteins based on their size, further analysis was required to confirm that the observed peaks are pCRP and mCRP. Therefore, fractions B4 & 5 and B7 & 8 were collected from all dissociation experiments and subject to SDS PAGE and Western Blot analysis. Prior to Western Blot analysis, protein quantification (see Section 2.2.5) revealed that up to 50% of the initial protein for all four dissociation samples had been lost through the purification and concentration process, as described in Section 2.2.3 and 2.2.4.

Western Blot analysis was carried out on fractions B4+5 and B7+8 from each of the dissociation experiments (2, 2.5, 3 and 4M urea) and the 3M urea dissociated mCRP sample which had been run through the PC-bound affinity column (as shown in Figure 2.10 & 2.11, also see section 2.3.4). All samples were run on an SDS PAGE then subjected to a Western Blot procedure, as described in section 2.2.6 and 2.2.7. Western Blot analysis was performed with a CRP specific, Clone-8 antibody produced in a mouse, (Sigma) to be confident that the band we had observed was CRP. Figure 2.10 shows the Western Blot results for the B4+5 fractions for each of the dissociation trials. All four samples show a positive band for the presence of CRP.

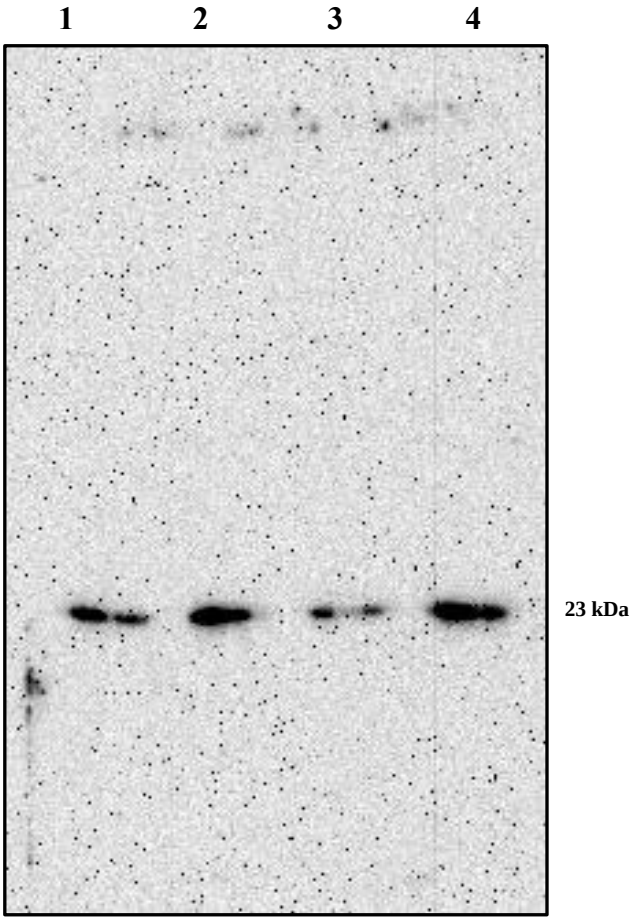

Figure 2.10 A Western Blot analyses of the B4+5 fractions for each of the CRP dissociation experiments. Lanes 1-4 contain 2, 2.5, 3 and 4M urea-dissociated samples respectively.

Figure 2.11a, shows the Western Blot results for each of the urea dissociated samples (2, 2.5, 3 and 4M from fractions B7+8). Each lane contains one band, corresponding to the expected mCRP molecular weight of 23kDa. Figure 2.11b is a sample of the 3M urea dissociation trial which was run through the PC-bound affinity column (see section 2.2.11 + 2.3.4). Like that observed in Figure2.11a, the sample displays one positive band for CRP at a molecular weight of around 23kDa. Figure ‘c’ contains the molecular weight markers that were run with the sample in order to roughly determine their molecular weight.

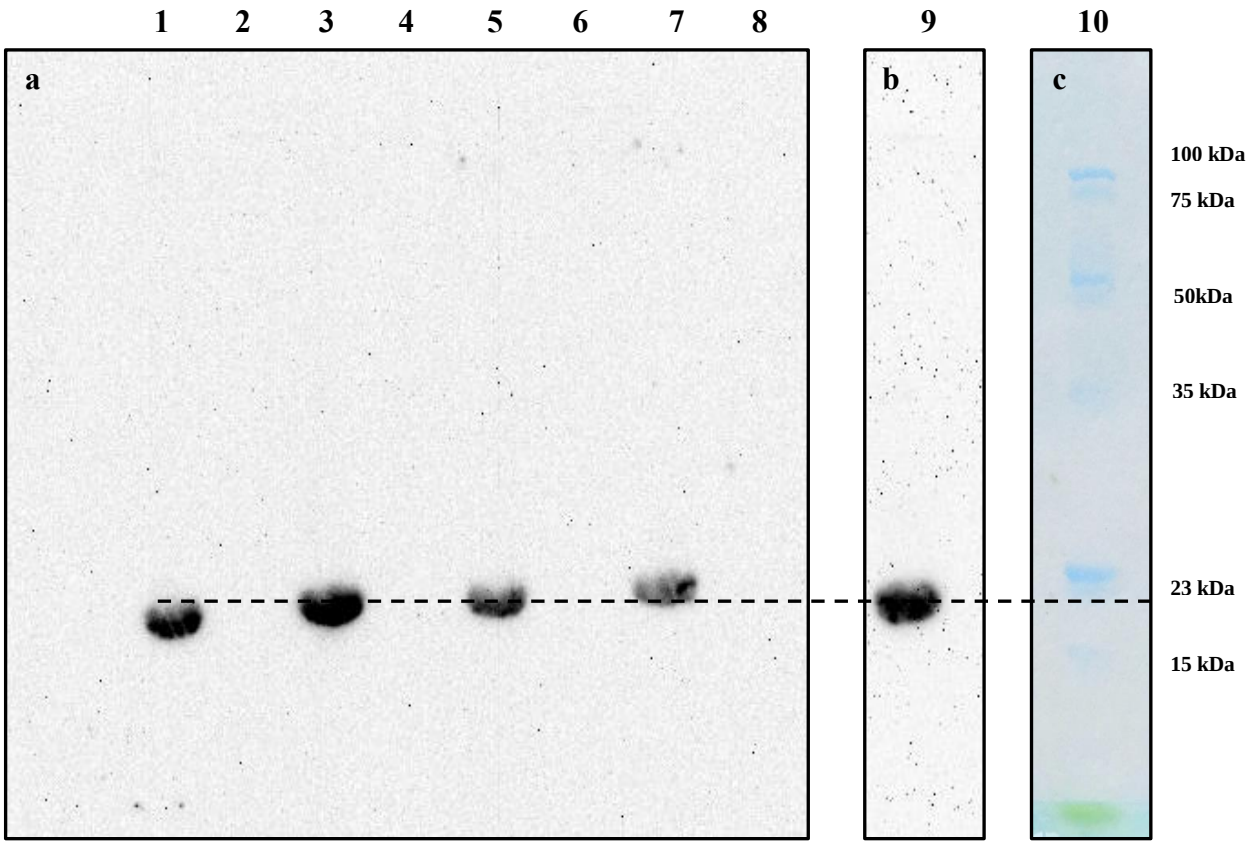

Figure 2.11 A Western Blot of the dissociated CRP samples. a) A Western Blot of the dissociated CRP samples (fractions B7+8) from the urea dissociation trials. Lane 1: 2M urea sample, lane 3: 2.5M urea sample, lane 5: 3M urea sample, Lane 7: 4M urea sample. All other lanes contained buffer. b) A Western Blot (from the same gel as a) of the 3M urea-produced mCRP sample which has been run through the PC-bound affinity column. c) Molecular weight markers (same gel) which have been stained in Coomassie Brilliant Blue.

2.3.4 Binding Monomeric and Pentameric C-reactive Protein with Phosphocholine

Native, pCRP binds to dead or damaged cells within the human body to generate an immune response. When cells become damaged, they express PC on their surface, for the recognition and binding of immune proteins. PC is pCRP's primary ligand, to which it binds with the highest affinity (Thompson *et al.*, 1999). To test whether the *in vitro* produced mCRP retained the ability to bind PC, a sample from the 3M urea dissociation trial was run through a PC-bound affinity column. The chromatography trace from the column run is

shown in Figure 2.12. The mCRP sample used was from the same stock of that produced in the 3M urea dissociation trial. Prior to running the sample through the column, it was pre-equilibrated with standard calcium buffer (see Section 2.2.1), an essential component to allow CRP to bind to PC. A total of 250µg was loaded and run through the column at a flowrate of 0.5ml/minute. Two main peaks were observed on the chromatography trace; these are labelled in Figure 2.12 as peaks 1 and 2. Peak 1 is shown 20 minutes after the application of the sample onto the column and gave an absorbance reading of 0.01AU. Once the UV absorbance reading had flat-lined, EDTA chelating buffer was run through the column. Peak 2 is shown 15 minutes after the chelating buffer was run through the column and gave an absorbance reading of 0.03AU. The UV absorbance was measured at 280nm.

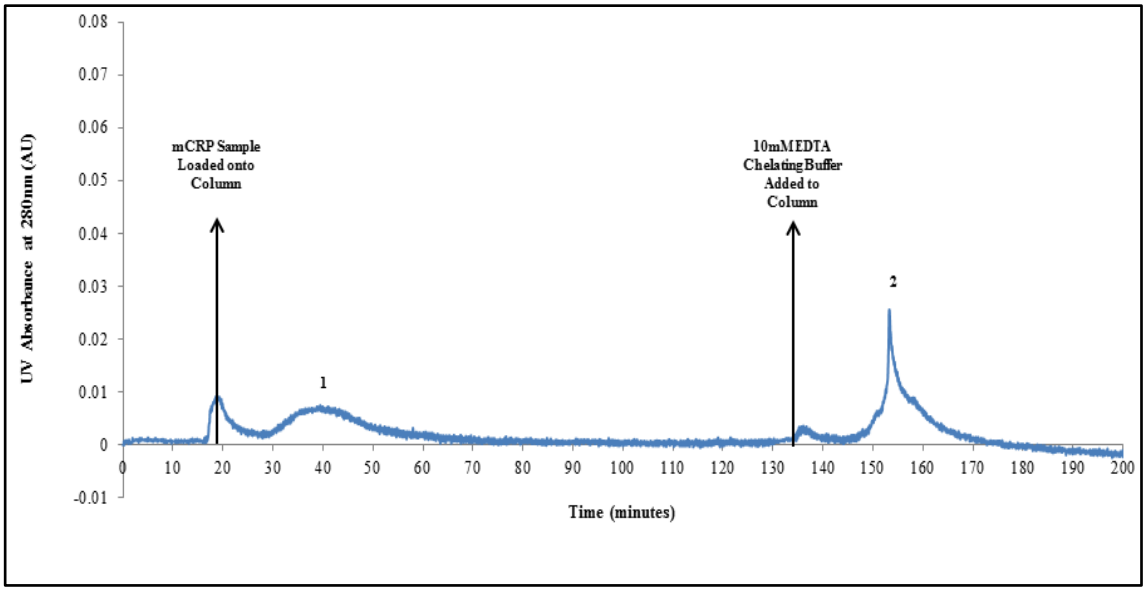

Figure 2.12 A chromatography trace of *in vitro* produced mCRP (from 3M Urea) being run through a PC-bound affinity column. A fluctuation in the UV absorbance reading was recorded, as shown by peak 1, due to the addition of the sample to the column (see Marker 1). Peak 2 represents the point at which the protein, mCRP, was eluted off the PC column through the addition of the calcium chelator EDTA (see Marker 2).

2.3.5 Precipitation Studies with C-reactive Protein

CRP was named due to its ability to bind and precipitate out the C-polysaccharide that is expressed on the cell wall surface of *Streptococcus pneumoniae* (McCarthy, 1982).

Previous experimental work carried out by Volanakis (1982) demonstrates that the precipitation of CRP with CWPS follows a general bell curve. These results are like that observed in antibody-antigen complexes; too little or too much ligand results in reduced precipitation, with an equivalence zone between the two displaying an increase in precipitation (Volanakis, 1982).

To determine whether the *in vitro* produced mCRP samples retained an ability to bind and precipitate with CWPS and follow the generic precipitation bell curve like that observed pCRP, samples were incubated with CWPS, with precipitation levels calculated via ELISA analysis on the remaining supernatant. Precipitation experiments were carried out on pCRP (SCRIPPS) and *in vitro* produced mCRP from a 3M urea dissociation experiment. Samples were incubated with CWPS to determine whether they would follow previously published precipitation trials (Volanakis, 1982). Prior to the precipitation experiments, ELISA calibration experiments were conducted for both pCRP and mCRP to determine the levels of CRP precipitated when combined with CWPS (as shown in Figure 2.13)

Graph a.

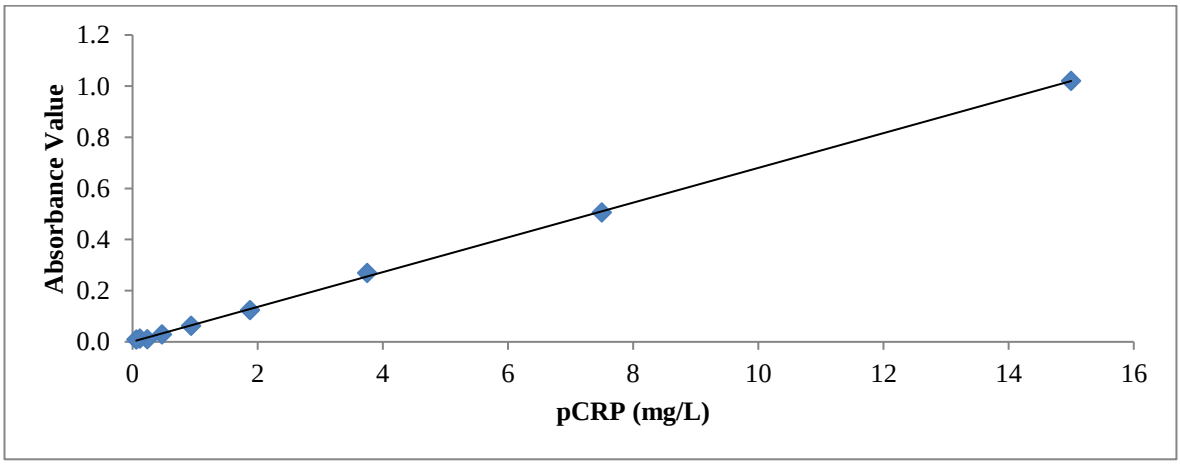

Graph b.

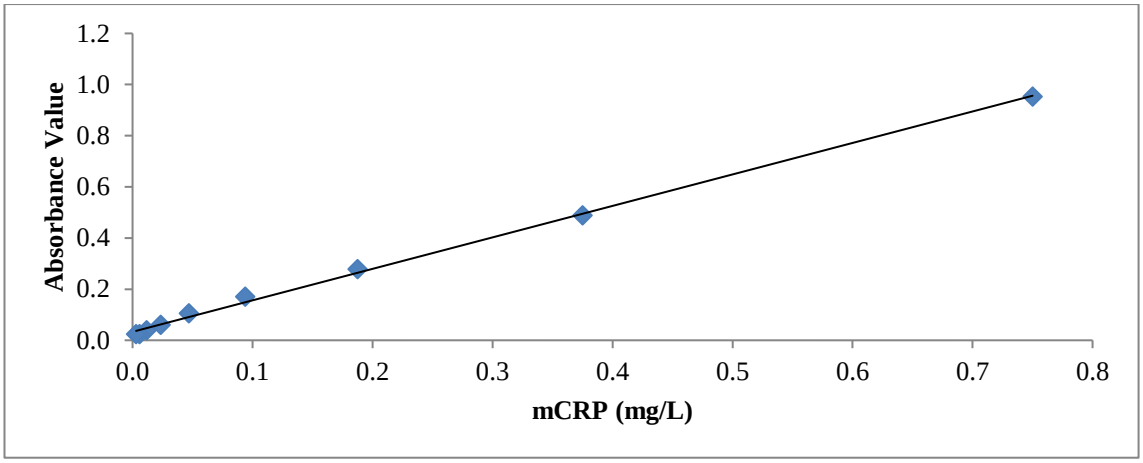

Figure 2.13 Monomeric and Pentameric CRP calibration graphs. a) The calibration graph for pCRP. Values are expressed in mg/L. The line equation is: y = 1.3587x + 0.0009. The R squared value is: 0.996. b) The calibration graph for mCRP. Monomeric CRP used was dissociated via a 3M urea trial. Values are expressed in mg/L. The line equation is: y = 1.2308x + 00332. The R squared value is: 0.9981. Both graphs display a positive correlation with an absorbance values below 1.0. This indicates that absorbance is proportional to concentration.

Figure 2.14 displays the levels of precipitation for both pCRP and *in vitro* produced mCRP when incubated with varying amounts of CWPS. The experimental work was adapted from the protocol documented by Volanakis, 1982, using radiolabelled CRP incubated with C-polysaccharide. Protein concentrations were determined via an ELISA and read at 450nm. The level of CRP precipitated was calculated based on the level of protein remaining in solution, post CWPS incubation.

Pentameric CRP displays little precipitation with CWPS at either end of the curve, where protein or ligand concentration is in excess, as shown in Figure 2.14. 2µg of pCRP precipitated out of solution when incubated with 0.1µg of CWPS, in addition to 5µg of pCRP precipitating out of solution when incubated with 300µg of CWPS. There is a clear equivalence zone is apparent which demonstrates high levels of protein precipitation. A range in the amount of ligand used from 10µg to 100µg shows an increased level in protein precipitation, which peaks at 20µg of CWPS, resulting in 16µg out of a total of 20µg of pCRP being precipitated. The levels of precipitation that is shown in Figure 2.14 is consistent

with what has previously been described when measuring pCRP precipitation (Volanakis, 1982).

Unlike that observed for pCRP, *in vitro* produced mCRP does not follow the general bell-shaped curve. The protein maintains a general baseline of precipitation of approximately 5µg when incubated with all the varying amounts of CWPS. The highest level or precipitation peaks at just over 7µg, when mCRP is incubated with 50µg, although these levels were still significantly lower than that of pCRP (approximately 15µg). The levels of precipitated protein for mCRP were calculated identical to that for pCRP; via ELISA analysis of the supernatant.

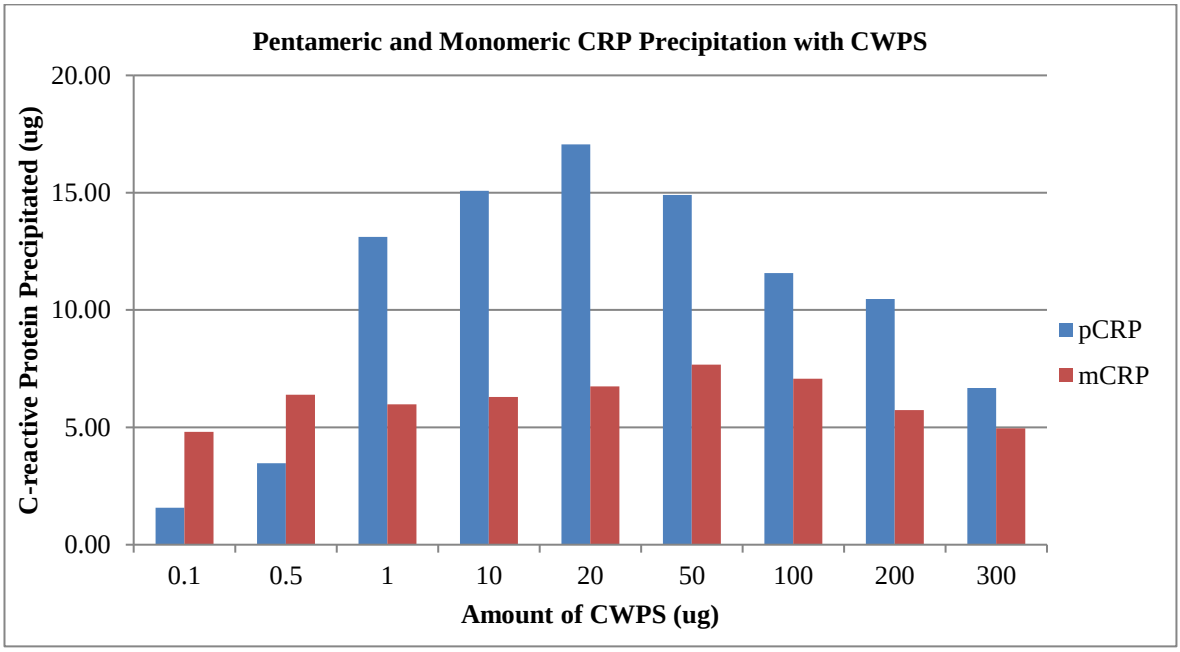

Figure 2.14 Precipitation studies of pCRP and mCRP with CWPS. 20µg CRP was incubated with varying amounts of CWPS for 1 hour at 37°C. Samples were freed of precipitate by centrifugation (4000 x g for 10 minutes) and protein concentration determined via ELISA. The red indicates the level of precipitation for pCRP whilst the blue represents the precipitation levels for *in vitro* produced mCRP (3M Urea).

2.4 Discussion

2.4.1 Optimisation of the Size Exclusion Chromatography Column

Size exclusion chromatography is the principle experimental used in the research here to isolate the different forms of CRP. Based on the results from the calibration of the column, the theoretical elution volumes for pCRP and mCRP were calculated to be 78.5ml and 94.5ml respectively. Although we initially did not have any mCRP to test whether these calculations were correct, the commercially available pCRP was run through the column as a standard (see Figure 2.5). The CRP sample was eluted off at 79ml, which corresponds to a molecular weight of 110kDa.

2.4.2 Production and Purification of Monomeric C-reactive Protein

CRP dissociation experiments using 2, 2.5, 3 and 4M urea were set down over a 10-week period to establish a suitable protocol which would result in the production of mCRP, whilst minimising the amount of urea required for dissociation. Although literature suggests that dissociation of pCRP is achievable through alternative methods, previous experimental work within our lab demonstrated that the treatment of pCRP with heat or acidic conditions results in complete denaturation of the protein. We did however aim to minimise the use of harsh conditions when dissociating pCRP as we were unclear how this would affect the protein's structure and function (Potempa, 1983). One thing that is essential when dissociating native pCRP is the removal of calcium ions; treatment with urea alone (without removal of calcium) is not sufficient to result in a high yield of dissociation. It is not entirely clear why this is the case, although the absence of calcium induces a major conformational change within the protein. Residues 140-150 form a large loop away from the body of the molecule, exposing hidden sites susceptible to proteolysis (Ramadan *et al*., 2002). This structural changes suggest that the calcium ions are crucial when maintaining the protein's

structural integrity, and an absence of these ions may weaken the inter-protein contacts which can then make it more liable to dissociation through urea treatment (Ramadan *et al*., 2002).

Partial dissociation was observed for all the urea concentrations used. The results show that the higher the concentration of urea used, the greater level of dissociation observed within the same timeframe, which agrees with previous dissociation experiments (Potempa, 1983). Eluted fractions (from all elution profiles) B4 and B5 corresponded to pCRP whereas the eluted fractions B7 and B8 were thought to be an *in vitro* produced form of mCRP based upon molecular weight calculations made from the calibration graph and Western Blot analysis. The lower concentration of 2M urea resulted in very little dissociation even after 10 weeks of incubation, based on the absorbance readings, around 90% of the protein eluted off was pCRP. Increasing the concentration to 2.5M suggests an increase in dissociation with higher levels of mCRP being eluted. There is however, still approximately 75% of the sample still being eluted off into fractions B4 and B5.

Both 3 and 4M urea dissociation trials resulted in almost complete dissociation (>90% total protein) of pCRP (see Figures 2.8 and 2.9). In contrast to previous dissociation experiments, a slight ‘shouldering’ effect was observed on the peaks representing pCRP (peak 1) on both chromatograms. These two ‘shoulders’ in Figures 2.8 and 2.9, based on the calculated molecular weights, were thought to signify a small level of un-dissociated or partially-dissociated pCRP (see Table 2.12). In several dissociation experiments, up to 50% of the initial CRP sample was recorded to be lost through the size exclusion chromatography and protein concentration processes. A slower flow-rate whilst purifying samples through both procedures was found to increase the protein yield, although significant losses was still recorded. As size exclusion chromatography is essential in the development of a sound methodology for the purification of *in vivo* CRP, it was important that where possible,

protein losses were reduced. Alongside optimisation of the column flowrate at 0.5ml/min, the centrifugation of samples was carried out at a reduced 'g' and the concentrate flow-through was quantified as described in section 2.2.5 to check for protein.

One of the main aims when producing an *in vitro* form of mCRP was to avoid using harsh conditions when dissociating the sample. When dissociating pCRP, it is expected that a small proportion will always remain in the pentameric form. Based on the 10-week period chosen it was decided that 3M urea would be the optimum concentration when dissociating pCRP for use in the remaining work described here.

Sample	**Elution Volume (ml)**	**Calculated Molecular Weight (kDa)**
2M Urea (B4+5)	79.00	110.23
2M Urea (B7+8)	95.65	21.35
2.5M Urea (B4+5)	79.09	109.26
2.5M Urea (B7+8)	95.68	21.28
3M Urea (B4+5)	79.60	103.90
3M Urea (B7+8)	94.97	22.83
4M Urea (B4+5)	79.27	107.34
4M Urea (B7+8)	94.90	22.99

Table 2.12 Elution volumes and their corresponding molecular weight values for each urea dissociation experiment. B4 and B5 corresponded to the elution of pCRP whilst B7 and B8 corresponded to the elution of mCRP.

It is unclear by what method urea dissociates proteins, and in turn, CRP. Furthermore, without further studies such as X-ray crystallography to determine the atomic structure, it is unclear what modifications urea-dissociation may have on the protein's structure and function. Due to its ability to disrupt non-covalent bonds within proteins, urea is one of the

most common denaturants used in proteomic studies (Sun *et al.,* 2014; Zou *et al.,* 1998). Urea can interact with both polar and non-polar components, which makes it such a powerful denaturant (Rossky, 2008). Interactions with hydrophilic groups are thought to occur by the formation of hydrogen bonds or other polar interactions, whereas it is thought to weaken hydrophobic interactions of a protein (Rossky, 2008; Zangi *et al.,* 2009).

There are two main mechanisms that have been postulated underlying urea-induced dissociation. The first, indirect mechanism involves urea disrupting the first shell of water molecules hydrating the protein. This change in the structure of water's hydrogen bond network around hydrophobic regions of the protein increases its solubility, weakening their hydrophobic effect and driving protein unfolding (Hua *et al.,* 2008; Stumpe & Grubmiller, 2007; Vanzi *et al.,* 1998). The second theory, or 'direct mechanism' postulates that urea interacts directly with hydrogen bonds, or electrostatic interactions within the protein through more favourable attractions, compared with water (Hua *et al.,* 2008) Interactions with urea and protein backbones and/or sidechains is stronger than for water, giving rise to an intrusion of urea into the protein's interior. These alterations to the protein's structure and stability are thought to be the initial driving force for the denaturation and protein unfolding. The latter theory is suggested to be the more widely accepted model for urea-induced dissociation, although it could potentially be a combination of the two (Stumpe & Grubmuller, 2007).

When in an aqueous solution urea can spontaneously dissociate to form cyanate and ammonia; this results in the formation of isocyanic acid. This in turn can then result in the carbamylation of the N termini of proteins and peptides, or side chain groups of lysine and arginine residues. Temperature, pH, concentration and incubation time are all known to affect the rate of urea dissociation and the degree of protein carbamylation (Sun *et al.,* 2014). Interprotomer contacts within pCRP's structure are majorly involved within the 115-123

loop of one protomer with residues from 40-42 and 197-202 on the next protomer. Salt bridges are formed between Glu101- Lys201, Lys123 – Glu197 and Arg118 to the carbonyl region of Pro202. These salt bridges between CRP promoters may be susceptible to carbamylation and could potentially explain why urea-dissociated CRP may not be able to re-associate. Furthermore, the removal of calcium dramatically results in a shift of the 140-150 loop, in addition to rearrangement of several side chains (Shrive *et al.,* 1996). This change in structure may also explain why removal of calcium is necessary for urea-induced CRP dissociation. Alterations in the protein's stability may aid denaturation by urea through one of the previously discussed mechanisms.

2.4.3 The Binding of Monomeric C-reactive Protein to the Phosphocholine-bound Affinity Column

To determine whether the *in vitro* produced mCRP retained its ability to bind PC, a sample from the 3M urea dissociation trial was run through a PC-bound affinity column. As samples were dissociated in a urea and EDTA containing buffer, they were eluted off the size exclusion column in a calcium containing buffer; crucial for CRP when binding to PC (Shrive *et al.*, 1996; Thompson *et al.,* 1999). Figure 2.12 shows the chromatography trace for when the mCRP sample was run through the column. Two main peaks were observed on the chromatogram (1 & 2). Peak 2 was subject to Western Blot analysis (as described in section 2.3.3), with mCRP confirmed from the eluted fraction (peak 2). The first peak was suggested to be an anomaly in the UV absorbance during sample loading. The second peak just 15 minutes after the addition of the chelating buffer displayed a marked increase in absorbance, reaching 0.03AU; a reading more indicative of the amount of protein loaded compared to peak 1(250µg). Our results disagree with previous studies that find dissociation through urea results in a complete loss to the binding of CWPS (which contains PC to which CRP would bind). This could be due to differences within the experimental conditions used

or due to CWPS being a much larger structure than PC, creating difficulties for protein binding. Although, Potempa, in addition to other published research does state they used concentrations of urea up to 8M (Potempa, 1983). Using such high concentrations of urea may result in alterations to the proteins structure and therefore loss of binding and/or protein function. This is shown through their reporting of mCRP's loss of ligand binding when dissociating the protein at these high concentrations.

What we have achieved through this experimental research is a set of optimum dissociation conditions, which uses the lowest concentration of urea possible, that results in almost complete dissociation of pCRP. Furthermore, we have demonstrated that the *in vitro* produced mCRP retains an ability to reversibly bind to PC, something that was previously established not to be possible when dissociating pCRP with urea. These results may not provide a direct confirmation of any structural modifications that may occur through urea-induced dissociation, but give an overall insight into stability and biological properties of the dissociated protein.

2.4.4 Western Blot Analysis of Monomeric and Pentameric C-reactive Protein Samples

Western Blot analysis was performed on the proposed pCRP and mCRP fractions from all the urea dissociation trials, and on the 3M urea sample which was run through the PC-bound affinity column. This confirmed the presence of CRP from the samples, alongside assessing the sample's purity. Pentameric CRP was confirmed to be present in all the trials, indicating that none of the dissociation trials induced complete dissociation of pCRP. All four samples of the proposed mCRP component from the dissociation trials gave a single band as expected. Comparison with molecular weight markers shown that all four samples corresponded to a protein with a molecular weight of around 23kDa, which fits in line with the molecular weight of mCRP (Shrive *et al.,* 1996). All samples appeared free from any

impurities with only one band being visible in each lane. The mCRP sample (peak 2, Figure 2.12) which had been run through the PC-bound affinity column was also subject to Western Blot analysis, to confirm whether the eluted protein peak was in fact CRP. As expected, the sample was positive for CRP, with a molecular weight of around 23kDa. Based on this experimental evidence it was concluded that the urea dissociation experiments successfully dissociated pCRP into its constituent subunits; an *in vitro* produced form of mCRP and that it retained its PC-binding ability.

2.4.5 Precipitation Studies with C-reactive Protein

One of the roles of pCRP within the human body is the activation of the classical complement pathway to provide a first line defence to the host. This is achieved through multiple interactions including; PC present upon the surface of dead or damaged cells and the C1q complement protein (Volanakis, 1982). Section 2.3.5 describes how the *in vitro* produced mCRP displays an ability to bind both PC and CWPS, although less successfully with the latter.

Figure 2.14 displays precipitation levels of pCRP and mCRP when incubated with increasing amounts of CWPS. As expected, pCRP follows the usual bell-shaped curve which fits in line with previous published work (Volanakis, 1982). A clear equivalence zone is shown ranging from around 10µg to 100µg of CWPS with levels of precipitated protein being reduced at either ends of the scale. It is believed that at this concentration range of ligand (and protein) that the two can form lattices, or aggregates, with cross-linking occurring resulting in the precipitation of the whole complex (Murphy *et al.*, 2008; Volanakis, 1982). Monomeric CRP displays a much lower level of precipitation. There is no clear equivalence zone, where precipitation of the protein is increased, but with more of a general baseline level of precipitation at around 5µg. This could be due to several reasons;

firstly, the monomeric form may be unable to form cross-linkages or large aggregates as there is only one PC binding site, compared to the five sites on pCRP. Secondly, treatment with urea could have altered the binding capacity of the protein with CWPS, or alternatively, diminished the effect of hydrophobic regions during dissociation. Although mCRP does not follow an identical trend to that of pCRP, the results from the precipitation curve do display an ability to bind and precipitate out low levels of CWPS.

2.4.6 Conclusions and Future Work

The experimental work discussed here provides a working protocol to produce a structurally and biologically stable *in vitro* form of mCRP. Evidence provided from both PC and CWPS binding studies show that mCRP retains an ability to interact and bind with these ligands; in contrast to previous research in the field. Dissociation with lower concentrations of urea can still produce almost complete dissociation of the pentameric molecule, but over a longer period. Furthermore, our results raise questions as to what effects such harsh conditions, like 8M urea, may have on the protein, which has been used in previous published research. Any potential future work involving either mass spectrometry or X-ray crystallography would be able to determine whether dissociation through urea treatment alters the protein in any way. Finally, the research that has been used within this chapter will be used to help develop and drive forward a sound methodology when testing human serum for an active form of mCRP.

Chapter 3.0 – Analysis of Human Serum Samples

3.1 Introduction

3.1.1 Overview

The role of pCRP within the human body is to bind to dead or damaged cells, opsonise particles for phagocytosis and regulate the immune response by the induction of cytokine synthesis (Pepys & Baltz, 1983). Rise in levels of this plasma protein is induced by interleukin (IL) 6, which elevate transcription levels of the CRP gene within hepatocytes (Mackiewicz *et al.*, 1990). Normal, healthy baseline levels of CRP can range from 1-3mg/L, but during an infection can increase up to 100-fold within 24-72 hours. It is therefore not surprising that CRP is routinely used as a clinical biomarker for injury, infection and inflammation (Pepys & Baltz, 1983; Shine *et al.*, 1981).

3.1.2 Measurement of C-reactive Protein in Human Serum

There are a wide range of standard clinical and immunochemical techniques which can be employed when measuring CRP levels within serum. These immuno-techniques utilise antibodies specific to their target antigen (in this case CRP) providing rapid and sensitive results which are applicable for routine analysis within a clinical laboratory (Koivunen & Krogsrud, 2006). Standard measurement of CRP levels for the evaluation of infection or inflammation within a clinical setting used to use enzyme-linked immunosorbent assays (ELISA). These are rapid and sensitive tools used for the measurement and detection of antigens among other components, within a serum sample. With modern day technology advancing at such a pace, these manual techniques can be quite time consuming and are usually only performed for anomalous samples that require a more in-depth analysis. Currently assays have moved to a more automated based system, such as latex-enhanced immunoturbidimetry assays. This is typically seen within the National Health Service

(NHS), which has an ever-increasing volume of samples to process whilst trying to make efficiencies within their workforce (Koivunen & Krogsrud, 2006; Rifai *et al.,* 1999; Siemens, 2014).

Measuring CRP levels in a clinical setting has been typical for assessing the severity of inflammation within an individual for many years. It is believed that elevated baseline levels (>3mg/L) can be a strong predictor for the development of diseases later of in life (Pepys & Hirschfield, 2003). Recent years has seen the development of high-sensitivity CRP tests which can detect subtler rises in the overall baseline levels of an individual, compared to levels commonly measured with standard CRP tests. As inflammation plays a major role in diseases such as cardiovascular disease, hypertension, atherothrombosis and even diabetes, the high-sensitivity measurement of inflammatory markers, such as CRP, over a period is thought to be a novel method of assessing an individual's risk of developing such conditions (Ridker, 2016; Rifai *et al.,* 1999; Sung *et al.,* 2003). It is crucial when performing high-sensitivity CRP tests that the patient is not suffering from infection or inflammation, as significantly raised levels of CRP will prevent accurate measurement of baseline CRP levels. The increase in sensitivity is based on the development of light-scattering immunoassays, sometimes called 'nephelometric assays'. Light is scattered from antigen-antibody complexes and measured based on the principle that a higher concentration of antigen results in an increase in the amount of light scattered (Krogsrud, 2006; Ridker, 2016; Rifai *et al.,* 1999; Sung *et al.,* 2003).

Shine *et al*., (1981) recorded that in young, healthy volunteers, the median baseline concentration of CRP is 0.8mg/L. The 90^{th} centile of the population has a CRP reading of 3.0mg/L and the 99^{th} centile measures at 10mg/L or over (Pepys & Hirschfield, 2003; Shine *et al*., 1981). Genetic polymorphisms are known to be partly responsible for increased baseline levels of CRP. Guanine and thymine repeats within the intron of the CRP gene are

connected to alterations in CRP levels in normal, healthy individuals and patients with systemic lupus erythematosus (Pepys & Hirschfield, 2003).

3.1.3 Monomeric C-reactive Protein within the Human Body

Research provided within Chapter 2 described previous documented literature for the *in vitro* production of mCRP and the development of a methodology which will be used to test human serum for this protein. Within this chapter the focus will also be on the more recent experimental work, which suggests that a monomeric form of CRP may be present within the human body. The biological relevance and production of this protein is yet to be fully established, but there is increasing evidence within the literature which suggests biological interactions with phosphocholine (PC), bound to the membranes of larger structures (cells, platelets), will readily dissociate the pentamer (Eisenhardt *et al.*, 2009; Habersberger *et al.*, 2012; Ji *et al.*, 2007; Ji *et al.*, 2009; Li *et al.*, 2012; Molins *et al.*, 2008; Slevin & Krupinski, 2009; Zhao & Shi, 2010).

It has also been proposed that mCRP imposes pro-inflammatory effects throughout the human body, contributing to various auto-inflammatory diseases. Activation of the classical complement pathway through binding to either native, or low-density lipoproteins alongside the complement protein C1q, has shown to result in intensified states of inflammation throughout the body (Ji *et al.*, 2006). Activation and dysfunction of endothelial cells has also been linked to mCRP; upregulation of monocyte chemoattractant protein, IL-8 and cell-cell adhesion molecules (ICAM-1 & VCAM-1) and E-selectin are just some examples. Furthermore, a study by Molins *et al.*, (2008) demonstrated how mCRP has shown to upregulate P-selectin, which stabilises platelet-platelet and platelet-leukocyte interactions. Coupled with the increase of tissue factor expression and alterations in fibrin clotting properties, it is clear these results are likely to be a contributing factor towards pro-thrombin

events routinely seen in the pathology of auto-inflammatory diseases (Li *et al.,* 2012; Molins *et al.,* 2008).

It is worth noting that several of these studies display pro-inflammatory effects for a membrane-bound form of mCRP, in addition to the experimental evidence being produced with *in vitro* dissociated CRP, as discussed in Chapter 2. Only previously has evidence come to light which suggests that mCRP may be able to be transported throughout the human body. In 2013, Habersberger *et al* proposed a model by which pCRP may dissociate and be transported around the body to areas of localised inflammation. They suggested lipids present on the surface of activated platelets mediate the binding and dissociation of pCRP. Upon activation, lipid membranes then undergo rapid changes within their membrane composition, resulting in the shedding of micro-particles (MP) (Eisenhardt *et al*., 2009; Habersberger *et al.,* 2013; Owens & Mackman, 2011; Verma *et al.,* 2004). These MP were demonstrated to bind and dissociate CRP following severe cardiovascular events (such as myocardial infarction), which can thus allow mCRP to interact with other cells within the body and impose a pro-inflammatory stimulus (Habersberger *et al.,* 2012).

More recently a study by Crawford *et al.,* (2016) has demonstrated the presence of mCRP and pCRP on the surface of circulating MP derived from endothelial cells. These two forms of CRP both displayed alternative biological effects within a vascular model, with mCRP inducing endothelial shedding and acting as a pro-inflammatory mediator, whereas pCRP induced anti-inflammatory effects through the reduction and regulation of migrating inflammatory immune cells (Crawford *et al*., 2016). They also state that not all current clinical tests may be able to measure levels of CRP that are bound to MP. High sensitivity CRP tests failed to detect correct levels, whereas flow cytometry did. This potential failure of standard plasma assays to detect sequestered levels of CRP could potentially have a knock-on effect for a patient's treatment within a clinical setting. Although, this is only a

suggested model, with mCRP used within their study being produced through 8M urea induced dissociation.

To our knowledge, there is only one experimental study which has claimed to have detected *in vivo* mCRP from human serum. Wang *et al*., (2015) tested for mCRP within the serum of patients who had recently suffered acute myocardial infarction (AMI), alongside patients suffering with unstable angina pectoris, stable angina pectoris and a control group. Their analysis revealed significantly increased levels of mCRP in AMI patients compared to other groups (20.96 ng/ml ±1.64). Their results also showed that circulating mCRP had considerable diagnostic accuracy for AMI, with nine patients who died before a 30-day follow up displaying plasma mCRP concentrations significantly higher than those who survived (36.70 ± 10.26 vs. 19.41 ± 1.43 ng/ml, P = 0.002). Wang and colleagues also discovered that mCRP levels were raised within patients who displayed raised levels of pCRP (Wang *et al.*, 2015). Their results came from a group of six patients with their plasma mCRP levels ranging from 5.73 - 122.74 ng/ml. Their methodology consisted of testing neat serum (via an ELISA) by using a monoclonal antibody specific to mCRP. As encouraging as these results are, pCRP has been documented to spontaneously dissociate upon binding to the bottom of an ELISA plate, which may expose hidden epitopes that would allow binding of a mCRP specific antibody (Eisenhardt *et al.*, 2011).

3.1.4 Experimental Aims

The robust, established methodology that was used to analyse human serum, was developed from our previous experimental research (Chapter 2) coupled with scientific evidence within the literature. Our methodology is capable of detecting both pCRP and mCRP from human serum. By distinguishing whether mCRP can be isolated and detected from human serum may provide a much-needed insight into current misconceptions concerning the protein. More important, if mCRP is found to be present within human serum, this may provoke further research by clinicians, to re-evaluate the current routine clinical care of patients when measuring their CRP levels. Steps may need to be taken to accommodate a monomeric form of CRP, which could display an entirely unique set of circumstances compared to that of its pentameric form.

3.2 Materials and Methods

3.2.1 Ethical Application

Prior to any experimental analysis, for our research to be legal and scientifically sound, approval was required by a peer review and ethical research committee respectively. This allowed the feasibility and risks of our study to be assessed, protecting both the researchers and participants.

3.2.1.1 Peer Review of the Ethical Application

An ethical application for peer review of our study was submitted to Keele University. The peer review system at Keele University is a local research community who assess the quality of the research. The panel scrutinises the supplementary scientific content provided, to ensure the research is viable, backed with sound knowledge. In addition, the system assesses the feasibility of the study and whether the methodology proposed is sufficient and scientifically accurate. The application was approved in April 2015.

3.2.1.2 The Integrated Research Application System

An application for the Integrated Research Application System (IRAS) was then submitted. The IRAS is an online system which provides regulation and governance for research applications. This ensured that the risks of the study were acknowledged, and all participants were provided with a detailed knowledge about the study, to make informed, autonomous decisions. IRAS was used for preparing applications to Research Ethics Committees and the NHS Research & Development offices. The application was approved in May 2015. The project was approved by: NRES Committee South Central – Oxford B / REC ref: 15/SC/0179.

3.2.1.3 Ethical Application Project Title and Research Question

The full title of the research project was:

'Do the current clinical methods, used for the evaluation of raised and baseline levels of C-reactive protein (CRP), allow for the potential presence of a monomeric form of CRP which could potentially display an alternative biological role within the human body, compared to that of pentameric CRP?'

The project was submitted as a student project and pilot study. The chief investigator (CI) was Dr. A. K Shrive. Other members of the study included Robert Williams (PhD student), Professor Trevor Greenhough (Co-supervisor) and Professor Anthony Fryer (collaborator at the University Hospital of North Midlands). The principal research question was:

'Is monomeric CRP found within the serum of patients with raised levels of CRP (>100mg/L)?

To reduce the risk of the study, inpatients at the University Hospital of North Midlands (UHNM), who were due to undergo a routine blood check, were recruited for the study. The unused serum from these blood tests would be used for our study, as opposed to being discarded after the routine tests were complete. This therefore means that no samples were specifically taken for our study.

3.2.1.4 Identification of Participants

The identification of participants took place at the University Hospital of North Midlands – The Royal Stoke University Hospital Participants eligible for the study were identified by Professor A. Fryer, or a member of his research team at UHNM. A criterion for participants eligible for the study was created. The inclusion criteria included:

i. Male or female over the age of 18 years.
ii. They are a case with a raised CRP level of >100mg/L
iii. They are inpatients at UHNM (Royal Stoke University Hospital) and are due to undergo a routine blood test as part of their routine clinical care.
iv. The exclusion criteria for the study were:
v. Any patient with a serum CRP <100mg/L will not be included.
vi. Patients under the age of 18 were not included.

3.2.1.5 Recruitment of Participants

All participants recruited for our study were inpatients at the UHNM. The participants who were eligible for our study were identified by either Professor A. Fryer, or a member of his research team. Eligible participants were approached by a research nurse or by a member of the participant's clinical care team and given a brief verbal explanation of our study. All participants who showed an interest in taking part in our study were guided through a participant information sheet (PIS, see Appendix 1).

The PIS outlines the risks, benefits and aims of our study. The research nurses explained to all participants that they will have the right to withdraw from the study at any time, without giving a reason. All participants were given as much time as required to decide if they wished to partake within our study. All participants were informed that as they were due to undergo a routine blood test, they would not have to undergo any procedures that would not be part of their routine clinical care, therefore making the research study very low risk. All participants were also informed that the information generated from this study was anonymous, and that none of them would be identifiable from the results generated.

If the participants were happy to take part in our study, and the research team member was happy that the participant had fully understood everything that had been discussed, the

participants were presented with a participant consent form (PCF, see appendix 2). All participants were given a PCF and asked to sign and date them. All PCF were stored at the UHNM in accordance with standard NHS procedures. Only members of the research team, or the participants clinical care team would have access to the PIS or PCS. Research members based at Keele University, carrying out the scientific analysis, would not have access to this information. All participants were informed that if they were to lose their mental capacity to make informed consent before, or during the study, they would be immediately removed from the study with their samples being destroyed.

3.2.2 Acquisition of Human Serum Samples

Once a participant had agreed to take part within our study, and the PCF had been signed and dated, venous blood was taken by a fully trained phlebotomist at the Royal Stoke University Hospital as per their routine clinical care. A standard phlebotomy technique was used and blood was collected into BD Vacutainer SST gel tubes without anticoagulant. The sample was then left for up to 30 minutes to allow the blood to clot. The sample was transferred to a centrifuge (Hettich Rotanta 460 Robotic Centrifuge, model number: C5680) and centrifuged at 3,500 x g at 25^{o}C for 7 minutes to separate out the serum from other components within the blood. The serum was stored in the hospital cold room at 4^{o}C until the routine analysis had been carried out. Once the analysis had been completed, 1-1.5ml, depending on the volume left over of the sample, was transferred into a cryovial tube and labelled. The sample was then stored in the cold room at 4^{o}C until collected and transferred to Keele University by Mr R. Williams.

The Human Serum samples were provided by UHNM with a unique code (e.g. CRP 001). These samples would not be in any way identifiable to the participant who provided them. Samples were taken and stored at Keele University, Huxley Building, Structural

Biology Research Group. All information generated from the study was stored on a password protected computer, with only the named investigators having access to the information.

Once the serum samples had been collected at UHNM they were transported in a chilled, sealed container to the Structural Biology Research Lab at Keele University. All serum samples were provided in a 1.5ml cryovial tube and stored at 4^{o}C (cold room temperature at Keele University). Samples were never frozen as it was unknown how this may affect the proteins within the serum. Sodium azide (0.02% v/v) was added to all samples upon arrival to Keele University. CRP and where possible, calcium levels, were provided by UHNM via an Excel Spreadsheet. A total of >1ml was provided per sample. Detailed records were kept for the sample collection date, sample ID, sample volumes, CRP and calcium concentrations, sample analysis and dates of when samples were discarded. Although the biological samples do not come under the jurisdiction of the Human Tissue Act 2004, Keele University requested a detailed account of the collection, storage and disposal of all human serum samples throughout our study. All relevant information was passed on to the relevant authorities at Keele University.

3.2.3 Purification of the Human Serum Samples

The affinity chromatography column system and software used were the same as described in section 2.2.3. Prior to the application of each human serum sample through the column, 10 column volumes of regeneration buffers 1 & 2 (see Table 3.1) were run through it. As serum contains many different proteins, it was important to ensure that any remnants residing in the column from the previous run were removed. The regeneration buffers were used to clean the column, ensuring that all CRP present within the serum could bind. The absorbance was measured at 280nm for all chromatography runs. The ultra-violet (UV) absorbance baseline was blanked prior to the addition of the regeneration buffers.

10 column volumes of equilibration buffer (see Table 3.1) were run through the column at a flowrate of 0.5ml/min. 0.9ml of each serum sample was diluted up to 10ml of equilibration buffer (see Table 3.1). The 10ml of diluted human serum was then passed through the column at a flowrate of 0.5ml/min. When the entire sample had been applied to the column, equilibration buffer was passed through and collected in a 50ml tube (Fisher Scientific) until the UV reading had returned to 0AU.

The chelating buffer (Table 3.1) was then run through the column at a flowrate of 0.5ml/min. The eluted protein was collected in a 50ml tube (Fisher). Once all the bound protein had been eluted from the column, 20 column volumes of equilibration buffer was run through the column until the absorbance reading had flat-lined to 0AU. The column was then ready for storage.

Buffer/Solution	**Components**	**Concentration**
Regeneration Buffer 1 pH 7.4	Sodium Chloride	500mM
	Tris	200mM
	EDTA	10mM
Regeneration Buffer 2 pH 7.4	Sodium Chloride	500mM
	Tris	50mM
	Calcium Chloride	10mM
Equilibration Buffer pH 7.4	Calcium Chloride	10mM
	Tris	50mM

	Sodium Chloride	150mM
	Sodium Azide	0.01%
Chelating Buffer pH 7.4	EDTA	10mM
	Tris	50mM
	Sodium Chloride	150mM
	Sodium Azide	0.01%

Table 3.1 A list of all the components for the buffers used on the phosphocholine-bound affinity chromatography column when purifying the human serum samples. Concentrations are also given for all the components used.

3.2.4 Concentration of the Eluted Fractions

The eluted fractions from the phosphocholine-bound affinity column were concentrated as described in section 2.2.4. Samples were concentrated to volumes that were appropriate for application onto the size exclusion column (0.1-2% of the column volume, see section 2.2.2).

3.2.5 Size Exclusion Chromatography of the Eluted Fractions

The size exclusion chromatography system and software used are the same as those described in section 2.2.2. The buffers used for preparing the column are outlined in Table 3.2. The column is stored in 20% ethanol and was purged with three column volumes of deionised water (one column volume is 120ml). The column and tubing were equilibrated with four column volumes of elution buffer (see Table 3.2). The pH of the elution buffer was adjusted by the addition of HCl. All buffers and solutions used on the column were filtered through a 0.2µm cellulose acetate filter (Sartorius Stedim Biotech, Geottingem, Germany) to remove any particulate matter that may clog the system and de-gassed, to avoid

introducing air into the system. All buffers and solutions were stored at 4^{o}C and allowed to equilibrate to room temperature before use.

Buffer/Solution	Components	Concentration
Storage Solution	Ethanol	20%
Wash Solution	Deionised H_2O	100%
Elution Buffer pH 7.4	Tris	20mM
	Sodium Chloride	280mM
	Calcium Chloride Hexahydrate	5mM

Table 3.2 A list of all the components for the buffers used on the size exclusion column when purifying the human serum samples. Concentrations are also given for all the components used.

The eluted samples were loaded onto the column via a 2ml sample injection loop. Based on the user guidelines, the sample volume did not exceed 0.1-2% of the column volume to obtain the best resolution and was accounted for when concentrating the sample. A flowrate of 0.5ml/min was used for all samples, with the absorbance measured at 280nm. Sample fractions of 5ml were collected up to one column volume (120ml) at room temperature. The size exclusion column was then prepared for storage. Four column volumes of wash buffer were run through the column, followed by four column volumes of 20% ethanol.

3.2.6 Concentration of the Eluted Fractions

Samples from the size exclusion column were concentration as described in section 2.2.4. The eluted fractions B4 & B5 and B7 & B8, for each serum sample, were combined

respectively. The fractions were concentrated to give final volumes varying between 50 and 800 µL. Protein concentrations subsequently determined will need to account for this variation.

3.2.7 Protein Quantification of the Eluted Serum Fractions

The protein content of the CRP samples was determined using a spectrophotometer as described in section 2.2.5.

3.2.8 SDS PAGE of the Eluted Serum Fractions

SDS PAGE gels were cast as described in section 2.2.6. All gels used for the analysis of the serum samples consisted of a 12.5%T resolving gel, a 4%T stacking gel at 0.75mm.

All samples were added to a non-reducing, SDS buffer at a ratio of 1:1. Samples were heated at 95^{o}C for a total of five minutes prior to loading on the gel. A total volume of 15µl was added to each well to maximise the total amount of protein run through the gel for each sample. Low range molecular weight markers were run alongside samples, but not transferred onto a Western Blot. Lanes containing the molecular weight markers were carefully cut off and stained with Coomassie Brilliant Blue, as described in section 2.2.6. B4+5 fractions eluted off the column were all run on separate gels to the B7+8 fractions. Positive pCRP controls (1µg) which had been subject to the same procedures as the samples were run alongside all B4+5 fractions. Positive *in vitro* produced mCRP (via 3M Urea) controls (1µg), which had been subject to the same procedures as the samples were run alongside all B7+8 fractions. Negative controls, which contained no protein sample and just running buffer, were included in all gels (not included in Figures). Gels were run on the same system as described in Chapter 2.

3.2.9 Enzyme-linked Immunosorbent Assay of the Eluted Serum Fractions

A calibration graph for known amounts of pCRP & mCRP were produced, to determine CRP levels within the human serum samples. Buffers and solutions used for the calibration experiments are the same as described are shown in Table 3.5. Both primary and secondary antibody dilutions used were as recommended by the supplier SCRIPPS. The ELISA was carried out on a sterile, 96-well plate (Costar). The plates were flat bottom plates, with a low evaporation lid, high binding affinity and made from polystyrene. All results from the experiment were triplicated. 100µl of calcium buffer was added to columns 2-10, rows A-C. 100µl of either pCRP or mCRP was added to column 1, rows A-C (0.75µg, 0.0075mg/ml). 100µl of either pCRP or mCRP was added to column 2, rows A-C. The contents of column 2, rows A-C was then mixed thoroughly, with 100µl being transferred to column 3, rows A-C. This process was repeated to column 9, rows A-F, where the additional 100µl was discarded to waste, leaving only calcium buffer in column 10, rows A-F (negative control). The plate was left to incubate overnight at 4^{o}C on the rocking machine (see Table 3.3).

The plate was washed thoroughly with wash buffer 3 times. Wash buffer consisted of phosphate buffered saline (PBS) and Tween (see Table 3.4). All components of wash buffer were purchased from Sigma. Any remnants of wash buffer within the wells were ‘flicked’ out into the waste. 100µl of blocking solution was then added to all wells. Blocking solution consisted of a 3% bovine serum albumin (BSA) solution in PBS-Tween (see Table 3.4). The BSA was purchased from Sigma with all blocking solution being made fresh prior to use. The plate was left for 2 hours at 4^{o}C on the rocking machine. The plate was washed thoroughly with wash buffer 3 times (see Table 3.4). Any remnants of wash buffer within the wells were ‘flicked’ out into the waste. The primary monoclonal antibody was thawed out prior to use. The primary antibody was diluted at 1:40,000 (the recommended dilution

from the supplier SCRIPPS) in wash buffer. 100µl of the diluted antibody was added to each well. The plate was left for 5 hours at 4°C on the rocking machine.

The plate was washed thoroughly with wash buffer 3 times. Any remnants of wash buffer within the wells were 'flicked' out into the waste. The secondary antibody was thawed out prior to use and was diluted at 1:40,000 in wash buffer (dilution based on recommendation from supplier SCRIPPS). 100µl of the diluted antibody was added to each well. The plate was left for 2 hours at 4°C on the rocking machine. The developing substrate used was 3,3',5,5' Tetramethylbenzidine (TMB) liquid substrate purchases from Sigma. The TMB is stored at 4°C, and prior to use allowed to equilibrate to room temperature. 100µl of TMB was added to all columns and developed for 10 minutes, or until the required colour intensity was reached. 100µl of 2M Sulphuric Acid was added to all columns. The tray was then read at 450nm on a BioTek EL800 plate reader using the Gen5 Software.

Pentameric and Monomeric CRP Calibration											
		1	**2**	**3**	**4**	**5**	**6**	**7**	**8**	**9**	**10**
A	**pCRP (µg)**	0.75	0.38	0.19	0.09	0.05	0.025	0.0125	0.00063	0.00021	Control
B		0.75	0.38	0.19	0.09	0.05	0.025	0.0125	0.00063	0.00021	Control
C		0.75	0.38	0.19	0.09	0.05	0.025	0.0125	0.00063	0.00021	Control
D	**mCRP (µg)**	0.75	0.38	0.19	0.09	0.05	0.025	0.0125	0.00063	0.00021	Control
E		0.75	0.38	0.19	0.09	0.05	0.025	0.0125	0.00063	0.00021	Control
F		0.75	0.38	0.19	0.09	0.05	0.025	0.0125	0.00063	0.00021	Control

Table 3.3 A Table showing the amounts of pentameric and monomeric CRP used in the ELISA calibration experiments.

Buffer/Solution	Components	Concentration
PBS pH 7.4 with HCl	Sodium Chloride	137mM
	Potassium Chloride	2.7mM
	Disodium Phosphate	10mM
	Monopotassium Phosphate	2mM
PBS – Tween (Wash Buffer)	PBS	1L
	Tween	0.5ml
PBS-Tween with 3% BSA (Blocking Solution)	PBS – Tween	20ml
	BSA	0.6mg
Calcium Buffer pH 7.4 with HCl	Tris	20mM
	Sodium Chloride	280mM
	Calcium Chloride	5mM
Primary Monoclonal Antibody 1:4,000 Dilution	Primary Antibody	1µl
	PBS - Tween	39.999ml
Secondary Antibody 1:40,000 Dilution	Secondary Antibody	1µl
	PBS – Tween	39.999ml

Table 3.4 A list of all the components used in the ELISA calibration experiment for pentameric and monomeric CRP. The concentration for each component used is also given.

The purified pCRP fractions (B4+5) fractions were subject to an ELISA to determine the levels of pCRP present, post-purification. The purified fractions were diluted in calcium buffer at 1:100. 50µl of each serum sample was added, in triplicate, to a 96-well plate. The blocking, washing, addition of antibodies and reading of the ELISA plates were carried out as described above for the calibration experiment. The primary and secondary antibody dilution used was 1:40,000. Positive controls were included.

The purified mCRP fractions (B7+8) fractions were subject to an ELISA to determine the levels of mCRP present, post-purification. The purified fractions were diluted in calcium buffer at 1:10. 50µl of each serum sample was added, in triplicate, to a 96-well plate. The blocking, washing, addition of antibodies and reading of the ELISA plates were carried out as described above for the calibration experiment. The primary and secondary antibody dilution used was 1:40,000. Positive controls were included.

Controls of pCRP (SCRIPPS) and mCRP (dissociated via 3M Urea) were included in all ELISA experiments. Both forms of CRP had been subject to the same purification methods as described in Sections 2.2.2, 2.2.3 and 2.2.4. Eluted fractions B4/5 were used for the positive pCRP control whilst fractions B7/8 were used for the negative control. Eluted fractions B7/8 were used for the positive control for mCRP, whilst fractions B4/5 were used for the negative control.

3.2.10 Western Blotting of the Eluted Serum Fractions

Samples which were used within the Western Blot transfer had previously been subject to SDS PAGE. Components and buffers used for the Western Blotting of human serum samples are the same as described in section 2.2.7.

Membranes were washed as described in section 2.2.7. The primary monoclonal antibody (mAb) was defrosted, prior to the addition to the nitrocellulose membrane. The

primary mAb was diluted in BLOTTO. For the purified pCRP fractions (B4+5), a 1: 1,000 mAb dilution was used. For the purified mCRP fractions (B7+8) a 1:400 mAb dilution was used. To increase the chances of detecting mCRP on the WB, a maximum volume of 15µL from each sample was loaded onto the gel. The primary antibody was left on the membrane overnight. A volume sufficient to completely immerse the membrane was used (>20ml). The secondary antibody was diluted in BLOTTO at 1:40,000. The secondary antibody was added to the nitrocellulose membranes for a minimum of 1 hour (for both fractions). A volume sufficient to completely immerse the membranes were used (>20ml).

The Clarity ECL Western Substrate was then added for a minimum of five minutes. The reagent was added at a 1:1 ratio of Clarity peroxide reagent and Clarity luminol/enhancer reagent, to a total volume of 7ml. All steps were carried out at 4^{o}C on the rocking machine, to encourage gentle agitation of the solution with the nitrocellulose membrane. The membranes were removed from the reagent and wrapped in Saran Wrap (protein side up) to prevent drying out. The membrane was then viewed on a digital image detector and exposed for up to 30 minutes, depending on the intensity of the band required. Control bands that fluoresced too brightly compared to that of the experimental samples were carefully cut off, with the remainder of the membranes exposed for a longer period of time.

3.2.11 Statistical Analysis

All graphs and Tables produced from the data generated from our research were created on Microsoft Excel 2010.

3.3 Results

3.3.1 Experimental Design

This sub-chapter highlights the experimental planning, design and initiative that was required during the preliminary stages of the study, and was thus used as a guide throughout its duration by all parties involved.

3.3.1.1 Ethical Application Approval

Prior to serum sample analysis, ethical approval was required by both Keele University and the online IRAS. Figure 3.1 displays an overview of the process that was required to obtain ethical approval for the project.

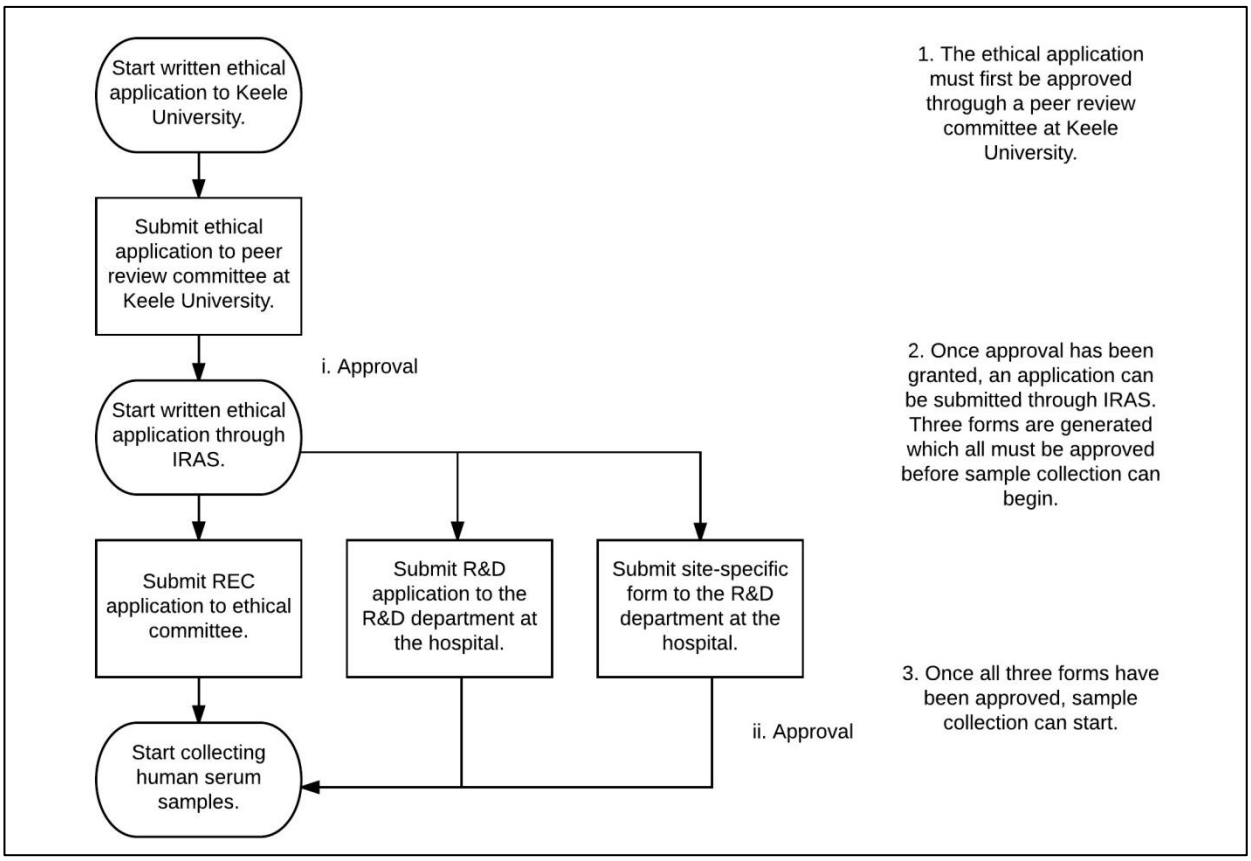

Figure 3.1 A flow diagram highlighting a step-by-step process used to obtain ethical approval through both Keele University, and IRAS. Preliminary questions provided through IRAS resulted in the generation of three separate forms, all which needed to be approved and signed off by the relevant bodies before sample collection could commence.

3.3.1.2 Determining the Sample Size Required for the Study

The primary outcome of this study is to determine whether human mCRP can be located within the serum of patients with raised levels of CRP (>100mg/L). For our study to be representative of the population alongside sample size calculations being a prerequisite for ethical approval, a sample size needed to be chosen to reflect this. To our knowledge, there is no readily available data for the average distribution of mCRP levels throughout the population in addition to very little information on whether mCRP is located within human serum. This therefore meant that we were unable to perform a sample size calculation, or generic power analysis for our study that would accurately represent the population.

We hypothesised that if mCRP were to be located within the serum of patients with raised levels of CRP (>100mg/L), then only a small portion of this total CRP would be mCRP, with the rest being native pCRP. This proportion was hypothesised to be 15%. From this, we were then able to calculate a confidence level (at 95%) for a chosen sample size. This was calculated with the following equation:

$$Confidence\ Level = \left(\hat{p} - Z\ \frac{\sqrt{\hat{p}\,(1-\hat{p})}}{n}, \hat{p} + \ Z\ \frac{\sqrt{\hat{p}\,(1-\hat{p}}}{n}\right)$$

Equation 3.1 The equation used to determine the Confidence Level for a sample size.

Equation 3.1 highlights how the confidence level for a sample size was calculated for this study. The $\hat{p}$ symbol represents the expected proportion of mCRP (15%), *n* represents the sample size a *Z* represents the critical value for the 95% confidence level. For the

confidence level to be determined for a chosen sample size, the critical value needed to be determined.

3.3.1.3 Calculation of the Critical Value for a Confidence Level

In statistical analysis, the critical value is the value given which corresponds to the chosen level of significance. This critical value, sometimes known as a 'cut off' value, is the boundary between the samples, in a test statistic, which can result in the decision to either reject, or fail-to-reject a null hypothesis. The calculation of the critical value for a two-tailed test is as follows (Chosen level of confidence = 95%):

i. Subtract the confidence level from 100%: 100% - 95% = 5%. This 5% represents both tail ends of the graph. These are the areas of the graph which are not included in the 95% confidence level.
ii. Convert the value from step 1 into a decimal: 5% = 0.05. This is usually denoted as the α value.
iii. Subtract α from 1: 1-0.05 = 0.95. This 0.95 represents that we are 95% confident that any one value will lie throughout the distribution of samples.
iv. Divide the value from step 3 by 2 as this is a two-tailed test: 0.95/2 = 0.475. A two-tailed test allows the test to be two sided, and to determine whether the sample is either greater or less than a certain range of values.
v. Input 0.475 into a *Z-Table* (see appendix), this gives a critical value of 1.96 (see appendix for *Z* Table).

3.3.1.4 Calculation of the Confidence Level

Equation 3.1 shows the equation used with Table 3.1 displaying the meaning and value of each symbol. This was calculated as follows:

i. Proportion = 15%

ii. 15% of 40 (n) = 6

iii. 6/40 = 0.15 = $\hat{p}$

iv. $= \left(0.15 - 1.96\ \frac{\sqrt{0.15(1-0.15)}}{40}, 0.15 + \ 1.96\ \frac{\sqrt{0.15\ (1-0.15}}{40}\right)$

v. = -0.039, +0.026

vi. = +/- 11.1%

vii. This therefore means that with a sample size of 40, we can be 95% confident that 15% of the serum samples analysed will contain mCRP +/-11.1%.

3.3.1.5 Overview of the Human Serum Sample Analysis Methodology

Once ethical approval had been granted, sample collection could begin. Human serum analysis was based on a three-step process; CRP purification from human serum via affinity chromatography, separation of potential CRP isoforms by use of size exclusion chromatography, followed by identification and quantification via Western Blot and ELISA analysis (see Chapter 2).

Human serum contains crude a mixture of components, including proteins, antigens, hormones and antibodies (Murphy *et al.*, 2008). We were therefore required to purify out the CRP within the serum, prior to application on the size exclusion column. Samples were run through a phosphocholine-bound affinity column, to which CRP can readily bind (Thompson *et al.,* 1999). Research within the literature demonstrates several models of pCRP dissociation, upon which is initiated through binding to the surface of cells at localised sites throughout the body, and even circulating platelets, all of which will contain PC constituents protruding from their membrane. (Eisenhardt *et al.,* 2009; Habersberger *et al.*, 2012; Ji *et al.*, 2007; Ji *et al.*, 2009; Li *et al.*, 2012; Molins *et al.*, 2008).

Coupled with the experimental evidence provided in Chapter 2, we were confident that potential forms of mCRP will be able to bind and interact with the PC column, and allow purification of the sample from serum. An overview of the entire purification, identification and quantification process for the human serum sample analysis is shown via a flow diagram in Figure 3.2.

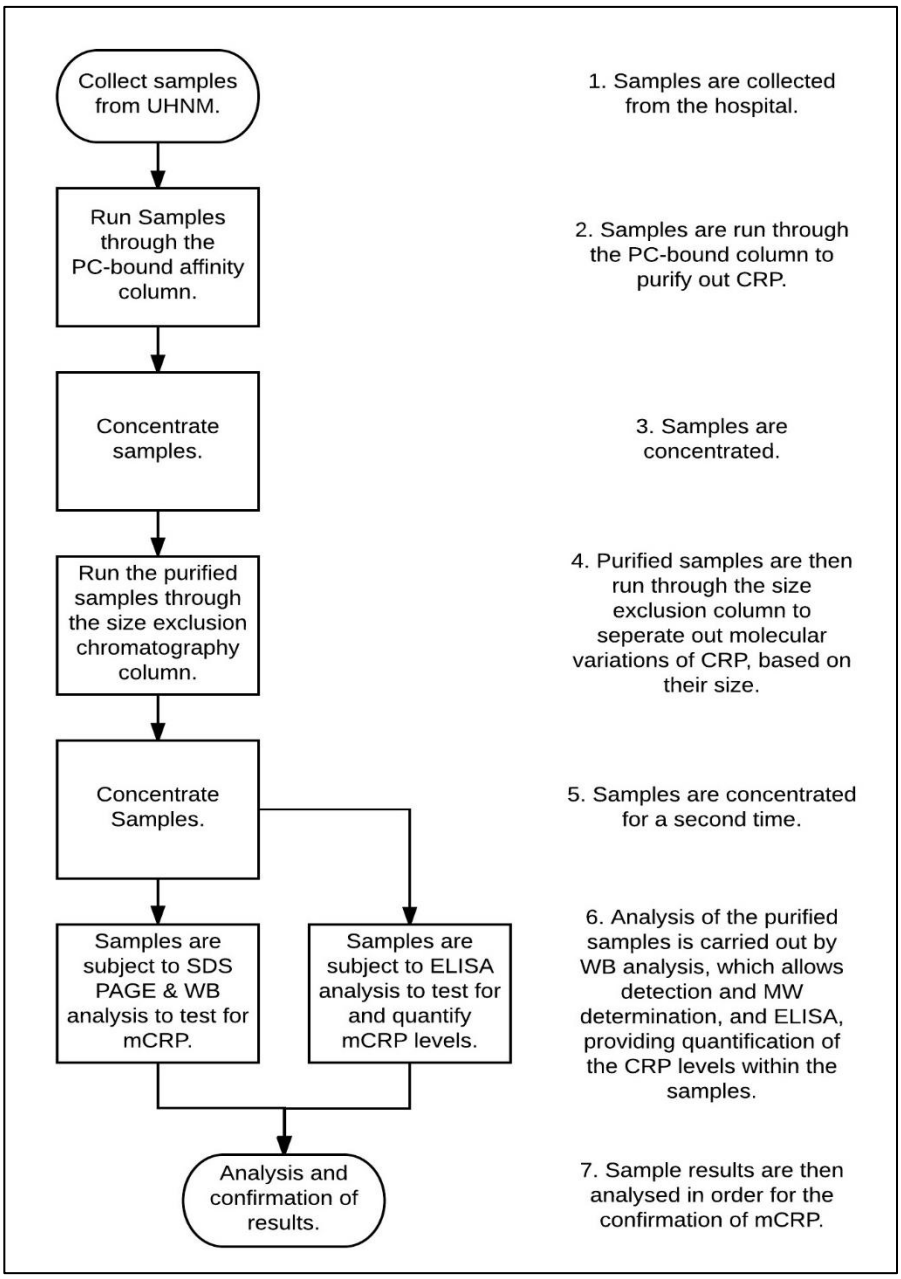

Figure 3.2 A flow diagram highlighting in a step-by-step process the methodology used for the analysis of human serum. Both Western Blot & ELISA analysis was performed on all samples.

3.3.2 Purification of the Human Serum Samples

A full list of all the CRP codes that were used within our study, their initial CRP concentrations based on reading provided by UHNM and their corresponding values (mg/L) from the purified serum ELISA results can be found within the appendix.

To purify all the potential forms of CRP from all other constituents within human serum, all samples were run through a phosphocholine-bound affinity column in the presence of calcium. This will allow binding of the pentraxins to their natural ligand, PC. A total of 40 human serum samples were obtained through the University Hospital of North Midlands from patients who exhibited raised levels of CRP (>100mg/L). The samples provided were anonymised and given a unique sample code (e.g. CRP 001). All 40 samples were analysed via the same methodology. Representative traces for the purification of human serum via affinity chromatography and size exclusion chromatography are shown in Figures 3.3 and 3.4 respectively. All the results obtained from both methods followed the same trend as shown in Figures 3.3 and 3.4.

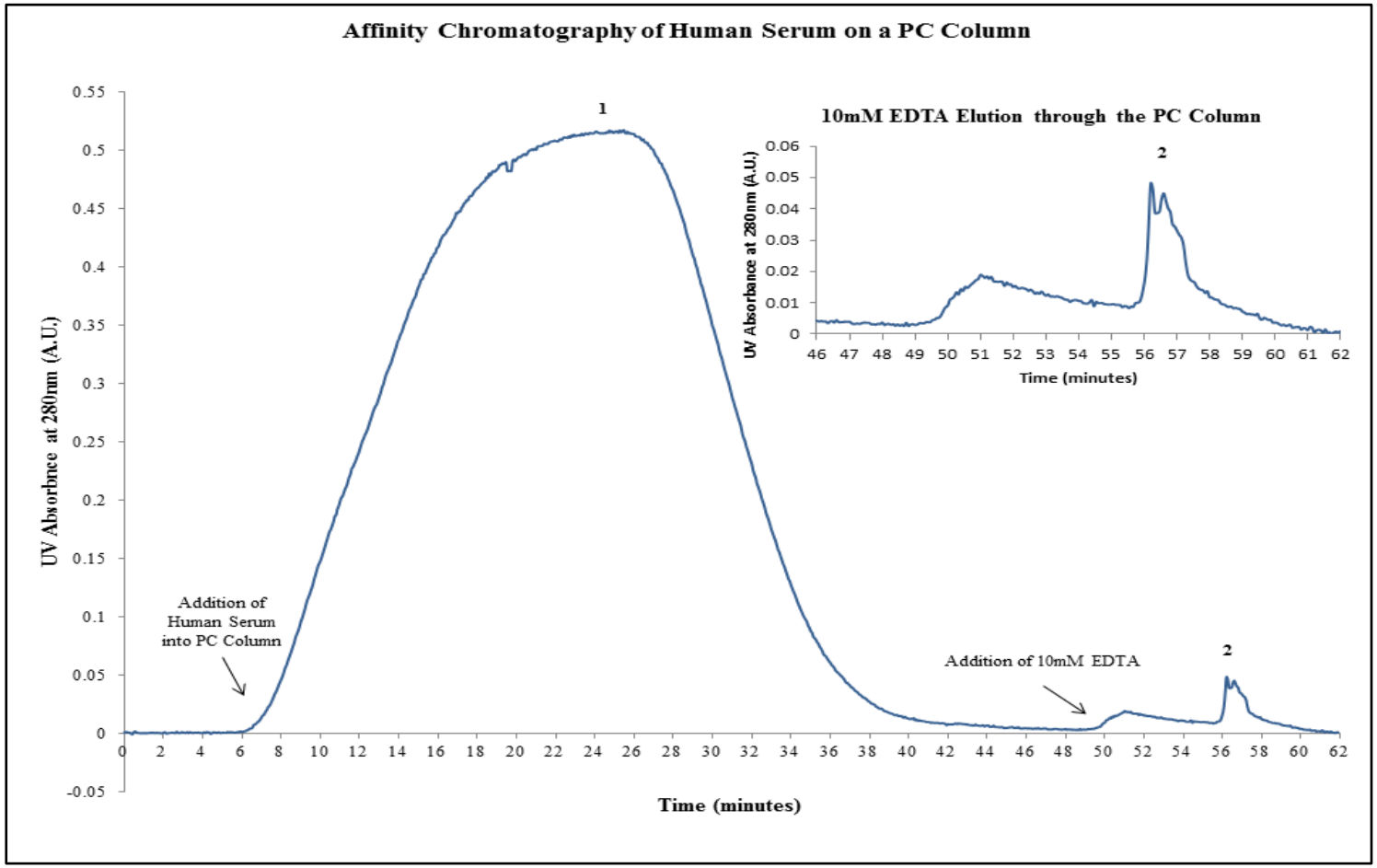

Figure 3.3 A chromatography trace of human serum ran through a phosphocholine-bound affinity column. Components within the serum which did not bind to the column, represented as peak 1, measured an absorbance reading of 0.54AU. Protein samples which bound to the column, peak 2, had an absorbance reading of 0.05AU.

The first peak gave a maximum absorbance reading of 0.54AU with the absorbance reading not returning to baseline levels (0AU) until just over 30 minutes had passed. The dip at the apex of peak represents where the entire sample had been loaded onto the column. Equilibration buffer was then run through the column until the absorbance reading had returned to baseline levels. The second peak on the chromatography trace occurs several minutes after the addition of the calcium chelator, Ethylenediaminetetraacetic acid (EDTA), which is shown from the second marker at the time point of around 46 minutes. The removal of calcium from the column by the addition of EDTA will result in the elution of any calcium dependent binding proteins, such as CRP, as they will no longer retain the ability to stay bound to phosphocholine. Peak 2 extends over a period of around 10 minutes and appears to exhibit a slight 'shoulder' before it reaches its apex, at an absorbance of 0.05AU. This magnified section is shown in Figure 3.3, which illustrates the 'shouldering' observed on the left-hand side of the peak, a common characteristic of the second peak in all the chromatography traces with human serum.

To separate out potential CRP forms based on their size, samples that had been run through the phosphocholine-bound affinity column were then run through a size exclusion chromatography column. The eluted sample obtained from peak 2 of the chromatography trace (see Figure 3.4) is a typical sample that was run through the size exclusion column. As all samples were run through the column using the same methodology, only one example image will be shown to represent the results acquired for the total cohort. The sample shown in Figure 3.4 (and 3.5) is from the sample labelled 'CRP 052'. Any anomalous results or outliers that did not fit with the size exclusion chromatography data would have been identified; fortunately, all results obtained from the affinity chromatography purification followed the same trend.

The sample was injected into the column at 0ml, with three main peaks observed and labelled as peaks 1, 2 and 3. The first peak in Figure 3.4 is broader and smaller than peaks 2 and 3, and eluted off the column at a volume of 59.05ml with an absorbance of 0.5mAU. The elution volume indicates a protein at a size of 787kDa. Due to the peak size and position on the trace, coupled with calculated molecular weight of the protein, which does not match any previous experimental work or research documented for CRP, it was disregarded as insignificant for this experimental study.

The second peak in Figure 3.4 was sharper than the first peak and gave an absorbance reading of 1.6mAU. The elution volume of the peak was 72.92ml, which equates to a protein with a molecular weight of approximately 200kDa. Based on the elution volume and calculated molecular weight, the protein was concluded not to be relevant to our research and the eluted fraction was not pursued for further experimental research.

The third peak represents the elution of pCRP from the human serum sample. The third peak displays a typical trace of pCRP when eluting off the size exclusion column, and is the most prominent and sharpest peak on the trace. The absorbance was measured at 6.5mAu and was eluted off at 79.01ml. Based on this elution volume the molecular weight was calculated to be approximately 110kDa. The elution peak observed within all the human serum samples for pCRP is similar to that recorded for the pCRP in the dissociation trials and pCRP control from SCRIPPS. Additionally, previous runs on the size exclusion column show that the pCRP is eluted off in the B4+5 fraction tubes, with *in vitro* produced mCRP eluting off into the B7 + 8 fraction tubes (see Chapter 2).

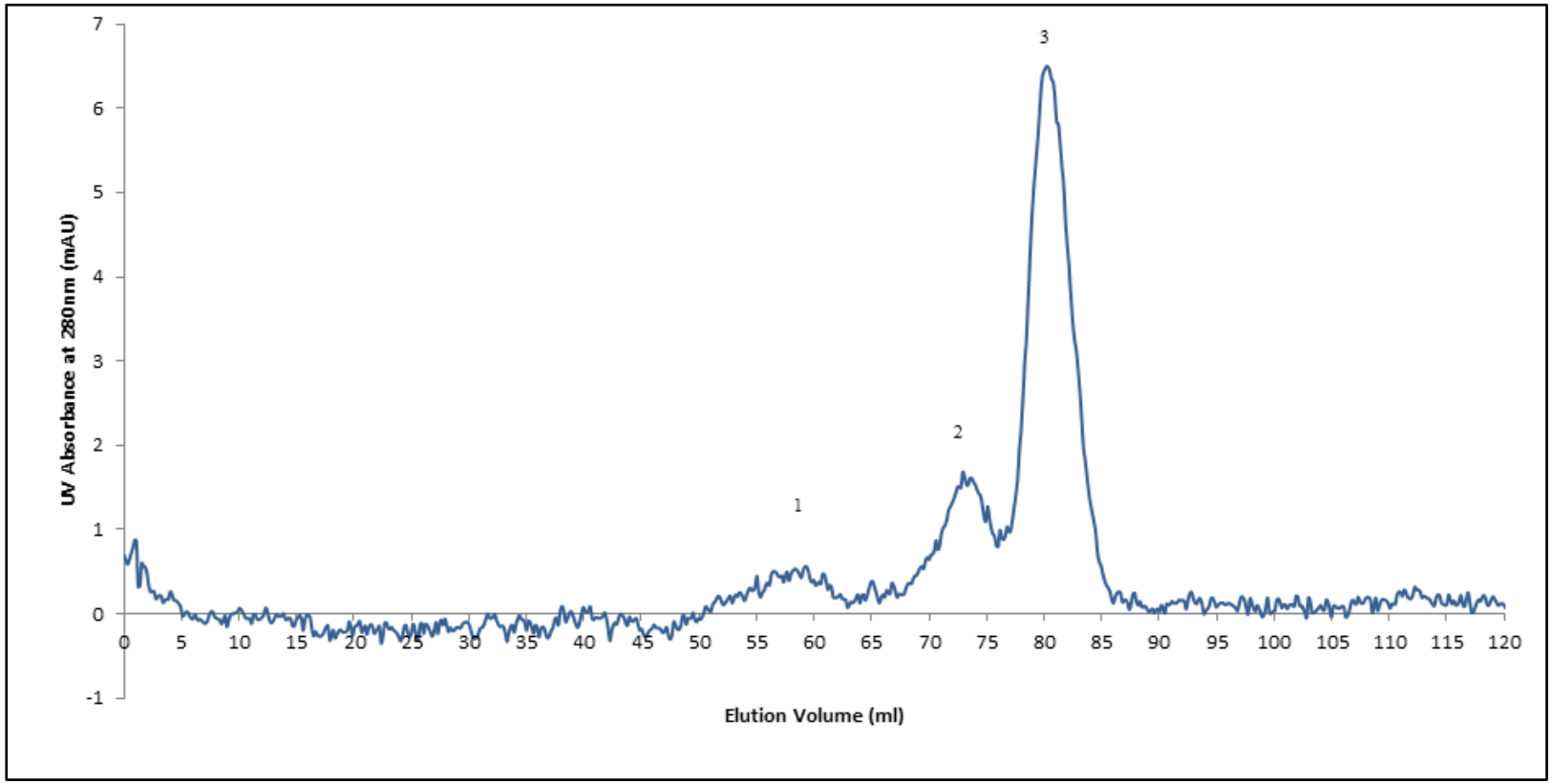

Figure 3.4 A chromatography trace from the size exclusion column, representing what is a typical trace when running the human serum samples through the column. Pentameric CRP, as shown in peak 3, displayed an elution volume of 79.01ml. Peaks 1 and 2 displayed elution volumes of 59.05 and 72.92ml respectively. It was unclear as to what these peaks represented.

Figure 3.5 displays a magnified area of the chromatography trace from elution regions of 70ml – 100ml, highlighting the elution volume and absorbance measurement for peak 3. Based on previous dissociation trials and size exclusion chromatography runs of control samples, markers 1 and 2 draw attention to where pentameric and monomeric CRP should elute off the column. Peak 3 is consistent with previous experimental work, as stated previously, but the absorbance reading remains at baseline level of around 0mAU at the region where mCRP elutes off (typically 94ml, giving a protein with the molecular weight of around 25kDa). Fractions B4 and 5, thought to contain pCRP were collected, in addition to fractions B7 and 8. Although no peaks were observed where mCRP should elute off, eluted fractions B7 and B8 were collected and tested nonetheless. This was to rule out mCRP levels being too little that the size exclusion column was unable to detect them, thus inducing an elution peak. All samples run through the size exclusion column were run at a flow rate of 0.5ml/min and the UV absorbance was measured at 280nm. Each of the pCRP and mCRP combined fractions was concentrated to give final volumes varying between 50 and 800µL, with this variation considered, when subsequently determining protein concentration of the samples.

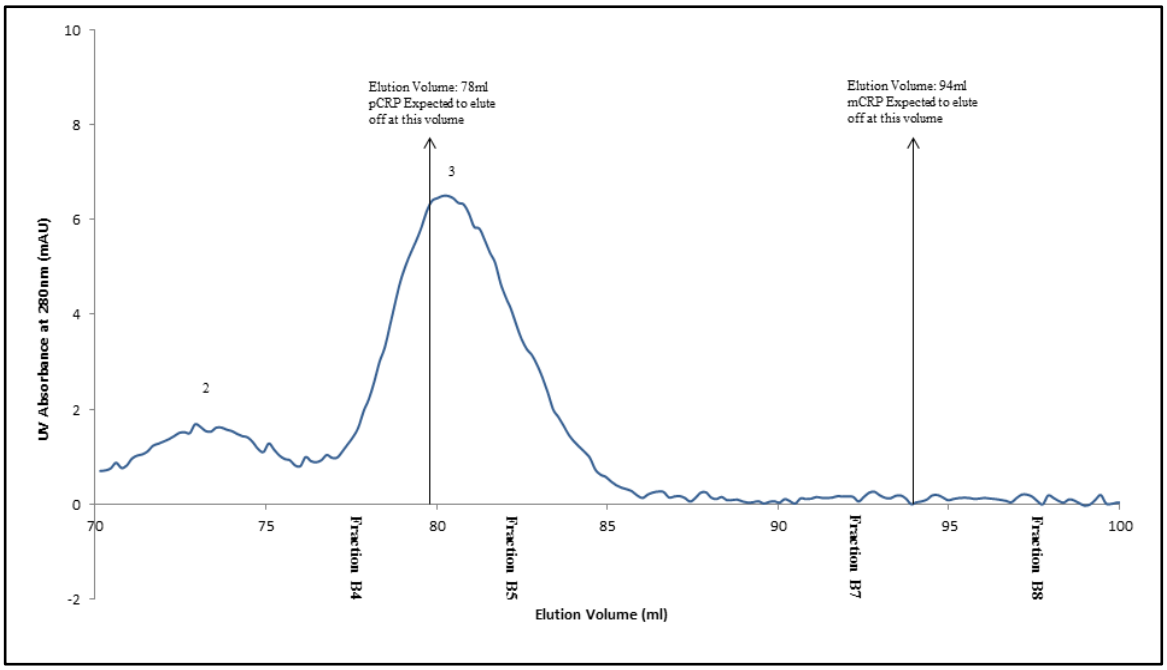

Figure 3.5 A magnified section of the size exclusion chromatography trace from Figure 3.2 (70-100ml). The region at which pCRP was eluted off the column is represented by marker 1. The region at which mCRP is expected to elute off, based on previous *in vitro* studies, is represented by marker 2. It is clear from these results that mCRP failed to induce a peak in any of the traces when running human serum samples through the size exclusion column.

3.3.3 Enzyme-linked Immunosorbent Assay of the Eluted Serum Fractions

All purified human serum samples (fractions B4 &5 and B7 & 8) were subject to analysis via an ELISA. Analysis via an ELISA will allow quantitative determination of both pCRP and mCRP levels in all samples. Furthermore, ELISA offers an increase level of sensitivity compared to Western Blot analysis, thus being able to detect levels of protein which may be initially missed. To determine the levels of CRP in both sets of fractions, a calibration experiment must first be carried out with both pentameric and monomeric control samples.

Graph a.

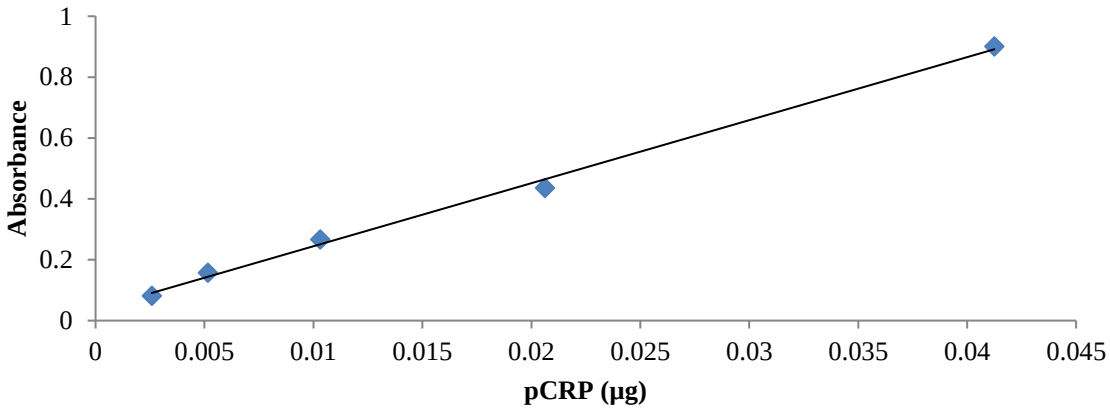

Graph b.

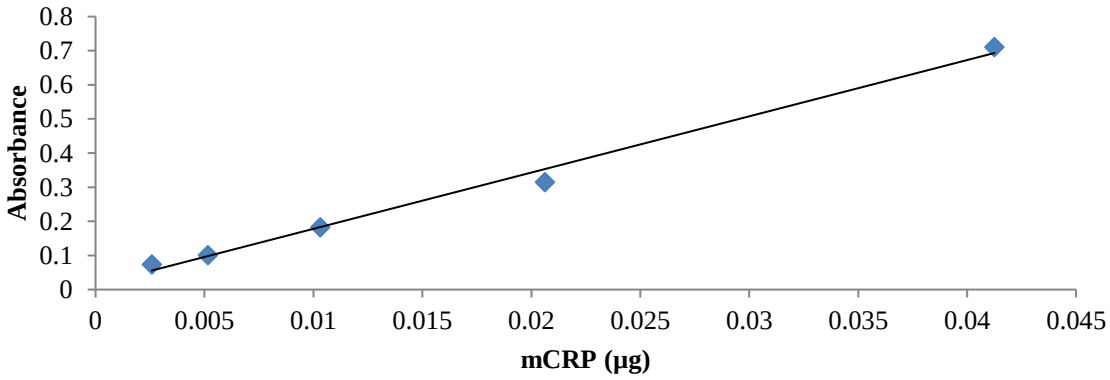

Figure 3.6. Calibration graphs for both monomeric and pentameric CRP. a) The calibration graph for pCRP. The line equation is: $y = 20.712x + 0.0372$. The R^2 value is: 0.9967. b) The calibration graph for mCRP. Monomeric CRP used was dissociated via a 3M urea dissociation trial. The line equation is: $y = 16.486x + 0.0132$. The R^2 value is 0.9922

Figure 3.6a and 3.6b displays the calibration graphs for both pCRP and mCRP respectively. The pCRP samples were purchased from SCRIPPS, whereas mCRP samples were produced *in vitro* from a 3M urea dissociation experiment (see Chapter 2). The R^2 displays a strong positive relationship between absorbance of protein concentration. Absorbance values are all below 1, indicating that absorbance is proportional to protein concentration for both calibration experiments. Line equations from both graphs were used to determine their respective CRP concentrations for the purified human serum samples.

Figure 3.7 displays the levels of pCRP present within each of the combined fractions (B4 and B5) from all 40 human serum samples as determined by ELISA. The values obtained from ELISA have been corrected per the appropriate concentrated volume post FPLC (see 3.3.2 and Appendix 5) to represent the concentration in the initial serum samples. All 40 of the samples tested positive for the presence of pCRP. The positive controls tested positive for pCRP whereas the negative controls did not (results are not included). Sample concentration is expressed in terms of mg/L and all results were triplicated. These results fit in line with those observed from the Western Blot analysis, which resulted in a positive band for all 40 samples (fractions B4 and B5). The lowest recorded value of pCRP within any of the samples was from CRP 021, which was calculated at 2.9mg//L, with the highest being recorded at 66.8mg/L for the sample 'CRP 012'. The average value of pCRP recorded was 23.3mg/L (SD for all 40 samples: 13.6, SE for all 40 samples ±2.1). As the requirement for participating in the study was to display an initial CRP reading of over 100mg/L, this indicates a significant loss of protein. This trend is also displayed throughout the main body of results, with none of the total forty samples displaying a CRP value >100mg/L, although as previously described, steps within the methodology used can result in losses of up to 50% of the sample with a poor return post-purification.

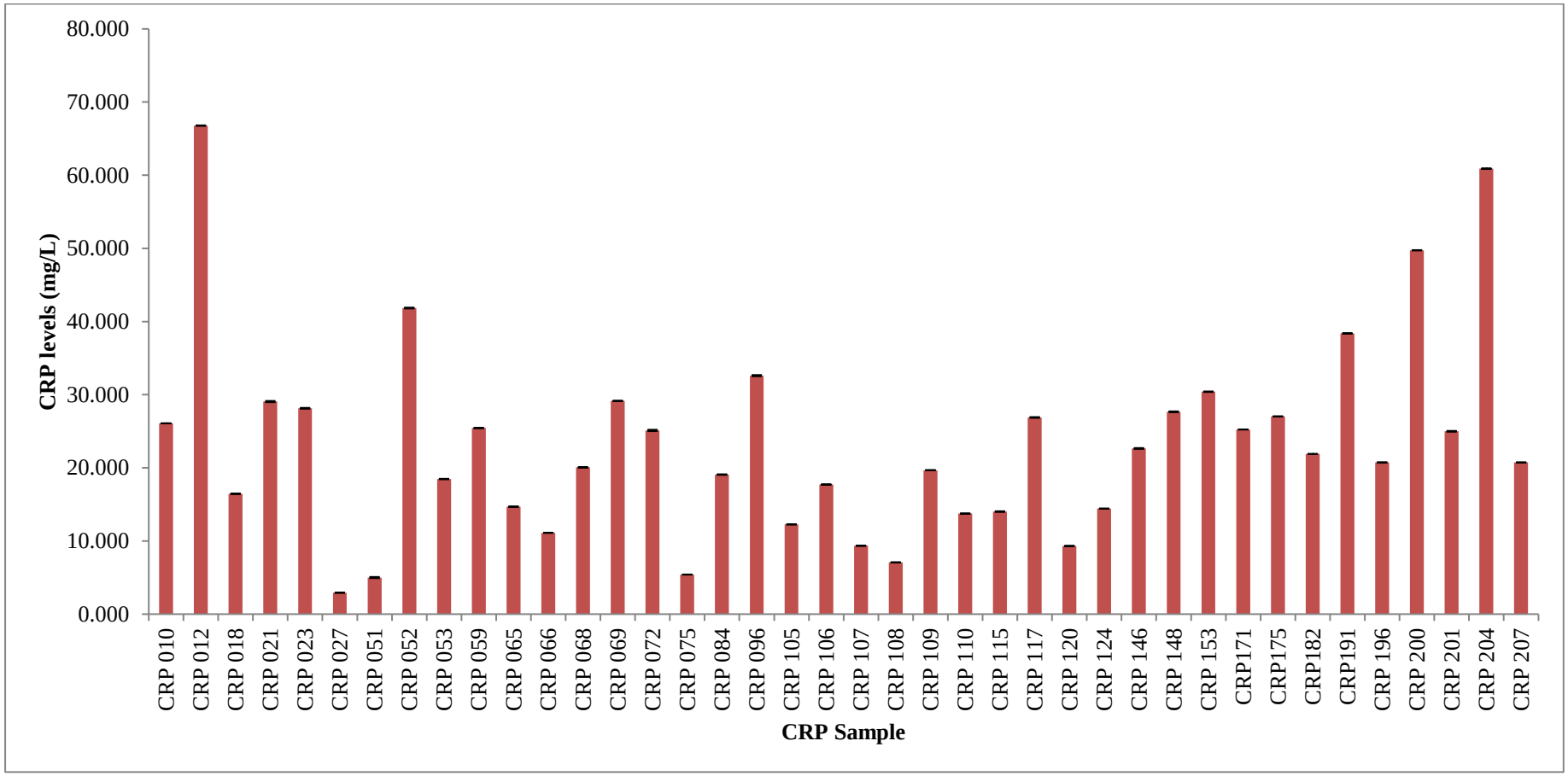

Figure 3.7 Pentameric human serum CRP levels in the serum samples as determined by ELISA of fractions B4 & B5 purified via the FPLC. The concentration of each sample is expressed in terms of mg/L. Samples were diluted 1:100 in triplicate. Scores shown are an average value minus the average control. Primary and secondary antibody dilutions used were 1:40,000. ELISA plates were developed with TMB and read at 450, n = 40. Error bars represented by SEM for each sample.

Purified pCRP (B4 + B5) samples were subject to additional protein quantification via the UV Spectrophotometer machine, as described in Section 2.2.5. The total CRP in the initial samples as calculated from the UV spectrophotometer measurements in the purified fractions was plotted against the levels calculated via the ELISA analysis to provide a quantifiable comparison. This comparison is shown in Figure 3.8 which provides an overview of the relationship between the two different techniques. The R^2 squared value of 0.46 indicates a slight correlation between the two sets of data; furthermore, observation of the chart clearly portrays a moderate, positive correlation within the data.

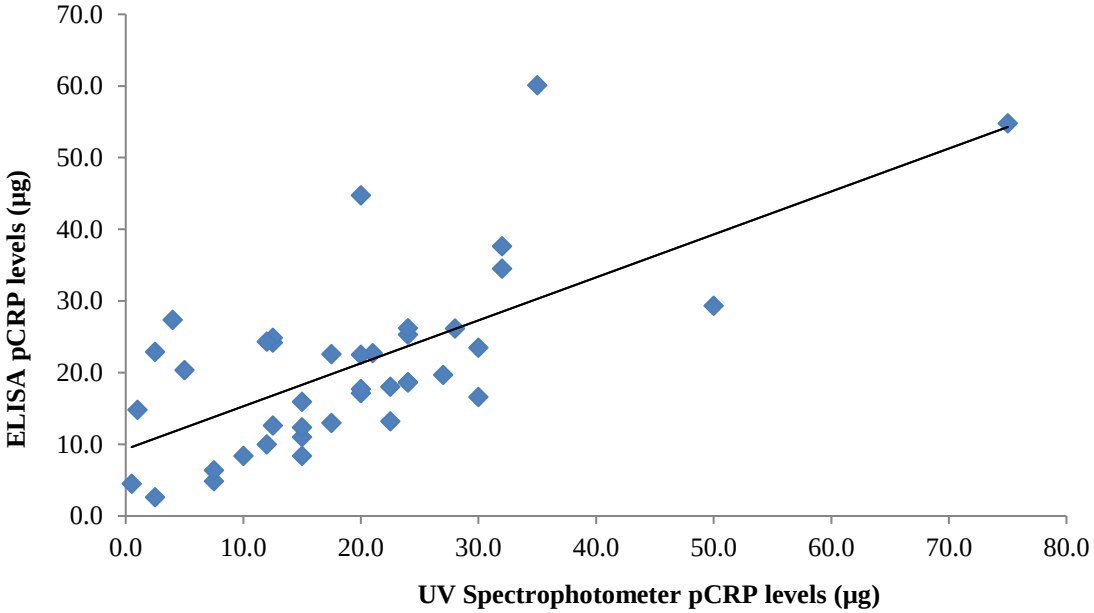

Figure 3.8. A comparison of the pCRP levels calculated from the ELISA analysis against the data provided through the UV Spectrophotometer. The R^2 value of the scatterplot was calculated at 0.46 and the line equation was as follows: y = 0.3994x + 9.313

Purified mCRP human serum fractions (B7 & B8) from the FPLC were subject to analysis via an ELISA. Figure 3.9 displays the levels determined by ELISA of mCRP present within each of these combined fractions (B7 and B8) from all 40 human serum samples. The values obtained from ELISA have been corrected per the appropriate concentrated volume post FPLC (see 3.3.2) to represent the concentration in the initial serum samples. The

positive controls tested positive for mCRP whereas the negative controls did not (results are not included). Sample concentration is expressed in terms of mg/L and all results were triplicated. The entire 40 samples tested positive for the presence of the monomeric form of CRP (denoted as 'mCRP'). These results show a significant increase in the number of positive samples compared to those observed from Western Blot analysis, which only detected positive bands for three samples (indicated by ELISA to be the three samples with the highest mCRP levels) highlighting the difference in sensitivity of the two techniques. Furthermore, this disproves the initial hypothesis that only 10% of the 40 patient samples would contain mCRP, when the actual value is 100% based on our results. The largest recorded value of mCRP within a sample was 3.5mg/L, with the average value from all 40 samples being 0.88mg/L (SD for all 40 samples: 0.89, SE for all 40 samples ±0.142). The purified mCRP (B7 + B8) was also subjected to additional quantification via the UV Spectrophotometer. Unfortunately, as mCRP levels of the purified, concentrated fractions were so low, protein levels were undetectable.

For the total cohort of 40 participants, all mCRP values recorded were significantly lower than those recorded for pCRP demonstrating an uneven split of these two proteins within serum. This was expected as raised CRP levels were a prerequisite to partake within this study and we hypothesised that pCRP would be the predominant form of CRP within human serum. It is worth noting that even though all 40 samples were positive for the presence of mCRP, some of these results were extremely low. These results are outlined in Table 3.5.

'CRP' Sample Code	**mCRP concentration (mg/L)**
027	0.08
051	0.13
096	0.04
105	0.06

Table 3.5 ELISA results from B7 and B8 fractions which recorded the lowest levels of mCRP out of those who tested positive. The concentrations are for the initial sample as calculated from the ELISA results.

A comparison of the remaining samples for mCRP highlights several which display markedly increased levels of the protein (see Table 3.6). The three highest of these samples (115, 148, and 204) are those giving positive results from the Western Blot analysis of the mCRP fractions B7 & B8 (see below and Figures 3.11 and 3.12).

'CRP' Sample Code	**mCRP concentration (mg/L)**
012	2.02
115	3.52
148	3.28
204	3.51
069	3.07

Table 3.6 ELISA results from the B7 & B8 fractions which displayed markedly increased levels of mCRP compared to the remaining positive results. The concentrations are for the initial sample as calculated from the ELISA results.

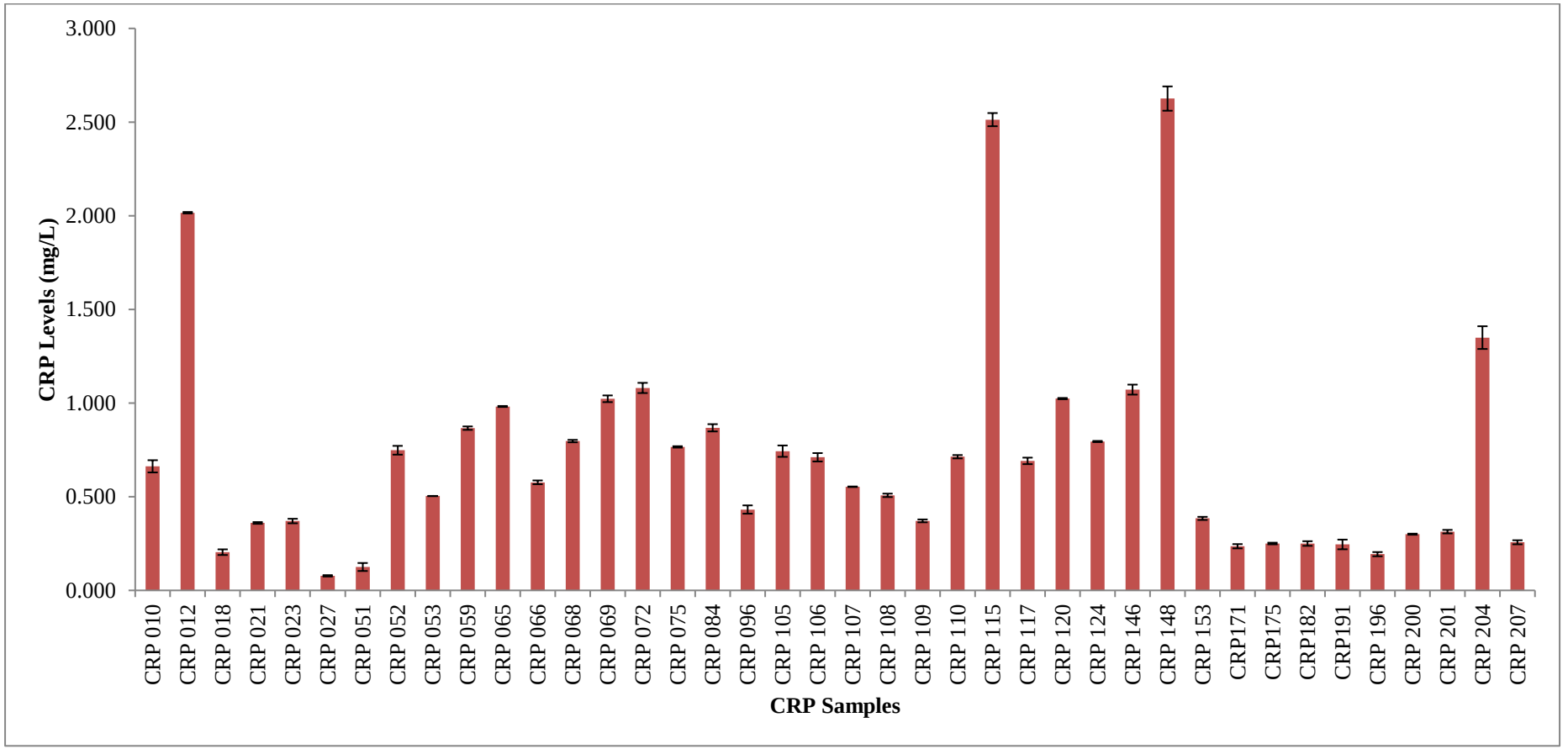

Figure 3.9 Monomeric human serum CRP levels in the serum samples as determined by ELISA of fractions B7 & B8 purified via the FPLC. The concentration of each sample is expressed in terms of mg/L. Samples were diluted 1:10 in triplicate. Scores shown are an average value minus the average control. Primary and secondary antibody dilutions used were 1:40,000. ELISA plates were developed with TMB and read at 450nm, *n* = 40. Error bars represented by SEM for each sample.

3.3.4 Western Blot Analysis of the Eluted Serum Fractions

To determine the presence of CRP in the samples collected from the size exclusion column, Western Blot analysis was carried out. A commercially available, CRP specific monoclonal antibody (Clone 8, Sigma), was used to test the samples for CRP. Previous experimental Western Blot analysis, (see Chapter 2) demonstrates that the monoclonal antibody can interact with and bind to both pentameric and *in vitro* produced mCRP. The previous successful Western Blot analysis with *in vitro* produced mCRP indicates that the epitope for antibody (Clone 8) binding remains identical and structurally intact when compared to that of pCRP. Although potential forms of mCRP within human serum may not be structurally identical to that of *in vitro* produced mCRP, one can assume that the same readily available epitope may be present for antibody binding with *in vivo* samples. Fractions B4 & B5, thought to contain pCRP, along with B7 & B8, thought to potentially contain mCRP, were combined respectively and concentrated as described in 3.2.6.

Figure 3.10 shows a typical Western Blot analysis of the CRP samples from the combined fractions B4 & B5. The samples used (going from lanes 1-9) were CRP 108, 109, 110, 115, 117, 120, 124, 146 and 148. All 9 of the samples tested were positive for the presence of pCRP through Western Blot analysis using a CRP specific monoclonal antibody (see Figure 3.4). Lane 10 consists of the pCRP control sample (from SCRIPPS), which the 9 CRP samples were compared against. The control image is separate to that of the serum samples as it was exposed for a shorter period (15 minutes), compared to that of the serum samples (30 minutes). All 10 of the bands (including the control sample) were present around the 23kDa mark when compared to the molecular weight markers (as shown on Figure 3.10), which corresponds correctly with the individual subunit size of CRP (Shrive *et al.,* 1996). The results shown in Figure 3.10 are typical of the Western Blot analysis seen for all combined fractions B4 & B5. Positive bands for pCRP were identified for all the 40 human

serum samples. All samples that were analysed via a Western Blot were compared to a positive control of pCRP and no anomalous results were found when testing fractions B4 & B5 for pCRP.

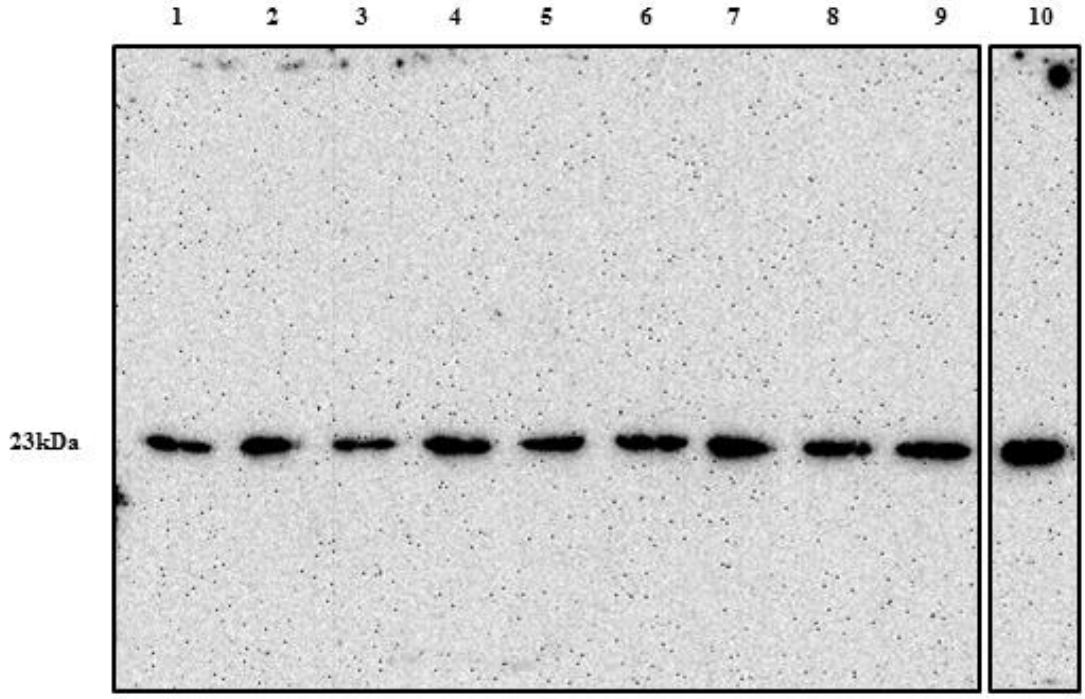

Figure 3.10 A Western Blot of the size exclusion fractions B4 and 5 for samples; 108, 109, 110, 115, 117, 120, 124, 146, 148. Samples are in lanes 1-9 respectively. Bands are present for all 9 of the serum samples tested. Lane 10 contains pCRP control (0.1µg). The primary mAb dilution was 1:1,000. The secondary mAb dilution was 1:40,000. Samples were exposed for up to 30 minutes.

Each of the mCRP samples collected from the size exclusion column were subjected to Western Blot analysis. Figure 3.11 and 3.12 shows the WB analysis of selected mCRP samples (going from lanes 1-9) 018, 021, 023, 109, 115, 148, 153, 175 and 207, 204, 201, 200, 196, 191, 182, 171, 146 respectively. These two figures include the only samples from combined fractions B7 & B8 from all 40 of the human samples which gave a positive Western Blot result for mCRP. Lane 9 and 10 in both Figures 3.11 & 3.12 respectively, contains an *in vitro* produced monomeric control from a 3M urea dissociation trial (as described in section 2.2.1). The control sample images are separate images as they were

exposed for a shorter period (of 15 minutes), compared to that of the serum samples, which were exposed for 45 minutes. As hypothesised in section 3.1.4, we believed that if mCRP were to be present within serum, only a small proportion of the total CRP would be mCRP. Therefore, a smaller mAb dilution was used to ensure even the smallest amounts of protein were detected. Figure 3.11 shows two samples which were positive for a monomeric form of CRP; samples 115 and 148. The bands shown were consistent in their migration distance with the *in vitro* mCRP control. Furthermore, the bands were present around the 23kDa mark when compared to molecular weight markers, corresponding correctly to the size of an individual subunit for CRP (Shrive *et al.*, 1996).

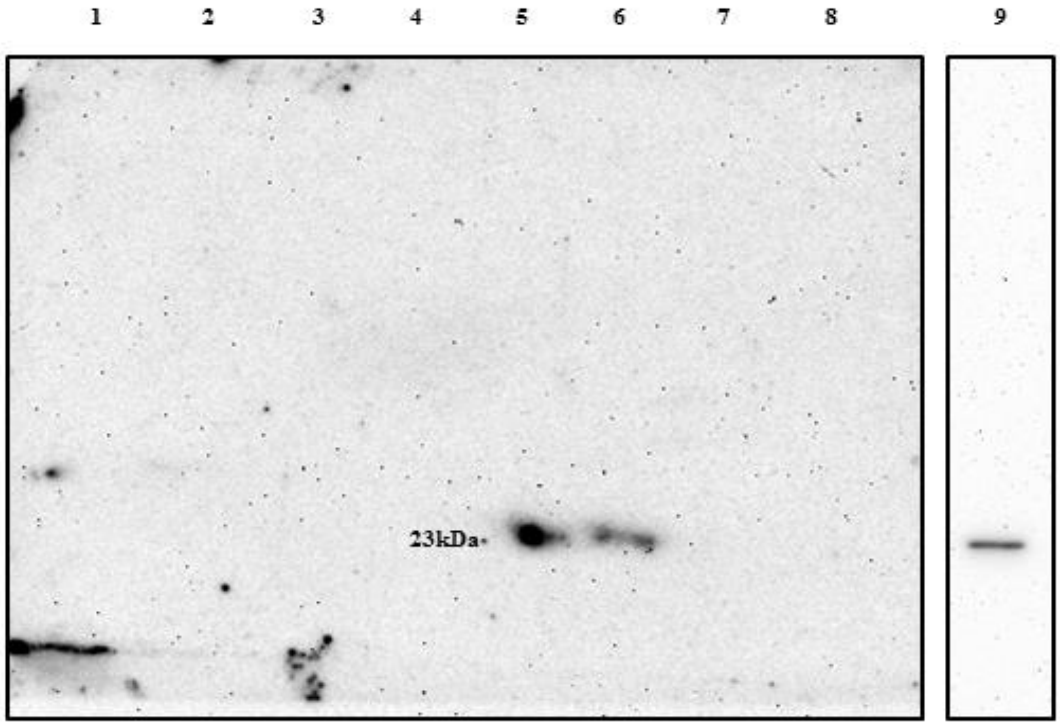

Figure 3.11 A Western Blot of the size exclusion fractions B7 and 8 for samples; 018, 021, 023, 109, 115, 148, 153 and 175. Samples are in lanes 1-8 respectively. Bands are present for samples 115 and 148. Lane 9 contains mCRP control (0.1µg). The primary mAb dilution used was 1:400. The secondary mAb dilution used was 1:20,000. Samples were exposed for up to 45 minutes.

Figure 3.12 shows the WB which gave a positive result for the human serum sample 204. It is worth noting that WB analysis was performed on all purified mCRP samples. Those

which gave a negative result for all samples on one blot were not shown. As stated previously, the control samples were from *in vitro* produced mCRP from 3M urea dissociation trials. The band shown in Figure 3.12 is consistent with the control sample in its migration distance throughout the gel. The sample is present around the 23kDa mark when compared to the molecular weight markers, again corresponding to the size of a single subunit of CRP (Shrive *et al.*, 1996). Unlike Figure 3.11, Figure 3.12 contains a considerable amount of background staining at the bottom of the membrane. This is due to two factors; the length of time which the samples were exposed for, in addition to small amounts of acrylamide sticking to the membrane post-SDS PAGE.

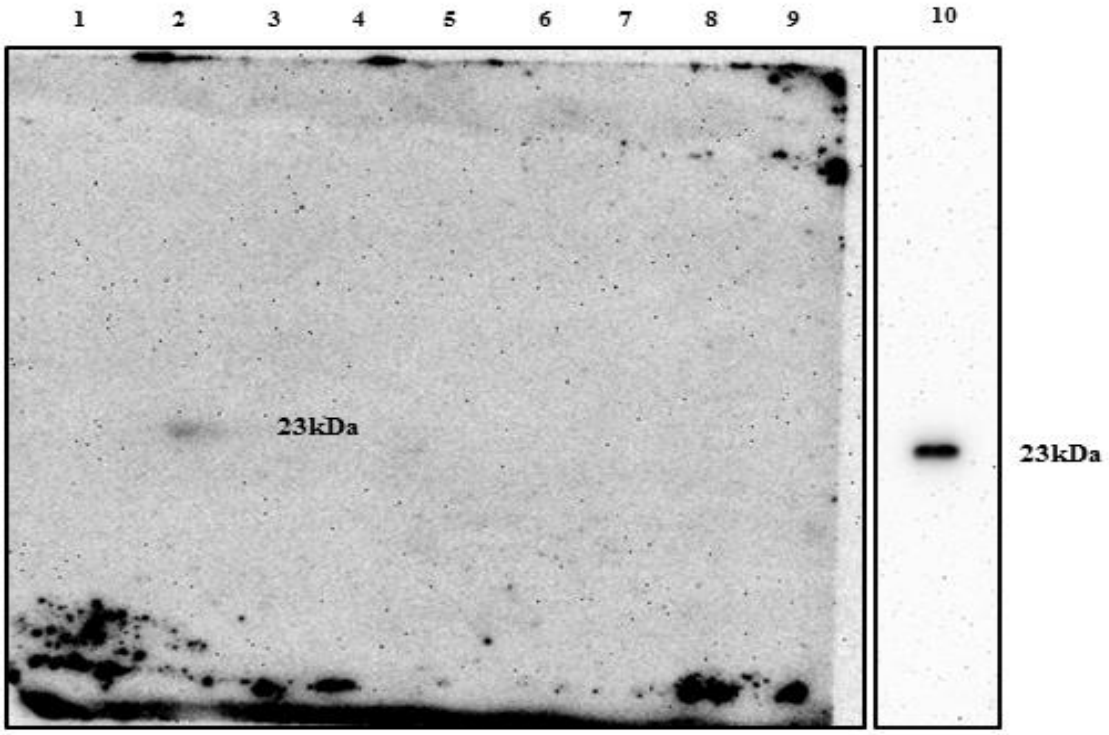

Figure 3.12 A Western Blot of the size exclusion fractions B7 and 8 for samples; 207, 204, 201, 200, 196, 191, 182, 171, 146. Samples are in lanes 1-9 respectively. A band is present for sample 204. Lane 10 contains mCRP control (0.1µg). The primary mAb dilution used was 1:400. The secondary mAb dilution used was 1:20,000. Samples were exposed for up the 45 minutes.

To ensure that results were not anomalous, or mistaken for background staining, the three samples which gave a positive result for the presence of CRP were tested several times.

3.4 Discussion

3.4.1 Overview

Here we describe the purification of human serum, through established procedures developed within our laboratory, alongside information provided within the scientific literature, to detect mCRP. We have successfully identified mCRP in all the 40 patient samples, with protein levels quantifiable via ELISA analysis. It was noted that purified levels of both pCRP and mCRP were markedly decreased when compared to the initial CRP concentrations provided by UHNM. Finally, we found that mCRP displays an ability to reversibly bind to PC through affinity chromatography, with Western Blot and size exclusion chromatography calculating the protein to have a molecular weight of approximately 23kDa. All CRP ELISA, UV Spectrophotometer and initial UHNM values can be found in a table in Appendix 5.

3.4.2 Human Serum Sample Purification

As human serum contains a crude mixture of proteins, platelets, hormones, among other components, a large proportion of the samples passed freely through the column, without interacting with the readily available PC units (Murphy *et al.*, 2008). This is shown through the large absorbance value of 0.54AU in peak 1 of Figure 3.3. Upon addition of the calcium chelator, EDTA, a smaller secondary peak was observed, measuring an absorbance of 0.05AU. The second peak exhibited a slight ‘shouldering’ effect, just left to the apex of the peak, which was typical for most traces seen when purifying the human serum samples. The ‘shouldering’ effect could be a result of the slow progression of various PC-binding serum proteins being eluted off the column based on their binding affinity to the ligand. Alternative ligands which display higher binding affinities to PC may need to be immersed within the chelating buffer before to elicit the elution of the protein; this may explain the

common ‘shoulder’ observed on all the serum traces. It was assumed the bulk of peak 2 represented the elution of CRP from the column, due to samples contained raised levels (>100mg/L), although other serum proteins are known to bind PC (Christner & Mortensen, 1994).

Like that shown in Figure 3.3, the chromatography trace in Figure 3.4 was typical of that seen for all 40 patient serum samples. Three main peaks (labelled 1-3) were observed, representing molecular weights of 787kDa, 200kDa and 110kDa respectively. As we are not aware of any serum calcium binding proteins with a molecular weight around 787kDa, we concluded that this protein was not relevant to our study, as this did not correspond to any of our expected protein sizes. Therefore, sample analysis of this fraction was not pursued. Similar to peak 1, it was unclear what peak 2 may represent, based on the elution volume and calculated molecular weight. One hypothesis was that this protein may represent decameric forms of CRP, or CRP aggregates. As described previously, this peak was concluded to be not relevant to our study and the eluted fraction was not pursued through additional experimental analysis. Based on the elution volume of peak 3, the molecular weight for the protein was calculated to be 110kDa. Coupled with the data provided from the dissociation trials in Chapter 2, it was concluded that protein was pCRP. This was extended to all B4 & B5 fractions of human serum, when run through the size exclusion column. All 40 of the serum samples tested failed to produce a peak for mCRP. Previous *in vitro* trials, alongside the column calibration has allowed calculation of where the monomer is expected to elute (~95ml, B7 & B8 fractions). This failure to produce a peak on the chromatogram could be down to mCRP levels being too low for detection. Therefore, fractions B7 and B8 were collected for each serum sample and tested regardless.

3.4.3 Western Blot Analysis

As expected, the Western Blot results for fractions B4 & B5 gave a positive result for all 40 human serum samples. Samples also corresponded with the molecular weight of the pCRP control sample. Coupled with the molecular weight calculations from the size exclusion column, it was accepted that these samples contained pCRP from human serum. Fractions B7 & B8 (thought to contain mCRP) gave a positive band for the presence of CRP from three of the human serum samples, despite no peak being recorded on the chromatogram (Figure 3.4). The samples which tested positive for CRP were 115, 148 and 204, the three highest serum mCRP concentrations as indicated by ELISA. The positive bands observed in Figures 3.11 and 3.12 corresponded to the molecular weight of the mCRP standard that was run alongside them (~23kDa). To our knowledge this is the first isolation and positive identification of mCRP through this procedure. Based on the molecular weight calculation from the size exclusion column, coupled with the positive bands from the Western Blot, these results suggest confirmation of the presence of a 'monomeric' form of CRP in human serum.

3.4.4 Enzyme-linked Immunosorbent Assay Analysis

ELISA analysis was carried out on all samples (fractions B4 & B5 and B7 & B8). A positive result was confirmed for all the 40 patient samples from fractions B4 & B5, which corresponds with the results observed from the Western Blot analysis. The average value of pCRP recorded was 23.3mg/L, with the minimum recorded value calculated to be 2.93mg/L and the maximum at 66.78mg/L. These results were further backed up by the additional quantification of the purified pCRP samples via the UV Spectrophotometer, as a comparison of the purified pCRP ELISA results with the quantified UV Spectrophotometer values suggested a weak positive correlation between the two sets of data. It is worth noting that

one of the main patient criteria for inclusion in this study was to have recorded CRP levels of >100mg/L. Comparison of these results with the CRP values provided through UHNM therefore suggests a large proportion of the protein within the sample was lost through the purification process. We have previously reported that large losses of the protein samples may occur through the concentrating and chromatography steps of the purification process (up to 50%), as described in Chapter 2.

ELISA analysis on fractions B7 & B8 resulted in all 40 patient serum samples being confirmed to contain mCRP. Comparison with the Western Blot analysis highlights a significantly larger proportion of mCRP samples went undetected; portraying the difference in sensitivity of the two different techniques. The average recorded level of mCRP within the serum samples was 0.88mg/L, with the minimum recorded value being 0.04mg/L and the maximum recorded value being 3.52mg/L (Sample 'CRP115'). Four out of the 40 samples which tested positive for mCRP displayed significantly lower results, as shown in Table 3.5. This ability of ELISA to detect even these low levels further highlights the difference in sensitivity of the two techniques. Overall, our results show that mCRP levels are significantly lower than those observed for pCRP, alongside levels being unevenly distributed throughout the cohort which tested positive for the protein. Our initial hypothesis was that we would expect to detect mCRP within 10% of our sample cohort, whereas ELISA analysis has confirmed mCRP to be present within all 40 samples, with Western Blot analysis confirming the presence of mCRP in 3 of the samples tested. What is significantly apparent, despite all the recorded loses when comparing the levels with those provided by UHNM, is that mCRP is still detectable at considerable levels when compared to previously published data (Wang *et al*., 2015).

Based on the methodology used we can also conclude that the isolated form of mCRP retains the ability to reversibly bind to PC. Published literature has previously suggested that

pCRP dissociation occurs through membrane insertion, with cholesterol being identified as a key lipid component for mediating this interaction (Ji *et al.,* 2009). *Pneumococcal* C-polysaccharide (which contains PC units) and polylysine are also other ligands which have been identified as being able to bind and dissociate CRP. A hydrophobic microenvironment has also been proposed as a key component for CRP dissociation; cell membranes contain mild hydrophobic environments which could lead to rapid dissociation of the pCRP subunits. The mCRP described here, which has been isolated from human serum, displays an ability to bind and interact with its high affinity ligand, PC. Our results are in line with previous experimental models whereby CRP binds to cell surfaces to induce dissociation and elicit a pro-inflammatory response (Ji *et al.,* 2007; Ji *et al.,* 2009).

Previous data published by Wang *et al.,* (2015) describe patients who recently suffered with an AMI with an average recorded mCRP serum level of 0.021mg/L (published as 20.96ng/ml, n = 101), with deceased patients recording higher levels up to 0.0367mg/L. Furthermore, a total of six patients out of 42 with raised levels of pCRP (3-285mg/L) displayed increased mCRP levels: 0.0057mg/L – 0.1227mg/. A comparison with the mCRP levels recorded from our study is an order of magnitude higher compared to those recorded by Wang *et al*., (2015). Our study however only enrolled patients with raised levels of (>100mg/L), whereas Wang *et al.,* do not give details on how many of those 6 positive samples displayed initial pCRP levels >100mg/L.

It is worth noting that a proportion of the protein sample was lost from each sample due to our methodology. The protein yields for the purified samples ranged from 5 up to 30%. This links in with what has been previously reported for the purification of *in* vitro produced mCRP, as described in Chapter 2, with losses of up to 50%, which is thought to occur during the concentration and chromatography steps within the methodology. Furthermore, purification of *in vivo* CRP samples must undergo both affinity and size

exclusion chromatography, in addition to two concentration steps, which may explain the large protein losses reported here. Although it is not clear as to what percentage of pCRP or mCRP has been lost for each sample. Overall, our results demonstrate that there is an uneven distribution of pCRP and mCRP within the serum samples. If one of the two proteins were more susceptible to losses during the purification process, this could explain why some results displayed larger losses than others.

Additional factors may need to be considered when evaluating mCRP levels and its production. Specific pathophysiological conditions commonly observed in certain inflammatory diseases may play a leading role in providing the essential conditions for the proteins formation. Epidemiological evidence associates high levels of CRP with the progression and development of inflammatory diseases such as atherosclerosis and heart disease. Common pathological features such as activated endothelial cells and platelets, and the production of circulating MP are all known to dissociate CRP. The production of reactive oxygen species in inflammatory diseases including atherosclerosis can permanently oxidise or modify proteins which may alter their biological and structural properties, although this is just theorising (Berlett & Stadtman, 1997; Mugge, 1998). Furthermore, mCRP has been detected within the serum of patients who have recently suffered an AMI, in addition to being identified in the extra-cellular matrix of patients suffering with Alzheimer's disease (Ji *et al.,* 2007; Ji *et al.,* 2009; Khreiss *et al.,* 2004; Salazar *et al.,* 2014; Slevin *et al.,* 2015). Alterations to normal physiological conditions during disease may provide the essential conditions needed for mCRP's formation. The human body's physiological pH range is from 7.35-7.45. At sites of intensified inflammation, it is known to become slightly more acidic. As pCRP is known to bind to a wider range of ligands in acidic conditions, this may also provide the stimulus needed for its dissociation (Hammond *et al*., 2010; Kellum *et al*., 2004 Sneck *et al*., 2005).

The evidence provided from our research, alongside the information we have discussed within the literature displays a strong consensus for an association between mCRP production and inflammatory disease. It is plausible that chronic inflammatory diseases may result in the formation of a vicious pro-inflammatory cycle involved around mCRP. The half-life of CRP is approximately 18 hours, with levels being determined by the rate of production and severity of the stimulus. This therefore means that following an acute infection, levels of CRP would drop down to baseline levels relatively quickly. However, during prolonged periods of chronic inflammation, this removal of CRP from localised sites within the body may be more onerous, thus resulting in the persistence of this cycle of inflammation.

These results may also have a significant impact in a clinical setting. As described previously, mCRP circulating on MP was undetectable through common plasma assays (Crawford *et al.,* 2016). As we have shown, a monomeric form of CRP can be purified and isolated from human serum, in more samples and at higher levels than we initially expected. Raised levels of either protein within a patient may dictate a completely different set of circumstances, and require completely different treatment. This is especially shown in studies researching the potential diagnostic values and biological properties of mCRP in patients suffering with cardiovascular disease and AMI (Crawford, *et al.,* 2016; Eisenhardt *et al.,* 2009; Habersberger *et al.,* 2013; Wang *et al.,* 2015). If current standard clinical techniques and practice, such as ELISA, immunoturbidimetry and nephelometric assays, are unable to distinguish between the two isoforms, this could dramatically impact on a patient's health and the treatment they receive.

3.4.5 Conclusions

To our knowledge, these are the first published results which demonstrate clearly the isolation and detection, via Western Blot and ELISA analysis, of a monomeric form of CRP located within human serum. Experimentally determined levels for both mCRP and pCRP differed from those provided by UHNM, highlighting the scale of potential losses which we have observed can occur through the methodology used. Quantification of pCRP levels via the ELISA was further backed up by the values provided via the UV Spectrophotometer machine, with levels recorded displaying a weak, positive correlation with those from the ELISA. Furthermore, mCRP displayed an ability to reversibly bind to PC, something with has previously been reported not to occur. Previous studies have detected a mCRP *in vivo,* although the possibility of pCRP spontaneously dissociating upon binding to an ELISA plate still exists. By use of Western Blot analysis and size exclusion chromatography we could independently confirm the presence of mCRP.

Our research has highlighted the need for development of a new methodology which could accurately determine mCRP levels from neat serum and provided several new avenues of research involving mCRP which may potentially be pursued. Furthermore, it is possible that this could instigate a change in the way we measure CRP levels in a clinical setting as increasing evidence for a monomeric form of CRP continues to emerge.

3.4.6 Future Work

Future work should involve researching into establishing a link between mCRP levels and inflammatory disease. It is crucial that we determine what predicts rises in levels of mCRP and furthermore what increased levels may correspond too. The formation of mCRP *in vivo* is also an avenue of research that should be pursued. Several research models currently exist with each one displaying overlapping elements. If we can uncover the

mystery of how this protein forms, it may provide us with an indication as to what biological role it may have within the body.

Finally, research needs to be focused on establishing a reliable methodology which could be used to accurately measure serum mCRP levels, without risk of the previously discussed complications. Multi-step methodologies also provide obvious complications such as low protein yield. The use of a mAb specifically for mCRP would allow measurement of the protein within neat serum; this removing the heavy losses sustained through the purification processes. These results highlight significant problems within a clinical setting, when measuring CRP, which need to be addressed. This research may provoke healthcare professionals to consider re-evaluating the way in which the approach CRP, both as a biomarker and mediator of inflammation and consider that research may be required to accommodate the testing of mCRP levels within the body.

Chapter 4.0 – Protein Crystallisation

4.1 Introduction

4.1.1 The Crystallisation of Proteins

Protein crystallisation is the formation of a protein crystal, predominately used for scientific and industrial research. Proteins can be prompted to form a crystal within a solution that is supersaturated. This supersaturation causes protein molecules to form a lattice of repeating units (each unit known as a unit cell), held together by non-covalent forces. Structural biology researchers grow these protein crystals to determine the protein's structure at an atomic level through X-ray diffraction. Incorporating additional proteins or ligands within crystal trials is also common, as this allows investigation into how proteins interact and/or bind with other components at an atomic level (Sherwood & Cooper, 2010). It is virtually impossible to predict the conditions at which a protein will crystallise, therefore suitable conditions must be found by trial and error. The protein solution must be at a sufficient concentration to promote crystal growth as well as being in a homogenous solution (Sherwood & Cooper, 2010). The protein solution should be 'pure', meaning that it is free from contaminating materials such as nucleotides, carbohydrates and other small molecules which may inhibit crystal growth. To grow protein crystals of sufficient quality that they will diffract to a high resolution, each unit cell, which forms the crystal lattice, needs to be identical. A homogenous solution promotes diffraction quality crystals as there is a higher chance of all the unit cells being identical (Lorber & Giege, 1992).

4.1.2 The Formation of Protein Crystals

There is no set time for which it takes a protein crystal to form; the crystallisation period can range from several hours up to several years. The formation of protein crystals occurs when protein molecules within the solution slowly aggregate together, because of

changes in energy dynamics, adopting one or a few identical orientations resulting in the formation of a three-dimensional lattice structure (Blundell & Johnson, 1976; Rhodes, 2000). Repeating units of this lattice structure are known as 'unit cells', which are the smallest possible repeating unit required to generate a protein crystal. Unit cells are held together through non-covalent interactions, such as hydrogen bonds with the water molecules in between them.

To achieve the formation of these ordered crystal lattices, proteins are slowly precipitated out of an aqueous solution. The aggregation of the protein sample within a well occurs due to the precipitant, usually varying types of salt-based solutions, or large molecular weight polyethylene glycol (PEG), which draws water molecules away from the protein. Temperature, solution pH, protein concentration, protein purity and ionic strength are all factors which can also affect whether a protein will precipitate out and form an ordered crystal lattice (Rhodes, 2000). The slow and controlled removal of water molecules by evaporation raises both the protein and precipitant concentration, which sometimes gives rise to the formation of protein crystals (Rhodes, 2000). Slow precipitation is more likely to produce larger crystals, whereas rapid precipitation may result in smaller, poorly formed crystals or even an amorphous solid (Rhodes, 2000).

Crystal formation occurs in two stages, nucleation and growth. The nucleation step consists of the initial formation of molecular clusters from which crystals will grow. This stage requires protein and/or precipitant concentrations higher than those optimal for slow precipitation. If nucleation conditions persist, it will result in the formation of many nuclei, which can result in many smaller crystals, instead of very few larger protein crystals (Rhodes, 2000).

The solubility of a protein also determines how it will crystallise. If a protein crystal were placed in a solvent which is free of protein, this crystal will begin to dissolve; the crystal will stop dissolving when the protein concentration within the solution reaches a specific value. At this specific value, the rate at which the crystal loses protein molecules is the same as the rate at which it gains protein molecules is equal, and is said to be in equilibrium. The concentration of proteins in the solution at equilibrium is classed as the solubility (Asherie, 2004). The solubility of a protein will vary on the solution conditions. Protein crystals will dissolve in under saturated solutions – where the protein concentration is below the protein solubility, but grow in supersaturated solutions. This supersaturation is needed to overcome the large activation energy barrier which exists when forming the crystal (Asherie, 2004). This barrier represents the free energy that is required to create the microscopic cluster of proteins – known as the nucleus – from which a protein crystal will eventually grow. Due to this energy barrier, nucleation rates can range from weeks to even years. If the supersaturation is too small, the nucleation rate will be too slow and crystals will not form in any reasonable amount of time. The point at which the rate of nucleation is large enough that spontaneous nucleation is observable is known as the ‘labile’ or ‘nucleation zone’ (see Figure 4.1). When the solution reaches the nucleation zone under the ideal conditions, protein molecules begin to aggregate and the concentration of free molecules falls. This process is shown in Figure 4.1.

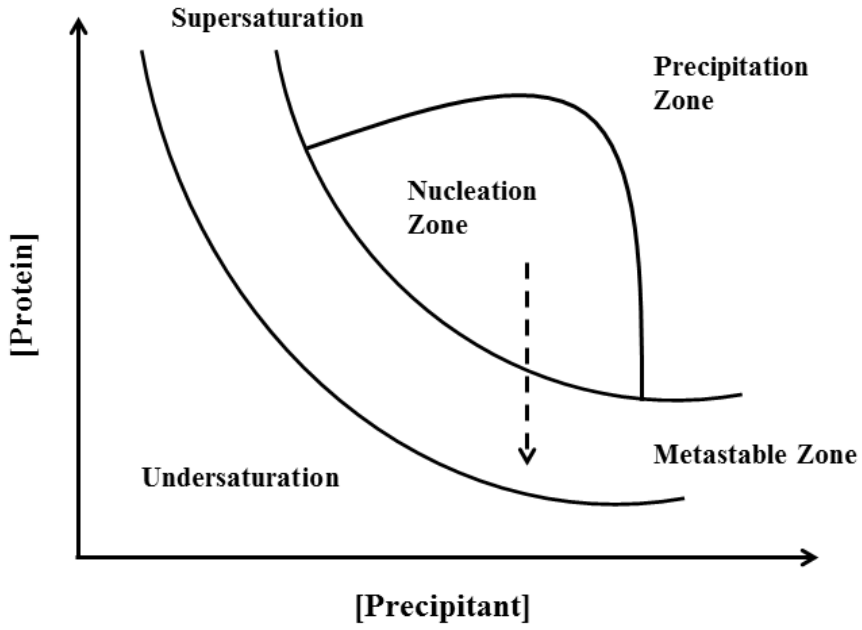

Figure 4.1. A diagram adapted from Foelsch, (2015), representing the required conditions for protein crystal growth. The process consists of increasing the supersaturation of the protein in a solution with an optimum concentration of precipitant. This supersaturation increases as water molecules diffuse to the reservoir until a crystal structure is nucleated. When this point is reached, the supersaturating should be reduced to allow the crystals to grow, as indicated by the south facing arrow.

This reduction of free molecules within the solution is the point at which the protein crystals can then start to grow larger within the metastable zone, as shown by the dotted arrow in Figure 4.1. If the nucleation rate becomes too high, small 'showers' of crystals may appear. This can be problematic as the crystals formed are often too small to test for diffraction. Finally, if the supersaturation zone is too high, this will result in the formation of precipitants or aggregates within the solution. This precipitation zone is unfavourable for crystal growth due to the formation as the disordered aggregates and precipitates form faster than the crystals (Asherie, 2004, Rhodes, 2000).

There are several well-known methods in which protein crystals can be grown, such as dialysis methods, batch methods or by vapour diffusion. There are also variations to the vapour diffusion technique, which differ depending on where the drop, containing the

protein solution, sits within the well. These are hanging drop, sitting drop and sandwich drop (Lorber & Giege, 1992). The sitting drop method of protein crystal growth is the technique used within this research project. The vapour diffusion method is carried out by using a tray with wells that contain different crystallisation conditions. Vapour diffusion is the most commonly employed diffusion technique used in protein crystallisation. For the sitting drop method, a droplet of the purified protein solution, buffer and precipitant are added to a small bridge sitting within the well, which contains a reservoir solution of the buffer and precipitant. The whole system is sealed, usually with a glass cover slip and vacuum grease. Over time, the reservoir solution, which contains a higher concentration of the precipitant, will equilibrate with the droplet, until the pressures in both are equal. As the droplet and reservoir solutions equilibrate, water within the droplet is removed, raising the concentration of the precipitant and protein solution. This system is represented in Figure 4.2.

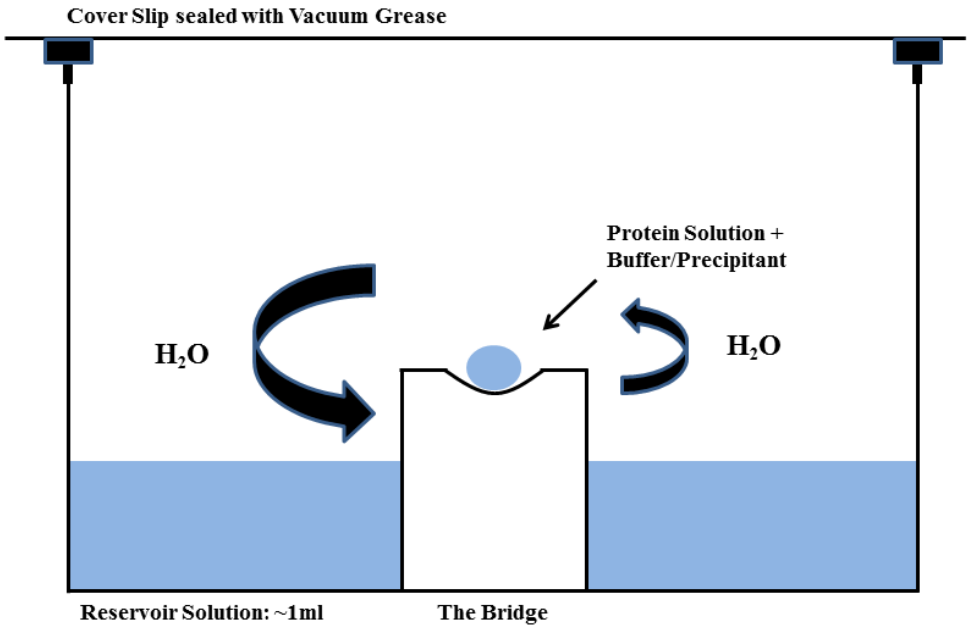

Figure 4.2. A diagram representing the vapour diffusion method used for the crystallisation of proteins. The protein solution is clearly displayed in the bridge, with the reservoir solution labelled below. The net diffusion of water molecules from the drop, represented by the arrows, to the reservoir slowly increases the protein concentration within the drop. Once optimal conditions are reached, protein crystals may form. The whole system is sealed with a cover slip and vacuum grease, as labelled above.

If the appropriate crystallisation conditions are reached within the droplet, the protein molecules within the droplet will slowly aggregate together to form a protein crystal (Glusker & Trueblood, 1985). Optimum crystallisation conditions for a protein (or complex) are usually unknown. In order to produce diffraction quality protein crystals that can be used for X-ray crystallography, many different trials will likely be used. Structure screens are commercially available which typically provide a set of 100 conditions that have previously been successful when growing protein crystals. When a specific condition produces a protein crystal, the condition can be 'screened'. Two-dimensional screening grids allow alterations of two variables (usually precipitant and ionic concentrations) to allow refinement of the condition in order to produce the best quality protein crystals (Rhodes, 2000).

There is a range of different precipitants that can be used in the formation of protein crystals. The most common precipitant used is salt-based precipitant, whereby the ions compete with the water molecules within the drop. This process is known as 'salting out'. Ions with a greater charge are usually better at salting out as they provide greater competition for the water molecules. As more water molecules are taken up, the proteins are forced closer together, which can result in the formation of a protein crystal. Other forms of precipitants commonly used for protein crystallisation are methyl pentanediol (MPD) and large molecular weight polyethylene glycol (PEG).

Other conditions which may affect the growth of protein crystals include pH and temperature. Alterations of the pH of a protein can change its solubility, and therefore its ability to form a protein crystal. Proteins with a larger charge, compared to those with no net charge at all tend to be more soluble, so subtle changes to this could alter both the quality of the crystal or even its ability to form. Crystals are often grown at room temperature. Crystals that are grown in 4^{o}C (for example) would have to be viewed in the temperature that they

were grown in, otherwise the crystal well would be forced to undergo temperature changes, adding unnecessary complications to the system (Lorber & Giege, 1992; Rhodes, 2000).

Protein crystals are also very fragile. Unlike small molecule crystals, the spaces between proteins within the crystal lattice are typically filled with a high percentage of solvent. The protein crystals are therefore never removed from their mother liquor for fear of drying out. Water loss from these protein crystals can thus result in the crystals cracking or even breaking apart, which would result in them being unusable, thus diminishing in their quality (Lorber & Giege, 1992).

Sometimes, during protein crystallisation trials, protein crystals may crystallise in more than one form (Rhodes, 2000). Often these crystal forms will differ in their quality of diffraction, ease of reproducibility and potentially in other properties too. Protein crystals which take more symmetrical shapes are preferred, as these are the crystals which diffract well and require less data collection, although with current advances in crystallography research, this is no longer a big issue (Rhodes, 2000). The slow precipitation of organic solvents or highly concentrated salt-based solvents within an aqueous solution can form crystals known as small molecule crystals (up to 200 atoms). The growth of small molecule crystals when trying to crystallise proteins can be problematic for some crystallographers, as it is difficult to distinguish between the two. The easiest method of determining a small molecule crystal will be upon X-ray diffraction, where diffraction patterns characteristic of small molecule crystals will be visible.

4.1.3 Cryoprotection of Protein Crystals

Protein crystals are flash-frozen in liquid nitrogen before they are exposed to X-ray radiation to provide diffraction patterns. The extremely cool temperatures of the liquid nitrogen help reduce the atomic vibration and diffusion as well as the level of radiation

damage by free radicals produced by the X-rays, increasing the resolution of the data collected (Rhodes, 2000). Prior to freezing the crystals, they must be soaked in a cryoprotectant, which displaces the water molecules within the crystal pores. This removal of water prevents ice forming within the crystal lattice, which can disrupt the lattice formation in addition to the formation of unwanted ice rings on the diffraction pattern (Lorber & Giege, 1992). Common cryoprotectants used are sugars including glucose or glycerol, as well as precipitants like MPD or a low molecular weight PEG. Once the protein crystal has been soaked in increasing volumes of cryoprotectant, it is removed by a loop where it is suspended in a thin film of the protectant, as shown in Figure 4.3. This is then flash frozen by immersing the loop into liquid nitrogen and kept in a cold stream of liquid nitrogen until testing (Rhodes 2000).

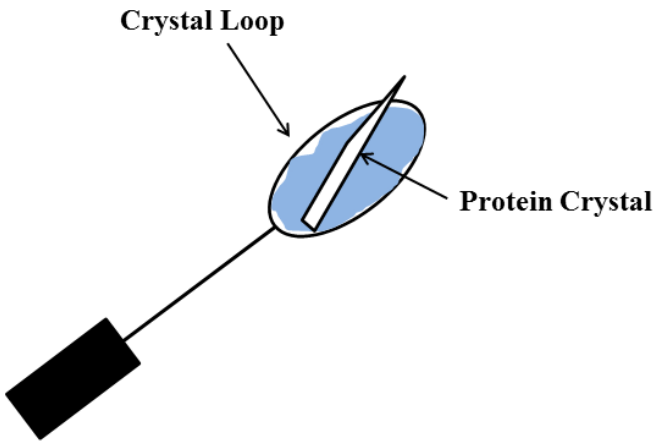

Figure 4.3. A diagram of the crystal loops which are used to transfer protein crystals from the well in which they were grown to a vial containing liquid nitrogen. Loop sizes will vary depending on the size of the protein crystal in question. The above diagram also displays a protein crystal immersed in a film of solvent and cryoprotectant. This helps prevent degradation of the crystal upon freezing. The crystal is flash-frozen into liquid nitrogen and stored until tested at DLS.

4.1.4 Monomeric C-reactive Protein in the Human Body

The atomic structure of native pCRP was first determined by Shrive *et al*., (1996), to a resolution of 3.0Å via X-ray crystallography. Following this, the structure for calcium-depleted pCRP and pCRP bound to PC was solved (Ramadan *et al*., 2002; Shrive *et al*., 1996; Thompson *et al*., 1999). These three-dimensional maps of native CRP provide a detailed insight into what the structural arrangement of a monomeric form of CRP *in vivo* could be. To our knowledge there are no current studies which have attempted to crystallise this native or ligand-bound structure. Doing so may provide an insight into the biological role of mCRP within the human body. Published reports within the scientific literature have postulated that mCRP is 'membrane-bound', 'modified' and 'a monomeric protein'. Dissociation models, supported by experimental research, suggest an ability of this protein to bind to cell membranes, thus stimulating dissociation of the native pentameric molecule. As previously discussed (Chapters 2 & 3), there is also increasing evidence for a pro-inflammatory role of mCRP within the human body, further linking this protein to the progression of disease. (Eisenhardt *et al.*, 2009; Habersberger *et al.*, 2012; Ji *et al.*, 2007; Ji *et al.*, 2009; Li *et al.*, 2012; Molins *et al.*, 2008; Slevin & Krupinski, 2009; Zhao & Shi, 2010).

4.1.5 The Interactions between C-reactive Protein, C1q GHR and CWPS

The binding mechanism between C1q and CRP has been debated over previous years to occur through either the collagen like region (CLR) of the C1q protein, or the globular head region (GHR) (Jiang *et al.*, 1991; Jiang *et al.*, 1992). More recent experimental research involving protein binding models coupled with amino acid mutagenesis studies provide a strong argument for binding to occur through the GHR; although this is still not known for certain (Agrawal *et al.*, 2001; Gaboriaud *et al.*, 2003; Kishore *et al.*, 2004). Furthermore, to

elicit a sufficient immune response, CRP must additionally be bound to its primary ligand phosphocholine exposed on the surface of dead or damaged cells (Shrive *et al.*, 1996; Thompson *et al.*, 1999; Volanakis, 1982). It is also unknown whether CRP undergoes any conformational changes upon binding to phosphocholine (PC) to provide this immunogenic stimulus within the human body.

4.1.6 Experimental Aims

The experimental aims of the research within this chapter are focused on the crystallisation of two different forms of CRP. The first involved *in vitro* produced mCRP from 3M urea dissociation studies described in Chapter 2. Although structural determination of this protein may not directly reflect that of an *in vivo* form of mCRP it will provide a general overview of the arrangement of a monomeric unit of CRP. Furthermore, it will uncover any modifications that may have occurred through treatment with urea.

The latter part of this research involves the crystallisation of the complex C1qGHR, CRP and CWPS. As described above, activation of the classical complement pathway requires binding to both C1q and a ligand, such as CWPS. By uncovering any structural changes that occur within CRP upon ligand binding, alongside the interactions between CRP and C1q will provide a greater understanding of pCRP's role within inflammation and the human body.

4.2 Materials and Methods

4.2.1 Preparation of Monomeric C-reactive Protein

All native human CRP used within the crystallisation trials is purchased in >99% purified form from SCRIPPS laboratories, San Diego, California, USA. Human pCRP was provided in a solution of: 20mM Tris, 280mM NaCl, 5mM $CaCl_2$, 0.1% NaN_3, pH 8.0. The protein was stored at 4^{o}C until use. Monomeric CRP used within all the crystallisation trials was produced and purified from the purified native human CRP as described in sections 2.2.1 and 2.2.2 of Chapter 2.

4.2.2 Crystallisation Trails of Monomeric C-reactive Protein

For the crystallisation trials, the human mCRP was used at a concentration of 4.3mg/ml (0.187M). All crystallisation trials consisted of mCRP with no ligand. All protein used within the crystallisation experiments had been stored at 4^{o}C within the lab for no longer than 6 months. Due to the lengthy process of mCRP production, coupled with a poor percentage yield from the purification process, a continuous flow of dissociation experiments was set up to replenish mCRP stocks. This therefore prevented the total exhaustion of the mCRP stocks, in addition to the purified protein being stored in the lab for extended periods of time.

All crystallisation trials used chemicals purchased from either Sigma or Fisher Scientific. Both structure screens 1 and 2 used in the initial crystallisation trials were purchased from Molecular Dimensions (cacodylate-free). All stock solutions of buffers were filtered through a 0.2µm Ministart Plus filter (Sartorius Vivascience, Hanover, Germany) to remove any particulate matter and microorganisms.

The sitting drop vapour diffusion crystallisation method was used with Linbro 24 well plates (MP Biomedicals Inc., Ohio, USA), microbridges (Molecular Dimensions), and coverslips (Menzel-Glaser, Braunschweig, Germany) sealed with high vacuum grease (Dow Corning, USA). A reservoir of 1ml crystallisation buffer was used per well containing the precipitating agent. Droplets of 1:1 ratio for protein to crystallisation buffer were placed in the microbridge at a total volume of 2µl, thus meaning the final concentration of mCRP within the drop was 2.15mg/ml (0.094M). All crystallisation plates were stored at room temperature and monitored for crystal growth using a Leica Mz16 microscope. Photographs of crystals were taken using a Pentax digital camera mounted on the microscope. The protein crystal dye IZIT (1µL) was added to one of the wells to determine whether the crystals grown were protein or small molecule.

4.2.3 Cryoprotection of Monomeric C-reactive Protein Crystals

The cryoprotectants used for crystals produced from crystallisation trials with mCRP were MPD and PEG 400 as both have previously shown to be reliable cryoprotectants within our research group. All cryobuffers were made with the cryoprotectants at 5, 10, 15 and 20% in the precipitant buffer specific to each well. The protocol for cryoprotection of crystals involved the addition of a 2µl droplet of the 5% cryoprotectant. This is followed by the addition of 2µl of the 10, 15 and 20% cryoprotectant at two to five minute intervals respectively. A further two drops of 2µl of the 20% cryoprotectant is added sequentially at two to five minute intervals. An exchange was then carried out by the removal of 10µl from the drop within the microbridge, and a replacement volume of 10µl of the 20% cryoprotectant added. Crystals were removed in the loop and immediately flash frozen in liquid nitrogen in which they were stored until tested at Diamond Light Source (DLS).

4.2.4 Data Collection at Diamond Light Source

All crystals that were produced from the human mCRP crystallisation trials were tested at DLS in Didcot, Oxfordshire. The stations that the crystals were tested were I02 and I04. The detector at the DLS stations for I02 and I04 was the ADSC Q315 CCD.

4.2.5 Production of the C1q Globular Head Region

Human C1q was purchased in a >99% chromatographically purified and lyophilised form from BioRad. Chemicals used for buffers for the digestion of intact C1q are highlighted in Table 4.1.

Buffer Used	Chemical Components
Solubilising Buffer A (pH 7.4)	0.1M Tris BASE
	0.2M NaCl
Solubilising Buffer B (pH 7.4)	0.1M Tris BASE
	0.2 NaCl
	0.05M Calcium Acetate
Dialysing Buffer 1 (pH 7.4)	0.1M Tris
Dialysing Buffer 2 (pH 7.0)	1M Sodium Citrate
	0.2M NaCl

Table 4.1 A Table listing all the chemical components used in the buffers for the enzymatic digestion of intact human C1q with the collagenase enzyme. Concentrations of all the chemical components used are also given.

1mg of lyophilised, intact C1q was dissolved in 5ml of solubilising buffer A and dialysed using tubing with 3.5 MWCO against 1L of dialysing buffer 1 overnight. The

sample was then removed from dialysis and transferred to a 15ml tube and spun in a centrifuge at 4^{o}C, 1000 x g for 15 minutes to collect the precipitate at the bottom of the tube. The supernatant was removed and transferred to a separate tube and stored at 4^{o}C. The precipitate was re-dissolved in 5ml of solubilising buffer B.

1mg of collagenase was dissolved in 1ml of deionised water. The C1q solution was heated in a water bath at 54^{o}C for 10 minutes, after which 200µl (0.2mg) of collagenase was added to the solution, which was then immediately removed from the water bath. The solution was left at room temperature for 1 hour, and then transferred to the cold room, at 4^{o}C, until a precipitate formed. The precipitate was removed from the digest by centrifugation at 4^{o}C, 1000 x g for 15 minutes. The supernatant was removed and dialysed in dialysis tubing with a 3.5 kDa MWCO against 1L of dialysing buffer 2 for up to 48 hours at 4^{o}C. The resulting precipitate was collected by centrifugation at 4^{o}C, 1000 x g for 15 minutes and re-dissolved in 100µl of solubilising buffer A. The following sample was denoted as C1qGHR. The protein concentration of the solution was determined by UV_{280nm} absorbance, as described in section 2.2.5, using the extinction coefficient for C1qGHR 0.982 (Gaboriaud *et al.,* 2003).

4.2.6 SDS PAGE of Human C1q Globular Head Region

Samples were run on a 12.5%T resolving, 4%T stacking SDS PAGE. Gels were cast as described in section 2.2.6. Reduced and non-reduced C1qGHR samples of 1µg were applied to the gel, alongside 1µg of intact C1q and molecular weight markers. Samples were prepared as described in section 2.2.6 in addition to the buffers used in the SDS PAGE.

Collagenase samples were also run on a separate SDS PAGE gel. 1µg of fresh collagenase was run alongside 1µg of collagenase that had been used for the digestion of intact C1q and molecular weight markers (all under non-reducing conditions). The

components used for the casting, running of the gel and sample preparation are as described in section 2.2.6. All gels were run for 45-50 minutes at 200V.

Once the enzyme control SDS PAGE had been run, the gel was transferred to Coomassie Brilliant Blue total-protein stain and left to develop for up to 30 minutes. The gel was rinsed with deionised water prior to imaging to remove any background staining. The SDS PAGE gel containing the C1qGHR samples was subject to silver staining, a highly sensitive method for staining protein gels compared to using Coomassie Brilliant Blue.

4.2.7 Silver Staining SDS PAGE Gels

All components used in the silver staining of SDS PAGE gels were purchased from either Sigma or Fisher Scientific. The gel containing the C1qGHR samples was washed twice with deionised water to remove any remaining running buffer from the surface of the gel. A 10% ethanol solution was added to the gel and left in a dark room on the rocking machine for ten minutes. The gel was then immersed in a second 10% ethanol solution of left for 30 minutes (the gel can be left overnight at this period). Following this a 0.7% nitric acid solution was added to the gel for 6 minutes and then washed thoroughly with deionised water. The gel was the immersed in 0.1% w/v silver nitrate and placed in a dark room on the rocking machine for 30 minutes. The gel was then rinsed thoroughly with deionised water and approximately 100ml of developing solution was then added (250µl of formaldehyde per 200ml of sodium carbonate solution, 22.9g/L). Once the developing solution appeared to turn a black/grey colour, it was disposed of, with fresh developing solution being added to the gel. Once the gel had been developed to the desired intensity the gel was covered 3% acetic acid and left for 5 minutes prior to imaging.

4.2.8 Initiation of the Complex Crystallisation Trails

All native human CRP used within these crystallisation trials is purchased in >99% purified form from SCRIPPS laboratories, San Diego, California, USA. The human CRP was provided in a solution of 20mM Tris, 280mM NaCl, 5mM $CaCl_2$, 0.11% NaN_3, pH 8.0. The protein was stored at 4^{o}C until use. The C1qGHR was purchased and produced as described in section 4.2.5. Pneumococcal CWPS was purchased from Statens Serum Institut, Copenhagen, Denmark in a lyophilised form. Upon use, CWPS was dissolved in 20mM Tris, 280mM NaCl, 5mM $CaCl_2$, 0.11% NaN_3, pH 8.0 to the appropriate concentration. The CRP and C1qGHR samples were concentrated to the appropriate concentration using Amicon 10kDa MWCO centrifugal filter devices, pre-rinsed with deionised water, at a force no higher than 1000 x g at 4^{o}C. The final concentration of the solution was measured using a spectrophotometer with UV absorbance at 280nm, as described in section 2.1.5. The protein samples (and CWPS) were either used immediately for crystallisation trials or stored at 4^{o}C.

Both ProPlex structure screens 1 and 2 used in the initial crystallisation trials were purchased from Molecular Dimensions (cacodylate-free). All stock solutions of buffers were filtered through a 0.2µm Ministart plus filter (Sartorius Vivascience, Hanover, Germany) to remove any particulate matter and microorganisms. For the crystallisation trials, the native, human CRP was used at a concentration of 13mg/ml (0.11mM). The C1qGHR was used at a concentration of 5.6mg/ml (0.11mM) and the CWPS was used in excess, at a concentration of 175mg/ml (26.66mM). CRP and C1qGHR were incubated 24 hours at a volume ratio of 1:1 prior to the addition of CWPS. The CWPS was then added to the solution at a volume ratio of 1:1:1, this was denoted as the complex stock solution.

The sitting drop vapour diffusion crystallisation method was used with Linbro 24-well plates (MP Biomedicals Inc., Ohio, USA), microbridges (Molecular Dimensions), and

coverslips (Menzel-Glaser, Braunschweig, Germany) sealed with high vacuum grease (Dow, Corning, USA). A reservoir of 1ml of crystallisation buffer was used per well containing the precipitating agent. Droplets of a 1:1 ratio for the complex stock solution to crystallisation buffer were placed in the microbridge at a total volume of 2µl. All crystallisation plates were stored at room temperature and monitored for crystal growth using a Leica Mz16 microscope. Photographs of crystals were taken using a Pentax digital camera mounted on the microscope.

4.2.9 Cryoprotection

The cryoprotectants used for crystals produced from crystallisation trials with native CRP, C1qGHR and CWPS were Glycerol, PEG 400 and PEG mono-methyl ether (MME) 550. The protocol for cryoprotection is as described in section 4.2.3. All cryobuffers were made with cryoprotectants at 5, 10, 15 and 20%. All crystals were removed in the loop and immediately flash frozen in liquid nitrogen in which they were stored until tested at DLS.

4.2.10 Diamond Light Source

All crystals that were produced from the complex crystallisation trials were tested at DLS in Didcot, Oxfordshire. The stations that the crystals were tested were I02 and I04. The detector at the DLS stations used was the ADSC Q315 CCD.

4.3 Results

4.3.1 Crystallisation Trails of Monomeric C-reactive Protein

The first half of these protein crystallisation experiments are dedicated to the crystallisation of an *in vitro* produced form of mCRP from our own developed methodologies (see Chapter 2). The initial crystallisation conditions involving the *in vitro* produced mCRP were chosen based on a range of conditions which have previously been successful in the crystallisation of pentraxins within our research group. These conditions, containing PEG, 2-(*N*-morpholino) ethane sulfonic acid (MES) and calcium chloride are shown in Table 4.2 Unfortunately after several months of monitoring these trials, no crystal growth was observed.

	1	**2**	**3**
A	4% PEG 6K, 10mM $CaCl_2$, 50mM MES, pH 7.0	7% PEG 6K, 10mM $CaCl_2$, 50mM MES pH 7.0	10% PEG 6K, 10mM $CaCl_2$, 50mM MES, pH 7.0

Table 4.2 Details of the initial crystallisation conditions for in vitro produced human mCRP. The conditions used were based on previous pentraxin crystallisation conditions which have proved successful in growing protein crystals.

Following on from the initial crystallisation trials, two structure screens containing a total of 50 conditions each, which have been documented to successfully grow protein crystals was used. Details for both structure screens used in the mCRP crystallisation trials can be found in Appendix 3. All conditions from the structure screens which showed a potential to grow protein crystals were further screened for optimisation of growth.

Several weeks after the initiation of structure screen 1, the condition 0.2M Ammonium Sulfate, 25% PEG 4000, 0.1M Sodium Acetate pH 4.6, produced two small rectangle shaped crystals, as shown in Figure 4.4.

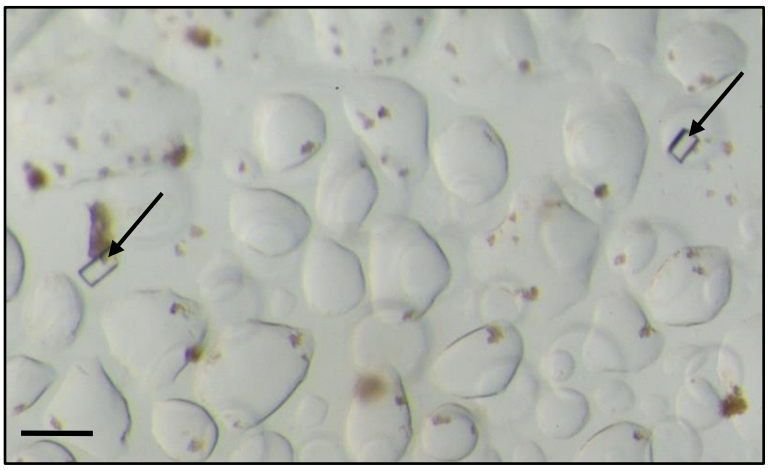

Figure 4.4 Two small rectangle shaped crystals produced from the condition 0.2M Ammonium Sulfate, 25% PEG 4000, 0.1M Sodium Acetate pH 4.6 from structure screen 1.Both crystals are identifiable by the arrows included in the Figure. The scale shown represents 200µm.

The crystal shown on the top right of Figure 4.4 was frozen in liquid nitrogen on the 13/04/2015 and tested at DLS on 19/04/2015. The crystal was cryoprotected prior to freezing. Whilst testing the crystal at DLS, it was noted that the crystal had degraded slightly in shape, with the edges appearing rounded. No diffraction pattern was observed from the crystal.

Four weeks after the start of the structure screen trial, three shard-like crystals, all joined together appeared in the well RW06A4 (see Figure 4.5). The condition of the well was 3.4M 1,6-Hexanediol, 0.2M Magnesium Chloride Hexahydrate, 0.1M Tris, pH 8.5.

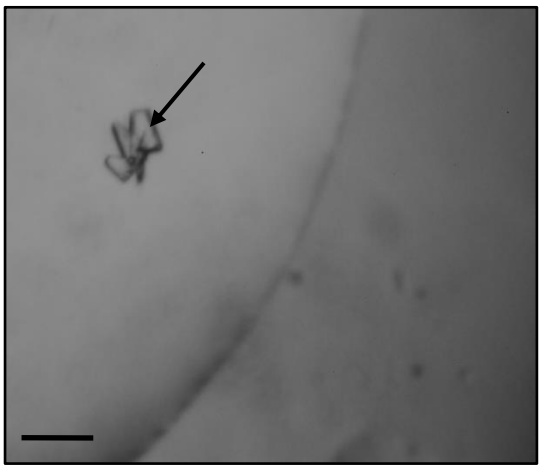

Figure 4.5 Three shard-like crystals, all joined together from the condition 3.4M 1,6-Hexanediol, 0.2M Magnesium Chloride Hexahydrate, 0.1M Tris, pH 8.5. The condition is from structure screen 1 of the mCRP crystallisation trials.The crystal cluster is identifiable via the arrow included in the Figure. The scale shown represents 100µm.

The crystal shown in Figure 4.5 was frozen in liquid nitrogen on the 01/12/2014 and tested at DLS on the 03/12/2014. Prior to the freezing of the crystal, it was broken apart into three separate pieces. Two out of the three crystals were tested, but unfortunately no diffraction patterns were observed. To improve the size and quality of the crystal shown in Figure 4.5, the condition was followed up with a three by three screen. The follow up trial involved the concentration of magnesium chloride and 1,6-hexanediol being altered by increments of 0.1 and 0.2M respectively either way. This is shown in Table 4.3.

	A	B	C
1	3.2M 1,6-Hexanediol, 0.1M Magnesium Chloride Hexahydrate, 0.1M Tris, pH 8.5	3.4M 1,6-Hexanediol, 0.1M Magnesium Chloride Hexahydrate, 0.1M Tris, pH 8.5	3.6M 1,6-Hexanediol, 0.1M Magnesium Chloride Hexahydrate, 0.1M Tris, pH 8.5
2	3.2M 1,6-Hexanediol, 0.2M Magnesium Chloride Hexahydrate, 0.1M Tris, pH 8.5	3.4M 1,6-Hexanediol, 0.2M Magnesium Chloride Hexahydrate, 0.1M Tris, pH 8.5	3.6M 1,6-Hexanediol, 0.2M Magnesium Chloride Hexahydrate, 0.1M Tris, pH 8.5
3	3.2 M 1,6-Hexanediol, 0.3M Magnesium Chloride Hexahydrate, 0.1M Tris, pH 8.5	3.4M 1,6-Hexanediol, 0.3M Magnesium Chloride Hexahydrate, 0.1M Tris, pH 8.5	3.6M 1,6-Hexanediol, 0.3M Magnesium Chloride Hexahydrate, 0.1M Tris, pH 8.5

Table 4.3 The conditions described above are a follow up study from the condition 3.4M 1,6-Hexanediol, 0.2M Magnesium Chloride Hexahydrate, 0.1M Tris, pH 8.5. See Figure 4.5 for the crystal produced from the initial crystallisation well. Conditions highlighted in yellow were those that further produced crystals in the follow up trial.

After several months of monitoring the follow up crystal trial, as described in Table 4.3, two rod shaped crystals appeared in the well C2, surrounded by thin spindle-like crystals. Both crystals from C2 smaller than previously seen in Figure 4.5. Small rectangular shaped crystals surrounded by thin, spindle-like crystals also appeared in C3. Conditions which produced crystals in the follow up study are highlighted in yellow (see Table 4.3). Images of the crystals grown in both follow up conditions are shown in Figure 4.6a and 4.6b.

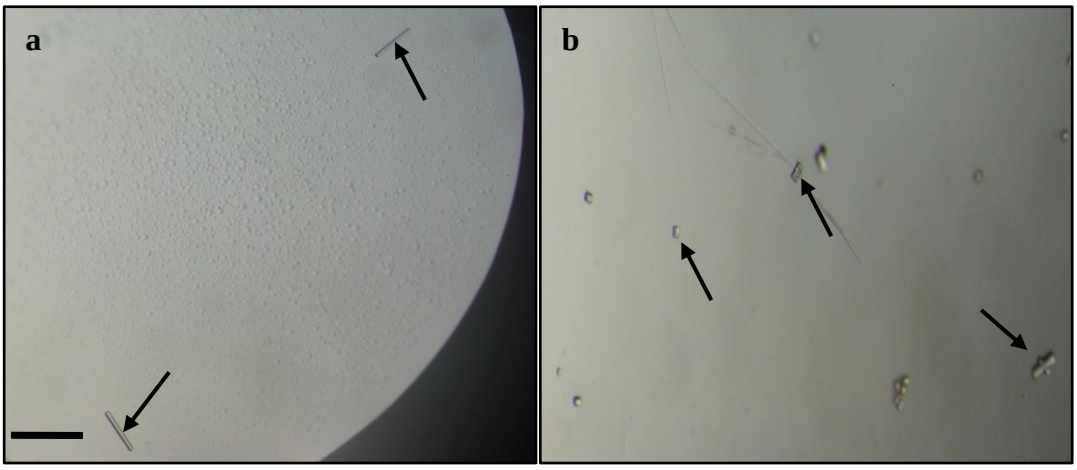

Figure 4.6. Rod-shaped crystals growing in both wells C2 and C3. a) Two rod shaped crystals surrounded by very thin spindle-like structures grown in C2 from the follow up study described in Table 4.3 (shown in yellow). b) Small rod shaped crystals, again surrounded by spindle-like structures within the well. The crystals shown were grown in C3 from the follow up study described in Table 4.3 (shown in yellow). The crystals in question are identifiable in both Figures via the arrows. The crystals observed in both Figures were noted to be a different form than the crystal grown in the original well (Figure 4.5). The scale in both images represents 100µm.

Crystals from both Figure 4.6a and 4.6b were frozen in liquid nitrogen on the 08/07/2015 and tested at DLS on the 12/07/2015. Due to the conditions that the crystals had been grown in, no cryoprotectant was used. One crystal was frozen from well C2 and two crystals were frozen from well C3. Unfortunately, when tested, the crystals appeared to be small molecule crystals, and not protein crystals based on their diffraction pattern.

Four weeks after the start of the first structure screen trial, tiny, rod-like crystals started to form (see Figure 4.7). The condition of this well was 70% MPD, 0.1M Sodium, 4-(2-Hydroxyethyl) Piperazine-1-Ethanesulfonic Acid (HEPES), pH 7.5. The crystal growth in the well is shown in Figure 4.7.

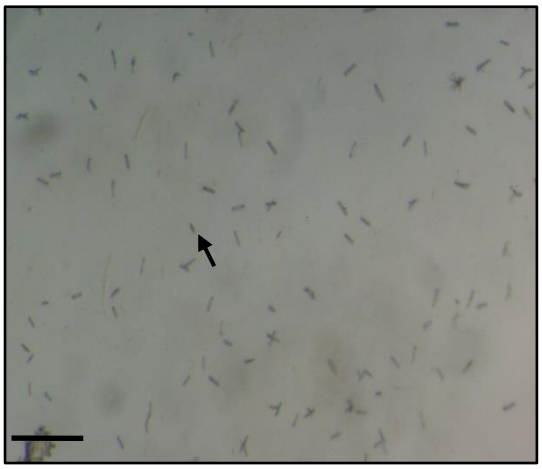

Figure 4.7 Small, rod-like crystals dispersed throughout the drop from the condition 70% MPD, 0.1M Sodium HEPES, pH 7.5. The condition is from structure screen 1 of the mCRP crystallisation trials. The arrow included in the Figure identifies one of the many crystals observed within the well. The scale shown represents 100µm.

The rod-like crystals shown in Figure 4.7 were too small for testing at DLS. In order to improve the size and quality of the crystals shown in Figure 4.7, the condition was followed up with a three by three screen. The concentration of MPD and sodium HEPES was varied by an increment of 5% and 0.05M respectively. Details for the crystallisation follow up study can be found in Table 4.4.

	A	**B**	**C**
1	70% MPD, 0.1M Sodium HEPES, pH 7.5	70% MPD, 0.1M Sodium HEPES, pH 7.5	70% MPD, 0.1M Sodium HEPES, pH 7.5
2	70% MPD, 0.1M Sodium HEPES, pH 7.5	70% MPD, 0.1M Sodium HEPES, pH 7.5	70% MPD, 0.1M Sodium HEPES, pH 7.5
3	70% MPD, 0.1M Sodium HEPES, pH 7.5	70% MPD, 0.1M Sodium HEPES, pH 7.5	70% MPD, 0.1M Sodium HEPES, pH 7.5

Table 4.4 The conditions described above are a follow up study from the condition 70% MPD, 0.1M Sodium, HEPES, pH 7.5. See Figure 4.7 for the crystals which were produced from the initial crystallisation trial. Wells which are highlighted in yellow were successful in growing crystals in the follow up trial.

After a week of monitoring the follow up crystallisation trial described in Table 4.4, rod shaped crystals appeared in the well A2. A large proportion of the rod-shaped crystals were multiple crystals, in addition, there were also several rhombus-shaped crystals dispersed throughout the drop. Both forms of crystals appeared to be larger than those previously shown (see Figure 4.7). A blue dye called IZIT (Hampton Research) was added to the well, which is known to stain some protein crystals dark blue, however the crystals did not take up the dye. An image of the crystals from the well A2 is shown in Figure 4.8. Unfortunately, the crystals did not stain through the addition of IZIT. The condition is highlighted in yellow in Table 4.4.

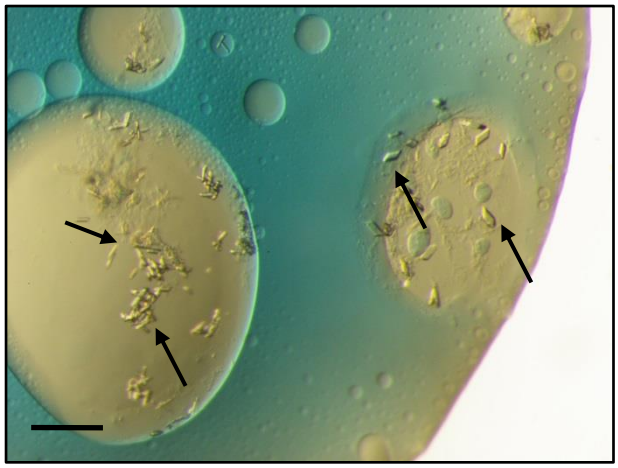

Figure 4.8 Small rod and rhombus shaped crystals from the *in vitro* mCRP trials that were dispersed throughout the drop. The crystals were grown in A2 of the follow up study described in Table 4.4 (highlighted in yellow). The arrows included in the Figure highlight clusters of the rod and rhombus shaped crystals within the well. See Figure 4.7 for the crystals which were produced from the initial crystallisation well. The scale shown represents 100µm.

The crystals shown in Figure 4.8 were frozen in liquid nitrogen on the 16/01/2015 and tested on the 18/01/2015 at DLS. Due to the conditions the crystals had been grown in, no cryoprotectant was used. Four crystals in total were frozen from the well A2, with only two being tested at DLS. Unfortunately, neither of the crystals that were tested showed any diffraction and were both thought to be small molecule crystals.

Several months after structure screen 2 had been initiated the well shown in Figure 4.9 started showing signs of crystal growth. Small, rounded crystalline structures appeared throughout the drop. The condition of the well was 4.3M Sodium Chloride, 0.1M Sodium HEPES, pH 7.5. The crystals are shown in Figure 4.9.

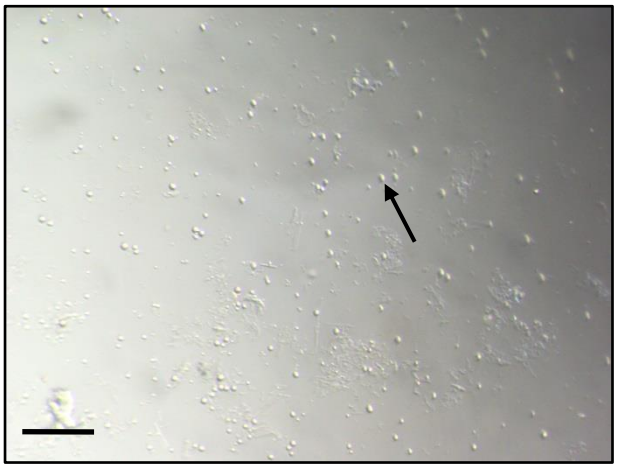

Figure 4.9 Small, rounded crystalline structures were dispersed throughout the drop from the mCRP crystallisation trials. The condition for the well was 4.3M Sodium Chloride, 0.1M Sodium HEPES, pH 7.5. The scale shown represents 100µm. The arrow highlights one of the small, rounded structures observed in the drop.

As the crystals were too small and had not formed properly, they were not tested at DLS. In order to improve the size and quality of the crystal shape, a follow up trial was carried out. The concentration of sodium chloride was altered by increments of 0.3M, with the pH of sodium HEPES also being varied. The conditions for the follow up study are outlined in Table 4.5.

	A	B	C
1	4M Sodium Chloride, 0.1M Sodium HEPES, pH 7.2	4.3M Sodium Chloride, 0.1M Sodium HEPES, pH 7.2	4.6M Sodium Chloride, 0.1M Sodium HEPES, pH 7.2
2	4M Sodium Chloride, 0.1M Sodium HEPES, pH 7.5	4.3M Sodium Chloride, 0.1M Sodium HEPES, pH 7.5	4.6M Sodium Chloride, 0.1M Sodium HEPES, pH 7.5
3	4M Sodium Chloride, 0.1M Sodium HEPES, pH 7.8	4.3M Sodium Chloride, 0.1M Sodium HEPES, pH 7.8	4.6M Sodium Chloride, 0.1M Sodium HEPES, pH 7.8

Table 4.5 The conditions described above are a follow up study from the condition 4.3M Sodium Chloride, 0.1M Sodium HEPES, pH 7.5. See Figure 4.9 for the crystal-like structures which were produced from the initial crystallisation trial. Wells which are highlighted in yellow were successful in growing crystals.

Four weeks after the trial had been set down; crystals had started growing in the well A2. The crystals appeared on the edge of the drop and appeared very similar to a shard of glass, as shown in Figures 4.10a and 4.10b.

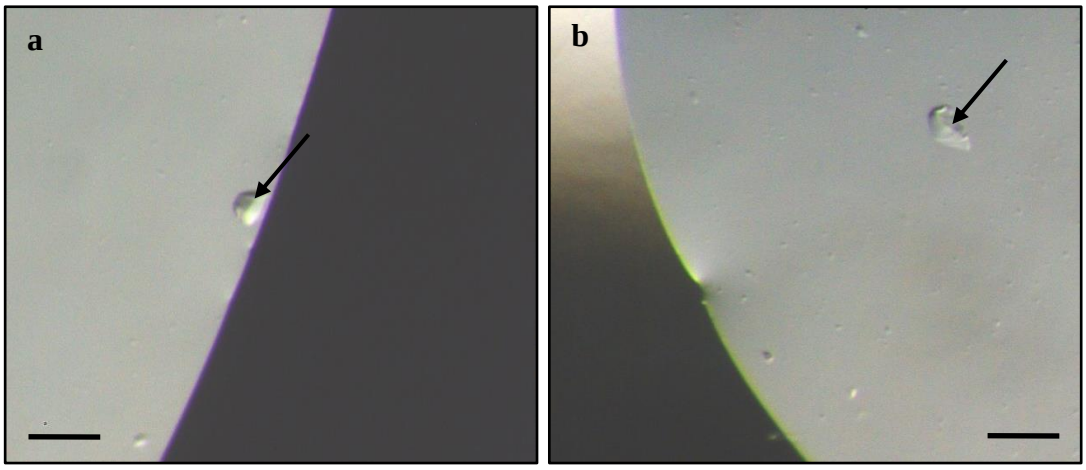

Figure 4.10 Crystals from both wells which resemble small shards of glass. a) The crystal grown from A2 appears like a shard of glass. b) Similar to a, the crystal also appears to resemble a shard of glass. Both crystals from a and b were grown in the well A2, as described in Table 4.5 (highlighted in yellow). Both crystals are identifiable via the arrows included in the Figure. Scale represents 200µm.

Both crystals were frozen in liquid nitrogen on the 09/12/2015 and tested at DLS on 13/12/2015. Prior to freezing the crystals were cryoprotected. The first crystal tested was extremely icy (Figure 4.10a) meaning visibility was poor. A grid scan was performed to determine where the crystal was located within the loop. Potential diffraction spots were observed from the grid scan, but due to the amount of ice on the loop no more information was collected. The second crystal tested (Figure 4.10b) unfortunately produced no diffraction spots.

Structure screen 2 also produced crystals which appeared as poorly formed plates that were rough round the edges (see Figure 4.11). The condition that the crystals grew in was 2.0M Ammonium Sulfate, 5% 2-propanol. The crystals are shown in Figure 4.11.

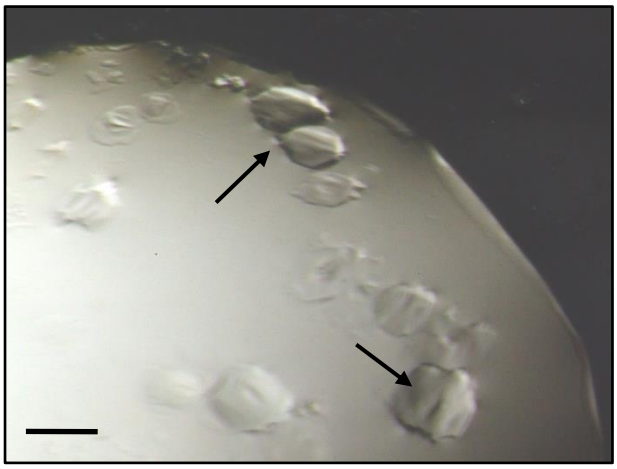

Figure 4.11 Poorly formed crystals dispersed throughout the drop from the mCRP crystallisation trials. The condition for the well was 2.0M Ammonium Sulfate, 5% 2-propanol. The scale shown represents 200µm. The two arrows included in the Figure highlight two of poorly formed crystals within the well.

Due to the poorly formed nature of the crystals shown in Figure 4.11 they were not tested at DLS. A follow up study was carried out, where the concentrations of ammonium sulfate and 2-propanol was varied. These conditions are shown in Table 4.6. Unfortunately, after months of monitoring the crystal trial, the follow up study described in Table 4.6 did not produced any crystals.

	A	**B**	**C**
1	1.0M Ammonium Sulfate, 3% 2-propanol	1.0M Ammonium Sulfate, 5% 2-propanol	1.0M Ammonium Sulfate, 7% 2-propanol
2	2.0M Ammonium Sulfate, 3% 2-propanol	2.0M Ammonium Sulfate, 5% 2-propanol	2.0M Ammonium Sulfate, 7% 2-propanol
3	3.0M Ammonium Sulfate, 3% 2-propanol	3.0M Ammonium Sulfate, 5% 2-propanol	3.0M Ammonium Sulfate, 7% 2-propanol

Table 4.6 The conditions described above are a follow up study from the condition 2.0M Ammonium Sulfate, 5% 2-propanol. See Figure 4.11 for the crystals which were produced from the initial crystallisation trial.

Analysis of all the conditions that were trialled with mCRP from both the structure screens and follow-up studies highlighted three conditions which demonstrated potential for growing protein crystals. These are highlighted in the summary Table 4.7. Several of these conditions are still being pursued with *in vitro* produced mCRP. In addition to this, varying the concentration of mCRP within the drop and the addition of co-crystallisation with a natural ligand is also being considered.

Condition	**Figure Reference**	**Diffraction Quality**
4M Sodium Chloride, 0.1M Sodium HEPES, pH 7.5	Figure 4.10a + 4.10b	Too icy to test properly at DLS
4.3M Sodium Chloride, 0.1M Sodium HEPES, pH 7.5	Figure 4.9	Small, rounded crystals not high quality enough for DLS (2x crystals)
2M Ammonium Sulfate, 5% 2-propanol	Figure 4.11	Small, rounded crystals not high quality enough for DLS

Table 4.7 A list of three conditions out of all those that were trialled which showed promise when attempting to crystallise mCRP.

4.3.2 Digestion of Human C1q with the Collagenase Enzyme

The CLR of C1q had to be removed through enzymatic digestion as the intact molecule was too floppy and would struggle to crystallise. Furthermore, digestion of the intact molecule helped to solubilise the C1q molecule, for the higher concentrations that were required for crystallisation. In addition, this aided in stabilising the complex within the crystal lattice, helping promote ordered crystal growth. To produce the GHR a protocol was used from established procedures (Paques *et al.*, 1979), which has previously been used

within our research group. Alternative protocols have also been trialled. Gaboriaud *et al*, 2003, successfully managed to cleave the GHR with the enzyme collagenase for crystallisation trials. Unfortunately, this protocol has previously yielded poor results within our lab and was not followed up.

The protocol used by Paques *et al*, 1979, uses the enzyme collagenase to cleave the CLR at specific points along the sequence; at the *x*-Gly bond within the sequence Pro-*x*-Gly-Pro, where *x* is a neutral residue. This therefore frees the GHR from the CLR, which can then be purified out of sample and used for crystallisation studies. The collagenase CLSPA used in the protocol is purchased from Worthington Biochemical Corporation (New Jersey, USA) and is provided in a chromatographically purified form from *Clostridium histolyticum.* The CLSPA collagenase used has a highly specific collagenase activity with little secondary enzyme activity, breaking down the collagen into a single stranded-form. In addition, bacterial collagenases can cleave at multiple sites along the chain, whereas mammalian collagenases are limited to one specific site.

SDS PAGE analysis was run on the C1qGHR sample to assess whether the digestion and production of C1qGHR had been a success and to assess the purity of the sample. Figure 4.12 shows the silver stained SDS PAGE of the C1q molecule post-digest. Molecular weight markers are shown in lane 1, with intact C1q in lane 3. Lanes 5 and 7 contain C1qGHR non-reducing and reducing respectively. As the three subunits of the GHR of C1q are not held together by disulfide bonds, the three bands observed in the non-reducing lane (5) displayed the same molecular weight as the bands from the reducing sample (lane 7). Molecular weight markers were used to estimate the molecular weight of each subunit and is shown on the left of the image. This matches the expected molecular weights based on previous experimental work that has published and within our lab, alongside previous published results (Gaboriaud *et al.*, 2003; Paques *et al.*, 1979).

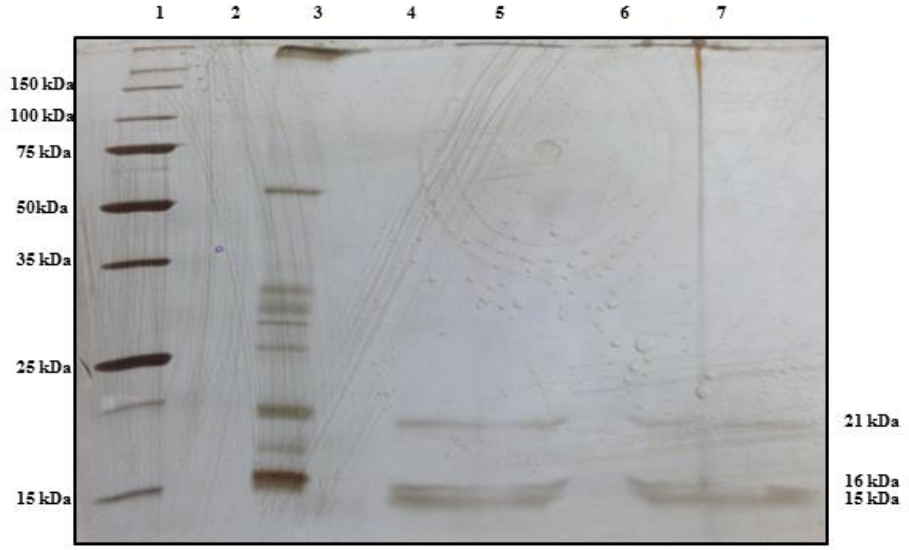

Figure 4.12 C1q digested by collagenase (silver stained), 12.5%T SDS-PAGE. Lane 1: molecular weight markers, lane 2: sample buffer, lane 3: undigested C1q, lane 4: sample buffer, lane 5: C1q GHR (non-reducing), lane 6: sample buffer, lane 7: C1q GHR (reducing).

Due to reports that the collagenase enzyme used in the digestion experiment has been known to degrade into smaller protein fragments once used, a second SDS PAGE was run to assess the enzyme's purity. A positive control of the enzyme alongside native collagenase is shown in Figure 4.13. Lanes 4 and 6 in Figure 4.13 both show identical bands whilst stained, indicating that the enzyme had not degraded.

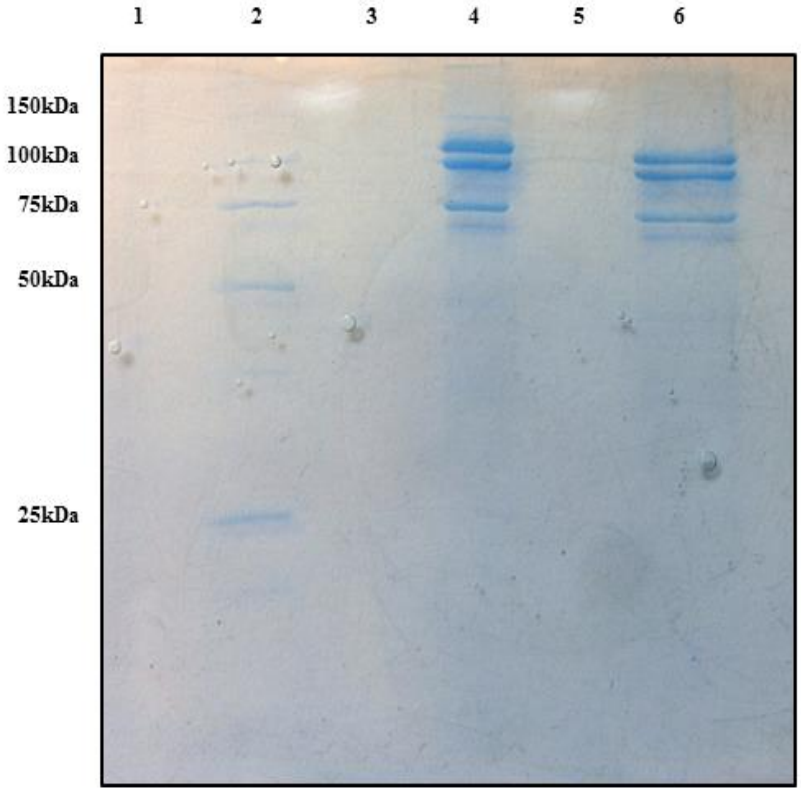

Figure 4.13 Collagenase from *Clostridium histolyticum*, Coomassie stained. Samples were run on a 12.5%T SDS-PAGE. Lane 1: sample buffer, lane 2: molecular weight markers, lane 3: sample buffer, lane 4: native collagenase, lane 5: sample buffer, lane 6: A control sample of collagenase which had not been subject to any experimental analysis.

4.3.2 Co-crystallisation of C-reactive Protein and C1qGHR with CWPS

The second half of the crystallisation studies is dedicated to the crystallisation of the complex structure involving CRP, C1QGHR and CWPS. Two structure screens purchased from Molecular Dimensions called the ProPlex were used in the complex (C1qGHR: pCRP: CWPS) crystallisation trials. The ProPlex contained two sets of 50 conditions which are known to have previously been successful when trying to crystallise large complexes. Details of the structure screens used in the complex trials can be found in Appendix 4. Crystallisation trials for the first ProPlex structure screen commenced on 24/06/2014.

After several weeks after the initiation of the first ProPlex structure screen trial, a large boulder shaped crystal had grown in the well RW01D4. The condition the crystal had grown in was 0.15M Ammonium Sulfate, 0.1M MES, pH 6.0, 15% PEG 4000. Unfortunately, there are no available images for this crystal. The large boulder shaped crystal was frozen in liquid nitrogen on 16/04/2015 after being cryoprotected. The crystal was tested at DLS on 05/05/2015 but no diffraction was observed.

In addition, long, hexagonal crystals started to grow in the well RW02B1 from the ProPlex structure screen trial 1. The condition for this well was 0.1M Sodium Citrate, pH 5.6, 20% PEG 4000, 20% 2-propanol. Unfortunately, there are no available images for this crystal. A long hexagonal shaped crystal was frozen in liquid nitrogen on 16/04/2015 after being cryoprotected. The crystal was tested at DLS on 05/05/2015 but no diffraction was observed.

Small, shard-like crystals appeared in from one of the wells in the ProPlex structure screen 1. The condition for this well was 0.2M Lithium Sulfate, 0.1M MES, pH 6.0, 20% PEG 4000. Unfortunately, there are no available images for this crystal and during

cryoprotection, the shard-like crystals dissolved (5% PEG 400). A follow up trial on this condition was therefore initiated, to improve the size, quality and stability of the crystal that was initially produced. The concentration of lithium sulfate and pH was varied throughout the trial. An additional two wells were also added, which was identical to the initial condition, except for the molecular weight of PEG used being changed to 2000 and 6000. The details of the crystallisation follow up study are shown in Table 4.8. The trial was initiated on 18/12/2015. As of yet, there are currently no crystals growing in the follow up wells. The well is being monitored for any sign of crystal growth.

	1	**2**	**3**
A	0.1M Lithium Sulfate, 0.1M MES, pH 5.8, 20% PEG 4000	0.2M Lithium Sulfate, 0.1M MES, pH 5.8, 20% PEG 4000	0.3M Lithium Sulfate, 0.1M MES, pH 5.8, 20% PEG 4000
B	0.1M Lithium Sulfate, 0.1M MES, pH 6.0, 20% PEG 4000	0.2M Lithium Sulfate, 0.1M MES, pH 6.0, 20% PEG 4000	0.3M Lithium Sulfate, 0.1M MES, pH 6.0, 20% PEG 4000
C	0.1M Lithium Sulfate, 0.1M MES, pH 6.2, 20% PEG 4000	0.2M Lithium Sulfate, 0.1M MES, pH 6.2, 20% PEG 4000	0.3M Lithium Sulfate, 0.1M MES, pH 6.2, 20% PEG 4000
D	0.2M Lithium Sulfate, 0.1M MES, pH 6.0, 20% PEG 2000	0.2M Lithium Sulfate, 0.1M MES, pH 6.0, 20% PEG 6000	Empty

Table 4.8 The conditions described above are a follow up study from the condition 0.2M Lithium Sulfate, 0.1M MES, pH 6.0, 20% PEG 4000. Additional trials involving PEG 2000 and 6000 were also set down (D1 + D2).

A year after the ProPlex structure screen 1 has been initiated, shard-like crystals were found to be growing in well RW01A5. They were then left for several months to continue growing, with regular checks made on the crystals. The crystals had stopped increasing in size several months later. The crystallisation condition of the well was 0.1M MES, pH 6.5, 15% PEG 500 MME. The well contained one large shard, with several smaller shards throughout the drop, as shown in Figure 4.14a and 4.14b.

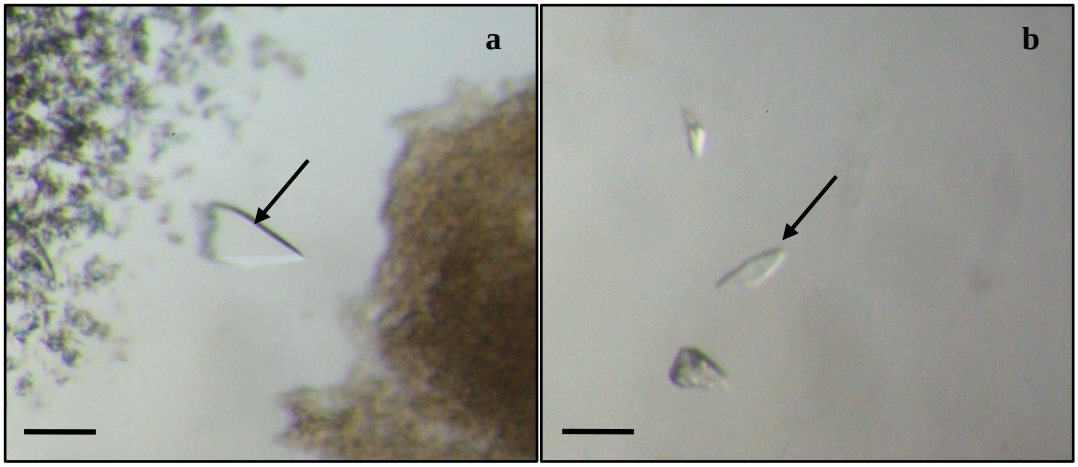

Figure 4.14 Large shard-like crystals grown in the complex crystallisation trials. a) A large, shard-like crystal from the complex crystallisation trials. b) A smaller, shard-like crystal from the complex crystallisation trials. Both crystals are from the crystallisation condition 0.1M MES, pH 6.5, 15% PEG 500 MME (well RW01A5). The scale represents 200µm. The arrows in both Figures highlight the position of the crystals within the drop.

The crystals had been grown in 15% PEG 500 MME, which could potentially act as a cryoprotectant for the crystal. As previous crystals from the complex trials have dissolved due to the addition of cryoprotectant, the largest crystal (Figure 4.14a) was frozen directly into liquid nitrogen. 20% of PEG 500 MME was added to the smaller, shard-like crystal as an additional cryoprotectant, and then frozen. Crystals were frozen on 09/12/2015. The crystals were tested at DLS on the 13/12/2015. The first crystal frozen (Figure 4.14a) was tested and diffracted to a resolution of around 9Å. A diffraction image for that crystal is shown in Figure 4.15. The second crystal diffracted to a resolution of around 10 Å.

Unfortunately, this resolution for both crystals was not high enough to warrant collection of a data set.

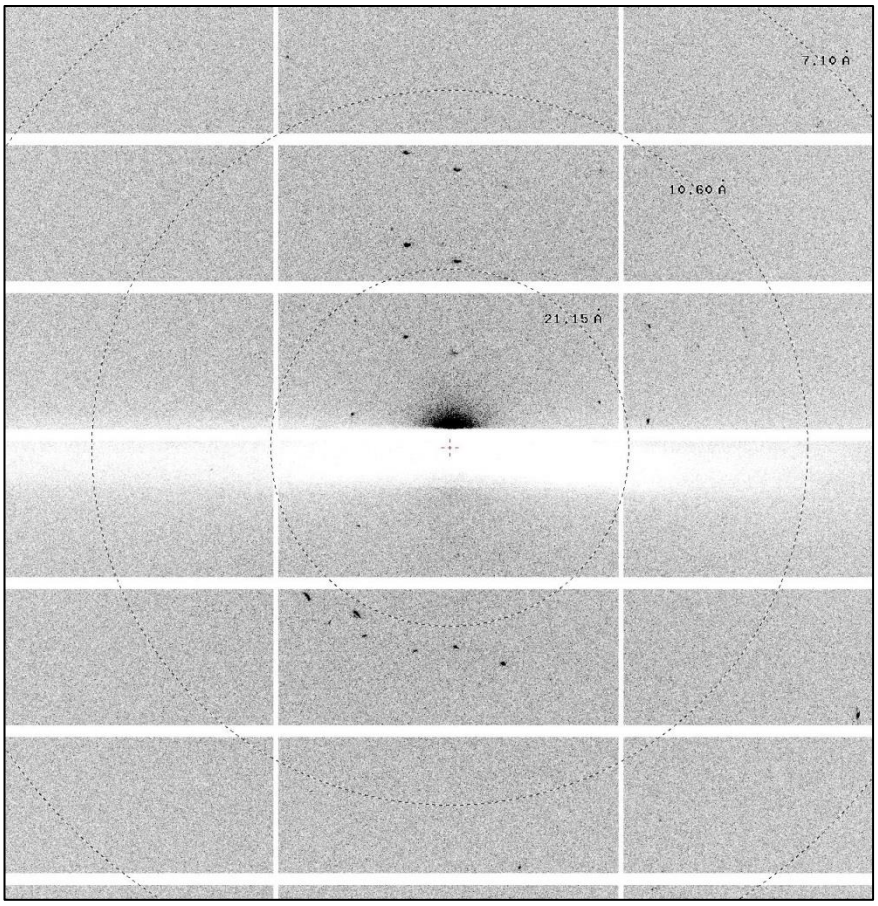

Figure 4.15. Enlarged section of one of the diffraction pattern images collected from a crystal of the protein complex C1qGHR, CRP and CWPS. The crystal which produced the diffraction patterns is shown in Figure 4.13a. Data was collected at DLS. Circles seen in black on the image represent approximate resolutions of (from inner to outer) 21.15Å, 10.60Å and 7.10Å.

To improve the size and quality of the crystals shown in Figure 4.14, the condition was followed up with a three by three screen. The concentration of PEG 550 MME was varied alongside the pH of the MES buffer. Details for the crystallisation follow up study can be found in Table 4.9. The trial was initiated on 18/12/2015. As of yet there are currently no crystals growing in the follow up wells. The well is being monitored for any sign of crystal growth.

	1	**2**	**3**
A	0.1M MES, pH 6.2, 10% PEG 500 MME	0.1M MES, pH 6.2, 15% PEG 500 MME	0.1M MES, pH 6.2, 20% PEG 500 MME
B	0.1M MES, pH 6.5, 10% PEG 500 MME	0.1M MES, pH 6.5, 15% PEG 500 MME	0.1M MES, pH 6.5, 20% PEG 500 MME
C	0.1M MES, pH 6.7, 10% PEG 500 MME	0.1M MES, pH 6.7, 15% PEG 500 MME	0.1M MES, pH 6.7, 20% PEG 500 MME

Table 4.9 The conditions described above are a follow up study from the condition 0.1M MES, pH 6.5, 15% PEG 500 MME. Crystals produced from the initial crystallisation trial are shown in Figure 4.14. As of yet, no crystals have been produced from this trial.

Crystallisation trials for the second ProPlex structure screen commenced on the 29/10/2014. Several weeks after the trial had been initiated; small oval shaped crystals started to grow (see Figure 4.16). The crystallisation condition of the well was 1.5M Ammonium Sulfate, 0.1M Sodium HEPES, pH 7.0. Unfortunately, there are no images available for the crystals produced. Crystals from the well were due to be frozen, but

dissolved due to the addition of cryoprotectant (5% MPD). A repeat trial was carried out for the same condition. After several weeks of monitoring the wells, a boulder-shaped crystal appeared, as shown in Figure 4.16 (top left of the image).

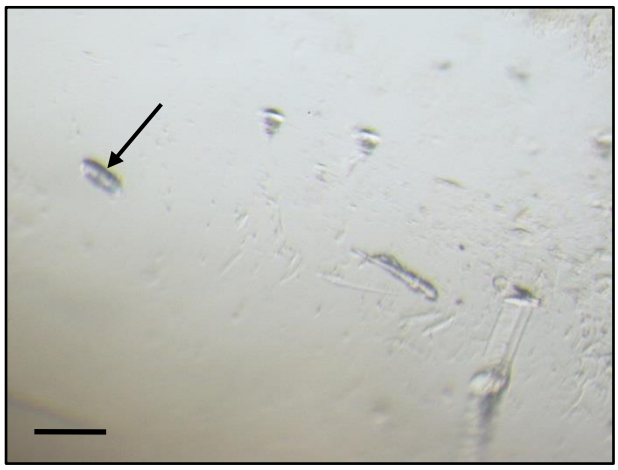

Figure 4.16 Boulder-shaped crystals from the complex structure screen 2. The condition for the well is 1.5M Ammonium Sulfate, 0.1M Sodium HEPES, pH 7.0. The scale shown represents 200µm. The arrow highlights the position of the crystal within the drop.

The boulder shaped crystal from Figure 4.16 was frozen on 16/10/2015 after being cryoprotected with glycerol. The crystal was tested at DLS on 18/10/2015 and diffracted to around 9Å. Data was not collected on the crystal as the resolution was not high enough. The well was continuously monitored for further crystal growth.

Small, oval shaped crystals also appeared in the well for the crystallisation condition of 2.0M Ammonium Sulfate, 0.1M Sodium Acetate, pH 5.0. Unfortunately, there are no images available for the crystals produced. Crystals from the well were due to be frozen, but dissolved due to the addition of cryoprotectant (20% PEG 400). A repeat trial was carried out on the same condition. Like the initial trial, small rounded crystals appeared in the well. These rounded crystals are shown in Figure 4.17 were too small to test at DLS and were left to see if they would increase in size. They are still currently being monitored.

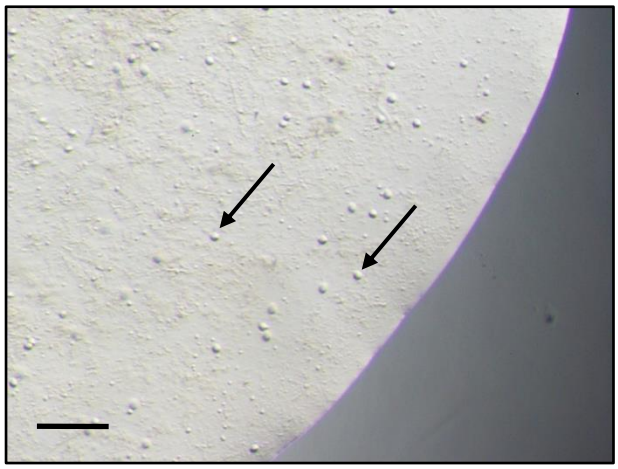

Figure 4.17 Small, rounded shaped crystals from the complex structure screen 2. The condition for the well is 2.0M Ammonium Sulfate, 0.1M Sodium Acetate, pH 5.0. The scale shown represents 100µm. The arrows highlight the appearance of two of the rounded crystals within the drop.

Several months after the initiation of the second ProPlex structure screen, small, rounded oval shaped crystals were found to be growing in the well RW14B4. The condition of the well was 1.6M Sodium/Potassium Phosphate, pH 6.5. The crystals produced in the well are shown in Figure 4.18.

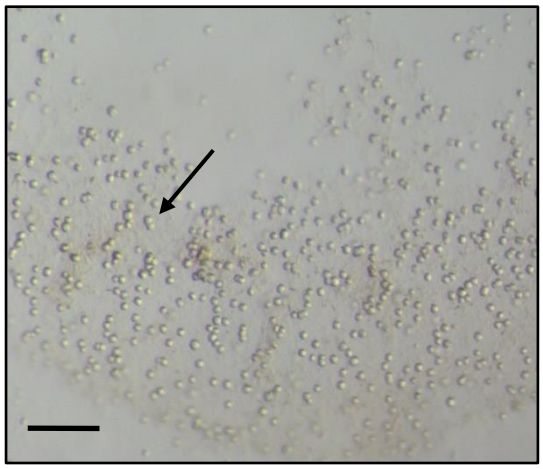

Figure 4.18 Small rounded shaped crystals from the complex structure screen 2. The condition for the well is 1.6M Sodium/Potassium Phosphate, pH 6.5. The scale represents 100µm. The arrow highlights the appearance of one of the rounded crystals within the drop.

A follow up study was commenced for the condition 1.6M Sodium/Potassium Phosphate, pH 6.5, as the crystals in Figure 4.18 were too small to test at DLS. The follow

up trial consisted of variations in the concentration of sodium/potassium phosphate and the pH. The conditions used are shown in Table 4.10.

	1	**2**	**3**
A	1.4M Sodium/Potassium Phosphate, pH 6.4	1.6M Sodium/Potassium Phosphate, pH 6.4	1.8M Sodium/Potassium Phosphate, pH 6.4
B	1.4M Sodium/Potassium Phosphate, pH 6.5	1.6M Sodium/Potassium Phosphate, pH 6.5	1.8M Sodium/Potassium Phosphate, pH 6.5
C	1.4M Sodium/Potassium Phosphate, pH 6.6	1.6M Sodium/Potassium Phosphate, pH 6.6	1.8M Sodium/Potassium Phosphate, pH 6.6

Table 4.10 The conditions described above are a follow up from the condition 1.6M Sodium/Potassium Phosphate, pH 6.5. As of yet, no crystals have been produced from this trial.

Unfortunately, the follow up study did not produce any crystals after several months of monitoring the trial. Several of the rounded crystals shown in Figure 4.18 (the initial crystal well) were transferred to B2 in the abovementioned follow up study (highlighted blue in Table 4.10). As the crystals, had not changed in size or form since they were discovered, they were transferred to B2 to determine if they would display signs of growth, or develop a more ordered form by providing a nucleation point for the protein within the well. Figure 4.19 shows the crystals that were transferred into B2. The crystal well is still being monitored but as of yet show no signs of growth.

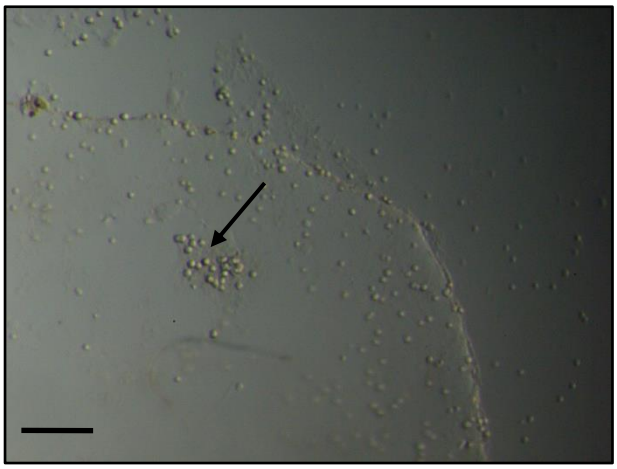

Figure 4.19 Small rounded crystals that were transferred from RW14B4 to the well B2 in the follow up study described in Table 4.10. Crystals were transferred in order to determine if they would improve in size or quality in an identical. The scale shown represents 100µm. A cluster of the rounded crystals is highlighted via the arrow.

Well RW14D1 also displayed signs of crystal growth. Similar to that previously observed in the second structure screen, small, rounded oval shaped crystals were identified within the well. The condition of the well is 0.1M Sodium Acetate, pH 5.0, 2% PEG 4000, 15% MPD. The crystals that were grown in the well are shown in Figure 4.20.

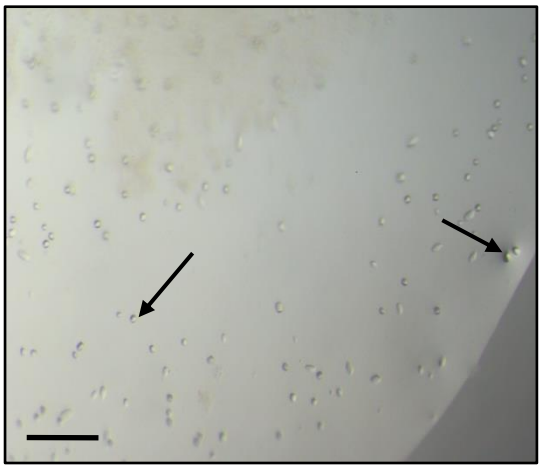

Figure 4.20 Small rounded shaped crystals from the complex structure screen 2. The condition for the well is 0.1M Sodium Acetate, pH 5.0, 2% PEG 4000, 15% MPD. The scale represents 100µm. The arrows highlight the appearance of the rounded crystals within the drop.

A follow up trial was commenced due to the crystals shown in Figure 4.20 being too small and poorly formed to be tested at DLS. The follow up trial consisted of variations in the concentration of MPD and buffer pH. The crystallisation conditions for the follow up

study are described in Table 4.11. The trial was initiated on 18/12/2015. Currently there are no crystals growing in the follow up wells. The well is being monitored for any sign of crystal growth.

	1	**2**	**3**
A	0.1M Sodium Acetate, pH 4.8, 2% PEG 4000, 10% MPD	0.1M Sodium Acetate, pH 4.8, 2% PEG 4000, 15% MPD	0.1M Sodium Acetate, pH 4.8, 2% PEG 4000, 20% MPD
B	0.1M Sodium Acetate, pH 5.0, 2% PEG 4000, 10% MPD	0.1M Sodium Acetate, pH 5.0, 2% PEG 4000, 15% MPD	0.1M Sodium Acetate, pH 5.0, 2% PEG 4000, 20% MPD
C	0.1M Sodium Acetate, pH 5.2, 2% PEG 4000, 10% MPD	0.1M Sodium Acetate, pH 5.2, 2% PEG 4000, 15% MPD	0.1M Sodium Acetate, pH 5.2, 2% PEG 4000, 20% MPD

Table 4.11 The conditions described above are a follow up from the condition 0.1M Sodium Acetate, pH 5.0, 2% PEG 4000, 15% MPD. As of yet, no crystals have been produced from this trial.

Well RW14A1 also produced crystals which displayed promising signs of growth. Small, oval shaped crystals were found within the well. The condition was 1.5M Ammonium Sulfate, 0.1M Tris, pH 8.0. The crystals that were grown within the well are shown in Figure 4.21.

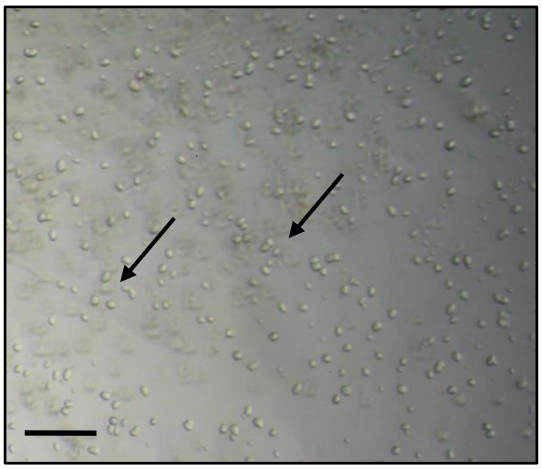

Figure 4.21 Small rounded shaped crystals from the complex structure screen 2. The condition for the well is 1.5M Ammonium Sulfate, 0.1M Tris, pH 8.0. The scale shown represents 100µm. The arrows highlight the appearance of the rounded crystals within the drop.

To improve the size and quality of the crystals grown in Figure 4.21, a follow up study was initiated. The follow up study for this trial was slightly altered to that of the previous ones carried out. It was noted, that high salt concentrations have repeatedly produced crystals throughout the complex crystallisation trials. This can be seen in the conditions which produced crystals in the Figures 4.14, 4.16 – 4.21. Therefore, in this follow up trial, high concentrations of ammonium sulfate was used, alongside variations in the pH. These conditions can be found in Table 4.12. The trial was initiated on 18/12/2015. Currently no crystals growing in the follow up wells. The well is being monitored for any sign of crystal growth.

	1	2	3
A	1.0M Ammonium Sulfate, 0.1M Sodium Acetate, pH 5.0	1.2M Ammonium Sulfate, 0.1M Sodium Acetate, pH 6.0	1.4M Ammonium Sulfate, 0.1M Sodium HEPES, pH 6.5,
B	1.6M Ammonium Sulfate, 0.1M Sodium HEPES, pH 7.0	1.8M Ammonium Sulfate, 0.1M Tris, pH 7.5	2.0M Ammonium Sulfate, 0.1M Tris, pH 8.0

Table 4.12 A set of conditions from previous complex crystallisation trials which have notably produced crystals from high-salt based buffers/precipitants. As of yet, no crystals have been produced from this trial.

Similar to that observed in the mCRP crystallisation trial. There were several conditions which displayed promise during the complex crystallisation trials (see Table 4.13). In addition, the respective crystal figures and their diffraction quality, where possible are given. Several of these conditions are currently being followed up alongside several of the wells being monitored due to the length of time previous crystals have taken to form.

Condition	Figure Reference	Diffraction Quality
0.2M Lithium Sulfate, 0.1M MES, 20% PEG 4K, pH 6.0	No Figure	Initially dissolved upon addition of cryoprotectant. No crystals produced from follow up
0.1M MES, 15% PEG 550 MME, pH 6.5	Figure 4.14	1 crystal to 10 Å 1 crystal to 9 Å
1.5M Ammonium Sulfate, 0.1M Sodium HEPES, pH 7.0	Figure 4.16	1 crystal to 9 Å

2M Ammonium Sulfate, 0.1M Sodium Acetate, pH 5.0	No Figure	Initially dissolved upon addition of cryoprotectant. No crystals produced from follow up
1.6M Sodium Potassium Phosphate, pH 6.5	Figure 4.18	Initial crystals not high enough quality for DLS. No crystals produced from follow up
0.1M Sodium Acetate, 2% PEG 4K, 15% MPD, pH 5.0	Figure 4.20	Initial crystals not high enough quality for DLS. No crystals produced from follow up

Table 4.13 A table of all the conditions from the complex crystallisation trials which displayed promise. Crystallisation conditions and their respective crystal Figures are displayed in addition to whether the crystals diffracted if grown.

4.4 Discussion

4.4.1 Crystallisation Trials of Monomeric C-reactive Protein

The crystallisation trials for mCRP failed to produce any crystals that were sufficient in size and quality that they could have been tested at DLS. Although no protein crystals were produced of sufficient quality, the crystal trials discussed here provide a basis of potential conditions which may be refined for future follow up crystallisation trials. These conditions are summarised in Table 4.7, whereby the well conditions, and quality of the crystals produced are given.

Several of the crystal trials involving mCRP produced crystals which either produced no diffraction spots at all, or were determined to be small molecule, based on the diffraction observed when tested at DLS. These crystals are highlighted in Table 4.14.

Condition	Figure Reference	Diffraction Observed
0.2M Ammonium Sulfate, 25% PEG 4000, 0.1M Sodium Acetate pH 4.6	Figure 4.4	No Diffraction Pattern Observed
3.4M 1,6-Hexanediol, 0.2M Magnesium Chloride Hexahydrate, 0.1M Tris, pH 8.5	Figure 4.5	No Diffraction Pattern Observed
3.6M 1,6-Hexanediol, 0.2M Magnesium Chloride Hexahydrate, 0.1M Tris, pH 8.5	Figure 4.6a (Follow on from Figure 4.5)	Confirmed Small Molecules Crystal

3.6M 1,6-Hexanediol, 0.3M Magnesium Chloride Hexahydrate, 0.1M Tris, pH 8.5	Figure 4.6b (Follow on from Figure 4.5)	Confirmed Small Molecules Crystal
70% MPD, 0.1M Sodium HEPES, pH 7.5	Figure 4.8 (Follow on from Figure 4.7)	No Diffraction Pattern Observed

Table 4.14 Crystallisation trials involving mCRP. Crystallisation conditions and their respective crystal Figures are shown for trials which produced small molecule crystals or crystals which did not diffract.

Initially, those crystals which displayed no diffraction upon testing with X-rays were suggested to potentially be poorly formed crystals. For proteins, X-rays are an ideal choice because their typical wavelength is 0.15nm, the approximate distance of the bond length in protein molecules. In principle, a single object will diffract X-rays; however, the use of a single molecule would produce too little intensity to observe any measurable diffraction. Consequently, scattering from many molecules is required to obtain a sufficient signal. Not only are a significant number of molecules required for the formation of a protein crystal, but an ordered orientation of the repeating units within the crystal lattice is also important. The quality of the diffraction patterns (and resolution) produced from protein crystal mirrors the symmetry and arrangement of the unit cells within the crystal. Thus, the formation of a poorly ordered lattice within the crystal structure will result in little or no diffraction at all (Merz Jr. *et al*., 2010). This can usually be rectified by refining the crystallisation conditions or protein concentration, thus promoting the formation of a well-ordered crystal. Additional methods are commercially available to help determine whether the crystals grown are protein. A protein dye called IZIT, was tested on the rod-shaped crystals that had been grown in 70% MPD, 0.1M Sodium HEPES, pH 7.5 (see Figure 4.8). The dye can distinguish between small molecule and protein crystals as it can penetrate the pores within protein

crystal contacts. As expected, the dye failed to stain the crystals observed in Figure 4.8, suggesting they were small molecule. Furthermore, due to the lack of reproducibility of the crystals displayed in Figure 4.4, a common trait in small molecule crystals, and lack of diffraction within the follow up studies from Figures 4.6 & 4.8, the abovementioned crystals were all deemed to be small molecule and were therefore not pursued any further.

Figure 4.9 displays small, rounded crystals throughout the drop, which were grown in the condition 4.3M Sodium Chloride, 0.1M Sodium HEPES, pH 7.5. These were initially considered to be protein crystals, due to their poor formation and quality; typical of protein crystal formation when initially trialling different conditions. The 'shower' of poorly formed crystals suggests that the nucleation rate of the crystal formation was too high (see Figure 4.1 for a graph on crystal growth). This prevents the formation of a well-ordered lattice alongside the growth of larger crystals as the concentration of free protein molecules have been depleted. Alterations within the proteins concentration or the precipitant used could help delay this growth rate, promoting the formation or larger, diffraction quality crystals. As they were too small to test at DLS a follow up was initiated (Table 4.5). The follow up trial produced two crystals which resembled shards of glass (see Figure 4.10a & b). This unique and random formation of the crystals suggested a poor quality of order within the crystal lattice structure. This was thus reflected within their diffraction quality. The crystal shown in Figure 4.10a showed potential diffraction spots via a grid scan, but due to heavy icing, visibility was too poor for any further analysis. The heavy icing also suggests the cryoprotectant used on that well (5-20% MPD) did not work. This could explain the poor diffraction quality observed as the formation of ice may have disturbed the crystal lattice. Unfortunately, the second crystal tested (see Figure 4.10b) produced no diffraction spots at all.

Figure 4.11 shows poorly formed crystal plates that were produced from the structure screen 2 condition 2.0M Ammonium Sulfate, 5% 2-propanol. Similar to that seen in Figure 4.9 and 4.10, the poorly formed order of the crystals suggested they may be protein. The shape and size of the crystals in Figure 4.11 does not suggest an issue with nucleation as previously suggested, but a lacking of order and homogeneity within the crystal lattice. This could be for several reasons, such as; the precipitant used was not optimal for mCRP, the protein concentration may need altering or the pH and or temperature may have affected the crystal growth within the drop (Blundell & Johnson, 1976). A follow up study was initiated, but unfortunately no crystals have since grown.

4.4.2 Future Crystal Trials of Monomeric C-reactive Protein

The protein crystallisation trials described here, involving mCRP, failed to produce any protein crystals of sufficient diffraction quality. The reasoning behind this is still unclear as there are several alternative factors which affect crystal growth. In addition, it is unclear whether treatment of native pCRP with urea, to induce dissociation, altered the protein's ability to crystallise. Table 4.7 summarises three conditions which provided the most promising results. It was noted that all three conditions contained high concentrations of salt precipitants. Furthermore, the use of alternative cryoprotectants may be warranted, as MPD failed to prevent ice rings when testing one of the crystals (Figure 4.10a). These conditions described here could potentially be pursued and refined in future research, when attempting to crystallise an *in vitro* or an *in vivo* form of mCRP.

Future research may also consider one variable that was not altered throughout the crystallisation trials; protein concentration. Typically, high protein concentrations (10-15mg/ml) are used within protein crystallisation trials to allow the formation of a nucleation point for crystal growth (Rhodes, 2000). Under-saturated solutions are unable to reach the

‘crystallisation zone’ whereby the ordered crystal lattice starts to form. Crystallisation drops for mCRP trials all remained relatively transparent, with no protein precipitation occurring (excluding the conditions that produced ‘showers’ of crystals). This further suggests an increase in concentration of mCRP may drive this nucleation and help form protein crystals in several of the trialled conditions. Future studies involving mCRP may also benefit from co-crystallisation with a ligand such as PC to which mCRP can bind. Introducing ligands within crystallisation trials can both stabilise the protein structure when bound, in addition to providing a nucleation point which aids in protein crystal formation (Rhodes, 2000).

4.4.3 Co-crystallisation Trials Involving C-reactive Protein and C1qGHR with CWPS

The protein crystallisation studies between pCRP, C1qGHR and CWPS aimed to provide an insight into the structural interactions between pCRP and C1q; therefore, determining which region of the C1q protein binds to pCRP. Currently structural data exists for pCRP bound to PC, determined by Thompson *et al*, but this may not be representative of what occurs *in vivo.* The binding of PC to pCRP, when complexed with C1q is not enough to elicit an immune response and activate complement (Volanakis, 1981; Volanakis, 1982). It is suggested that PC is required to be bound to the polysaccharide from the cell wall for this to occur.

Initial crystallisation trials involving the complex produced two crystals, which when tested at DLS, produced no diffraction spots at all. These conditions and their corresponding crystal Figures are summarised in Table 4.15.

Condition	Figure Reference	Diffraction Observed
0.15M Ammonium Sulfate, 0.1M MES, pH 6.0, 15% PEG 4000	No Figure Available	No Diffraction Pattern Observed
0.1M Sodium Citrate, pH 5.6, 20% PEG 4000, 20% 2-propanol	No Figure Available	No Diffraction Pattern Observed

Table 4.15 Crystallisation trials of the complex. Crystallisation conditions and their respective crystal Figures are shown for trials which produced crystals which did not diffract.

As discussed previously, if a crystal displays no diffraction it does not necessarily mean it is a small molecule crystal; the crystal may be a poorly formed protein crystal. Although, based on their lack of reproducibility from their follow up trials, and as no diffraction was observed from the initial crystals, these were concluded to be small molecule and thus we did not pursue them any further. Cryoprotection of complex crystals proved to be problematic, as several of the crystals grown from the complex trials dissolved upon addition of the cryoprotectant. Table 4.16 highlights the crystallisation conditions of the failed cryoprotectants that were used.

Condition	Figure/Well	Cryoprotectant Used	Follow Up Study
0.2M Lithium Sulfate, 0.1M MES, pH 6.0, 20% PEG 4000	No Figure Available – RW02A4	5-20% PEG 400	No crystals grown from the follow up study (see Table 4.8)
1.5M Ammonium Sulfate, 0.1M Sodium HEPES, pH 7.0	No Figure Available – RW13D6	5% MPD	Crystals grown in follow up (see Figure 4.16)
2.0M Ammonium Sulfate, 0.1M Sodium Acetate, pH 5.0	No Figure Available – RW14A2	5-20% MPD	Crystals grown in follow up (see Figure 4.17)

Table 4.16 A table highlighting crystallisation conditions of the complex trials which produced crystals that dissolved upon addition of the cryoprotectant. Information regarding crystal growth in the respective follow up studies is also provided.

Table 4.16 highlights two different common cryoprotectants which proved to be damaging to the crystals grown in the complex crystallisation trials. A follow up study from the well RW13D6 (described in the above Table 4.16) produced a boulder shaped crystal, as shown in Figure 4.16. Cryoprotection of this crystal with glycerol proved successful with the crystal diffracting to 9Å when tested at DLS. Furthermore, one the two crystals from RW01A5, shown in Figure 4.14a & b was successfully cryoprotected with PEG 550 MME and diffracted to 10Å (with the other crystal diffracting to 9Å). The cryoprotectants used here were sufficient in helping protect the crystal from ice formation and radiation damage,

but unfortunately this was not high enough resolution from either trial to warrant data collection. These conditions clearly need to be refined in further follow up studies to improve their diffraction quality. The addition of various cryoprotectants to crystals can result in said crystal dissolving prior to being frozen, as demonstrated in Table 4.16. The protein and the precipitant and buffer solution can largely dictate what cryoprotectant is used. Certain cryoprotectants will disrupt the hydrogen-bond network that runs through the crystal contacts when attempting to displace the water molecules. This can therefore result in the crystal structure breaking apart, and thus dissolving the crystal into solution (Blundell & Johnson, 1976; Chayen, 2004; Glusker & Trueblood, 1985; Heras & Martin, 2005)

The follow up study for the trial RW14A2, as described in Table 4.16, produced a 'shower' of small rounded crystals throughout the drop (see Figure 4.18). Alongside this, several other complex crystallisation trials produced similar crystals. These are summarised in Table 4.17.

Condition	Figure	Crystal Description	Follow Up Study
2.0M Ammonium Sulfate, 0.1M Sodium Acetate, pH 5.0	Figure 4.17	Small Rounded Crystals	No Further Crystals Produced
0.1M Sodium Acetate, pH 5.0, 2% PEG 4000, 15% MPD	Figure 4.20	Small Rounded Crystals	No Further Crystals Produced
1.6M Sodium/Potassium Phosphate, pH 6.5	Figure 4.18	Small Rounded Crystals	Crystals transferred to additional well (see Table 4.10, Figure 4.19). No Further Crystal Growth
1.5M Ammonium Sulfate, 0.1M Tris, pH 8.0	Figure 4.21	Small Rounded Crystals	No Further Crystals Produced

Table 4.17 A summary of all the crystallisation conditions from the complex trials which produced small rounded crystals of poor quality. Their respective Figures and follow up information is also given.

Table 4.17 summarises a list of conditions from the complex crystallisation trials which resulted in the growth of small, poorly formed, rounded crystals. The results described here in Table 4.17 are like the crystals growth observed in Figure 4.9 from the mCRP crystallisation trials. This poor crystal quality described above could be due to several

reasons. Firstly, the nucleation rate during crystal growth could be too high, thus forming the small 'showers' of crystals throughout the drop, therefore the crystals are to form an ordered lattice and grow to a larger size. Secondly, poorly formed crystals could be due to refinement needed in the concentration of precipitant and buffers used. A more realistic option would be a combination of several variables which require refining, including changes to the pH, or the concentration of buffer, precipitant or protein sample used. The crystals produced from the condition 1.6M Sodium/Potassium Phosphate, pH 6.5 (Figure 4.18) failed to produce any crystals in their follow up study (Table 4.10). A process adopted from the seeding technique was attempted, whereby fragments of protein crystals are transferred from one well to another identical well, which thus acts as a nucleation point for the protein within that well (Blundell & Johnson, 1976; Chayen, 2004; Stura & Wilson, 1991). Unfortunately, after several months of monitoring the well, no crystal growth was observed. Looking forward, alternative micro/macro seeding techniques such as adding crushed crystals to a well at the start of the experiment could be employed to promote crystal growth (Rhodes, 2000).

The follow up trial for the condition 1.5M Ammonium Sulfate, 0.1M Tris, pH 8.0 (see Figure 4.21), which produced small rounded crystals (Table 4.17) was slightly altered to that of previous follow-up experiments. Previous crystallisation trials which had yielded protein crystals which diffraction to low resolution data, alongside those described in Table 4.17 all had one variable in common: high salt-based precipitant. A follow up trial was therefore carried out containing a range of ammonium sulfate concentrations (1-2M, 0.2M increments) and a range of different pH's (5.0-8.0) to accommodate this observation. Any visible crystals are yet to appear from these trials, but are being closely monitored. This could be due to several reasons. The temperature within the lab may have had an effect of crystal formation within the well. In addition, the range of conditions covered may not be

suitable for the complex, with more follow up trials required. Although, it is worth noting that initial trials did take up to 12 months for crystals to form (Blundell & Johnson, 1976; Chayen, 2004; Rhodes, 2000)

4.4.4 Future Crystal Trails of the Complex: C-reactive Protein, C1qGHR and CWPS

Protein crystallisation for the complex of C1qGHR, CRP and CWPS produced several crystals which diffracted to a low resolution of 9-10Å. Unfortunately, no crystals were produced which diffracted to a higher resolution. Common cryoprotectants which have provided successful previously within our research group failed to successfully cryoprotect three of the complex crystals. Moreover, this highlights two cryoprotectants (PEG 550 MME and Glycerol) which could also be used in future studies. A typical feature observed within these trials was poorly formed rounded crystals. Future experimental work should address this issue of a more ordered crystal growth by through further follow up studies. Fortunately, the trials described here have highlighted several key areas which could be pursed for future crystallisation studies. Conditions which have been highlighted in Table 4.17 show a range of high salt-based conditions which could be further pursued and refined to grow diffraction quality crystals. Furthermore, alterations in the proteins concentration may be a key area to address for further experimental work.

Chapter 5.0 – Discussion, Conclusions and Future Work

5.1 General Overview

CRP was initially classed as a biological marker for the presence of infection, inflammation or tissue damage within the body (Baltz *et al*., 1982; Pepys & Hirschfield, 2003). Since its discovery, experimental research has highlighted conflicting roles for the acute phase protein. Published research has postulated that molecular variations of CRP can exert pro-inflammatory stimuli within the body, exacerbating the pathology commonly observed in inflammatory diseases (Pepys & Hirschfield, 2003; Torzewski *et al.*, 1998; Zhang *et al.*, 1999; Zhang *et al*., 2012). Furthermore, it is widely accepted that raised baseline levels of pCRP is a strong indicator for the development of said diseases later in life (Pepys & Hirschfield, 2003). Alternative evidence has suggested an immune-regulatory role of CRP within the body, helping to manage and control not only inflammation, but other components of the immune system (Skoglund *et al*., 2008).

The main aims of this research include the purification & identification of molecular variations of human CRP from serum, alongside determination of the structural interactions occurring between native CRP and its natural ligands. Here we provide experimental evidence which contributes towards our overall understanding of CRP within the human body. We describe the identification of a monomeric form of CRP from human serum, through both Western Blot and ELISA analysis within our laboratory. Furthermore, based on our crystallisation studies, we can report a set of experimental conditions to which one may follow up to refine the crystallisation of mCRP and a complex of CRP, C1qGHR and CWPS.

5.2 Production, Purification and Characterisation of Monomeric C-reactive Protein

The experimental evidence provided in Chapter 2 discusses the production, purification and characterisation of *in vitro* produced mCRP. A large proportion of the research documented within the literature, which describes the potential pro-inflammatory effects of mCRP, uses similar methods of urea-induced dissociation to produce mCRP for their experiments. Our dissociation trials helped determine the optimum conditions required to produce mCRP within the most realistic timeframe possible for our research. Although we could not be certain of any modifications urea-induced dissociation may have on the CRP protein, additional characterisation experiments carried out provide an insight into the structural and biological stability of the protein. Interestingly, re-introducing mCRP into a standard storage calcium buffer for extended periods of time did not result in re-association. We hypothesised this is due to urea-induced modifications to the lysine residues involved in the non-covalent interactions occurring between the CRP protomers; fortunately, this did not seem to alter structural or biological properties of the protein. Confirmation of this could be achieved through successful crystallisation of the mCRP protein.

Dissociation trials within our research group demonstrated that urea alone was not sufficient to induce dissociation of the native CRP molecule; EDTA, a calcium chelator was required. The dependence on the removal of calcium highlights its importance in maintaining structural integrity of the protein. Moreover, Shrive *et al.*, (1996), have previously demonstrated the removal of calcium results in structural changes and exposure of sites which are susceptible to proteolysis (Ramadan *et al.*, 2002; Shrive *et al.*, 1996). Calcium was also shown to be crucial in maintain the protein's biological activity when interacting with ligands.

Purification of the mCRP samples via size exclusion chromatography not only provided us with a method of assessing the level of dissociation, but also allowed calculation of the elution volume for mCRP. Due to the lower levels of mCRP that we discovered within serum compared to that of pCRP, the protein failed to produce any elution peak when being run through the size exclusion column. The elution volume established through previous dissociation trials proved to be crucial when calculating where potential *in vivo* mCRP samples may elute off the column. Furthermore, identification of *in vitro* produced mCRP via Western Blot analysis suggested that the commercially available mAb could detect similar epitopes present on an *in vivo* form of mCRP. The experimental evidence from the precipitation studies highlighted several important features regarding mCRP. Firstly, the protein failed to follow the generic precipitation curve, like pCRP. This may be due to mCRP only displaying one binding site to phosphocholine (PC), whereas pCRP contains five. This therefore prevents mCRP forming 'cross-linkages' with the ligand in an equivalence zone, which generates large levels of precipitation; a reaction commonly seen in antibody-antigen agglutination reactions. Alternatively, mCRP displayed an ability to bind and precipitate in smaller amounts, to larger, PC-bound ligands. As there are large volumes of literature referring to a 'membrane-bound CRP' form, one may assume that an *in vivo* form of mCRP could exhibit similar features (Ciubotaru *et al.,* 2005; Ji *et al.,* 2009; Li *et al.,* 2012; Zhao & Shi, 2010).

5.3 Analysis of Human Serum Samples

We tested 40 patient's serum samples for the presence of mCRP, who displayed raised levels of pCRP (>100mg/L). We hypothesised that to increase our chances of detecting mCRP; we would recruit participants who already displayed significantly raised levels of pCRP. Additionally, we hypothesised that out of the 40 human samples that we tested, 15% (6 participants) would test positive for the presence of mCRP. Analysis of the

serum from all participants revealed that all 40 samples tested positive for mCRP. To our knowledge, this is the first report of the presence of mCRP identified through both Western Blot and ELISA analysis, post-serum purification.

Previous research has reported the detection of mCRP within the serum of patients who had suffered a myocardial infarction (20.96 ± 1.64ng/ml) (Wang *et al.*, 2015). Furthermore, they also described the isolation of mCRP within patients with raised levels of pCRP (>3mg/L). The clinical data provided from this study, coupled with our experimental research, further contributes towards the hypothesis that mCRP is present within the human body. Comparison between levels detected within both studies highlights differences in the mean levels detected, although these figures are only provided from 6 participants, with further research needed. Dissimilar to our research, Wang *et al*, identified and measured mCRP levels through ELISA analysis of neat serum, which may encounter complications as pCRP has been reported to dissociate upon binding to ELISA plates (Eisenhardt *et al.*, 2011). In our study, we have overcome this by providing a unique additional analysis which demonstrates ability for PC binding, alongside molecular weight determination through size exclusion chromatography and Western Blot analysis.

We provide here evidence of a monomeric form of CRP within serum through two separate established procedures. We also conclude that standard quantitative tests, such as ELISA can measure levels of both *in vitro* mCRP and pCRP, but do not distinguish between the two isoforms. The same is plausible for the automated systems used within clinical practice, as these also rely on the same formation of the antigen-antibody complex. This research should therefore provoke clinicians to consider re-evaluating the methods in which they measure CRP levels within serum. Scientific evidence suggests a pro-inflammatory role for mCRP, with others suggesting raised levels acting as a biomarker in life-threatening circumstances (Wang *et al.*, 2015). This inability for current automated systems to

differentiate between levels of pCRP and mCRP may result in patients receiving the wrong care and/or treatment. Monomeric CRP has also been detected on the surface of various cells within the body (Habersberger *et al.*, 2012). As we have shown, *in vitro* mCRP can bind to PC; it is entirely plausible that membrane-bound CRP also exists, with membrane binding potentially contributing to its formation.

5.4 Crystallisation Trials

The crystallisation trials involving mCRP failed to produce any protein crystals of sufficient diffraction quality, we do however provide a list of potential conditions which may be followed up. High salt-based precipitants were found to be the most successful in producing small crystal-like structures which may have acted as nucleation points to allow crystal growth. Successful crystallisation of these conditions may eventually allow us a greater understanding of this proteins atomic structure. Although it may not be identical to that located within the human body, it will provide a more detailed structural knowledge of a monomeric unit of CRP, in addition to any modifications sustained through urea-induced dissociation.

Crystallisation studies with the complex involved pCRP, C1qGHR and CWPS. Similar to that observed within the mCRP crystallisation trails, we failed to produce any protein crystals which would diffract to a high enough standard for structural determination. The complex itself is extremely large which can sometimes prove difficult when trying to crystallise proteins within a uniformly organised lattice. That said, what we have achieved is a set of conditions which one could refine, and follow up, to promote the growth of sufficient, diffraction quality crystals. A series of high salt based precipitants were found to be the most successful when producing crystals, an observation which was common in both complex and mCRP crystallisation trials. Small, poorly formed showers of crystals were also

commonly seen in these trials, suggesting alterations are required in the concentration of proteins used.

As previously stated, CRP precipitates out with CWPS. Based on established precipitation studies (Volanakis, 1982) we managed to determine the ratio of CRP and CWPS which would result in low levels of precipitation when combining the samples. Furthermore, incubation of CRP with C1qGHR was thought to stabilise this interaction, further reducing precipitation levels. Several of the crystals which were produced dissolved upon the addition of cryoprotectant, with glycerol proving to be the most stable. This additional knowledge could also be used in the future studies; alongside the conditions we have provided should more follow-up conditions be trialled.

5.5 Conclusion

The research described here provides evidence for a monomeric form of human CRP through both ELISA and Western Blot analysis. The identification of mCRP through two separate procedures was crucial within our research as it not only synergistically backed up our experimental methodology but also provided us with both the molecular weight and quantifiable levels of the protein. Our methodology was further supported by samples which recorded the highest values through ELISA analysis also displaying positive bands on the Western Blots. Furthermore, the quantification of pCRP levels via the ELISA analysis was additionally reinforced by the UV Spectrophotometer readings of the purified samples. Unfortunately, the purified samples did display significant differences to the initial CRP concentrations, which could be down to several reasons, such as losses through the methodology used, or CRP may already have been ligand-bound, thus resisting purification. What is remarkable is that despite these losses, mCRP was still identified within all 40 of the human samples at relatively high concentrations compared to previous research, raising

the question of what levels of mCRP might be within neat human serum. Interestingly, the purified mCRP from human serum displayed similar characteristics to that of *in vitro* produced mCRP. This may provide further insight into the potential characteristics of the protein which been used heavily to document its pro-inflammatory properties. The formation of mCRP within the human body may not be solely linked to increased levels of pCRP, as we initially hypothesised. We speculate that alternative pathophysiological conditions within the human body may be required for its formation. In addition, structural determination of both mCRP and the complex will further aid in our understanding of both pentameric and monomeric CRP, and how they interact with their respective ligands.

The full clinical significance of this research is yet to be established. Important points that have previously been raised need to be addressed before a realistic approach for the re-evaluation of clinical CRP tests can be considered. What is clear from this research is that there is sound justification for further studies involving mCRP. Only through the recruitment of larger cohorts from the population can we begin to answer some of these questions and fully understand CRP's role within the human body.

References.

Abernethy, T. J. & Avery, O.T. (1941) The occurrence during acute infections of a protein not normally present in the blood. Distribution of the reactive protein in patient's sera and the effect of calcium on the flocculation reaction with C-polysaccharide of pneumococcus. *Journal of Experimental Medicine.* **73,** 173-182.

Abernethy, T. J., & Francis, T. (1937) Studies on the somatic polysaccharide of pneumococcus: I. Cutaneous and serological reactions in pneumonia. *Journal of Experimental Medicine.* **65**, 59-73.

Agrawal, A. CRP after 2004. (2004) *Molecular Immunology*. **42**, 927-930.

Agrawal, A., Shrive, A.K., Greenhough, T.J., Volanakis, J.E. (2001) Topology and structure of the C1q-binding site on C-reactive protein. *Journal of Immunolgy.* **166**, 3998-4004.

Albert, M. A., Danielson, E., Rifai, N., Ridker, P. M. (2001) Effect of statin therapy on levels: the pravastatin inflammation/CRP evaluation (PRINCE): a randomised trial and cohort study. *JAMA.* **286**, 64-70.

Alberts, B., Johnson, A., Lewis, J., Raff, M., Roberts, K., Walter, P. (2008) Molecular Biology of the Cell, New York, Garland Science.

Algarra, M., Gomes, D., Esteves da Silva, J.C.G. (2013) Current analytical strategies for C-reactive protein quantification in blood. *Clinica. Chemica. Acta.* **415**, 1-9.

Amatayakul-Chantler, S., Dwek, R. A., Tennent, G. A., Pepys, M. B., Rademacher, T. W. (1993) Molecular characterisation of Limulus Polyphemus C-reactive protein. II. Asparagine-linked oligosaccharides. *European Journal of Biochemistry.***214**, 99-110.

Amersham Biosciences. Protein separations handbook collection. Gel Filtration & affinity chromatography. Principles and methods. **18**, 1022-29.

Arlaud, G. J. & Colomb, M. G. (2001) Complement: Classical Pathway. In: *Encyc. Life. Sci*. http://www.els.net, 1-9.

Armstrong, P. B., Swarnakar, S., Srimal, S., Misguith, S., Hahn, E. A., Aimes, R. T., Quigley, J. P. (1996) A cytolytic function for a sialic acid-binding lectin that is a member of the pentraxin family of proteins. *Journal of Biological Chemistry.* **271**, 14717-14721.

Ash, R. (1933) Nonspecific precipitins for pneumococci fraction C in acute infections. *J. Journal of Infectious Diseases.* **53,** 89-97.

Asherie, N. (2004) Protein crystallization and phase diagrams. *Methods*. **34**, 266-272.

Aydin, S. (2015) A short history, principles, and types of ELISA, and our laboratory experience with peptide/protein analysis using ELISA. *Peptides.* **72**, 4-15.

Ballou, S. P., & Macintyre, S. S. (1990) Absence of a binding reactivity of human C-reactive protein for immunoglobulin or immune complexes. *Journal of Laboratory and Clinical Medicine.* **115**, 332-338.

Baltz, M.L., Beer, F.C., Feinstein, A., Munn, E.A., Milstein, C.P., Flecther, T.C., March, J.F., Taylor, J., Bruton, C., Clamp, J.R., Davies, A.J.S., Pepys, M.B. (1982) Phylogenetic aspects of C-reactive protein and related proteins. *Annual New York Academy of Science.* **389**, 49-57.

Berg, J. M., Tymoczko, J, L., Stryer, L. (2012) Biochemistry: International Edition, Basingstoke, UK, W. H. Freeman and Company.

Berger, P., McConnell, J. P., Nunn, M., Kornman, K. S., Sorrell, J., Stephenson, K., Duff, G. W. (2002) C-reactive protein levels are influenced by common IL-1 gene variations. *Cytokine*. **17**, 171-174.

Berlett, B. S., & Stadtman, E. R. (1997) Protein oxidation in aging, disease and oxidative stress. *The Journal of Biological Chemistry*. **272**, 20313-20316.

Bhakdi, S., Torzewski, M., Klouche, M., Hemmes, M. (1999). Complement and atherogenesis: binding of CRP to degraded, nonoxidised LDL enhances complement activation. *Atherosclerosis, Thrombosis and Vascular Biology*. **19**, 2348-2354.

Black, S., Kushner, I., Samols, D. (2004) C-reactive protein. *Journal of Biological Chemistry*. **279**, 48487-48490.

Blake, G. J., & Ridker, P. M. (2002) Inflammatory bio-markers and cardiovascular risk prediction. *Journal of Internal Medicine.* **252**, 283-294

Blundel. T. L., & Johnson, L. (1976) Protein Crystallography. United States. Academic Press.

Bryan, T., Luo, X., Bueno, P.R., Davis, J.J. (2013) An optimised electrochemical biosensor for the label-free detection of C-reactive protein in blood. *Biosensors. Bioelectronics.* **29**, 94-98.

Carland, T. M., Gerwick, L. (2010) The C1q domain containing proteins: Where do they come from and what do they do? *Develop. Comparative Immunology.* **34**, 785-790.

Cartwright., J. R., Tharia, H. A., Burns, I., Shrive, A. K., Hoole, D., Greenhough, T. J. (2004) Isolation and characterisation of pentraxin-like serum proteins from the common carp, Cyprinus carpio. *Development and comparative Immunology*. **28**, 113-125.

Cermak, J., Key, N. S., Bach, R. R., Balla, J., Jacob, H. S., Vercellotti, G. M. (1993) C-reactive protein induces peripheral blood monocytes to synthesize tissue factor. *Blood*. **82**, 513-520.

Chang, M. K., Binder, C. J., Torzewski, M., Witztum, J. L (2002) C-reactive protein binds to both oxidised LDL and apoptotic cells through recognition of a common ligand: Phosphorylcholine of oxidised phospholipids. *PNAS*. **99**, 13043-13048.

Chayen, N. E. (2004) Turning protein crystallisation from an art into science. *Current opinion in structural biology*. **14**, 577-583.

Chen, H., Locke, D., Liu, Y., Liu, C., Kahn, M. L. (2002) The platelet receptor GPVI mediates both adhesion and signalling responses to collagen in a receptor density-dependent fashion. *The Journal of Biological Chemistry*. **277**, 3011-3019.

Choi, H.W., Sakata, Y., Kurihara, Y., Ooya, T., Takeuchi, T. (2012) Label-free detection of C-reactive protein using relfectometric interference spectroscopy-based sensing system. *Analytica. Chimica. Acta.* **728**, 64-68.

Ciliberto, G., Arcone, R., Wagner, E. F., Ruther, U. (1987) Inducible and tissue-specific expression of human C-reactive protein in transgenic mice. *The EMBO Journal.* **6**, 4017-4022.

Cirillo, P., Golino, P., Calabro, P., Cali, G., Ragni, M., De Rosa, S., Cimmino, G., Pacileo, M., De Palma, R., Forte, L., Gargiulo, A., Corigliano F. G., Angri, V., Spagnuolo, R., Nitsch, L., Chiariello, M. (2005) C-reactive protein induces tissue factor expression and promotes smooth muscle and endothelial cell proliferation. *Cardiovascular Research.* **687**, 47-55.

Ciubotaru, I., Potempa, L.A., Wander, R.C. (2005) Production of modified C-reactive protein in U937-derived macrophages. *Experimental Biology in Medicine.* **230**, 762-70.

Clos, T. W. D. (1989) C-reactive protein reacts with the U1 small nuclear ribonucleoprotein. *Journal of Immunology.* **143**, 2553-9.

Clos, T. W. D., & Mold, C. (2004) C-reactive protein: an activator of innate immunity and a modulator of adaptive immunity. *Immunology Research.* **30**, 261-277.

Cook, M. T., Hayball, P. J., Nowak, B. F., Hayball, J. D. (2005) The opsonising activity of a pentraxin-like protyein isolated from snapper (Pagrus auratus, Sparidae) serum. *Development and comparative Immunology*. **29**, 703-712.

Coons, A.H., Creech, H.J., Jones, R.N. (1941) Immunological properties of an antibody containing a fluorescent group. *The Society of Experimental Biology in Medicine.* **47**, 200-202.

Coppinger, J. A., Cagney, G., Toomey, S., Kislinger, T., Belton, O., McRedmond, J. P., Cahill, D. J., Emili, A., Fitzgerald, D. J., Maguire, P. B. (2004) Characterisation of the proteins released from activated platelets leads to localisation of novel platelet proteins in human atherosclerotic lesions. *Blood*. **103**, 2069-2104.

Courtoy, P. J., Lombart, C., Feldmann, G., Moguilevsky, N., Rogier, E. (1981) Synchronous increase of four acute phase proteins synthesised by the same hepatocytes during the inflammatory reaction: a combined biochemical and morphological kinetics study in the rat. *Laboratory Investigation*. **44**, 105-115.

Crawford, J. R., Trial, J., Nambi, V., Hoogeveen, R. C., Taffet, G. E., Entman, M. L. (20160 plasma levels of endothelial microparticles bearing monomeric C-reactive protein are increased in peripheral artery disease. *Journal of Cardiovascular Translational Research.* **9**, 184-193.

Crosby, W. H. (1971) In the Platelet. Brinkhous, K. M., Shermer, R. W., Mostofi, F. K., Williams and Wilkins, Baltimore.

Cybulsky, M. I., & Gimbrone, M. A. Jr. (1991) Endothelial expression of a mononuclear leukocyte adhesion molecule during atherogenesis. *Science*. **251**, 788-791.

Danenberg, H, D., Kantak, N., Grad, E., Swaminathan, R. V., Lotan, C., Edelman, E. R. (2007) C-reactive protein promotes monocyte-platelets aggregation: an additional link to the inflammatory thrombotic intricacy. *European Journal of Heamatology.* **78**, 246-252.

Danesh, J., Whincup, P., Walker, M., Lennon, L., Thomson, A., Appleby, P., Gallimore, J. R., Pepys, M. B. (2000) Low grade inflammation and coronary heart disease: propestive study and updated meta-analyses. *BMJ.* **321,** 199-204.

de Beer, F. C., & Pepys, M. B. (1982c) Isolation of human C-reactive protein and serum amyloid P component. *Journal of Immunological Methods*. **50**, 17-31.

de Beer, F. C., Baltz, M. L., Munn, E. A., Feinstein, A., Taylor, J., Bruton, C., Clamp, J. R., Pepys, M. B. (1982a) Isolation and characterisation of C-reactive protein and serum amyloid P component in rat. *Immunology*. **45**, 55-70.

de Beer, F. C., Soutar, A. K., Baltz, M. L., Trayner, I., Feinstein, A., Pepys, M. B. (1982b) Low density and very low density lipoproteins are selectively bound by aggregated C-reactive protein. *Journal of Experimental Medicine.* **156**, 230-242.

Deegan, O., Walshe, K., Kavanagh, K., Doyle, S. (2003) Quantitative detection of C-reactive protein using phosphocholine-labelled enzyme or microspheres. *Analytical Biochemistry.* **312**, 175-181.

Sherwood, D., & Cooper, J. (2010) Crystals, X-rays and proteins: comprehensive protein crystallography. United States. OUP Oxford.

Dong, Q., & Wright, J. R. (1996) Expression of C-reactive protein by alveolar macrophages. *Journal of Immunology.* **156**, 4815-4820.

Dunbar, B. S. (1994) Protein Blotting: A Practical Approach. United States. Oxford University Press.

Eisenhardt, S, U., Habersberger, J., Oliva, K., Lancaster, G. I., Ayhan, M., Woolard, K. J., Bannasch, H., Rice, G. E., Peter, K. (2011) A proteomic analysis of C-reactive protein stimulated THP-1 monocytes. *Proteome. Sci.* **9,** 1-12.

Eisenhardt, S. U., Thiele, J. R., Bannasch, H., Stark, B., Peter, K. (2009) C - reactive protein, how conformational changes influence inflammatory properties. *Cell. Cycle*. **8**, 3885-3892.

Filep, J. G. (2009) Platelets affect the structure and function of C-reactive protein. *Circulation Research.* **105**, 109-111.

Emsley, J., White, H. E., O'Hara, B. P., Oliva, G., Srinivasan, N., Tickle, I. J., Blundell, T. L., Pepys, M. B., Wood, S. P. (1994) Structure of pentameric human serum amyloid P component. *Nature*. **367**, 339-345.

Enghild, J. J., Thogersen, I. B., Salvesen, G., Fey, G. H., Figler, N. L., Gonias, S. L., Pizzo, S. V. (1990) Alpha-macroglobulin from Limulus Polyphemus exhibits proteinase inhibitory activity and participates in a haemolytic system. *Biochemistry*. **29**, 10070-10080.

Engvall, E., Perlmann, P. (1971) Enzyme-linked immunosorbant assay (ELISA). Quantitative assay of immunoglobulin. *Immunochemistry.* **8**, 871-874.

Foelsch, K. (2015) Monitoring protein crystallisation via dynamic light scattering and in-situ diffraction in microfluidic devices. University of Osnabrueck. Germany.

Fredrickson, D. S., Levy, R. I., Lees, R. S. (1967) Fat transport lipoproteins – an intergrated approach to mechanisms and disorders. *The New England Journal of Medicine.* **276**, 34-44.

Gaboriaud, C., Juanhuix, J., Gruez, A., Lacroix, M., Darnault, C., Pignol, D., Verger, D., Fontecilla-Camps, J.C., Arlaud, G.J. (2003) The crystal structure of the globular head of complement protein C1q provides a basis for its versatile recognition properties. *Journal of Biological Chemistry.* **278**, 46974-82.

Gaboriaud, C., Thielens, N. M., Gregory, L. A., Rossi, V., Fontecilla-Camps, J. C., Arlaud, G. J. (2004) Structure and activation of the C1 complex of complement: unravelling the puzzle. *Trends in Immunology.* **25**, 368-373.

Gan, S. D., & Patel, K. R. (2013) Enzyme immunoassay and enzyme-linked immunosorbent assay. *Journal of Investigative Dermatology.* **133**, 1-3.

Ganaptahii, M. K., Rzewnicki, D., Samols, D., Jiang, S. L., Kushner, I. (1991) Effect of combinations of cytokines and hormones on synthesis of serum amyloid A and C-reactive protein in Hep 3B cells. *Journal of Immunology.* **147**, 1261-1265.

Gasteiger, E., Gattiker, A., Hoogland, C., Ivanyi, I., Appel, R. D., Bairoch, A. (2003) ExPASy: the proteomics server for in-depth protein knowledge and analysis. *Nucleic Acid Research.* **31**, 3784-3788.

Gan, S.D. & Patel, K.R. (2013) Enzyme Immunoassay and Enzyme-Linked Immunosorbent Assay. *Journal of Investigative Dermatology.* **133**, 1-3.

Garlanda, C., Bottazzi, B., Bastone, A., Mantovani, A. (2005) Pentraxins at the crossroads between innate immunity, inflammation, matrix deposition and female fertility. *Annu. Rev. Immunol.* **23**, 337-366.

Gershov, D., Kim, S.J., Brot, N. Elkon, K. B. (2000) C-reactive protein binds to apoptotic cells, protects the cells from assembly of the terminal complement components, and sustains an anti-inflammatory innate immune response: Implication for system autoimmunity. *J. Exp. Med.* **18**, 1353-63.

Gewurz, H., Mold, C., Siegel, J., Fiedel, B. (1982) C-reactive protein and the acute phase response. *Advances in Internal Medicine.* **27**, 345-72.

Gill, R., Kemp, J. A., Sabin, C., Pepys, M. B. (2004) Human C-reactive protein increases cerebral infarct size after middle cerebral artery occlusion in adult rats. *Journal of Cerebral Blood Flow and Metabolism.* **24**, 1214-1218.

Girija, U. V., Gingras, A. R., Maeshall, J. E., Panchal, R., Sheikh, M. A., Gal, P., Schwaeble, W. J.m Mitchell, D. A., Moody, P. C., Wallis, R. (20130) Structural basis of the C1q/C1s interaction and its central role in assembly of the C1 complex of complement activation. *PNAS*. **110**, 13916-13920.

Glusker, J. P., & Trueblood, K. N. (1985) Crystal structure analysis: A primer. United States. Oxford University Press.

Gotschlich, E. C. (1982) Binding of C-reactive protein to C-carbohydrate and PC-substituted Protein. *Annals of the New York Academy of Sciences*. **389**, 163-171.

Gotschlich, E. C., & Liu, Y. (1966) Structural and Immunological Studies on the pneumococcal C-polysaccharide. *Journal of Biological Chemistry*. **242**, 463-470.

Griselli, M., Herbert, J., Hutchinson, W. L., Taylor, K. M., Sohail, M., Krausz, T., Pepys, M. B. (1999) C-reactive protein and complement are important mediators of tissue damage in acute myocardial infarction. *Journal of Experimental Medicine.* **190**, 1733-1740.

Hack, C.E., Wolbink, G.J., Schalwijk, C., Speijer, H., Hermens, W.T., Bosch, H.V.D. (1997) A role for secretory phospholipase A2 and C-reactive protein in the removal of injured cells. *Immunology Today.* **18**, 111-5.

Habersberger, J., Frederik, S., Scheichl, A., Htun, N., Bassler, N., Merivirta, R., Diehl, P., Krippner, G., Meikle, P., Eisenhardt, S.U., Mereditch, I., Peter, K. (2012) Circulating micro-particles generate and transport C-reactive protein in patients with myocardial infarction. *Cardiovascular Research.* **96**, 64-72.

Hames, B. D. (1998) Gel Electrophoresis of Proteins: A Practical Approach. United States. OUP Oxford.

Hammond, D. J., Singh, S. K., Thompson, J. A., Beeler, B. W., Rusinol, A. E., Pangburn, M. K., Potempa, L. A., Agrawal, A. (2010) Identification of acid pH-dependent ligands of pentameric C-reactive protein. *The Journal of Biological Chemistry.***285**, 36235-36244.

Hansson., G. K., & Libby, P. (2006) The immune response in atherosclerosis: a double-edged sword. *Nature.* **6**, 508-519.

Heras, B., & Martin, J. L. (2005) Post-crystallization treatments for improving diffraction quality of protein crystals. *Biological Crystallography*. **61**, 1173-1180.

Hjerten, S. (1962) "Molecular sieve" chromatography of polyacrylamide gels, prepared according to a simplified method. *Archives of Biochemistry and Biophysics.* **1**, 147-151.

Hohenester, E., Hutchinson, W.L., Pepys, M.B., Wood, S.P. (1997) Crystal structure of decameric complex of human amyloid P component with bound dAMP. *Journal of Molecular Biology.* **269**, 570-578.

Hornbeck, P., Winston, S. E., Fuller, S. A. (2001) Enzyme-linked immunosorbent assays. *Current Protocols in Immunology.* Chapter 2, Unit 2.1.

Hornung, M. (1972) Growth inhibition of melanoma cells by C-reactive protein activated lymphocytes. *Proceedings of the Society for Experimental Biological Medicine.* **139,** 1166-1169.

Hua, L., Zhou, R., Thirumalai, D., Berne, B. J. (2008) Urea denaturation by stronger dispersion interactions with proteins than water implies a 2-stage unfolding. *PNAS.* **105,** 16928 – 16933.

Hutchinson, W. L., Hohenester, E., Pepys, M. B. (2000) Human serum amyloid P component is a single uncomplexed pentamer in whole serum. *Molecular Medicine*. **6**, 482-493.

Islam, S. & Kang, S.H. (2011) Chemiluminescence detection of label-free C-reactive protein based on catalytic activity of gold nanoparticles. *Talanta.* **84**, 752-758.

Jabs, W. J., Logering, B. A., Gerke, P., Kreft, B., Wolber, E. M., Klinger, M. H., Fricke, L., Steinhoff, J. (2003) The kidney as a second site of human C-reactive protein formation in vivo. *European Journal of Immunology.* **33**, 152-161.

Janeway, C. A., & Medzhitov, R. (2002) Innate Immune Recognition. *Annu. Rev. Immunology.* **20,** 197-216.

Ji, S., Ma, L., Bai, C., Shi, J., Li, H., Potempa, L.A., Filep, J.G., Zhao, J., Wu, Y. (2009) Monomeric C-reactive protein activates endothelial cells *via* interaction with lipid raft microdomains. *FASEB. J.* **23**, 1806-16.

Ji, S., Wu, Y., Zhu, L., Potempa, L.A., Sheng, F., Lu, W., Zhao, J. (2007) Cell membranes and liposomes dissociate C-reactive protein (CRP) to form a new, biologically active structural intermediate: $mCRP_m$. *FASEB. J.* **21,** 284-94.

Jialal, I., & Devaraj, S. (2001) Inflammation and atherosclerosis: the value of the high sensitivity C-reactive protein assay as a risk marker. *American Journal of Clinical pathology.* **116**, 108-115.

Jialal, I., Devaraj, S., Venugopal, S. K. (2004) C-reactive protein: risk marker or mediator in atherothrombosis? *Hypertension*. **44**, 6-11.

Jiang, H., Robey, F.A., Gewurz, H. (1992) Localisation of sites through which C-reactive protein binds and activates complement to residues 14-26 and 76-92 of the human C1q A chain. *Journal of Experimental Medicine.* **175**, 1373-1379.

Jiang, H., Sigel, J.N., Gewurz, H. (1991) Binding and complement activation by C-reactive protein via the collagen-like region of C1q and inhibition of these reactions by monoclonal antibodies to C-reactive protein and C1q. *Journal of Immunology.* **146**, 2324-30.
Johnstone, A., & Thorpe, R. (1987) Immunochemistry in Practice. United States. Blackwell Scientific Publications.

Jonasson, L., Holm, J., Skalli, O., Bondjers, G., Hansson, G. K. (1986) Regional accumulation of T cells, macrophages, and smooth muscle cells in the human atherosclerotic plaque. *Atherosclerosis.* **6**, 131-138.

Kaplan, M.K. & Volanakis, J.E. (1974) Interaction of C-reactive protein complexes with the complement system. *Journal of Immunology.* **112**, 2135-47.

Kellum, J. A., Song, M., Li, J. (2004) Extracellular acidosis and the immune response: clinical and physiological implications. *Critical Care*. **8**, 331-336.

Kemeny, D. M. (1991) A practical guide to ELISA. United States. Pergamon.

Khera, A., de Lemos, J. A., Peshock, R. M., Lo, H. S., Stanek, H. G., Murphy, S. A., Wians F. H. Jr., Grundy, S. M., McGuire, D. K. (2006) Relationship between C-reactive protein and subclinical atherosclerosis: the Dallas heart study. *Circulation.* **113**, 38-43.

Khreiss, T., Josef, L., Potempa, L. A., Filep, J. G. (2004) Conformational rearrangement in C-reactive protein is required for proinflammatory actions on human endothelial cells. *Circulation.* **109,** 2016-2022.

Kim, H., Lee, S., Jeon, W.B., Lyu, H., Lee, S.W., Jeong, S.W. (2008) Detection of C-reactive protein on a functional poly(thiophene) self-assembled monolayer using surface plasmon resonance. *Ultramicroscopy.* **108**, 1379-1383.

Kim, I., Moon, S., Kim, S. H., Kim, H. J., Koh, Y. S., Koh, G. Y. (2001) Vascular endothelial growth factor expression of intercellular adhesion molecule 1 (ICAM-1), vascular cell adhesion molecule 1 (VCAM-1), and E-selectin through nuclear factor-κB activation in endothelial cells. *The Journal of Biological Chemistry*. **276**, 7614-7620.

Kinne, R. W., Stuhlmuller, B., Burmester, G. (2007) Macrophages. *Arthritis Research & Therapy.* **9**, 1-16.

Kishore, U., Ghai, R., Greenhough, T. J., Shrive, A. K., Bonifati, D. M., Gadjeva, M. G., Waters, P., Kojouharova, M. S., Chakraborty, T., Agrawal, A. (2004) Structural and functional anatomy of the globular domain of complement protein C1q. *Immunology Letters*. **95**, 113-128.

Kishore, U., Kojouharova, M. S., Reid, K. B. M. (2002) Recent progress in the understanding of the structure-function relationships of the globular head reagions of C1q. *Immunobiology*. **205**, 355-364.

Kishore, U. & Reid, K. B. M. (2000) C1q: Structure, function and receptors. *Immunopharmacology*. **49**, 159-170.

Kjelgaard-Hansen, M., Martinez-Subiela, S., Petersen, H.H., Jensen, A.L., Ceron, J.J. (2007) Evaluation and comparison of two immunoturbidimetric assays for the heterologous determination of porcine serum C-reactive protein. *Vet. J.* **173**, 571-577.

Klinger, M. H. F. (1997) Platelets and inflammation. *Anatomy and Embryology.* **196**, 1-11.

Koenig, W., Sund, M., Frohlich, M., Fischer, H. G., Lowel, H., Doring, A., Hutchinson, W. L., Pepys, M. B. (1999) C-reactive protein, a sensitive marker of inflammation, predicts the future risk of coronary heart disease in initially healthy middle-ages men: results from MONICA. *Circulation.* **99**, 237-242

Koivunen, M.E. & Krogsrud, R.L. (2006) Principles of immunochemical techniques used in clinical laboratories. *Laboratory Medicine.* **37**, 490-7.

Kresl, J.J., Potempa, L.A., Anderson, B.E. (1998) Conversion of native oligomeric to a modified monomeric form of human C-reactive protein. *International Journal Of Biochemistry and Cell Biology*. **30**, 1415-26.

Kushner, I., Kaplan, M. H. (1961) Studies of acute phase protein. I. An immunohistochemical method for the localisation of Cx-reactive protein in rabbits.

Association with necrosis in local inflammatory lesions. *Journal of Experimental Medicine.* **114**, 961-974.

Lee, W., Chen, Y., Lin, H., Shiesh, S., Lee, G. (2011) An integrated microfluidic system for fast automatic detection of C-reactive protein. *Sensors and Actuators. B.* **157**, 710-721.

Lei, K., Liu, T., Zon, G., Soravia, E., Liu, T., Goldman, N. D. (1985) Genomic DNAQ sequence for Human C-reactive protein. *The Journal of Biological Chemistry.* **260**, 13377-13383.

Li, R., Ren, M., Luo, M., Zhang, Z., Luo, B., Wy, J. (2012) Monomeric C-reactive protein alters fibrin clot properties on endothelial cells. *Thrombosis Research.* **129**, 251-6.

Li, S., & Goldman, N. D. (1996) Regulation of Human C-reactive protein and gene expression by two synergistic IL-6 responsive elements. *Biochemistry*. **35**, 9060-9068.

Li, S., Liu, T., Goldman, N. D. (1990) *cis*-Acting elements responsible for interleukin-6 inducible C-reactive protein gene expression. *The Journal of Biological Chemistry.* **265**, 4136-4142.

Libby, P. (2002) Inflammation in atherosclerosis. *Nature*. **420**, 868-874.

Libby, P., Ridker, P. M., Hansson, G. K. (2011) Progress and challenges in translating the biology of atherosclerosis. *Nature*. **473**, 317-324.

Liu, T., & Gotschlich, E. C. (1963) The chemical composition of Pneuomococcal C-polysaccharide. *The Journal of Biological Chemistry*. **233**, 1928-1934.

Lorber, B., & Giege, R. (1992) Preparation and handling of biological macromolecules for crystallization. New York. IRL Press.

Luchetti, M. M., Piccinini, G., Mantovani, A., Peri, G., Matteucci, C., Pomponio, G., Fratini, M., Fraticelli, P., Sambo, P., Di Loreto, C., Doni, A., Introna, M., Gabrielli, A. (2000) Expression and production of the long pentraxin PTX3 in rheumatoid arthritis (RA). *Clinical Experimental Immunology.* **119**, 196-202.

Lund, V., & Olafsen, J. A. (1998) A comparative study of pentraxin-like proteins in different fish species. *Developmental and Comparative Immunology.* **22,** 185-194.

Lundberg, A. M., & Hansson, G. K. (2010) Innate Immune Signals in Atherosclerosis. *Clinical Immunology*. **134**, 5-24.

Mackiewicz, A., Ganapathi, M.K., Schultz, D., Brabenec, A., Weinstein, J., Kelley, M.F., Kushner, I. (1990) Transforming growth factor β_1 regulates the production of acute phase proteins. *PNAS.* **87,** 1491-95.

Mantovani, A., Bussolino, F., Dejana, E. (1992) Cytokine regulation of endothelial cell function. *FASEB.* **6**, 2591-2599.

Marnell, L., Mold, C., Du Clos, T. W. (2005) C-reactive protein: ligands, receptors and role in inflammation. *Clinical Immunology.* **117**, 104-111.

Mauri, N., Offermann, M. K., Swerlick, R., Kunsch, C., Rosen, C. A., Ahmad, M., Alexander, R. W., Medford, R. M. (1993) Vascular cell adhesion molecule-1 (VCAM-1) gene transcription and expression are regulated through an antioxidant-sensitive mechanism in human vascular endothelial cells. *Journal of Clinical Investigation.* **92**, 1866-1874.

Mayrose, I., Graur, D., Ben-Tal, N., Pupko, T. (2004) Comparison of site-specific rate-interference methods for protein sequences: Empirical Bayesian methods are superior. *Molecular Biology and Evolution.* **9**, 1781-91.

McCarthy, M. (1982) Historical perspective on C-reactive protein. *Annals of the New York Academy of Sciences.* **389**, 1-10.

McGrath, F. D., Brouwer, M. C., Arlaud, G. J., Daha, M. R., Hack, C. E., Roos, A. (2006) Evidence that complement protein C1q interacts with C-reactive protein through its globular head region. *Journal of Immunology.* **176**, 2950-2957.

McGrowder, D., Riley, C., Morrison, E. Y. St. A., Gordon, L. (2010) The role of high-density lipoproteins in reducing the risk of vascular diseases, neurodegenerative disorders and cancer. *Cholesterol.* **2011**, 1-9.

McNicholas, S., Potterton, E., Wilson, K. S., Noble, M. E. M. (2011) 'Presenting your structures: the CCP4mg molecular-graphics softwarfe'. *Acta. Crys.* **67**, 386-394.

Mihlan, M., Blom, A. M., Kupreishvili, K., Lauer, N., Stelzner, K., Bergstrom, F., Niessen, H. W., Zipfel, P. F. (2011). Monomeric C-reactive protein modulates classical complement activation on necrotic cells. *FASEB Journal.* **25**, 4198-4210.

Merz Jr., K. M., Ringe, D., Reynolds, C. H. (2010) Drug Design. Structure- and Ligand-Based Approaches. New York. Cambridge University Press.

Mitra, S., & Bhattacharya, S. (1992) Purification of C-reactive protein from Channa punctatus (Bloch). *Indian Journal of Biochemistry and Biophysics*. **29**, 508-511.

Mold, C., Gewurz, H., Du Clos, T. W. (1999) Regulation of complement activation by C-reactive protein. *Immunopharmacology*. **42**, 23-30.

Mold, C., Rodgers, C. P., Richards, R. L., Alving, C. R., Gewurz, H. (1981) Interaction of C-reactive protein with liposomes. III. Membrane requirements for binding. *Journal of Immunology.* **126**, 856-860.

Molins, B., Pena, E., Vilahur, G., Mendieta, C., Slevin, M., Badimon, L. (2008) C-reactive protein isoforms differ in their effect on thrombus growth. *Atherosclerosis, Thrombosis and Vascular Biology.* **28**, 2239-46.

Mortensen, R. F., & Duszkiewicz, J. A. (1977) Mediation of CRP-dependent phagocytosis through mouse macrophage Fc-receptors. *Journal of Immunology.* **119**, 1611-1616.

Mortensen, R. F., Marcelletti, J. F., Johnson, C. S., Furmanski, P. (1982) Human C-reactive protein (CRP): A selective regulator of bone-marrow monocyte progenitor cells. *Annals of the New York Academy of Sciences.* **389**, 457-458.

Mortensen, R. F., Osmand, A. P., Gewurz, H. (1975) Effects on C-reactive protein on the lymphoid system. I. Binding to thymus-dependent lymphocytes and alteration of their functions. *The Journal of Experimental Medicine.* **141**, 821.839.

Mortensen, R. F., & Gewurz, H. (1976) Effects of C-reactive protein on the lymphoid system. II. Inhibition of mixed lymphocyte reactivity and generation of cytotoxic lymphocytes. *Journal of Immunology.* **116**, 1244-1250.

Mugge, A. (1998) The role of reactive oxygen species in atherosclerosis. *German Journal of Cardiology*. **87**, 851-864.

Murphy, K., Travers, P., Walport, M. (2008) Janeway's Immunobiology Seventh Edition, New York, Garland Science.

Nakanishi, Y., Kodama, H., Murai, T., Mikami, T., Izawa, H. (1991) Activation of rainbow trout complement by C-reactive protein. *American Journal of Veterinary Research. **52**, 397-401*.

Narkates, A.J. & Volanakis, J.E. (1982) C-reactive protein binding specificities: Artificial and natural phospholipid bilayers. *Annals of the New York Academy of Science.* **389**, 172-82.

Navratil, J. S., Korb, L. C., Ahearn, J. M. (1999) Systemic lupus erythematosus and complement deficiency: clues to a novel role for the classical complement pathway in the maintenance of immune tolerance. *Immunopharmacology*. **42**, 47-52.

Nieswandt, B., & Watson, S. P. (2003) Platelet-collagen interaction: is GPVI the central receptor? *Blood*. **102**, 449-461.

Nguyen, N. Y., Suzuki, A., Boykins, R. A., Liu, T. (1986) The amino acid sequence of *Limulus* C-reactive protein. *The Journal of Biological Chemistry.* **261**, 10456-10465.

Osmand, A.P., Friedenson, B., Gewurz, H., Painter, R.H., Hofmann, T., Shelton, E. (1977) Characterization of C-reactive protein and the complement subcomponent C1t as homologous proteins displaying cyclic pentameric symmetry (pentraxins). *PNAS.* **74**, 739-43.

Owens, A. P., & Mackman, N. (20110 Microparticles in hemostasis and thrombosis. *Circulation Research.* **108**, 1284-1297.

Paffen, E., Vos, H. L., Bertina, R. M. (2004) C-reactive protein does not directly induce tissue factor in human monocytes. *Atherosclerosis, Thrombosis and Vascular Biology.* **24**, 975-981.

Pasceri, V., Cheng, J. S., Willerson, J. T., Yeh, E. T. (2001) Modulation of C-reactive protein-mediated monocyte chemoattractant protein-1 induction in human endothelial cells by anti-atherosclerosis drugs. *Circulation.* **103**, 2531-2534.

Pasceri, V., Willerson, J. T., Yeh, E. T. (2000) Direct proinflammatory effect of C-reactive protein on human endothelial cells. *Circulation.***102**, 2165-2168.

Paques, E.P., Huber, R., Priess, H. (1979) Isolation of the Globular Region of the subcomponent q of the C1 Component of Complement. *Physiological Chemistry*. **360**, 177-83.

Pepys, M.B. & Baltz, M.L. (1983) Acute phase proteins with special reference to C-reactive protein and related proteins (pentraxins) and serum amyloid A protein. *Adv. Immunology* **34,** 141-212.

Pepys, M.B., & Hirschfield G.M. (2003) C-reactive protein: A critical update. *Journal of Clinical Investigation.* **111**, 1805-12.

Pepys, M.B., Beer, F.C., Milstein, C.P., March, J.F., Feinstein, A., Butress, N., Clamp, J.R., Taylor, J., Bruton, C., Flecther, T.C. (1982) C-reactive protein and serum amyloid P component in the plaice (*Pleuronectes platessa L.)* a marine teleost, are homologous with their human counterparts. *Biochemica, Biophysica. Acta.* **704**, 123-133.

Pepys, M. B., Dash, A.C., Fletcher, T.C., Richardson, N., Munn, E.A., Feinstein, A. (1978a) Analogues in other mammals and in fish of the human plasma proteins, C-reactive protein and amyloid P component. *Nature.* **273**, 168-70.

Pepys, M. B., Dash, A.C., Markham, R.E., Thomas, H.C., Williams & Aniva, B.D. (1978b) Comparative clinical study of protein SAP (amyloid P component) and C-reactive protein in serum. *Journal of Clinical Experimental Immunology.* **32**, 119-124.

Pepys¸ M. B., Hirschfield, G. M., Tennent, G. A., Gallimore, J. R., Kahan, M. C., Bellotti, V., Hawkins, P. N., Myers, R. M., Smith, M. D., Polara, A., Cobb, A. J. A., Ley, S. V., Aquilina, J. A., Robinson, C. V., Sharif, I., Gray, G. A., Sabin, C. A., Jenvey, M. C., Kolstoe, S. E., Thompson, D., Wood, S. P. (2006) Targeting C-reactive protein for the treatment of cardiovascular disease. *Nature*. **440**, 1217-1221.

Pepys, M. B., Rowe, I. F., Baltz, M. L. (1985) C-reactive protein: binding to lipids and lipoproteins. *Internal Review of Experimental Pathology*. **27**, 83-111.

Pied, S., Nussler, A., Pontet, M., Miltgen, F., Matile, H., Lambert, P., Mazier, D. (1989) C-reactive protein protects against preerythrocytic stages of malaria. *Infection and Immunity*. **57**, 278-282.

Potempa, L.A., Maldonado, B.A., Laurent, P., Zemel, E.S., Gewurz, H. (1983) Antigenic, electrophoretic and binding alterations of human C-reactive protein modified selectively in the absence of calcium. *Mol. Immunology.* **20**, 1165-75.

Poxton, I. R., Tarelli, E., Baddiley, J. (1978) The structure of C-Polysaccharide from the walls of *Streptococcus pneumoniae*. *Biochemistry Journal.* **175,** 1033-1042.

Punyadeera, C., Dimeski, G., Kostner, K., Beyerlein, P., Cooper-White, J. (2011) One-step homogenous C-reactive protein assay for saliva. *Journal of Immunology.* **373**, 19-25.

Ramadan, M. A., Shrive, A. K., Holden, D., Myles, D. A., Volanakis, J. E., DeLucas, L. J., Greenhough, T. J. (2002) The three-dimensional structure of calcium-depleted human C-reactive protein from perfectly twinned crystals. *Acta Crysallographica Section D Biological Crystallography.* **58**, 992-1001.

Rhodes, G. (2000) Crystallography made crystal clear. United States. Academic Press.

Richards, R. L., Gewurz, H., Osmand, A. P., Alving, C. R. (1977) Interactions of C-reactive protein and complement with liposomes. *PNAS.* **74**, 5672-5676.

Ridker, P. M. (2003) Clinical application of C-reactive protein for cardiovascular disease detection and prevention. *Circulation.* **107**, 363-369.

Ridker, P. M., (2016) From C-reactive protein to interleukin-6 to interleukin-1: Moving upstream to identify novel targets for atheroprotection. *Clinical Research.* **118**, 145-156.

Ridker, P. M., Cannon, C. P., Morrow, D., Rifai, N., Rose, L. M., McCabe, C. H., Pfeffer, M. A., Braunwald, E. (2005) C-reactive protein levels and outcomes after statin therapy. *New England Journal of Medicine.* **352,** 20-28.

Ridker, P. M., Rifai, N., Lowenthal, S. P. (2001) Rapid reduction in C-reactive protein with cerivastatin among 785 patients with primary hypercholesterolemia. *Circulation*. **103**, 1191-1193.

Ridker, P. M., Rifai, N., Pfeffer, M. A., Sacks, F., Braunwald, E. (1999) Long-term effects of pravastatin on plasma concentration of C-reactive protein. The cholesterol and recurrent events (CARE) investigators. *Circulation.* **100**, 230-235.

Rifai, N., Ballantyne, C.M., Cushman, M., Levy, D., Myers, G.L. (2006) High–sensitivity C-reactive protein and cardiac C-reactive protein assays: Is there a need to differentiate? *Clinical Chemsitry.* **52**, 1254-57.

Rifai, N., Ridker, P. M. (2001) High-sensitivity C-reactive protein: A novel and promising marker of coronary heart disease. *Clinical Chemistry.* **43**, 403-411.

Rifai, N., Tracy, R. P., Ridker, P. M. (1999) Clinical efficacy of an automated high-sensitivity C-reactive protein assay. *Clinical Chemistry*. **45**, 2136-2141.

Robey, F. A., & Liu, T. (1981) Limulin: A C-reactive protein from *Limulus Polyphemus. The Journal of Biological Chemistry.* **256**, 969-975.

Ross, R. (1999) Atherosclerosis – An inflammatory disease. *Mechanisms of Disease.* **340**, 115-126.

Rossky, P. J. (2008) Protein denaturation by urea: slash and bond. *PNAS.* **105,** 16825-16826.

Ruggeri, Z. M. (2002) Platelets in atherothrombosis. *Nature Medicine*. **8**, 1227-1234.

Sampson, A. P. (2000) The role of eosinophils and neutrophils in inflammation. *Clinical and Experimental Allergy.* **30**, 22-27.

Sato, A., Oe, K., Yamanaka, H., Yokoyama, I., Ebina, K. (2014) C-reactive protein specifically enhances platelet-activating factor-induced inflammatory activity in vivo. *European Journal of Pharmacology.* **754**, 46-51.

Schwalbe, R. A., Dahlback, B., Coe, J. E., Nelsestuen, G. L. (1992) Pentraxin family of proteins interact specifically with phosphorylcholine and/or phosphorylethanolamine. *Biochemistry.* **20**, 4907-15.

Shine, B., de Beer, F.C., Pepys, M.B. (1981) Solid phase radioimmunoassays for human C-reactive protein. *Clin. Chim. Acta.* **117**, 13-23.

Shrive, A.K., Metcalfe, A.M., Cartwright, J.R., Greenhough, T.J. (1999) C-reactive protein and SAP-like pentraxin are both present in *Limulus Polyphemus* haemolymph: Crystal structure of *Limulus* SAP. *Journal of Molecular Biology.* **290**, 997-1008.

Shrive, A.K., Cheetham, G.M.T., Holden, D., Myles, D.A.A., Turnell, W.G., Volanakis, J.E., Pepys, M.B., Bloomer, A.C., Greenhough, T. J. (1996) Three-dimensional structure of human C-reactive protein. *Nature Structure Biology.* **3**, 346-54.

Siegel, J., Rent, R., Gewurz, H. (1974) Interactions of C-reactive protein with the complement system. *Journal of Experimental Medicine.* **140**, 631-647.

Siemens (2014) Siemens Healthcare Diagnostics. ADIVA Chemistry. C-reactive Protein assay.

Singh, U., Devaraj, S., Dasu, M. R., Ciobanu, D., Reusch, J., Jialal, I. (2006) C-reactive protein decreases interleukin-10 secretion in activated human monocyte-derived macrophages via inhibition of cyclic AMP production. *Atherosclerosis, Thrombosis and Vascular Biology.* **26**, 2469-2475.

Sjowall, C., & Wettero, J. (2007) Pathogenic implication for autoantibodies against C-reactive protein and other acute phase proteins. *Clinical Chimica Acta.* **378**, 13-23.

Skoglund, C., Wettero, J., Skogh, T., Sjowall, C., Tengvall, P., Bengtsson, T. (2008) C-reactive protein and C1q regulate platelet adhesion and activation on adsorbed immunoglobulin G and albumin. *Immunology Cell Biology.* **86**, 466-474.

Slevin, M. & Krupinski, J. (2009) A role for monomeric C-reactive protein in regulation of angiogenesis, endothelial cell inflammation and thrombus formation in cardiovascular/cerebrovascular disease? *Histology and Histopathology.* **24**, 1473-8.

Sneck, M., Kovanen, P. T., Oorni, K. (2005) Decrease in pH strongly enhances binding of native, proteolyzed, lipolyzed and oxidized low density lipoprotein particles to human aortic proteoglycans. *The Journal of Biological Chemistry*. **280**, 37449-37454.

Steel, D. M., & Whitehead, A. S. (1994) The major acute phase reactants: C-reactive protein, serum amyloid P component and serum amyloid A protein. *Immunology Today*. **15**, 81.88.

Steinb, M. P., Edberg, J. C., Kimberly, R. P., Mangan, E. K., Bharadwaj, D., Du Clos, T. W. (2000) C-reactive protein binding to FcgammaRIIa on human monocytes and neutrophils is allele-specific. *Journal of Clinical investigation.* **105**, 369-376.

Stumpe, M. C. & Grubmuller, H. (2007) Interaction of urea with amino acids: implications for urea-induced protein denaturation. *The Journal of the American Chemical Society.* **129,** 16126-16131.

Stura, E. A., & Wilson, I. A. (1991) Applications of the streak seeding technique in protein crystallisation. *Journal of Crystal Growth.* **110**, 270-282.

Sun, S., Zhou, J., Yang, W., Zhang, H. (2014) Inhibition of protein carbamylation in urea solution using ammonium-containing buffers. *Analytical Biochemistry*, **446,** 76-81.

Sung, K. C., Suh, J. Y., Kim, B. S., Kang, J. H., Kim, H., Lee, M. H., Park, J. R., Kim, S. W. (2003) High sensitivity C-reactive protein as an independent risk factor for essential hypertension. *American Journal of Hypertension.* **16**, 429-433.

Syin, C., Gotschilch, E. C., Liu, T. Y. (1986) Rabbit C-reactive protein. Biosynthesis and characterisation of cDNA clones. *Journal of Biological Chemistry*. **261**, 5473-5479.

Szalai, A. J., van Ginkel, F. W., Wang, Y., McGhee, J. R., Volanakis, J. E. (2000) Complement-dependent acute-phase expression of C-reactive protein and serum amyloid P-component. *Journal of Immunology.* **165,** 1030-1035.

Tabas, I. (2010) Macrophage death and defective inflammation resolution in atherosclerosis. *Nature Reviews Immunology*. **10**, 36-46.

Takeuchi, O., & Akira, S. (2010) Pattern Recognition Receptors and Inflammation. *Cell*. **6,** 805-820.

Tennent, G. A., Butler, P. J. G., Hutton, T., Woolfitt, A. R., Harvey, D. J., Rademacher, T. W., Pepys, M. B. (1993) Molecular characterisation of *Limulus Polyphemus* C-reactive protein I. Subunit composition. *European Journal of Biochemistry.* **214,** 91-97.

Thompson, D., Pepys, M.B., Wood, S.P. (1999) The physiological structure of human C-reactive protein and its complex with phosphocholine. *Structure.* **7**, 169-77.

Tillett, W.S. & Francis, T. (1930) Serological reactions in pneumonia with non-protein somatic fraction of pneumococcus. *Journal of Experimental Medicine.* **52**, 561-571.

Torzewski, M., Rist, C., Mortensen, R. F., Zwaka, T. P., Bienek M., Waltenberger, J., Koeing, W., Schmitz, G., Hombach, V., Torzewski, J. (2000) C-reactive protein in the arterial intima: role of C-reactive protein receptor-dependent monocyte recruitment in atherogenesis. *Atherosclerosis, Thrombosis and Vascular Biology.* **20**, 2094-2099.

Torzewski, J., Torzewski, M., Bowyer, D. E., Frohlich, M., Koenig, W., Waltenberger, J., Fitzsimmons, C., Hombacj, V. (1998) C-reactive protein frequently colocalises with the terminal complement complex in the intima of early atherosclerosis lesions of human coronary arteries. *Atherosclerosis, Thrombosis and Vascular Biology.* **18**, 1386-1392.

Towbin, H., Staehelin, T., Gordon, J. (1979) Electrophoretic transfer of proteins from polyacrylamide gels to nitrocellulose sheets: Procedure and some applications. *PNAS*. **76**, 4350-4354.

Tracy, R. P., Lemaitre, L., Psaty, B. M., Ives, D. G., Evans, R. W., Cushman, M., Meilahn, E. N,m Kuller, L. H. (1997) Relationship of C-reactive protein ro risk of cardiovascular disease in the elderly. Results from the cardiovascular health study and the rural health promotion project. *Atherosclerosis, Thrombosis and Vascular Biology.* **17,** 1121-1127.

Tron, K., Manolov, D. E., Rocker, C., Kachele, M., Torzewski, J., Nienhaus, G. U. (2008) C-reactive protein specifically binds to Fcgamma receptor type 1 on a macrophage-like cell line. *European Journal of Immunology*. **38**, 1414-1422.

Tucci, A., Goldberger, G., Whitehead, A. S., Kay, R. M., Woods, D. E., Colten, H. R. (1983) Biosynthesis and postsynthetic processing of human C-reactive protein. *Journal of Immunology.* **5**, 2416-2419.

Van-Weemen, B.K. & Schuurs, A.H. (1971) Immunoassay using antigen-enzyme conjugates. *FBES. Lett.* **15**, 232-236.

Vanzi, F., Madan, B. Sharp, K. (1995) Effect of the protein denaturants urea and guanidinium on water structure: a structural and thermodynamic study. *The Journal of the American Chemical Society.* **120,** 10748-10753.

Vashist, S.K., Czilwik, G., Oordt, T.V., Stetten, F.V., Zengerle, R., Schneider, E.M., Luong, J.H.T. (2014) One-step kinetics-based immunoassay for the highly selective detection of C-reactive protein in less than 30min. *Analytical Biochemistry.* **456**, 32-37.

Vashist, S.K., Schneider, E.M., Zengerle, R., Stetten, F.V. (2015) Graphene-based rapid and highly sensitive immunoassay for C-reactive protein using a smartphone-based colorimetric reader. *Biosensors and Bioelectronics.* **66**, 169-176.

Verma, S., Szmitko, P. E., Yeh, E. T. (2004) C-reactive protein: structure affects function. *Circulation.* **109**, 1914-1917.

Vermeeren, V., Grieten, L., Vanden-Bon, N., Bijnens, N., Wenmackers, S., Janssens, S.D., Haenen, K., Wagner, P., Michiels, L. (2011) Inpedimetric, diamond-based immunosensor for the detection of C-reactive protein. *Sensors. Actuators.* **157**, 130-138.

Vetter, M. L., Gewurz, H., Hansen, B., James, K., Baum, L. L. (1983) Effects of C-reactive protein on human lymphocyte responsiveness. *Journal of Immunology.* **130**, 2121-2126.

Vickers, M. A., Green, F. R., Terry, C., Mayosi, B. M., Julier, C., Lathrop, M., Ratcliffe, P. J., Watkins, H. C., Keavney, B. (2002) Genotype at a promoter polymorphism of the interleukin-6 gene is associated with baseline levels of plasma C-reactive protein. *Cardiovascular Research.* **53**, 1029-1034.

Villems, R. & Toomik, P. I. (1993) Handbook of affinity chromatography. Chromatographic science series. Volume 63. Editor: Kline T. Published: Marcel Dekker Inc., New York.

Volanakis, J.E. (1982) Complement activation by C-reactive protein complexes. *Annals of the New York Academy of Sciences.* **389**, 235-50.

Volanakis, J.E. (2001) Human C-reactive protein: expression, structure and function. *Molecular Immunology.* **38**, 189-97.

Volanakis, J.E. & Kaplan, M.H. (1971) Specificity of C-reactive protein for choline phosphate residues of *Pneumococcal* C-polysaccharide. *Proceedings of the Society in Experimental Biology and Medicine.* **136**, 612-4.

Volanakis, J.E. & Narkates A.J. (1981) Interaction of C-reactive protein with artificial phosphatidylcholine bilayers and complement. *Journal of Immunology.* **126**, 1820-25.

Voleti, B., & Agrawal, A. (2006) Stating and nitric oxide reduce C-reactive protein production while inflammatory conditions persist. *Molecular Immunology.* **43**, 891-896.

Walport, M. J. (2001) Complement: First of two parts. *Advances in Immunology*. **344**, 1058-1066.

Wang, J., Tang, B., Liu, X., Wu, X., Wang, H., Xu, D., Guo, Y. (2015) Increased monomeric CRP levels in acute myocardial infarction: A possible new and specific biomarker for diagnosis and severity assessment of disease. *Atherosclerosis*. **239,** 343-349.

Whitehead, A. S., Bruns, G. A., Markham, A. F., Colten, H. R., Woods, D. E. (1983) Isolation of human C-reactive protein complementary DNA and localisation of the gene to chromosome 1. *Science*. **4605**, 69-71.

Wilcheck, M. & Chaiken, I. (2000) An overview of affinity chromatography – in methods in molecular biology. Affinity chromatography: methods and protocols. Editors: Bailon, P., Ehrlich, G. K., Fung, W. J., Berthold, W. Published: Human Press Inc., USA. **147**, 1-6.

Williams, R. C., Kilpatrick, K. A., Kassaby, M., Abdin, Z. H. (1978) Lymphocytes binding C-reactive protein during acute rheumatic fever. *The Journal of Clinical Investigation*. **61**, 1384-1393.

Wood, P. (2006) Understanding Immunology, Dorchester, UK, Pearson Education Limited.

Wu, J., Stevenson, M. J., Brown, J. M., Grunz, E. A., Strawn, T. L., Fay, W. P. (2008) C-reactive protein enhances tissue factor expression by vascular smooth muscle cells: mechanisms and in vivo significance. *Atherosclerosis, Thrombosis and Vascular Biology*. **28**, 698-704.

Yalow, R.S & Berson, S.A. (1960) Immunoassay of endogenous plasma insulin in man. *Journal of Clinical Investigations* **39**, 1157-1175.

Yudkin, J. S., Kumari, M., Humphries, S. E., Mohamed-Ali, V. (2000) Inflammation, obesity, stress and coronary heart disease: is interleukin-6 the link? *Atherosclerosis*. **148**, 209-214.

Yue, C. C., Muller-Greven, J., Dailey, P., Lozanski, G., Anderson, V., Macintyre, S. (1996) Identification of a C-reactive protein binding site in two hepatic carboxylesterases capable of retraining C-reactive protein within the endoplasmic reticulum. *The Journal of Biological Chemistry.* **271,** 22245-22250.

Zangi, R., Zhou, R., Berne, B. J. (2009) Urea's action on hydrophobic interactions. *Journal of the American Chemical Society.* **131,** 1535-1541.

Zhang, L., Liu, S., Wright, T. T., Shen, Z., Li, H., Zhu, W., Potempa, L. A., Ji, S., Szalai, A. J., Wu, Y. (2015) C-reactive protein directly suppresses Th1 cell differentiation and alleviates experimental autoimmune encephalomyelitis. *The Journal of Immunology.* **194**, 5243-5252.

Zhang, Y. X., Cliff, W. J., Schoefl, G. I., Higgins, G. (1999) Coronary C-reactive protein distribution: its relation to development of atherosclerosis. *Atherosclerosis.* **145**, 375-379.

Zhang, Z., & Ni, H. (2011) C-reactive protein as a predictor of mortality in critically ill patients: a meta-analysis and systematic review. *Anaesthesia and Intensive Care Journal*.**39,** 854-861.

Zhang, Z., Yang, Y., Hill, M. A., Wu, J. (2012) Does C-reactive protein contribute to atherothrombosis via oxidant-mediated release of pro-thrombic factors and activation of platelets? *Frontiers in Physiology.* **3**, 1-6.

Zhao, J. & Shi, X. (2010) A study of the interaction of the C-reactive protein monomer with the U937 monocyte. *Cell and Molecular Biology Letters.* **15**, 485-95.

Zhu, Y., Thangamani, S., Ho, B., Ding, J. L. (2005) The ancient origin of the complement system. *EMBO Journal.* **24**, 382-394.

Zou, Q., Habermann-Rottinghaus, S. M., Muphy, K. P. (1998) Urea effects on protein stability: hydrogen bonding and the hydrophobic effect. *Proteins: Structure, Function and Bioinformatics.* **31,** 107-115.

Zouki, C., Haas, B., Chan, J. S., Potempa, L. A., Filep, J. G. (2001) Loss of pentameric symmtery of C-reactive protein is associated with promotion of neutrolphil-endothelial cell adhesion. *Journal of Immunology.* **167**, 5355-5361.

Zwaka, T. P., Hombach, V., Torzewski, J. (2001) C-reactive protein-mediated low density lipoprotein uptake by macrophages. *Circulation*. **103**, 1194-1197.

Websites

http://web.expasy.org/protparam/

Appendix 1.

University Hospitals of North Midlands NHS
NHS Trust

University Hospitals of North Midlands

The Royal Stoke University Hospital

Newcastle Rd,

Stoke-on-Trent

Staffordshire

ST4 6QG

01782 715444

PATIENT INFORMATION SHEET

We would like to invite you to take part in a new research study. Before you decide whether to take part, it is important that you understand why the research is being done and what it would involve for you. One of the research team will go through the information sheet with you and will answer any questions you may have. We expect this should take no more than 15 minutes. If you are happy to participate we will ask you to sign a written consent form to acknowledge this.

Study title: *Is monomeric C-reactive Protein present within Human Serum?*

What is the purpose of the study?

The purpose of this study is to determine whether a specific version of a protein (known as C-reactive Protein or CRP) can be found within the serum of patients who have already been identified as having raised levels of CRP through a routine blood test. There is evidence that the version of the protein we are looking for may contribute to inflammation. It is thought that current blood tests for CRP do not include the version of the protein we are looking for in their measurements. The research will be carried out using the serum left over after all of the routine blood tests have been done; there will be no need to collect any extra blood from you.

Why have I been invited to take part?

You have been invited to take part in this study because your routine blood tests have shown raised CRP levels (>100mg/L). We would like to use the serum sample that is left over following completion of all of your routine blood tests.

Do I have to take part?

No, taking part in the study is voluntary. If you do decide to take part you will be asked to sign a consent form and you should keep this information sheet for future reference. You will retain the right to withdraw from the study at any time.

What will I have to do if I take part?

You will not need to do anything other than sign the consent form. If you decide to take part you will:

(i) Agree to read through, sign and date one of our participant consent forms (2x copies).
(ii) Agree for us to use any excess blood taken from your routine blood test procedure (that would normally be discarded), in order to test for a specific type of CRP.

You will not be required to undergo any procedure that is not already part of your routine clinical care at the hospital. This will complete your role within the study.

What is the benefit of taking part?

Although you will not benefit directly from the study, the data we collect will help us determine whether a specific type of CRP is located within human blood serum. We hope to identify whether current clinical practice, when measuring CRP levels, needs to be reconsidered.

Will taking part change my treatment and care?

Taking part in the study will not influence your treatment and care. This will continue as directed by your Doctor. There will be no further risk to you outside that already present in the routine collection of blood.

Will my information be kept confidential?

Your name will be included on your consent form, but all other study information and data will be kept confidential, anonymous and securely. You will never be identified by name in any communications or publications arising from the research.

What will happen to the samples I donate?

The samples will be used in a series of laboratory tests to determine whether a specific type of CRP is present within the blood. Once our study is completed, serum samples will be transferred back to the Hospital and stored for up to five years for potential future research. Your sample will remain anonymised and you will never be identified in any communications or publications from any research. Information generated from this study will be included within the thesis write up by Mr Robert Williams, PhD student at Keele University.

Who is conducting the research?

The research is led by Dr Annette Shrive (Keele University). Her co-investigators are Mr Robert Williams and Professor Tony Fryer (Keele University and University Hospitals of North Midlands respectively). The laboratory tests will be conducted at Keele University. It is being funded by Keele University.

Who should I contact for more information?

Patients can contact the Patient Advice and Liaison service (PALS) by telephone on 01782 676450/676455 or via email to patient.advice@uhns.nhs.uk for an independent contact point where they can seek general advice about taking part in research.

In addition, for further information about this study, patients can also contact the researchers listed below.

Mr Robert Williams
Postgraduate Researcher
Huxley Building, Keele University
Keele
ST5 5BG
Tel: 01782 734441

Dr Annette Shrive
Structural Biology Researcher & Lecturer
Huxley Building, Keele University
Keele
ST5 5BG
Tel: 01782 734441

Appendix 2.

University Hospitals of North Midlands NHS
NHS Trust

University Hospitals of North Midlands

The Royal Stoke University Hospital

Newcastle Rd,

Stoke-on-Trent

Staffordshire

ST4 6QG

01782 715444

PATIENT CONSENT FORM

Title of Project: Is monomeric C-reactive Protein present within the serum of patients with raised levels of C-reactive Protein (>100mg/L)?

Name of Researcher: *Dr A. Shrive, Mr R. Williams, Prof T. Fryer, Prof T. Greenhough*

Study Centre: *Royal Stoke University Hospital / Keele University*

Study Number: *CRP1*

Patient ID Number for this study: *A001*

Please initial box

1. I confirm that I have been guided through and understand the information sheet dated 25th March 2015, version 2, for the above study, and have had the opportunity to ask questions. ☐

2. I understand that my participation is voluntary and that I am free to withdraw at any time, without giving any reason and without my medical care or legal rights being affected. ☐

3. I understand that sections of my medical notes may be looked at by responsible individuals from regulatory authorities, the NHS trust or from the Sponsor (Keele University), where it is relevant to my taking part in this research. I give permission for these individuals to have access to my data. ☐

4. I understand that once the study has been completed, my serum sample will be transferred back to the Royal Stoke University Hospital, and kept for up to 5 years for potential future research. ☐

5. I agree to take part in the above study. ☐

_____	_____	_____
Name of Patient	Date	Signature
_____	_____	_____
Name of Person taking consent	Date	Signature

Appendix 3.

Structure Screen 1

Structure Screen 1 & 2 Conditions A1 – D12 MD1-30

Well #	Conc.	Units	Salt 1	Conc.	Units	Buffer	pH	Conc.	Units	Precipitant 1	Conc.	Units	Precipitant 2
A1	0.02	M	Calcium chloride dihydrate	0.1	M	Sodium acetate	4.6	30	% v/v	MPD			
A2	0.2	M	Ammonium acetate	0.1	M	Sodium acetate	4.6	30	% w/v	PEG 4000			
A3	0.2	M	Ammonium sulfate	0.1	M	Sodium acetate	4.6	25	% w/v	PEG 4000			
A4	2.0	M	Sodium formate	0.1	M	Sodium acetate	4.6						
A5	2.0	M	Ammonium sulfate	0.1	M	Sodium acetate	4.6						
A6				0.1	M	Sodium acetate	4.6	8	% w/v	PEG 4000			
A7	0.2	M	Ammonium acetate	0.1	M	Sodium citrate	5.6	30	% w/v	PEG 4000			
A8	0.2	M	Ammonium acetate	0.1	M	Sodium citrate	5.6	30	% v/v	MPD			
A9				0.1	M	Sodium citrate	5.6	20	% w/v	PEG 4000	20	% v/v	2-Propanol
A10	1.0	M	Ammonium phosphate monobasic	0.1	M	Sodium citrate	5.6						
A11	0.2	M	Calcium chloride dihydrate	0.1	M	Sodium acetate	4.6	20	% v/v	2-Propanol			
A12	1.4	M	Sodium acetate trihydrate	0.1	M	Sodium cacodylate	6.5						
B1	0.2	M	Sodium citrate tribasic dihydrate	0.1	M	Sodium cacodylate	6.5	30	% v/v	2-Propanol			
B2	0.2	M	Ammonium sulfate	0.1	M	Sodium cacodylate	6.5	30	% w/v	PEG 8000			
B3	0.2	M	Magnesium acetate tetrahydrate	0.1	M	Sodium cacodylate	6.5	20	% w/v	PEG 8000			
B4	0.2	M	Magnesium acetate tetrahydrate	0.1	M	Sodium cacodylate	6.5	30	% v/v	MPD			
B5	1.0	M	Sodium acetate trihydrate	0.1	M	Imidazole	6.5						
B6	0.2	M	Sodium acetate trihydrate	0.1	M	Sodium cacodylate	6.5	30	% w/v	PEG 8000			
B7	0.2	M	Zinc acetate dihydrate	0.1	M	Sodium cacodylate	6.5	18	% w/v	PEG 8000			
B8	0.2	M	Calcium acetate hydrate	0.1	M	Sodium cacodylate	6.5	18	% w/v	PEG 8000			
B9	0.2	M	Sodium citrate tribasic dihydrate	0.1	M	Sodium HEPES	7.5	30	% v/v	MPD			
B10	0.2	M	Magnesium chloride hexahydrate	0.1	M	Sodium HEPES	7.5	30	% v/v	2-Propanol			
B11	0.2	M	Calcium chloride dihydrate	0.1	M	Sodium HEPES	7.5	28	% v/v	PEG 400			
B12	0.2	M	Magnesium chloride hexahydrate	0.1	M	Sodium HEPES	7.5	30	% v/v	PEG 400			
C1	0.2	M	Sodium citrate tribasic dihydrate	0.1	M	Sodium HEPES	7.5	20	% v/v	2-Propanol			
C2	0.8	M	Potasium sodium tartrate tetrahydrate	0.1	M	Sodium HEPES	7.5						
C3	1.5	M	Lithium sulfate	0.1	M	Sodium HEPES	7.5						
C4	0.8	M	Sodium phosphate monobasic monohydrate/	0.1	M	Sodium HEPES	7.5						
	0.8	M	Potasium phosphate monobasic										
C5	1.4	M	Sodium citrate tribasic dihydrate	0.1	M	Sodium HEPES	7.5						
C6	2.0	M	Ammonium sulfate	0.1	M	Sodium HEPES	7.5	2	% v/v	PEG 400			
C7				0.1	M	Sodium HEPES	7.5	20	% w/v	PEG 4000	10	% v/v	2-Propanol
C8	2.0	M	Ammonium sulfate	0.1	M	Tris	8.5						
C9	0.2	M	Magnesium chloride hexahydrate	0.1	M	Tris	8.5	30	% w/v	PEG 4000			
C10	0.2	M	Sodium citrate tribasic dihydrate	0.1	M	Tris	8.5	30	% v/v	PEG 400			
C11	0.2	M	Lithium sulfate	0.1	M	Tris	8.5	30	% w/v	PEG 4000			
C12	0.2	M	Ammonium acetate	0.1	M	Tris	8.5	30	% v/v	2-Propanol			
D1	0.2	M	Sodium acetate trihydrate	0.1	M	Tris	8.5	30	% w/v	PEG 4000			
D2				0.1	M	Tris	8.5	8	% w/v	PEG 8000			
D3	2.0	M	Ammonium phosphate monobasic	0.1	M	Tris	8.5						
D4	0.4	M	Potasium sodium tartrate tetrahydrate										
D5	0.4	M	Ammonium phosphate monobasic										
D6	0.2	M	Ammonium sulfate					30	% w/v	PEG 8000			
D7	0.2	M	Ammonium sulfate					30	% w/v	PEG 4000			
D8	2.0	M	Ammonium sulfate										
D9	4.0	M	Sodium formate										
D10	0.05	M	Potassium phosphate monobasic										
D11								30	% w/v	PEG 1500			
D12	0.2	M	Magnesium formate dihydrate										

Structure Screen 2

Structure Screen 1 & 2 — Conditions E1 – H12 — MD1-30

Well #	Conc.	Units	Salt 1	Conc.	Units	Buffer	pH	Conc.	Units	Precipitant 1	Conc.	Units	Precipitant 2
E1	0.1	M	Sodium chloride	0.1	M	BICINE	9.0	30	% v/v	PEG 500 MME			
E2	2.0	M	Magnesium chloride hexahydrate	0.1	M	BICINE	9.0						
E3				0.1	M	BICINE	9.0	10	% w/v	PEG 20000	2	% v/v	1,4-Dioxane
E4	0.2	M	Magnesium chloride hexahydrate	0.1	M	Tris	8.5	3.4	M	1,6-Hexanediol			
E5				0.1	M	Tris	8.5	25	% v/v	tert-Butanol			
E6	1.0	M	Lithium sulfate/	0.1	M	Tris	8.5						
	0.01	M	Nickel(II) chloride hexahydrate										
E7	1.5	M	Ammonium sulfate	0.1	M	Tris	8.5	12	% v/v	Glycerol			
E8	0.2	M	Ammonium phosphate monobasic	0.1	M	Tris	8.5	50	% v/v	MPD			
E9				0.1	M	Tris	8.5	20	% v/v	Ethanol			
E10	0.01	M	Nickel(II) chloride hexahydrate	0.1	M	Tris	8.5	20	% w/v	PEG 2000 MME			
E11	0.5	M	Ammonium sulfate	0.1	M	Sodium HEPES	7.5	30	% v/v	MPD			
E12				0.1	M	Sodium HEPES	7.5	10	% w/v	PEG 6000	5	% v/v	MPD
F1				0.1	M	Sodium HEPES	7.5	20	% v/v	Jeffamine® M-600			
F2	1.6	M	Ammonium sulfate/	0.1	M	Sodium HEPES	7.5						
	0.1	M	Sodium chloride										
F3	2.0	M	Ammonium formate	0.1	M	Sodium HEPES	7.5						
F4	1.0	M	Sodium acetate trihydrate	0.1	M	Sodium HEPES	7.5						
	0.05	M	Cadmium sulfate $^{8}/_{3}$-hydrate										
F5				0.1	M	Sodium HEPES	7.5	70	% v/v	MPD			
F6	4.3	M	Sodium chloride	0.1	M	Sodium HEPES	7.5						
F7				0.1	M	Sodium HEPES	7.5	10	% w/v	PEG 8000	8	% v/v	Ethylene glycol
F8	1.6	M	Magnesium sulfate heptahydrate	0.1	M	MES	6.5						
F9	2.0	M	Sodium chloride/	0.1	M	MES	6.5						
	0.1	M	Potassium phosphate monobasic/										
	0.1	M	Sodium phosphate monobasic monohydrate										
F10				0.1	M	MES	6.5	12	% w/v	PEG 20000			
F11	1.6	M	Ammonium sulfate	0.1	M	MES	6.5	10	% v/v	1,4-Dioxane			
F12	0.05	M	Cesium chloride	0.1	M	MES	6.5	30	% v/v	Jeffamine® M-600			
G1	0.01	M	Cobalt(II) chloride hexahydrate	0.1	M	MES	6.5						
	1.8	M	Ammonium sulfate										
G2	0.2	M	Ammonium sulfate	0.1	M	MES	6.5	30	% w/v	PEG 5000 MME			
G3	0.01	M	Zinc sulfate heptahydrate	0.1	M	MES	6.5	25	% v/v	PEG 500 MME			
G4				0.1	M	Sodium HEPES	7.5	20	% w/v	PEG 10000			
G5	2.0	M	Ammonium sulfate	0.1	M	Sodium citrate	5.6						
	0.2	M	Potassium sodium tartrate tetrahydrate										
G6	1.0	M	Lithium sulfate	0.1	M	Sodium citrate	5.6						
	0.5	M	Ammonium sulfate										
G7	0.5	M	Sodium chloride	0.1	M	Sodium citrate	5.6	4	% v/v	Polyethyleneimine			
G8				0.1	M	Sodium citrate	5.6	35	% v/v	tert-Butanol			
G9	0.01	M	Iron(III) chloride hexahydrate	0.1	M	Sodium citrate	5.6	10	% v/v	Jeffamine® M-600			
G10	0.01	M	Manganese(II) chloride tetrahydrate	0.1	M	Sodium citrate	5.6	2.5	M	1,6-Hexanediol			
G11	2.0	M	Sodium chloride	0.1	M	Sodium acetate	4.6						
G12	0.2	M	Sodium chloride	0.1	M	Sodium acetate	4.6	30	% v/v	MPD			
H1	0.01	M	Cobalt(II) chloride hexahydrate	0.1	M	Sodium acetate	4.6	1.0	M	1,6-Hexanediol			
H2	0.1	M	Cadmium chloride hemi(pentahydrate)	0.1	M	Sodium acetate	4.6	30	% v/v	PEG 400			
H3	0.2	M	Ammonium sulfate	0.1	M	Sodium acetate	4.6	30	% w/v	PEG 2000 MME			
H4	2.0	M	Sodium chloride					10	% w/v	PEG 6000			
H5	0.5	M	Sodium chloride/										
	0.1	M	Magnesium chloride hexahydrate/										
	0.01	M	CTAB										
H6								25	% v/v	Ethylene glycol			
H7								35	% v/v	1,4-Dioxane			
H8	2.0	M	Ammonium sulfate					5	% v/v	2-Propanol			
H9				1.0	M	Imidazole	7.0						
H10								10	% w/v	PEG 1000	10	% w/v	PEG 8000
H11	1.5	M	Sodium chloride					10	% v/v	Ethanol			
H12				1.6	M	Sodium citrate	6.5						

Abbreviations:
Bicine; N,N-Bis(2-hydroxyethyl)glycine, **CTAB**; cetyltrimethylammonium bromide, **Sodium HEPES**; 2-(4-(2-Hydroxyethyl)-1-piperazinyl)ethanesulfonic Acid Sodium Salt, **MES**; 2-(N-morpholino)ethanesulfonic acid, **MME**; Monomethylether, **MPD;** 2,4-methyl pentanediol, **PEG**; Polyethylene glycol, **Tris**; 2-Amino-2-(hydroxymethyl)propane-1,3-diol., ***tert*-butanol**; 2-methyl-2-propanol; **Jeffamine M-600** is titrated to pH 7 prior to use.

Appendix 4.

ProPlex Structure Screen 1

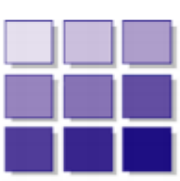

moleculardimensions.com

ProPlex Screen HT-96 Rows A - D MD1-42

HT-96 Well	Salt	Buffer	pH	Precipitant	Additive
A1	None	0.1 M Tris	8.0	25 % v/v PEG 350 MME	None
A2	0.1 M calcium acetate	0.1 M MES	6.0	15 % v/v PEG 400	None
A3	0.1 M lithium Chloride	0.1 M Na HEPES	7.5	20 % v/v PEG 400	None
A4	None	0.1 M Tris	8.0	25 % v/v PEG 400	None
A5	None	0.1 M MES	6.5	15 % v/v PEG 550 MME	None
A6	0.2 M sodium chloride	0.1 M Na/K phosphate	6.5	25 % w/v PEG 1000	None
A7	0.1 M ammonium sulfate	0.1 M Tris	7.5	20 % w/v PEG 1500	None
A8	0.2 M ammonium sulfate	0.1 M sodium acetate	5.5	10 % w/v PEG 2000 MME	None
A9	0.2 M sodium chloride	0.1 M MES	6.0	20 % w/v PEG 2000 MME	None
A10	0.1 M potassium chloride	0.1 M Tris	8.0	15 % w/v PEG 2000 MME	None
A11	None	0.1 M Na HEPES	7.5	25 % w/v PEG 2000 MME	None
A12	0.2 M sodium acetate	0.1 M sodium citrate	5.5	5 % w/v PEG 4000	None
B1	0.2 M lithium sulfate	0.1 M Tris	7.5	5 % w/v PEG 4000	None
B2	0.1 M calcium acetate	0.1 M sodium acetate	4.5	10 % w/v PEG 4000	None
B3	0.2 M sodium acetate	0.1 M sodium citrate	5.5	10 % w/v PEG 4000	None
B4	0.2 M sodium chloride	0.1 M MES	6.5	10 % w/v PEG 4000	None
B5	0.1 M magnesium chloride	0.1 M Na HEPES	7.5	10 % w/v PEG 4000	None
B6	None	0.1 M Na HEPES	7.0	10 % w/v PEG 4000	10 % v/v 2-propanol
B7	0.2 M ammonium acetate	0.1 M sodium acetate	4.0	15 % w/v PEG 4000	None
B8	0.1 M magnesium chloride	0.1 M sodium citrate	5.0	15 % w/v PEG 4000	None
B9	None	0.1 M sodium cacodylate	6.0	15 % w/v PEG 4000	None
B10	0.15 M ammonium sulfate	0.1 M MES	6.0	15 % w/v PEG 4000	None
B11	None	0.1 M Na HEPES	7.0	15 % w/v PEG 4000	None
B12	0.1 M magnesium chloride	0.1 M Na HEPES	7.0	15 % w/v PEG 4000	None
C1	0.15 M ammonium sulfate	0.1 M Tris	8.0	15 % w/v PEG 4000	None
C2	None	0.1 M sodium citrate	4.5	20 % w/v PEG 4000	None
C3	0.2 M ammonium acetate	0.1 M sodium acetate	5.0	20 % w/v PEG 4000	None
C4	0.2 M lithium sulfate	0.1 M MES	6.0	20 % w/v PEG 4000	None
C5	None	0.1 M Tris	8.0	20 % w/v PEG 4000	None
C6	0.15 M ammonium sulfate	0.1 M Na HEPES	7.0	20 % w/v PEG 4000	None
C7	None	0.1 M sodium citrate	5.6	20 % w/v PEG 4000	20 % v/v 2-propanol
C8	0.2 M sodium chloride	0.1 M Tris	8.0	20 % w/v PEG 4000	None
C9	None	0.1 M sodium cacodylate	5.5	25 % w/v PEG 4000	None
C10	0.15 M ammonium sulfate	0.1 M MES	5.5	25 % w/v PEG 4000	None
C11	None	0.1 M sodium cacodylate	6.5	25 % w/v PEG 4000	None
C12	0.2 M potassium iodide	0.1 M MES	6.5	25 % w/v PEG 4000	None
D1	0.2 M sodium chloride	0.1 M Na HEPES	7.5	25 % w/v PEG 4000	None
D2	None	0.1 M MES	6.5	10 % w/v PEG 5000 MME	12 % v/v 1-propanol
D3	0.1 M potassium chloride	0.1 M Na HEPES	7.0	15 % w/v PEG 5000 MME	None
D4	0.2 M ammonium sulfate	0.1 M Tris	7.5	20 % w/v PEG 5000 MME	None
D5	0.1 M magnesium chloride	0.1 M MES	6.0	8 % w/v PEG 6000	None
D6	0.15 M sodium chloride	0.1 M Tris	8.0	8 % w/v PEG 6000	None
D7	None	0.1 M sodium citrate	5.5	15 % w/v PEG 6000	None
D8	0.1 M magnesium acetate	0.1 M sodium cacodylate	6.5	15 % w/v PEG 6000	None
D9	None	0.1 M MES	6.5	15 % w/v PEG 6000	5 % v/v MPD
D10	0.1 M potassium chloride	0.1 M Na HEPES	7.5	15 % w/v PEG 6000	None
D11	None	0.1 M Tris	8.5	15 % w/v PEG 6000	None
D12	None	0.1 M Tris	8.5	20 % w/v PEG 6000	None

ProPlex Structure Screen 2

moleculardimensions.com

ProPlex Screen HT-96 **Rows E - H** **MD1-42**

HT-96 Well	Salt	Buffer	pH	Precipitant	Additive
E1	0.1 M magnesium acetate	0.1 M sodium acetate	4.5	8 % w/v PEG 8000	None
E2	None	0.1 M sodium citrate	5.0	8 % w/v PEG 8000	None
E3	0.2 M sodium chloride	0.1 M sodium cacodylate	6.0	8 % w/v PEG 8000	None
E4	None	0.1 M Na HEPES	7.0	8 % w/v PEG 8000	None
E5	None	0.1 M Tris	8.0	8 % w/v PEG 8000	None
E6	0.1 M calcium acetate	0.1 M sodium cacodylate	5.5	12 % w/v PEG 8000	None
E7	None	0.1 M sodium phosphate	6.5	12 % w/v PEG 8000	None
E8	0.1 M magnesium acetate	0.1 M MOPS	7.5	12 % w/v PEG 8000	None
E9	0.2 M sodium chloride	0.1 M Na HEPES	7.5	12 % w/v PEG 8000	None
E10	0.2 M ammonium sulfate	0.1 M Tris	8.5	12 % w/v PEG 8000	None
E11	None	0.1 M sodium citrate	5.0	20 % w/v PEG 8000	None
E12	0.2 M ammonium sulfate	0.1 M MES	6.5	20 % w/v PEG 8000	None
F1	None	0.1 M Na HEPES	7.0	20 % w/v PEG 8000	None
F2	0.2 M lithium chloride	0.1 M Tris	8.0	20 % w/v PEG 8000	None
F3	0.1 M magnesium acetate	0.1 M MES	6.5	10 % w/v PEG 10 000	None
F4	None	0.1 M Na HEPES	7.0	18 % w/v PEG 12 000	None
F5	0.1 M sodium chloride	0.1 M Tris	8.0	8 % w/v PEG 20 000	None
F6	None	0.1 M Na HEPES	7.0	15 % w/v PEG 20 000	None
F7	None	0.1 M MES	6.5	0.5 M ammonium sulfate	None
F8	None	0.1 M sodium acetate	5.0	1 M ammonium sulfate	None
F9	None	0.1 M MES	6.5	1 M ammonium sulfate	None
F10	None	0.1 M Tris	8.0	1 M ammonium sulfate	None
F11	None	0.1 M sodium acetate	5.0	1.5 M ammonium sulfate	None
F12	None	0.1 M Na HEPES	7.0	1.5 M ammonium sulfate	None
G1	None	0.1 M Tris	8.0	1.5 M ammonium sulfate	None
G2	None	0.1 M sodium acetate	5.0	2 M ammonium sulfate	None
G3	None	0.1 M Na HEPES	7.0	2 M ammonium sulfate	None
G4	None	0.1 M Tris	8.0	2 M ammonium sulfate	None
G5	1 M potassium chloride	0.1 M Na HEPES	7.0	1 M ammonium sulfate	None
G6	None	0.1 M sodium acetate	5.0	2 M sodium formate	None
G7	None	0.1 M Tris	7.5	3 M sodium formate	None
G8	None	None	7.5	0.8 M Na/K hydrogen phosphate	None
G9	None	None	7.0	1.3 M Na/K hydrogen phosphate	None
G10	None	None	6.5	1.6 M Na/K hydrogen phosphate	None
G11	None	0.1 M Na HEPES	7.5	1 M sodium acetate	None
G12	None	0.1 M Na HEPES	7.0	1 M sodium citrate	None
H1	None	0.1 M sodium citrate	6.0	2 M sodium chloride	None
H2	None	0.1 M MES	6.5	1 M lithium sulfate	None
H3	None	0.1 M Tris	8.0	1.6 M lithium sulfate	None
H4	None	None	6.0	1.4 M sodium malonate	None
H5	None	0.1 M Tris	8.0	1.2 M Na/K tartrate	None
H6	None	0.1 M MES	6.5	1.6 M magnesium sulfate	None
H7	None	0.1 M sodium acetate	5.0	15 % v/v MPD	2 % w/v PEG 4000
H8	0.05 M calcium acetate	0.1 M sodium cacodylate	6.0	25 % v/v MPD	None
H9	None	0.1 M imidazole	7.0	50 % v/v MPD	None
H10	0.05 M magnesium Chloride	0.1 M MES	6.5	10 % v/v 2-propanol	5 % w/v PEG 4000
H11	0.2 M ammonium acetate	0.1 M Na HEPES	7.5	25 % v/v 2-propanol	None
H12	0.1 M sodium chloride	0.1 M Tris	8.0	15 % v/v ethanol	5 % v/v MPD

Abbreviations:
HEPES; N-(2-hydroxyethyl)-piperazine-N'-2-ethanesulfonic acid, **MES**; 2-(N-morpholino)ethanesulfonic acid, **MME**; Monomethylether, **PEG**; Polyethylene glycol, **Tris**; 2-Amino-2-(hydroxymethyl)propane-1,3-diol, **MOPS**; 3-(N-Morpholino)-propanesulfonic acid;

Appendix 5.

CRP Concentrations for UHNM and Purified Samples, Volumes of Purified Samples and UV Spectrophotometer Readings for the Purified Samples (mCRP & pCRP)

Sample Code	Concentration of CRP Provided by UHNM (mg/L)	pCRP Concentrations in Purified Samples (mg/L)	Volume of Purified pCRP Samples (ml)	mCRP Concentrations in Purified samples (mg/L)	Volume of Purified mCRP Samples (ml)
CRP 010	117.20	26.08	0.83	0.66	0.30
CRP 012	263.90	66.78	0.78	2.02	0.90
CRP 018	176.00	16.45	0.11	0.20	0.10
CRP 021	320.90	29.06	0.22	0.36	0.20
CRP 023	203.50	28.13	0.22	0.37	0.15
CRP 027	108.40	2.93	0.28	0.08	0.05
CRP 051	111.20	5.00	0.06	0.12	0.05
CRP 052	172.10	41.84	0.89	0.75	0.50
CRP 053	121.70	18.46	0.83	0.50	0.35
CRP 059	239.60	25.44	0.28	0.87	0.50
CRP 065	109.90	14.68	0.28	0.98	0.70
CRP 066	198.70	11.12	0.22	0.58	0.70
CRP 068	103.20	20.06	0.28	0.34	0.30
CRP 069	144.90	29.14	0.33	3.07	0.90
CRP 072	115.80	25.11	0.28	0.22	0.10
CRP 075	354.30	5.41	0.17	0.31	0.20
CRP 084	109.10	19.07	0.28	0.26	0.15
CRP 096	279.80	32.60	0.28	0.04	0.05
CRP 105	131.10	12.26	0.28	0.06	0.05
CRP 106	101.70	17.72	0.28	0.71	0.50
CRP 107	303.00	9.35	0.28	0.55	0.35
CRP 108	215.40	7.08	0.28	0.72	0.50
CRP 109	138.40	19.68	0.56	0.58	0.70
CRP 110	131.00	13.75	0.28	0.62	0.70
CRP 115	106.90	14.01	0.28	3.52	0.70
CRP 117	112.50	26.88	0.28	0.32	0.30
CRP 120	119.20	9.31	0.28	0.79	0.50
CRP 124	173.90	14.43	0.28	0.79	0.50
CRP 146	130.80	22.64	0.28	1.07	0.50
CRP 148	262.10	27.66	0.28	3.28	0.50
CRP 153	209.80	30.40	0.44	1.15	0.60
CRP171	149.90	25.24	0.33	0.79	0.50
CRP175	387.80	27.03	0.44	0.58	0.35
CRP182	126.70	21.89	0.33	0.58	0.35

CRP191	139.40	38.37	0.44	0.74	0.45
CRP 196	149.20	20.73	0.44	1.03	0.80
CRP 200	254.50	49.74	0.56	0.75	0.50
CRP 201	125.40	24.99	0.56	1.02	0.65
CRP 204	448.60	60.90	0.56	3.51	0.65
CRP 207	168.00	20.73	0.44	0.43	0.50

Sample Code	**Purified pCRP Concentrations from UV Spectrophotometer (mg/ml)**	**Purified mCRP Concentrations from UV Spectrophotometer (mg/ml)**
CRP 010	0.040	0.010
CRP 012	0.050	0.010
CRP 018	0.010	0.010
CRP 021	0.140	0.010
CRP 023	0.120	0.010
CRP 027	0.010	0.000
CRP 051	0.010	0.000
CRP 052	0.040	0.010
CRP 053	0.040	0.000
CRP 059	0.010	0.000
CRP 065	0.090	0.010
CRP 066	0.060	0.000
CRP 068	0.090	0.000
CRP 069	0.080	0.000
CRP 072	0.070	0.000
CRP 075	0.050	0.010
CRP 084	0.080	0.000
CRP 096	0.200	0.000
CRP 105	0.060	0.010
CRP 106	0.060	0.000
CRP 107	0.040	0.000
CRP 108	0.030	0.000
CRP 109	0.040	0.000
CRP 110	0.060	0.000
CRP 115	0.050	0.000
CRP 117	0.050	0.000
CRP 120	0.060	0.000
CRP 124	0.070	0.000
CRP 146	0.020	0.000
CRP 148	0.050	0.020
CRP 153	0.010	0.000

CRP171	0.070	0.000
CRP175	0.030	0.000
CRP182	0.090	0.000
CRP191	0.080	0.000
CRP 196	0.060	0.000
CRP 200	0.040	0.000
CRP 201	0.040	0.000
CRP 204	0.150	0.010
CRP 207	0.060	0.000